ISSN 0250-7625

IIASA REPORTS

International Institute for Applied Systems Analysis

Volume 6 Number 2 October–December 1982
Completing Volume 6

IIASA
REPORTS

Volume 6 (1982)
Completing Volume 6

Cover

Photograph: F.K. Nebuda

International Standard Serial Number 0250-7625

IIASA Reports presents research conducted at IIASA that has been independently reviewed before publication. However, the views and opinions it expresses are not necessarily those of the Institute or the National Member Organizations that support it or of the institution that sponsored the research.

TWO GLOBAL SCENARIOS: THE EVOLUTION OF ENERGY USE AND THE ECONOMY TO 2030

Verne G. Chant
International Institute for Applied Systems Analysis, Laxenburg, Austria
and
Hickling-Partners Incorporated, Ottawa, Ontario, Canada

SUMMARY

Energy in a Finite World: A Global Systems Analysis *documents the seven-year study of the future balance of energy supply and demand made by the IIASA Energy Systems Program. Part IV of this book, "Balancing Supply and Demand: The Quantitative Analysis," presents results based on two scenarios of global and regional development; these scenarios specify population growth, aggregate economic development in five sectors, and detailed energy use and supply for seven global regions. This report outlines how these scenarios were derived and interprets their quantitative projections in terms of energy–price, energy–income, and substitution elasticities and technological development. The data used are those also used in the book.*

This report defines the scenarios in terms of population, GDP, and primary and final energy-use projections in sufficient detail for the economic interpretation analysis. For all seven regions, it examines the energy linkage in the aggregate in terms of energy use per unit of GDP and the energy–GDP elasticity, after which it defines an economic framework and simple aggregate models for interpreting the scenario projections. One model allows for separating the effects of energy prices and energy growth on energy requirements; another, based on a production-function formulation, allows one to examine technological development and the substitution of nonenergy for energy inputs primarily in the industrial sector. Finally, the report defines appropriate measures of energy price increases over the projection period and uses them, along with the economic models, to analyze the scenarios in economic terms.

1 INTRODUCTION

A scenario is a logically consistent statement or characterization of a possible future state of the world. Often a scenario statement also specifies a sequence of events that could transform a reference state into the postulated future state. This postulated state may represent the consensus of many experts or be outrageously absurd, provided that it is internally consistent and follows from the assumptions made. A scenario in this sense, therefore, is not a prediction, but simply one future state that might be realized.

Scenario definition is necessarily subjective. Many assumptions must be made which cannot be proven or tested. Depending on one's purpose, certain assumptions are more appropriate and more useful, than others. We use our scenario projections as a tool to explore the interrelationships among many variables. We have developed two quantitative scenarios in detail which we label High and Low. Neither represents our expected or most likely future. But the range of the High and Low is sufficient to span many possible future states which are useful to explore.

No one would claim that the product of the IIASA Energy Systems Program was, in whole or in part, two scenarios. Scenarios *were* developed, *were* used as a learning tool, and formed a framework within which to describe results in an internally consistent and quantitative manner. The drive for consistency demanded quantification, usually to a precision well beyond what would be justified based on data availability and known relationships. That is the nature of the analytic tool. One must not forget, however, the purpose of the quantification and the scenario projections; the message must be interpreted.

Most of the work documented in this report involved the interpretation, in economic terms, of scenario projections that were derived in noneconomic terms. That is to say, our scenario projections were derived based on assumptions about population, production, resources, costs, development, technology, and life-styles with the assistance of a set of detailed models. These projections were then interpreted in economic terms using energy prices, income and price elasticities, technological development and substitution. The purpose of these interpretations was twofold. Firstly, to use the interpretation as part of the assessment of the scenario during the iterative development process with respect to consistency, reasonableness, and continuity. Secondly, to provide, as in this report and other publications, a similar interpretation of the resulting scenarios to facilitate understanding and comparisons with other work. This report also serves another purpose in providing a more detailed scenario data base, both historical and projected, than Energy Program Group 1981.

1.1 Two Scenarios

Our two scenarios were developed to enable the analysis of the global energy problem to be specific, regional, and quantitative. In a highly aggregated way, these scenarios provide a high and a low energy use picture for each of seven regions of the globe. These regions are illustrated in Figure 1 and are defined in Appendix B.

To begin the scenario development process, assumptions were made with respect to population growth and urbanization. Population projections for the seven regions exhibit continually decreasing growth rates reaching a stable population of some nine billion people a few decades after our projection period. During the projection period (1975–2030), global population doubles from four billion to eight billion – an abrupt change in historical perspective. Also the population share in developing regions increases from 71

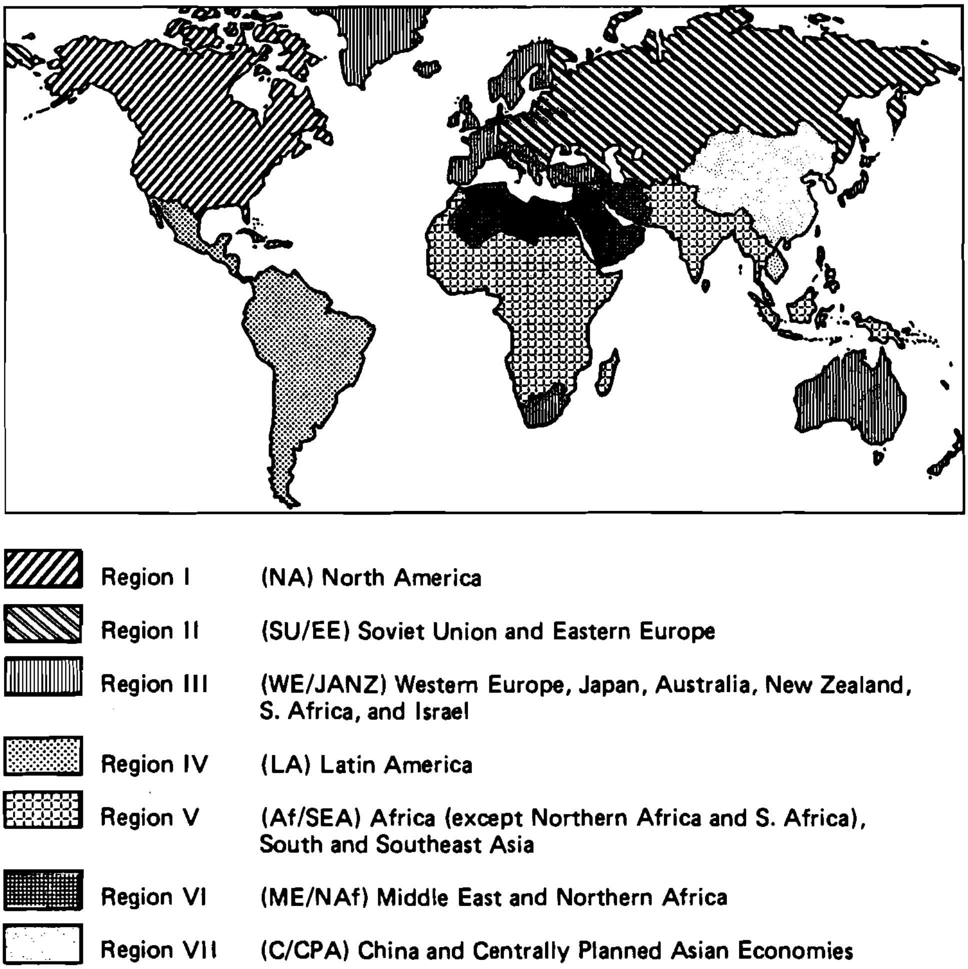

FIGURE 1 The IIASA world regions.

percent to 80 percent; the population ages such that two-thirds as many people are in the labor-force age bracket (15–65 years) per person over age 65; and urbanization increases dramatically from 30 percent to 60 percent in the developing regions and from less than 70 percent to 90 percent in developed regions. The same population projection was used in both scenarios and it was not changed during the iterative process.

A second major starting point in the scenario development process was projection of gross domestic product (GDP) for each region. Two projections were made, a high and a low. GDP was included within the iterative process so that initial projections were not necessarily our final projections. These scenarios exhibit ever-decreasing growth rates through the projection period, on both a per-capita and absolute basis. Also the developing region growth rates were consistently higher than those in Regions I and III, again, even on a per-capita basis. GDP projections were disaggregated into five major sectors including manufacturing which was further disaggregated for purposes of analyzing energy requirements. The sectoral shifts during the projection period included an increasing share of services in developed regions and an increasing share of the industry sector (replacing agriculture) in the developing regions.

Energy requirements were projected in detail for household and commercial use, for transportation, for economic sectors, and for feedstocks. These requirements were defined at the useful energy level wherever possible and were transformed into requirements for final energy. Total final energy projections increase 4-fold in the High scenario (from 5.8 to 22.8 TWyr/yr) and 2.5-fold in the Low scenario (from 5.8 to 14.6 TWyr/yr). (See Appendix C for energy units and conversion factors.)

Primary energy requirements were computed with a cost minimizing model designed to meet energy demand while accounting for constraints on total resources, build-up rates, maximum production levels and availability of imports. Global primary energy projections increase 4.3 times in the High scenario (from 8.2 to 35.7 TWyr/yr) and 2.7 times in the Low scenario (from 8.2 to 22.4 TWyr/yr). On a per-capita basis, global average primary energy increases from 2.1 to 4.5 kWyr/yr (High) and 2.8 kWyr/yr (Low).

1.1.1 IIASA Energy Models

These scenario projections were developed in detail for each region with the help of the IIASA set of energy models (Basile 1980). Population and economic projections were used as basic driving variables for determining energy consumption requirements in final and useful energy terms by means of the MEDEE model as depicted in Figure 2. This model, which accounts for all forms of energy end-uses, is primarily involved with physical relationships. Projections used in the model are made based on a general hypothesis of higher energy prices and conservation rather than on energy prices and price elasticities directly.

This detailed specification of energy demand is translated for use as the driving input for an optimizing supply model called MESSAGE (Schrattenholzer 1981). This model devises a minimum cost strategy for satisfying the energy demands taking account of resource availabilities and costs, technology costs, new technology build-up constraints, and availabilities of imported energy resources. The results are projections of primary energy requirements by region and shadow costs for each constraint. Several iterations are required to obtain a satisfactory solution in terms of both interregional balances of traded energy and intraregional consistency between energy demand by fuel type and energy supply. As shown in Figure 2, the results of the supply strategy are then analyzed in further detail to determine capital requirements and economic impacts.

Also shown in this figure is an economic interpretation block which takes data from the basic input assumptions, the MEDEE model, and the MESSAGE model, in order to determine energy prices and various elasticities. It is this block which is the focus of this report.

The purpose of performing this economic interpretation is two-fold. One purpose is to derive a better understanding of the implications of the scenario projections and, if necessary, to provide guidance for changing these projections. A second purpose is to interpret the scenario projections, that were made primarily without using energy prices and elasticities, in economic terms in order to facilitate comparisons with other studies and to allow others to interpret our projections in different ways.

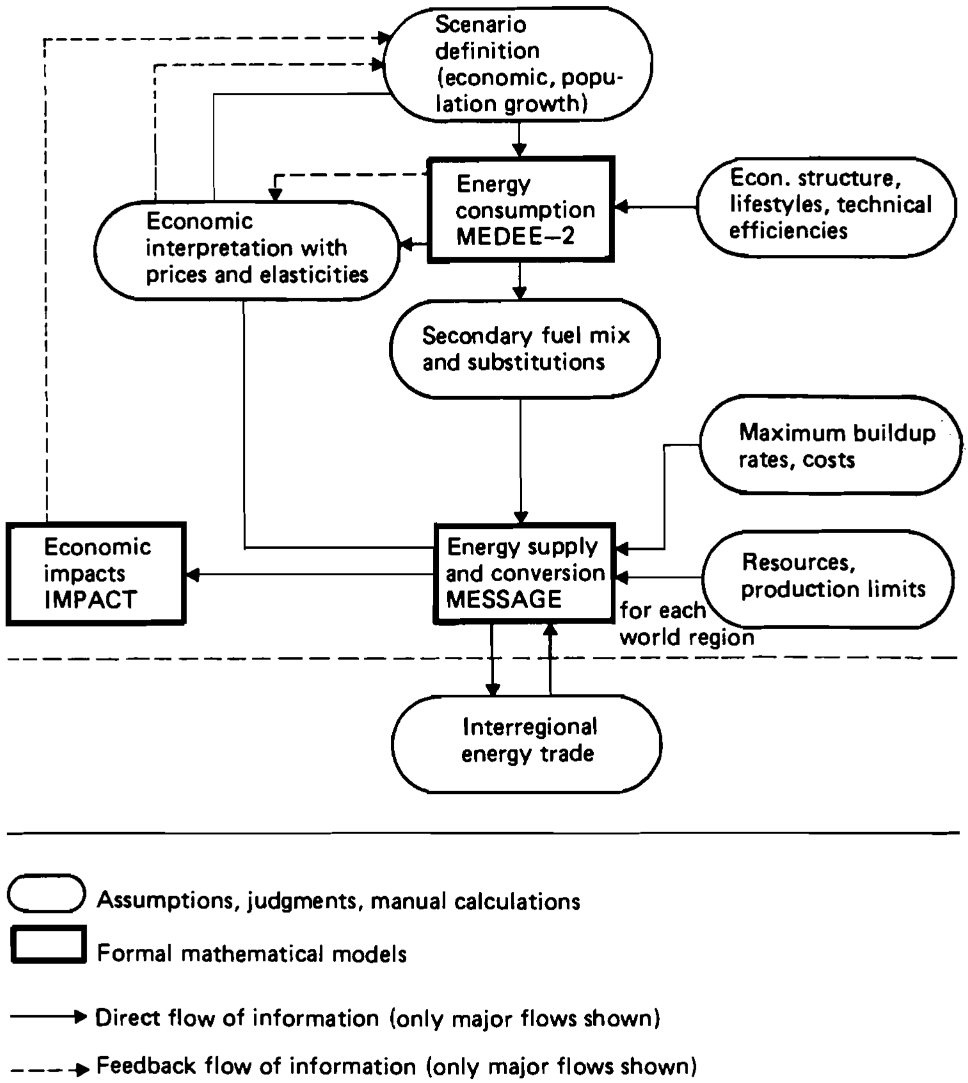

FIGURE 2 The IIASA set of models for energy program scenario development.

1.1.2 Aggregate Energy–Economy Linkage

A convenient way of specifying the linkage between energy requirements and economic growth is by means of the energy–GDP elasticity. An elasticity of unity implies that energy growth and economic growth go hand in hand: a 10 percent increase in GDP requires a 10 percent increase in energy. Lower values of elasticity imply that energy requirements increase proportionally less than GDP increases. For primary energy, historical values of this elasticity are close to unity for Region I and Region III but the scenario projections exhibit much lower values of about 0.7. This indicates that energy conservation is included in the projections. In the short term (to 2000) in Region I, much smaller values of about 0.4 indicate the potential for strong conservation, especially in the transportation sector. The developing regions, on the other hand, exhibit elasticities much greater than unity. These values do not imply increasing inefficiency, but are caused by a changing economic structure toward increasing energy use in agriculture and toward energy-intensive industry during the development process. These elasticities do drop from historical values of 1.2 to 1.5 down to near unity in the course of the projection period.

1.1.3 Energy Prices

The aggregate energy–GDP elasticity does not separate the effect of energy prices on energy use. It is clear that energy prices are increasing and prices do make a difference. Another simple model has been used to separate the effects of energy consumption increases due to GDP increases and energy conservation due to energy price increases. In this model, two elasticities are defined, one analogous to the aggregate energy–GDP elasticity mentioned above and another to measure the response to price increases. Energy price increases appropriate for use in this model are for final (delivered) energy, in real (constant) terms (excluding general inflation). It is argued that price increases relative to 1972 price levels are most appropriate even though the study base year is 1975. The reason is that the ultimate effects of real price increases between 1972 and 1975 (about 40 percent) had not taken place by 1975. As a guide for defining prices, projected increases in energy production and distribution costs are examined. Long-term price increases for final energy (averaged over all forms of energy including electricity) are then set at a factor of three for all regions except Region III. This region had relatively high prices in 1972 and so the long-term increase there was set at 2.4.

Using these projected price increases and the scenario projections for GDP and total final energy, combinations of energy–income elasticities (same as elasticities mentioned above *if* prices are constant) and energy–price elasticities were calculated consistent with the scenarios. These price elasticities ranged from − 0.2 to − 0.85 in the developed regions and from 0.0 to − 0.5 in the developing regions.

1.1.4 Payments for Energy

The combination of increasing energy use and increasing energy prices results in greatly increased payments for energy over the projection period. In the developed regions, energy conservation (energy–GDP elasticities less than unity) softens the impact of increasing energy prices such that payments for energy increase, relative to GDP, from 20 to 35 percent in High scenario and from 40 to 70 percent in Low scenario. The greatest impact, however, is in the developing regions where increasing energy intensiveness, coupled with price increases, result in 3- and 4-fold increases in payments as a share of the GDP. These increases are staggering and signal ever-increasing strains on world economic order.

1.1.5 Sectoral Energy Use

Energy requirements must be modeled on a detailed basis. The aggregate analyses summarized above are useful for understanding the overall scenario projections. More insight is gained by examining the various uses of energy and how these uses are related to economic activity and energy prices.

We distinguish between energy used as a factor of production in the economy and energy purchased by consumers. The former is an intermediate input to a production process that requires other inputs as well, most importantly capital and labor. Energy purchased by consumers for household use or for passenger transport, we call final demand energy. Final demand energy is used directly by the consumer while intermediate input energy is used indirectly.

A comparison of final demand and intermediate input energy use in the scenario projections indicates that the energy–income and energy–price elasticities are different for the two categories of energy use. For the developed regions, energy conservation is more pronounced for final demand energy than intermediate input energy (very strong in the High and less strong in the Low scenario). For the developing regions, the opposite is indicated, but less pronounced. The linkage of final demand energy to population and the great potential for conservation in developed regions would explain these results.

1.1.6 Substitution and Technological Development

A framework for analyzing the substitution between energy as a factor of production, and capital and labor as other factors of production is defined in the report. This framework is based on a constant elasticity of substitution production function incorporating an exponential (with time) technological development factor which allows for more production from the same inputs as time progresses. Making use of the economic concept of setting prices equal to marginal productivity, energy and other factor prices are defined. It is shown how, with the assumed technological development factor, factor prices must increase over time in real terms to keep up with their marginal productivity. Energy price increases greater than those accounted for by technological development cause a substitution of other factors of production (capital and labor) for energy. The reduction in energy growth due to technological development and substitution is most evident in one summary equation that expresses the energy–GDP elasticity ϵ in terms of the exponential growth rates of GDP g, of technological development δ, and of energy prices π, and the elasticity of substitution σ (which is shown in the report to be closely related to an energy–price elasticity):

$$\epsilon = 1 - \delta/g - \sigma(\pi - \delta)/g$$

As indicated in this equation, energy growth relative to GDP growth is less than unity due to technological development (the strength of the effect due to the ratio of technological development "growth" δ and GDP growth g) and due to substitution provided energy prices π increase faster than what is accounted for by technological development δ. In the examples calculated in the report consistent with the scenario projections, the relative contribution of these two terms in reducing ϵ is shown to be somewhat less than one half due to technological development.

In the application of the substitution model to the industry sector of six regions, technological development ranges from 0.2 to 0.6 percent per year. Region II indicates the largest values, Regions I and III next with the developing regions having the lowest values. Similarly, the elasticities of substitution (closely related numerically to energy price elasticities) range from 0.2 to 0.6 with the same regional variation. The model also indicates that the increase in other factors of production due to energy price increases and substitution would be relatively small: between 0.7 and 1.9 percent for all regions except Region II which would be about 2.5 percent.

These relatively small increases in use of nonenergy factors of production due to substitution result from price increases of only energy. Other resource-based inputs are expected to exhibit real price increases as well which will cause their own substitution effect.

2 TWO SCENARIOS: DEFINITION AND ENERGY–ECONOMY LINKAGE IN THE AGGREGATE

This section is divided into two parts. The first part summarizes the two IIASA Energy Program scenarios. The scenarios are defined by specifying the population projections for seven world regions for the period 1975–2030, by specifying two economic projections (a High economic growth and a Low economic growth), and by specifying the energy consumption accompanying these projections (a High and a Low). The energy projections, which are based on the population and economic projections as major inputs, are described in Energy Program Group (1981) from the demand, as well as the supply, points of view.

The second part examines the demand linkage between the economy and energy consumption for the aggregate regional economies. This aggregate analysis is performed in terms of energy–GDP ratios, energy–GDP elasticities, and income and price elasticities for all seven regions.

2.1 Scenario Definition

2.1.1 Population Projections

The population of the world is already in excess of four billion (10^9) with over 70 percent in developing regions. At current growth rates, the population would double in 35 years. No present day demographer, however, would project world population for the next 35 or 50 years with today's growth rate.

Examination of the world population over the past two centuries shows that growth rates have varied considerably. As shown in Table 1, the growth rate for the world as a whole has increased from 0.4 percent per year in 1750 to 1.9 percent per year in 1975. These world average growth rates, however, do not indicate the large changes that have taken place separately in the more developed and less developed countries. The more developed countries have experienced a rapid increase in growth rate up to the middle of the nineteenth century and a gradual leveling off. The less developed countries have had very low and decreasing growth rates in the previous century but have recently shown very high growth rates.

For projection purposes, the factors that influence birth rates and death rates must be well understood. By making assumptions about these factors, conditional projections can then be made. Under certain conditions, it is possible and desirable to link these factors to other scenario parameters and projections (e.g., economic development, energy use) and, therefore, to make population projections scenario dependent. This was not done.

TABLE 1 World population for two centuries.

	1750		1800		1850		1900		1950		1975
Population											
($\times 10^6$)	791		978		1,262		1,650		2,492		3,946
Distribution											
(percent)											
More developed countries	26		26		28		35		34		27
Less developed countries	74		74		72		65		66		73
Growth rates											
(percent/year)											
More developed countries		0.4		0.7		1.0		0.8		0.9	
Less developed countries		0.4		0.5		0.3		0.8		2.2	
World		0.4		0.5		0.5		0.8		1.9	

We preferred to work with a single, fixed projection of population that fell within the range of our own population projections as well as numerous other recent population projections. This is not to deny the existence or importance of economic and environmental factors on population. This approach was taken partly in order to reduce the complexity of analysis but mainly to focus our attention on the energy and energy–economic implications of the global energy system.

The population projections we have used are based on the assumptions of achieving a bare replacement level of fertility in developing regions by 2015 (Keyfitz 1977). These population projections for the seven geographical world regions are presented in Table 2 and are illustrated in Figure 3. The current population growth rate and the assumed future decline in growth rate are put into perspective with the historical data from Table 1.

A more detailed look at the projected growth of the world population shows a gradual decrease from its current peak of 2 percent per year to less than 1 percent per year by 2030. The growth rates of the less developed regions (IV, V, and VI), however, are more than three times the growth rates of the more developed regions (I, II, and III). As shown in Table 3, the projected growth rates for Region VII, are in between those of the Regions I, II, and III and Regions IV, V, and VI.

There is a striking change in the age structure as this projected stable population is approached. As a result of a lower birth rate and an increasing life expectancy, especially in developing regions, the fraction of population over age 65 increases substantially. Since this has an impact on average economic productivity and growth potential, it is an important factor in setting scenario values. To see this effect look at the ratio of population between the ages of 15 and 64 to the population age 65 and over. In simplistic terms, this ratio indicates the number of people who must produce not only for themselves and their children, but also for one additional adult who has retired from economic production. In 1975 in Region I, there were 6.4 persons between 15 and 64 years for each person 65 and over. By 2030, this ratio will be 4. Regions II and III exhibit a similar pattern by dropping from 6.7 and 5.7 respectively to about 4 by 2030. Regions IV, V, and VI will change more dramatically by dropping from a range of 15–18 down to 8–9 by 2030 while Region VII drops from 11 to 5.5.

TABLE 2 Scenario definition part 1: Population projection by region[a].

	Population ($\times 10^6$)				
	Base year (actual[b]) 1975	1985	Projection[c] 2000	2015	2030
Region I North America	237	257	284	302	315
Region II The Soviet Union and E.Europe	363	393	436	467	480
Region III W. Europe, Japan, Australia, New Zealand, S. Africa, and Israel	560	611	680	727	767
Region IV Latin America	319	424	575	693	797
Region V Africa (except Northern Africa and S. Africa), South and Southeast Asia	1,422	1,860	2,528	3,080	3,550
Region VI Middle East and Northern Africa	133	176	247	302	353
Region VII China and Centrally Planned Asian Economies	912	1,097	1,330	1,550	1,714
World	3,946	4,818	6,080	7,121	7,976

[a]See Appendix B for a complete listing of countries in each region.
[b]Mid-year estimates from UN 1978.
[c]Same population projection for both High and Low scenarios.

2.1.2 Economic Projections

Global economic production exceeded 6×10^{12} US dollars in 1975 (base year for projections). Many caveats and explanatory notes must be added to this statement before it can be properly interpreted. It is, however, the measure of the "size" of the global economic system that we have chosen to use.

The explanatory notes include the following: we use 1975 US dollars, 1975 official exchange rates and prices (except for centrally planned economies*), and we measure GDP by country, then aggregate to our seven regions and finally the globe. The caveats

*For the centrally planned economies we used the estimates of GDP given by World Bank (1977). These estimates are based on a comparison of physical indicators of economic product among centrally planned and market economies for 1965 (this comparison was done by the UN Economic Commission for Europe). Then data for real growth for both centrally planned and market economies were used to estimate the GDP of the centrally planned economies for 1975.

include the obvious ones involved whenever GDP estimates of different countries are compared or aggregated into regions. Economic structures are very different from country to country (especially from developing to developed economies) and so GDP estimates are not really comparable; and also official monetary exchange rates do not necessarily reflect "real" equivalences.

Given these caveats, the estimates of GDP for 1975 for our seven regions are given in Table 4. The historical growth rates of GDP are also given for the period 1950–1975 for GDP as measured in constant prices of 1975. The same data are given in per-capita terms in Table 5.

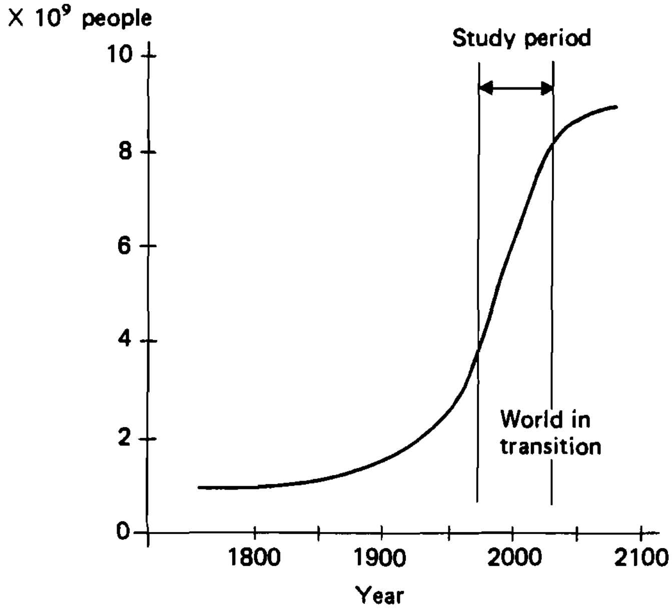

FIGURE 3 World population: historical and projected.

TABLE 3 Population growth rates.

	Average annual growth rate (percent/year) 1950–1975	1975–1985	1985–2000	2000–2015	2015–2030
Developed regions (I + II + III)	1.2	0.8	0.7	0.4	0.3
Developing regions (IV + V + VI)	2.4	2.8	2.1	1.3	1.0
Region VII (C/CPA)	1.7	1.9	1.3	1.0	0.7
World	1.9	2.0	1.6	1.1	0.8

TABLE 4 Estimates of GDP for 1975 and historical growth rates[a].

Region	Growth rate (percent/year) 1950–1960	1960–1975	1950–1975	GDP $\$10^9$ 1975
I (NA)	3.3	3.4	3.4	1,670
II (SU/EE)	10.4	6.5	8.0	930
III (WE/JANZ)	5.0	5.2	5.1	2,385
IV (LA)	5.0	6.1	5.7	340
V (Af/SEA)	3.9	5.5	4.9	340
VI (ME/NAf)	7.0	9.8	8.6	190
VII (C/CPA)	8.0	6.1	6.9	320
World	5.0	5.0	5.0	6,175

[a]GDP in 1975 dollars and prices using official exchange rates for market economies. See Table A.2 in Appendix A.

TABLE 5 Estimates of per capita GDP for 1975 and historical per capita growth rates.

Region	Per capita growth rate (percent/year) 1950–1960	1960–1975	1950–1975	Per capita GDP $ 1975
I (NA)	1.5	2.2	1.9	7,050
II (SU/EE)	8.8	5.4	6.7	2,560
III (WE/JANZ)	3.9	4.1	4.0	4,260
IV (LA)	2.1	3.4	2.9	1,070
V (Af/SEA)	1.8	2.9	2.5	240
VI (ME/NAf)	4.3	6.6	5.7	1,430
VII (C/CPA)	6.3	4.3	5.1	350
World	3.1	3.1	3.1	1,565

We chose to make two projections of economic growth to the year 2030. GDP is the single most important determinant of energy use and its future values are somewhat uncertain. Having a range of values in our projections, therefore, allowed us to examine the linkage of many variables to GDP. We examined in detail a High and a Low economic projection. Neither the High nor the Low was intended to represent a prediction, forecast, or even best guess. But an attempt was made to span a sufficiently wide range of values so that expected values would be included.

For making these projections, we relied on the projections and results of other similar recent studies including those of WAES (1977) and WEC (1978). Our projections differ from these in that we lowered economic growth, and consequently energy demand, so that energy supply and demand would balance given a "reasonable" energy supply situation. A central guidance for extending our projections to the year 2030 and for developing the two scenarios in greater detail was the constant checking for internal consistency and consistency among world regions. Even though the application of these guidelines is judgmental, we found that the procedure was very useful for eliminating potential scenario values that on the surface might appear reasonable. Achievement of consistency within a scenario at any level of detail is clearly only a necessary condition for reasonableness and not a sufficient condition.

As part of the exercise of setting economic projections, therefore, there were several iterations of making assumptions, analyzing implications, checking for consistency and making refinements of assumptions. The projections presented here are the result of this process and we will not dwell on the intermediary values.

Our two projections for the growth rate of regional gross domestic product are given in Table 6. The general trend in these projections which is exhibited in all regions is the

TABLE 6 Scenario definition part 2: Growth rates of GDP by region High and Low scenarios (percent/year).

Region	1975–1985	1985–2000	2000–2015	2015–2030
	High scenario			
I (NA)	4.3	3.3	2.4	2.0
II (SU/EE)	5.0	4.0	3.5	3.5
III (WE/JANZ)	4.3	3.4	2.5	2.0
IV (LA)	6.2	4.9	3.7	3.3
V (Af/SEA)	5.8	4.8	3.8	3.4
VI (ME/NAf)	7.2	5.9	4.2	3.8
VII (C/CPA)	5.0	4.0	3.5	3.0
World	4.7	3.8	3.0	2.7
	Low scenario			
I (NA)	3.1	2.0	1.1	1.0
II (SU/EE)	4.5	3.5	2.5	2.0
III (WE/JANZ)	3.1	2.1	1.5	1.2
IV (LA)	4.7	3.6	3.0	3.0
V (Af/SEA)	4.8	3.6	2.8	2.4
VI (ME/NAf)	5.6	4.6	2.7	2.1
VII (C/CPA)	3.3	3.0	2.5	2.0
World	3.6	2.7	1.9	1.7

ever-decreasing growth rates in later and later periods. We believe that many factors will contribute to this trend but the two most important factors are decreases in population growth rates and the increasing scarcity of basic resources. Decreases in population growth rates in our projections have already been indicated in 2.1.1. As shown by the growth rates of GDP per capita in Table 7, however, the general trend of decreasing growth rates is still evident in these projections. This decline in per-capita growth rates is attributed mainly to the depletion of resources and the concomitant increase in real cost of these resources. In our studies this factor is most evident with respect to energy resources, but other basic resources are expected to follow a similar pattern.

We have not examined the interregional trade implications of these regional economic projections. We have made the assumption, however, that because of the dependency of

TABLE 7 Per capita GDP growth rates for two scenarios to 2030 (percent/year).

Region	High scenario 1975–2000	2000–2030	Low scenario 1975–2000	2000–2030
I (NA)	2.9	1.9	1.7	0.7
II (SU/EE)	3.6	3.2	3.1	1.9
III (WE/JANZ)	3.0	1.8	1.7	0.9
IV (LA)	3.0	2.4	1.6	1.9
V (Af/SEA)	2.8	2.4	1.7	1.4
VI (ME/NAf)	3.8	2.8	2.4	1.2
VII (C/CPA)	2.8	2.4	1.6	1.4
World	2.4	1.9	1.3	0.9

the developing regions on trade with the developed regions as a major stimulant for growth, the developing economies will be limited in their growth potential to one or two percentage points greater than the growth rates of the developed economies. This assumption has been used in some World Bank studies, in particular in a contribution to the WAES study. (See also Hicks et al. 1976.) This interregional linkage of economic growth rates is not universal and may prove unfounded for our projection period, but we have made the projections based on this assumption. Some countries, notably those of the Middle East in Region VI, are assumed not to be limited by this linkage but rather by their capability to absorb the favorable trade balances due to large oil exports.

Although these aggregate projections of population and GDP by region are the principal determinants of our energy projections, both of these projections must be divided into more detailed components for making the energy projections. For GDP in particular, the five sectors agriculture, mining, manufacturing, construction, and services are projected separately and manufacturing is further disaggregated into four subsectors depending upon energy intensity (Energy Program Group 1981, Lapillonne 1978). As an example of the differences in GDP formation in various regions for 1975 and as projected for our study period, Table 8 gives the shares of agriculture, industry (which comprises mining, manufacturing, construction, and energy) and service sectors for all regions except Region VII for which this detailed approach was not used. These sector shares, also illustrated in Figure 4, show that developing region economies are much more agriculture based than developed regions but that this share is projected to decrease markedly by 2030. The industry sector shows a greater share of GDP in the developed regions but is decreasing in time whereas the developing regions begin from a relatively low share in industry and increase in time as economic development progresses.

2.1.3 Energy Projections

Detailed energy projections were made for all regions except Region VII where the general lack of data necessitated our using a more aggregated projection approach. These

TABLE 8 Shares of agriculture, industry, and services for six regions (percent GDP).

Region	1975	High scenario 2000	2030	Low scenario 2000	2030
Agriculture					
I (NA)	3	2	1	2	2
II (SU/EE)	11	7	4	9	7
III (WE/JANZ)	6	5	3	4	3
IV (LA)	12	8	5	10	7
V (Af/SEA)	36	26	16	30	23
VI (ME/NAf)	7	4	2	5	4
Industry					
I (NA)	32	30	29	32	32
II (SU/EE)	50	46	41	46	43
III (WE/JANZ)	46	43	39	44	42
IV (LA)	36	42	47	40	43
V (Af/SEA)	26	32	38	30	35
VI (ME/NAf)	66	57	47	54	54
Service					
I (NA)	65	68	70	66	66
II (SU/EE)	39	47	55	45	50
III (WE/JANZ)	48	52	58	52	55
IV (LA)	52	50	48	50	50
V (Af/SEA)	38	42	46	40	42
VI (ME/NAf)	27	39	51	41	42

projections were made using the population and GDP projections as basic inputs, and are reported in detail separately (Energy Program Group 1981, Khan and Hölzl 1981, Chant 1981). Many further assumptions were made to provide more detail for these scenarios and the resulting projections are for final (or delivered) energy for each of the GDP sectors as well as transportation, households, and nonenergy feedstocks. These projections are given in some detail in Appendix A (Tables A.11 and A.12). Table 9 shows the growth rates in per-capita final energy for the historical period 1950–1975 and for the projection period to 2030. As is clear in this table, the projections call for much greater increases in use of energy in the developing regions than in the developed regions even on a per-capita basis.

These projections for final energy requirements were given by fuel type as input to an optimizing energy supply model (Energy Program Group 1981). This model determined the minimum cost energy supply strategy for each region taking account of energy resource costs and production constraints, new technology maximum buildup rates and energy import availabilities. The results which we use here are the requirements for primary energy for each region. These are given in some detail in Appendix A (Tables A. 7 and A. 9) and are summarized in Table 10. The trends in per-capita primary energy use for the High scenario are shown in Figure 5 for the historical period 1950–1975 as well as for the projection period.

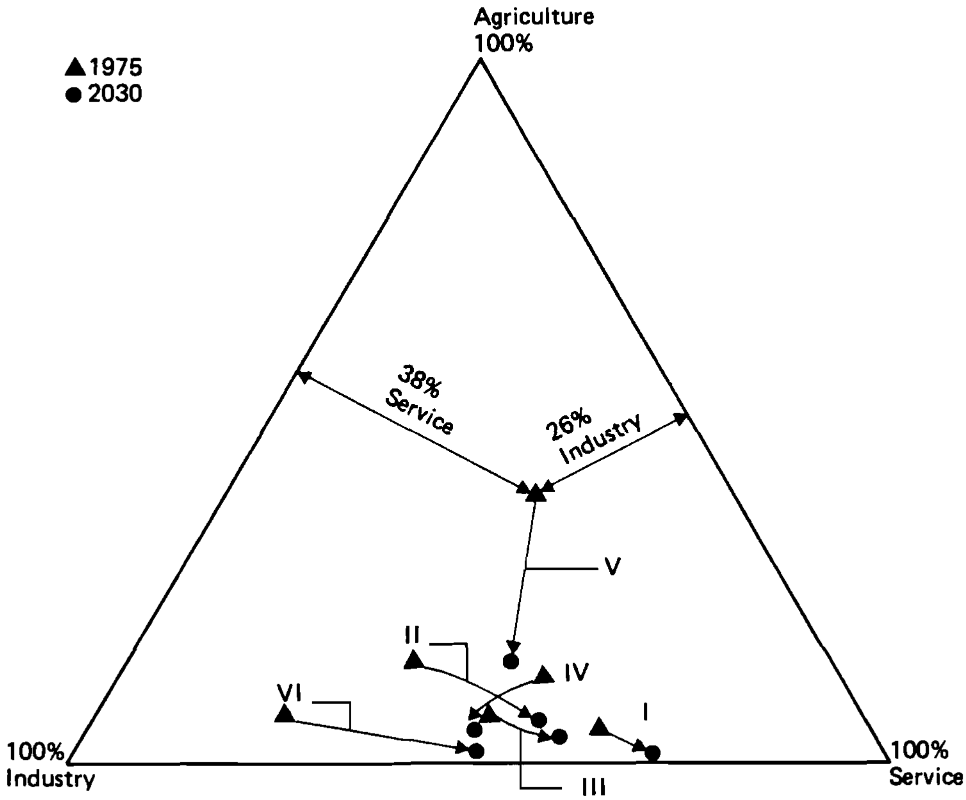

FIGURE 4 Sectoral evolution of GDP by region, High scenario.

TABLE 9 Final energy[a] per capita 1975 and growth rates: historical and two scenarios to 2030.

Region	Growth rate (percent/year) 1950–1975	Final energy per capita (kW/cap) 1975	Growth rate of FE per capita (percent/year) High scenario 1975–2000	High scenario 2000–2030	Low scenario 1975–2000	Low scenario 2000–2030
I (NA)	1.3	7.89	0.6	0.8	0.03	0.2
II (SU/EE)	3.9	3.52	1.8	1.5	1.4	0.7
III (WE/JANZ)	3.3	2.84	1.8	0.8	0.8	0.3
IV (LA)	4.0	0.80	3.2	2.2	1.9	1.6
V (Af/SEA)	4.3	0.18	3.5	2.6	2.3	1.7
VI (ME/NAf)	7.4	0.80	4.4	2.3	3.2	1.1
VII (C/CPA)	9.0	0.43	3.1	2.3	1.6	1.3
World	2.4	1.46	1.2	1.2	0.3	0.5

[a]Total final energy including nonenergy feedstocks but excluding noncommercial sources of energy (wood, animal waste, etc.).

TABLE 10 Summary of scenario energy projections: primary energy[a].

Primary energy for 1950, 1975, and projections to 2030 for the High and Low scenarios, by region (TW).

Region	Historical 1950	1975	High scenario 2000	2030	Low scenario 2000	2030
I (NA)	1.14	2.65	3.89	6.02	3.31	4.37
II (SU/EE)	0.42	1.84	3.69	7.33	3.31	5.00
III (WE/JANZ)	0.67	2.26	4.29	7.14	3.39	4.54
IV (LA)	0.06	0.34	1.34	3.68	0.97	2.31
V (Af/SEA)	0.06	0.33	1.43	4.65	1.07	2.66
VI (ME/NAf)	0.01	0.13	0.77	2.38	0.56	1.23
VII (C/CPA)	0.03	0.46	1.44	4.46	0.98	2.29
World	2.39	8.21[b]	16.8	35.7	13.6	22.4

Primary energy growth rates for 1950–1975 and projections to 2030 for the High and Low scenarios, by region (percent/year).

Region	Historical 1950–1975	High scenario 1975–2000	2000–2030	Low scenario 1975–2000	2000–2030
I (NA)	3.4	1.5	1.5	0.9	0.9
II (SU/EE)	6.1	2.8	2.3	2.4	1.4
III (WE/JANZ)	5.0	2.6	1.7	1.6	1.0
IV (LA)	7.1	5.7	3.4	4.3	2.9
V (Af/SEA)	7.1	6.1	4.0	4.8	3.1
VI (ME/NAf)	10.7	7.5	3.9	6.2	2.6
VII (C/CPA)	11.1	4.7	3.8	3.1	2.9
World	5.1	2.9	2.5	2.0	1.7

[a]Including nonenergy feedstocks but excluding noncommercial energy.
[b]Including 0.21 TW for bunkers.

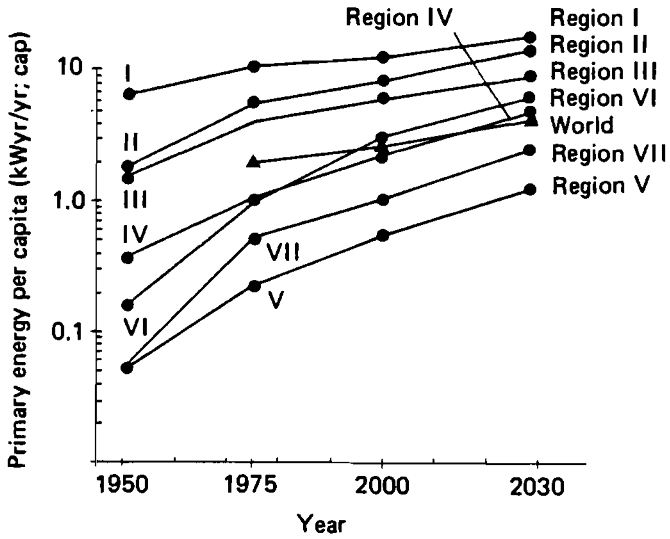

FIGURE 5 Primary energy per capita by region, 1950–2030, High scenario.

2.2 Energy–Economy Linkage in the Aggregate

The objective of the analysis that is reported here is not to develop scenarios but to interpret the linkage between the economic variables and the associated energy usage projections *in an economic sense*. In so doing, we gain insight into the nature of this linkage that was postulated in noneconomic terms and we can interpret projected relative changes in terms of elasticities involving GDP, energy prices, and substitution of nonenergy inputs for energy. We begin this analysis by examining the energy–economy linkage at the most aggregated level.

2.2.1 Energy–GDP Ratios and Elasticities

One simple way to examine the linkage between energy and GDP is to calculate the ratio of energy consumption to GDP. Using the data from Appendix A for primary energy and GDP, both historical and projected, we can plot primary energy per unit GDP versus GDP per capita as shown in Figure 6. The abscissa (GDP per capita) in this plot is an aggregate measure of economic development, thus the graph indicates the changing energy intensity of economies as they develop. The developing regions exhibit a trend of increasing energy usage per unit of GDP as their economies have developed between 1950 and 1975 and this trend continues in our projections, although less severely. The developed regions, in general, surpassed the point where energy intensity is increasing and are on a downward

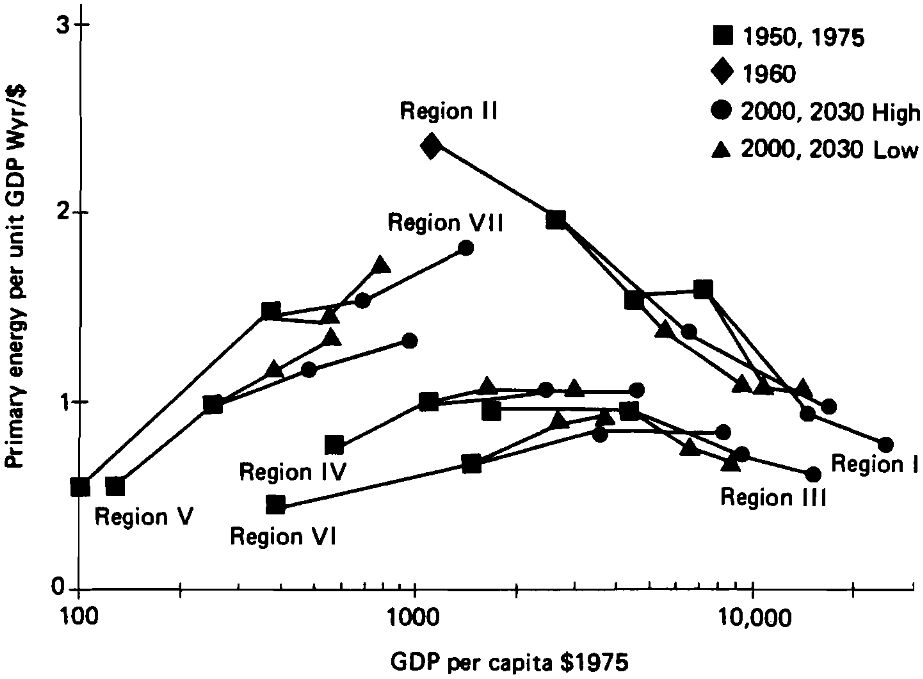

FIGURE 6 Primary energy per unit GDP versus GDP per capita. Historical (1950–1975) and scenario projections to 2030.

trend in the projections. The points plotted for 2030 in all regions except Regions IV and VI indicate more primary energy consumption than the trend would indicate (especially for Regions I and VII) because in these regions the supply strategy includes large amounts of coal liquefaction. This technology for satisfying the requirements for liquid fuel involves 40 percent losses in conversion from coal to liquid fuel and consequently requires higher levels of primary energy.

Another simple way to examine the linkage between energy and GDP is to relate primary energy per capita to GDP per capita. As an example of this relationship over a long historical period, Figure 7 presents a graph of primary energy per capita versus GDP per capita (in constant dollars) for the USA, for the period 1910–1978. Even though the annual variations as shown in this figure are both increases and decreases, the long-term trend is unmistakable. And, of course, in our scenario projections to the year 2030 it is the long-term trends that interest us rather than the annual fluctuations.

If we change the scale of the graph of Figure 7, replace the detailed curve between 1910 and 1978 by a straight line, and correct for the addition of Canada we obtain the historical period part of Figure 8. This second figure now has the primary energy and GDP projections to the year 2030 added for both the High and Low scenarios for Region I. The change in slope between the historical period and the scenario projections is immediately apparent. It is the purpose of this analysis to examine the nature of this change in detail for all regions. What may be pointed out immediately is that, especially for Region I, our scenario projections include large effects of energy conservation and efficiency improvements over and above what has occurred in the past.

There are two points shown on Figure 8 which require further comment. The actual scenario projections and energy supply strategies for Region I, lead to large increases in

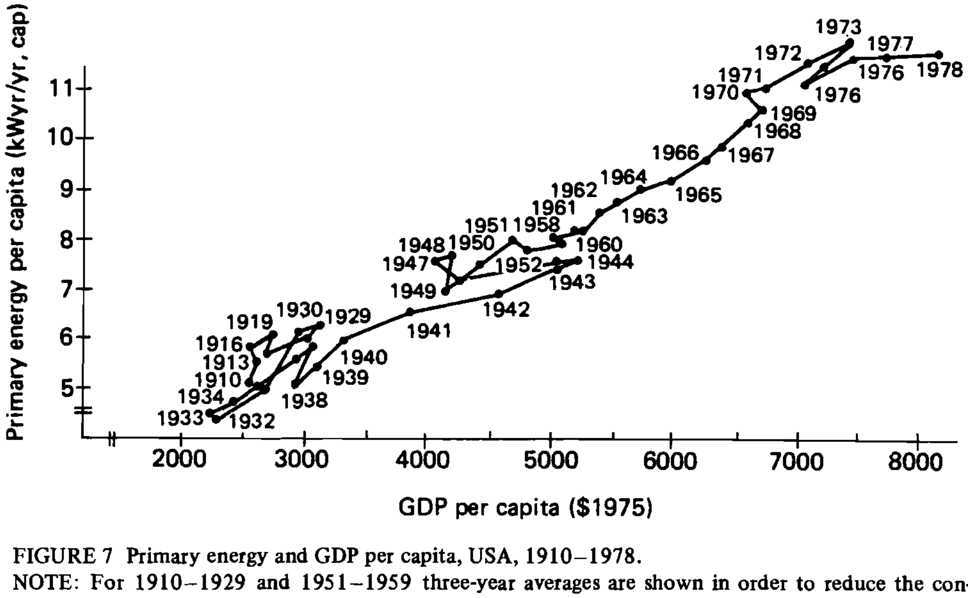

FIGURE 7 Primary energy and GDP per capita, USA, 1910–1978.

NOTE: For 1910–1929 and 1951–1959 three-year averages are shown in order to reduce the confusion of point clusters.

SOURCE: Based on data from Alterman (1977) and Bureau of the Census (1978).

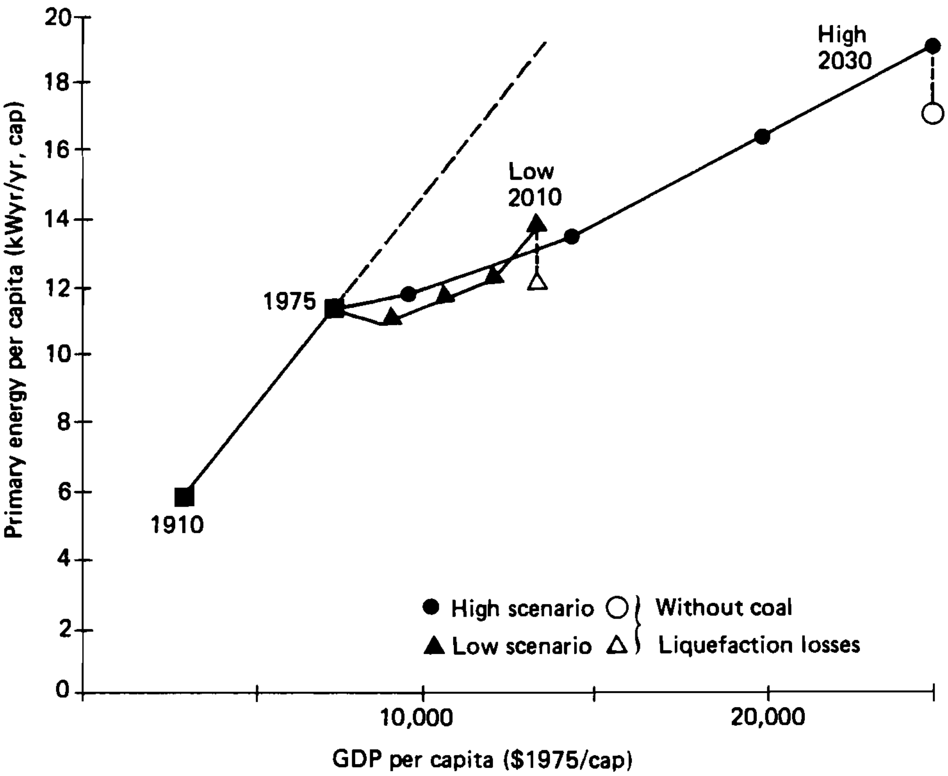

FIGURE 8 Primary energy and GDP per capita, Region I, 1910–2030.

primary energy consumption between 2015–2030. As mentioned earlier, this is due in large part to the necessity of using coal liquefaction with large losses as a supply technology for liquid fuel demand. If these losses are subtracted from the 2030 primary energy consumption in Region I, the corresponding energy consumption drops significantly. This brings the 2030 Low scenario point onto the projected long-term trend line and drops the 2030 High scenario point below this line.

This trend of conservation and increasing efficiency of energy use is projected for all regions but to different and lesser extents than for Region I. Figure 9, using a logarithmic scale, shows these trends for all regions. The historical period is limited to 1950–1975 but the long-term trend evident in the projections is clear.

Perhaps the simplest way to quantify this changing long-term trend between energy use and GDP is to calculate the energy–GDP elasticity. This elasticity ϵ is defined by the following equation:

$$\frac{E(t_2)}{E(t_1)} = \left[\frac{\mathrm{GDP}(t_2)}{\mathrm{GDP}(t_1)}\right]^{\epsilon} \tag{1}$$

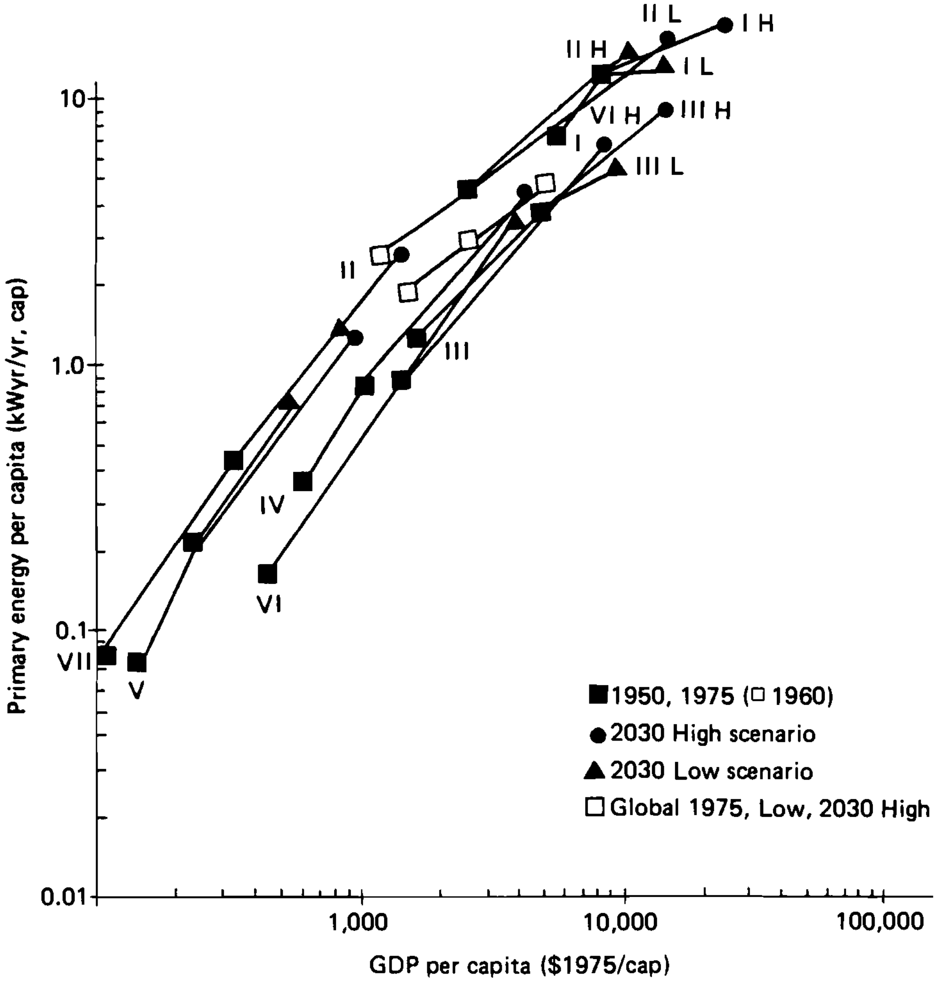

FIGURE 9 Primary energy and GDP per capita, IIASA regions, 1950–2030.

where t_1 and t_2 are two points in time, E represents energy consumption (which can be either primary or final in our applications) and GDP is in real terms. With this definition, the elasticity ϵ is the average (constant) value for the time period from t_1 to t_2. For small changes in energy use and GDP over a short period, say one year, this parameter can be interpreted simply as the ratio of the percentage change in energy to the percentage change in GDP.

Analyses of historical data indicate that values of ϵ less than unity are common for developed economies where increases in GDP are associated with somewhat smaller (in percentage terms) increases in energy consumption. This result can be interpreted as increases in the efficiency of the use of energy or in changes in the nature of GDP such that less energy-intensive sectors gain a larger share of total GDP. For developing economies, the values of this elasticity are typically greater than unity such that GDP increases are associated with greater than commensurate increases in energy consumption. Usually this result does not imply a decrease of efficiency but a rapidly changing economy that is increasing the share of industry and mechanization of agriculture at the expense of more traditional techniques.

Primary energy–GDP elasticities ϵ_p are given for all seven regions in Table 11 for the historical period 1950–1975 and for the projection period 1975–2030 for both scenarios. For the historical period, these parameters were determined by fitting a straight line to the logarithmic transformation of eqn. (1), using the 5-yearly data given in Appendix A. For the projection period, since no data smoothing was necessary, only the period end points are required to calculate the elasticities.

TABLE 11 Primary energy–GDP elasticities ϵ_p 1950–2030.

Region	Historical[a] 1950–1975	High scenario 1975–2000	High scenario 2000–2030	Low scenario 1975–2000	Low scenario 2000–2030
I (NA)	1.03	0.42	0.67	0.36	0.89[b]
II (SU/EE)	0.77	0.65	0.67	0.62	0.62
III (WE/JANZ)	0.96	0.70	0.77	0.65	0.73
IV (LA)	1.28	1.04	0.98	1.06	0.97
V (Af/SEA)	1.52	1.15	1.11	1.18	1.19
VI (ME/NAf)	1.20	1.16	0.96	1.23	1.10
VII (C/CPA)	1.57	1.06	1.17	0.98	1.27[b]
World	0.99	0.70	0.90	0.67	0.93

[a] Historical values were computed by linear regression on logarithmic transformation of eqn. (1) using 5-yearly data. Values for the projection period result from the scenario data.

[b] The primary energy–GDP elasticity is unusually high for Regions I and VII in the Low scenario because of coal liquefaction losses (see page 20). If these losses are subtracted from primary energy consumption in 2030, the resulting elasticities are 0.53 and 0.94 for Regions I and VII respectively. The same effect is present in the High scenario for Regions I, II, III and VII but is less pronounced in the elasticity because GDP growth is higher.

The elasticities for the historical period follow the well-observed trend of being lesss than unity for developed economies and greater than unity for developing economies. Regions V and VII exhibit the largest value of ϵ_p for the historical period but these average values mask an apparent trend from even higher values at the beginning to lower values near the end of this period.

For the projection period, the developing regions continue the trend of decreasing elasticities as the economies become more developed and approach the unity value. Region VII is a notable exception to this trend, but as we have pointed out before this is again evidence of the coal liquefaction losses in that region. Indeed, the elasticity for Region I, Low scenario 2000–2030 reflects this same effect most visibly because the GDP growth projection is very small for that time period so that any increase in primary energy consumption yields an unusually high value for the primary energy–GDP elasticity.

These energy–GDP elasticities can be calculated with respect to final energy eliminating the unusual effects near 2030 due to large amounts of coal liquefaction. Table 12

TABLE 12 Final Energy–GDP Elasticities ϵ_f 1950–2030.

Region	Historical[a] 1950–1975	High scenario 1975–1985	1985–2000	2000–2015	2015–2030	Low scenario 1975–1985	1985–2000	2000–2015	2015–2030
I (NA)	0.84	0.31	0.43	0.53	0.48	0.24	0.38	0.53	0.46
II (SU/EE)	0.68	0.59	0.58	0.52	0.53	0.54	0.57	0.50	0.41
III (WE/JANZ)	0.84	0.77	0.65	0.58	0.51	0.67	0.64	0.60	0.49
IV (LA)	1.21	1.07	1.01	0.97	0.90	1.10	1.03	0.95	0.88
V (Af/SEA)	1.42	1.20	1.08	1.05	1.01	1.19	1.12	1.14	1.06
VI (ME/NAf)	1.17	1.12	1.07	0.95	0.81	1.21	1.11	1.01	0.93
VII (C/CPA)	1.53	1.10	1.02	1.02	0.96	1.02	0.98	0.99	0.90
World	0.87	0.69	0.73	0.78	0.77	0.64	0.73	0.79	0.74

[a]See footnote *a*, Table 11.

gives these elasticities for the historical period 1950–1975 and for four periods during the projection period 1975–2030. The trend of decreasing elasticities as economies develop (both developed and developing economies) is now quite clear. The only exception is Region I which has very low values for the initial years of the projection period. This results from our assumptions that Region I has a great conservation potential that it can and will take advantage of as rapidly as possible. A large part of this conservation before 2000 is due to fuel efficiency improvements in automobiles which have been mandated in the USA and Canada.

It should be noted that as the primary energy–GDP elasticities are biased upward because of coal liquefaction losses, the final energy–GDP elasticities can be considered to be biased downward because of the increasing share of electricity in our projections. This share doubles in most regions between 1975 and 2030, increasing from 12.5 percent to 24–25 percent in Regions I and III, from 9 percent to 20–21 percent in Region II, and from 6 percent to 12 percent in developing regions. (See Table A.13 of Appendix A.)

2.2.2 Income and Price Elasticities

The analyses reported here are at a very aggregate level. It is recognized that there are many factors which determine the relationship between energy consumption and economic growth. One of the factors that tends to make energy growth smaller than economic growth is technological development. Another factor is the changing nature of economic activity that, for developed economies, is usually away from energy-intensive industry toward services; and for developing economies, is away from low energy-consuming agriculture toward energy-intensive industry. These two factors can, in the aggregate, explain the energy–GDP relationships noted in 2.2.1.

Energy consumption is also affected by price. It is instructive to separate these two effects for the projection period when we expect price increases to play an important role in determining energy consumption. The two factors mentioned above (technological development and changing texture of GDP) and others that depend upon GDP we call the *income effect*.* Factors that are related to price we call the *price effect*.* The separation of energy demand into these two effects is very useful but, of course, in application can be somewhat arbitrary. For example, the mandated motor vehicle efficiency improvement in Region I is not exactly an income or price effect but is an important factor affecting projected energy consumption for this region.

The income effect relates changes in energy consumption to changes in GDP when there is no price change and is measured by the energy–income elasticity γ. The price effect relates changes in energy consumption to changes in energy price when there is no change in GDP and is measured by the energy–price elasticity β. These relationships are formalized by the equation:

$$\frac{E(t_2)}{E(t_1)} = \left[\frac{\mathrm{GDP}(t_2)}{\mathrm{GDP}(t_1)}\right]^{\gamma} \left[\frac{P(t_2)}{P(t_1)}\right]^{\beta} \tag{2}$$

*These definitions should not be confused with those in traditional economics where a price effect is divided into a substitution effect and an income effect.

where, in addition to the variables of eqn. (1), $P(t)$ is the appropriate price of energy (in real terms) that applies at time t. (Prices are discussed in detail below.) For periods when there are no changes in the price of energy then the energy–income elasticity γ is exactly the same as the energy–GDP elasticity ϵ. As with the elasticity ϵ, the elasticities γ and β may be defined for either primary energy or final energy.

In the application of eqn. (2), we examine the scenario data for GDP and final energy for the entire projection period 1975–2030, thus defining t_1 as 1975 and t_2 as 2030. Since the data for energy and GDP are given, then once the appropriate price increase is specified, eqn. (2) defines a linear relationship between γ and β as follows:

$$\beta = \frac{\log E_r}{\log P_r} - \gamma \frac{\log \mathrm{GDP}_r}{\log P_r} \tag{3}$$

where the subscript r denotes the value of the variable relative to the base year value. The GDP and final energy data are given in Appendix A, Tables A.3 and A.11 for each region and the relative price increase assumptions are discussed below.

Energy Prices

It should be immediately clear that the energy price that is appropriate for eqn. (2) is *not* the international price of crude oil even though this is the price often quoted when energy price increases are referred to. If energy price is to help explain the consumption of energy then the price must be the price to the *user* and must be quoted in real terms or in relation to other prices. Thus we specify the energy price for final (delivered) energy, averaged over all forms of final energy, and we specify real price increases relative to a base year value.

Before specifying the relative price increases that will be used for interpreting the scenario projections, it is useful to look at recent energy prices. Gathering, reconciling, and aggregating price data for (delivered) final energy products is a tremendous task even for one country. There is a multiplicity of energy products at the user level, and even the same product is sold at vastly different prices to different users.

What can be done is to select important representative energy commodities and gather price data on these according to aggregate user categories. At a minimum, petroleum products used for transportation should be separated because of the large taxes that are usually levied on these products. Also the user categories of the industry sector and of the residential and commercial sector should be separated because the typically large energy users in industry pay a lower unit price for energy. Prices for different years must be adjusted for inflation. Data for different fuel types within these user categories can be aggregated on a calorific quantity basis, but one must recognize that this procedure is not ideal because of different end use efficiencies, environmental effects, ease of use, and the like. The user categories can also be aggregated on the calorific quantity basis with the same caveat. Finally, data for countries within a geographic region can be aggregated on the same basis after choosing an appropriate measure of the equivalences of different national currencies.

This procedure was followed by Hogan (1980) to produce the data of Table 13. For Region I in 1972, for example, the delivered energy prices varied significantly for the three

TABLE 13 Real prices for final (delivered) energy (1975 $ per kWyr).

	Industry sector	Transport sector	Residential-commercial sector	All sector aggregate
Region I (NA)				
1972	30	116	83	70
1975	52	144	108	97
1975–1972	1.73	1.24	1.30	1.35
Region III (WE/JANZ)				
1972	62	254	135	113
1975	92	338	174	159
1975–1972	1.48	1.33	1.29	1.41

NOTE: $100 per kWyr is equivalent to $19.40 per barrel of oil equivalent, $3.34 per million Btu, and $0.011 per kWhr. These prices are calculated from data contained in Hogan 1980. Data on current prices were adjusted for inflation using a GNP deflator; currency conversions were based on a purchasing power parity conversion rate. The data reported here for Region III are for the aggregation of data for the four largest energy-using countries only: France, FRG, the UK, and Japan.

user categories, with the transport sector prices ($116/kWyr)* being almost four times the industry sector prices ($30/kWyr). For the all sector aggregate price, Region III prices were approximately 60 percent higher than Region I. Also, on average, 1975 delivered energy prices were only about 40 percent greater (in real terms) than 1972 prices in either region. Clearly, the international price of crude petroleum increased by a much greater factor during this same 3-year period, even in real terms, but crude petroleum prices are not the only prices of interest in analyzing the user demand for energy.

Hogan aggregated fuel types within sectors and across sectors using a Cobb-Douglas function formulation to estimate another average energy price. His procedure assumed that interfuel substitutions would occur to take advantage of different relative fuel price increases. His average price index indicated that 1975 prices would be only 22 percent higher than 1972 prices for the USA and Canada and that price increases in other countries would be as follows: France, 11 percent; the FRG, 15 percent; the UK, 33 percent; and Japan, 31 percent.

The conclusion is that real prices to the user for delivered energy had not increased by more than 40 percent between 1972 and 1975, on average, and possibly less depending on aggregation methods.

Energy Price Projections

Energy price projections are required for interpreting the scenario projections in terms of income and price elasticities. The price projection required is for final energy delivered to the user and for real price increases relative to 1972 and not relative to the base year 1975, for reasons explained below.

There is a variable lag between the time a price change is made and the effect in the economy is noticed. In some situations the time lag can be zero when the activity requiring

*Prices are quoted in constant (1975) US dollars.

the energy can be immediately changed or foregone, as for example, pleasure travel. In most situations, however, the time lag is very long, up to two or three decades before industrial processes can be redesigned and new equipment can be economically replaced. Even though the price increases of 1973 and 1974 have had a noticeable effect in some categories of energy consumption by 1975, we assume that a negligible part of the ultimate reaction to these price increases had yet occurred by 1975. Thus, since energy consumption will still be reacting to these earlier price increases, we must include these price increases in our definition of relative price appropriate for eqn. (2). The lagged effect of later price increases is accounted for by assuming that the actual relative price increases for energy will be in existence by approximately 2010 so that their full effect will be represented in the scenario projections for 2030.

Having defined the appropriate energy price, we now must be specific about the magnitude of the increase to be used in our analysis. As a guideline, we begin by examining energy production cost increases that result from the optimized supply scenarios resulting from our modeling exercise (Energy Program Group 1981, Chapter 17). Production costs are not, however, the only determinant of energy prices to the user so these can be used only as a guideline, as outlined below, for establishing our scenario price increases.

For our current purposes, we use the cost data for each supply technology, the resource cost data, and the mix of technologies that define the supply strategy and calculate an average cost per unit of final energy. These costs include all resource costs including imported crude at world trade prices and all energy conversion costs for refineries, electric power plants, etc. Costs are averaged over all final energy produced so that energy losses are accounted for. For each case, the total annual cost of supply of all fuel types and electricity was calculated. This total cost was then allocated per unit of final energy that would result from this total production. Thus, for example, the cost of production of electricity was calculated for the amount of secondary energy (gross power station output) required, but this cost was divided by the net amount of final energy (electricity delivered to the user) produced. All costs downstream from the power plant or refinery – administrative costs, interest payments and profit, transmission, transportation and distribution costs, trade margins and taxes – are *not* counted in this calculation.

Production and conversion costs are shown in Table 14 for 2030 along with 1972 costs estimated using the same procedure. Average production and conversion costs would be within the range of \$101 to \$126 per kWyr of final energy for 2030 for both the High and the Low scenarios. These 2030 costs would be between 3.4 and 4.2 times the 1972 costs for Regions I and IV, and between 2.9 and 3 for Region III in both scenarios. The apparently low costs for Region II reflect very high shares of relatively inexpensive central sources of heat – district heat and cogeneration plants.

A comparison of final energy prices for 1972 from Table 13 with production and conversion costs of energy shows that in 1972 these costs comprised only 43 percent of final energy prices for Region I and 35 percent for Region III. The difference consists of taxes, downstream costs, administrative and other costs. All taxes and other costs are not likely to increase at the same rate as energy production and conversion costs; some of these other costs should not increase at all, while others will increase to varying degrees, and taxes will vary from country to country. It is simply an assumption, adopted here, that these taxes and other costs will little more than double their 1972 value. Combining these components of costs results in approximately a 3-fold increase in prices for Region I

TABLE 14 Energy production and conversion cost estimates, \$(1975) per kWyr[a] of final energy.

Region	1972	High scenario 2030	Low scenario 2030
I (NA)	30	126	118
II (SU/EE)	ne	108	103
III (WE/JANZ)	40	119	114
IV (LA)	30	104	102
V (Af/SEA)	ne	105	101

ne–not estimated.
[a] \$100 per kWyr is equivalent to \$19.40 per barrel of oil equivalent, \$3.34 per million BTU and \$0.011 per kWhr.

and a 2.4-fold increase for Region III. The lower price increase for Region III is due to the relatively high level of prices already in place in this region in 1972. Since these price levels did not prevail throughout the other regions in 1972, the relative price increase for all other regions is defined to be 3-fold.

In summary, the implied price evolutions employed in the interpretation of scenario projections in this report are as follows:

- Energy prices are for final energy (delivered to the user) averaged for all fuels on a calorific content basis.
- Energy prices are for real increases relative to 1972.
- Energy prices are projected to increase by a factor of 2.4 for Region III and by a factor of 3 for all other regions.

Elasticities

For the historical period (1950–1975), real energy prices did not change significantly; they actually dropped slightly in most countries. Without taking account of these small price changes during this period, the values of the income elasticity γ would be the same as those given in Tables 11 and 12 for the energy–GDP elasticity ϵ for primary energy and for final energy, respectively.

For the scenario projection period 1975–2030, energy prices do increase and therefore both income elasticity γ and price elasticity β must be considered. If the scenario projections for GDP increases and final energy increases are specified (as in Tables A.3 and A.11 in Appendix A), and if energy price increases are also specified (as above), then the corresponding combinations of γ and β consistent with the scenario projections can be calculated. These combinations of γ and β are shown in Figure 10 for the High scenario and in Figure 11 for the Low scenario. These figures apply to the all sector aggregate of GDP and final energy projections for the period 1975–2030. The grouping of the developed regions (I, II, and III) with values of γ less than unity and of the developing regions (IV, V, VI, and VII) with values of γ greater than unity is as expected. A comparison of the two figures for the two scenarios indicates that the High scenario has higher price elasticities or lower income elasticities than the Low scenario for all regions. This result indicates that the High scenario projections represent better assumed efficiency improvements and stronger assumed conservation effects than the Low scenario.

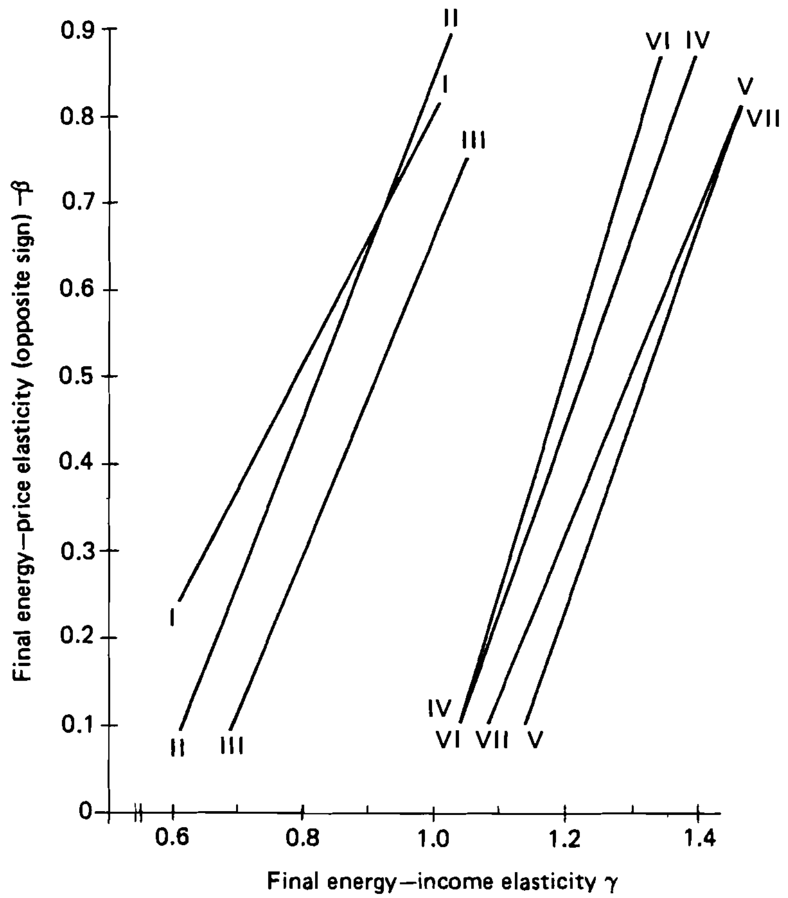

FIGURE 10 Income and price elasticities for aggregate final energy, High scenario.

Particular numerical values for γ and β may be selected for any region on the basis of Figures 10 and 11. For example, if the income elasticity were unity (that is, energy use increases in step with GDP increases if there were no price increase), then the price elasticities represented by the scenario projections are -0.81 and -0.52 for the High and the Low scenarios in Region I, respectively. For the historical value of the income elasticity for this region (for final energy it is 0.84), the corresponding price elasticities would be -0.58 and -0.39 for the two scenarios. Table 15 presents a range of values of both γ and β for all regions. As indicated in this table, the price elasticities for aggregate final energy are lower for the developing regions than for the developed regions. This result is not an irrefutable conclusion because the range of income elasticities shown was chosen arbitrarily and larger price elasticities would result if larger income elasticities were chosen. Based on the historical values of the income elasticities, however, the range of values shown seems reasonable. Accepting these ranges for γ, the associated price elasticities

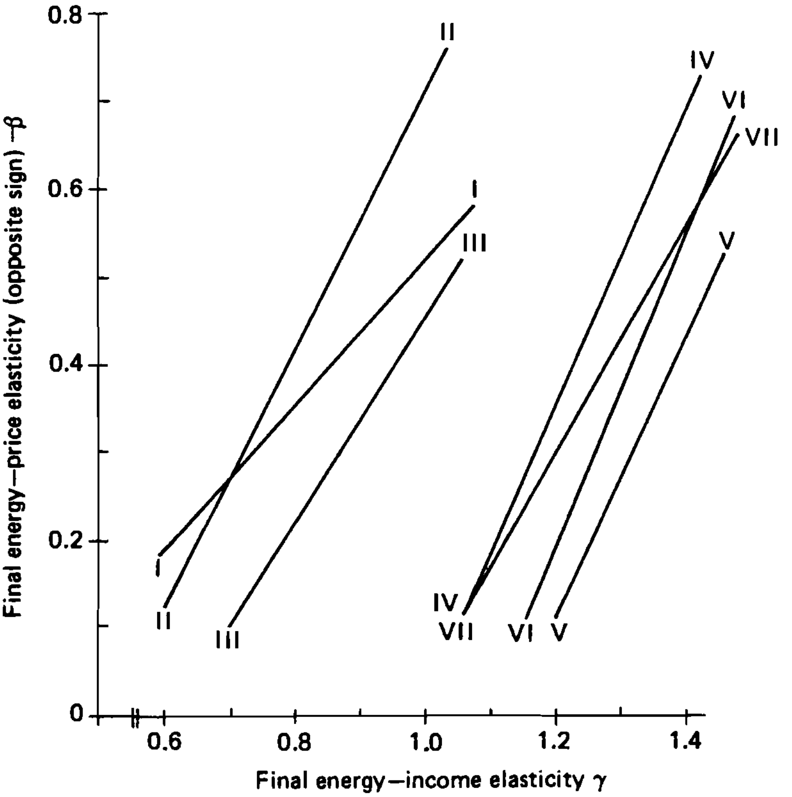

FIGURE 11 Income and price elasticities for aggregate final energy, Low scenario.

shown are evidence of strong price-induced conservation that is represented in the scenario projections. This conservation is strongest in the developed regions and in the High scenario.

Payments for Energy

A simple calculation demonstrates the burden that the developing countries will have as they develop their economies during a period of significant energy price increases. The projected energy consumption increases can be combined with the projected energy price increases to calculate the increases in the payments for energy. Since our price increases are relative to the 1972 price level of energy, these increases in payments must be interpreted also as increases from 1972. These increases in payments can be related to projected increases in GDP to obtain a relative measure of their magnitude.

Table 16 shows the results of these calculations. For Region I, High scenario final energy use is projected to almost double (1.96) between 1975 and 2030. Combined with a 3-fold increase in final energy prices, this implies nearly a 6-fold (5.88) increase in total payments for energy. The High scenario implies, however, a 4.75-fold increase of GDP for Region I so that energy payments would increase, in a relative sense, only 24 percent

TABLE 15 Final energy–income and energy–price elasticities.

	High scenario		Low scenario	
Region	Income elasticity γ	Price elasticity β	Income elasticity γ	Price elasticity β
I (NA)	(0.8, 1.0)	(−0.52, −0.81)	(0.8, 1.0)	(−0.35, −0.52)
II (SU/EE)	(0.8, 1.0)	(−0.46, −0.85)	(0.8, 1.0)	(−0.42, −0.71)
III (WE/JANZ)	(0.8, 1.0)	(−0.30, −0.66)	(0.8, 1.0)	(−0.22, −0.45)
IV (LA)	(1.1, 1.2)	(−0.23, −0.44)	(1.1, 1.2)	(−0.18, −0.35)
V (Af/SEA)	(1.2, 1.3)	(−0.24, −0.45)	(1.2, 1.3)	(−0.11, −0.27)
VI (ME/NAf)	(1.1, 1.2)	(−0.24, −0.49)	(1.1, 1.2)	(−0.02, −0.20)
VII (C/CPA)	(1.2, 1.3)	(−0.32, −0.50)	(1.2, 1.3)	(−0.30, −0.43)

NOTE: Final energy price elasticities are all sector aggregates for the period 1975–2030, calculated according to eqn. (2) to be consistent with GDP and final energy (including feedstocks) scenario projections and with the assumed range of values for the income elasticities shown. The historical values for 1950–1975 for γ are given in Table 12 under the assumption that real prices did not change during that period. These values are, respectively, 0.84, 0.68, and 0.84 for Regions I, II, and III and 1.21, 1.42, 1.17, and 1.53 for Regions IV, V, VI, and VII. The high values for the developing regions should not be applied to the projection period; the range shown in this table would be more appropriate.

TABLE 16 Increase in payments for energy relative to increase in GDP.

Region	GDP projected increase	Final energy projected increase	Final energy price increase	Increase in energy payment divided by increase in GDP[a]
High scenario				
I (NA)	4.75	1.96	3.0	1.24
II (SU/EE)	8.23	3.25	3.0	1.18
III (WE/JANZ)	4.90	2.75	2.4	1.35
IV (LA)	10.50	10.36	3.0	2.96
V (Af/SEA)	10.26	12.56	3.0	3.67
VI (ME/NAf)	15.36	15.45	3.0	3.02
VII (C/CPA)	7.66	8.13	3.0	3.18
Low scenario				
I (NA)	2.50	1.41	3.0	1.69
II (SU/EE)	5.07	2.31	3.0	1.37
III (WE/JANZ)	2.79	1.88	2.4	1.62
IV (LA)	6.56	6.49	3.0	2.97
V (Af/SEA)	5.87	7.42	3.0	3.79
VI (ME/NAf)	6.90	8.19	3.0	3.56
VII (C/CPA)	4.20	4.04	3.0	2.89

[a]For example, if energy use doubles and price triples by 2030, payments increase 6-fold but if GDP also increases 4-fold then this index is 6/4 = 1.50. Thus, the relative increase in energy payments is 50 percent. GDP and final energy projections are given in Appendix A.

(5.88/4.75 = 1.24). As shown in the table, the other developed regions would experience 18 percent and 35 percent increases in the High scenario or from 37 percent to 69 percent in the Low scenario. It is the developing regions, however, which exhibit astonishing relative increases of from 3-fold to almost 4-fold. Region IV, for example, would experience a 30-fold increase in energy payments while only a 10-fold increase in GDP. It would be difficult, indeed, to maintain such a growth pattern.

In this section, we have defined two scenarios of global evolution of economy and energy consumption. The linkage between the economic development and the energy consumption was defined originally in noneconomic terms, that is without using prices explicitly. We have examined this linkage in an aggregate manner in this section by looking at energy–GDP elasticities and income and price elasticities. To understand this linkage better, we now proceed to examine some of the major energy consuming sectors independently. The following section outlines the framework for analyzing these sectors and examines the household use of energy with the (γ, β) model of eqn. (2). A production function type model is then described in Section 4 which accounts for technological development and substitution of nonenergy inputs (capital and labor) for energy. This model is applied then to the nonenergy sector of the economy and to the industry sector.

3 SECTORAL ANALYSIS: ENERGY AS AN INPUT AND AS FINAL DEMAND

We have two objectives for examining energy use by sector. The first is to gain a better understanding of the energy–economy linkage than can be learned from aggregate analyses as in Section 2. Indeed, in our energy projections using the accounting framework of the MEDEE model, we use a detailed sectoral breakdown for determining energy use. Here we examine this projected energy demand by sector in order to understand the economic interpretation of these projections.

The second objective for sector analysis is to study the question of the shift in capital intensiveness of the economy. There are two important causes of a shift toward a more capital-intensive economy. The most readily apparent cause is the projected increased capital intensiveness in energy production. The era of readily available cheap oil and gas is over. All of the alternative forms of energy are, to varying degrees, more capital intensive. Increased electricity production whether from coal, nuclear, or solar sources is very capital intensive. The production of synthetic liquids, methanol, or hydrogen is even more capital intensive. On a long-run marginal cost basis, it is not necessary that a shift to capital-intensive production of energy implies a large increase in cost. It could be that these alternatives are just slightly higher in cost and therefore have heretofore not been implemented but now with relatively small changes in the energy sector these alternatives are attractive. Unfortunately, the current assessments of these alternatives, and particularly their costs, imply that indeed these alternatives do lead to much higher unit energy costs. It is this assessment that causes the second shift to more capital intensiveness in the economy as a whole. In sectors other than energy where energy is an important factor of production, the increase in unit cost of energy to the user will cause him to reassess his production possibilities including his use of energy and where possible shift to alternatives that use less energy. Assuming that he was operating efficiently to begin with (that is, that he cannot arbitrarily reduce his energy use and maintain production exactly as before) then shifting to processes that use less energy will necessarily use more of something else (per unit of output). This "something else", in the economy-wide analysis, must be value-added factors of production, that is, capital and labor. Thus we have the shift to more capital-intensive production of energy (a major effect in a small sector) and a second shift to more capital-intensive production in the remaining sectors of the economy due to a change in price of energy (a relatively minor effect in a very large sector).

There are two other important factors that affect the overall capital intensiveness of the developed economies. Effects similar to the one described above for energy are projected to occur in many other primary sectors of the economy. Resource extraction industries in general are experiencing the disappearance of easily accessible deposits of minerals resulting in higher exploration, development, and extraction costs, usually due to increased capital intensiveness. These costs are reflected in the prices of minerals that are used in the economy so the secondary impact in the production processes of the remaining sectors of the economy is also present. A second factor which affects the capital intensiveness of the overall economy is the development of the so-called postindustrial society. Projections for developed economies have been made that continue the recent trend of an increasing share of services and a decreasing share of industry in the economy. Since on average the service sector is less capital intensive than the industrial sector, this trend contributes to a decreasing capital–output ratio. The effects that have been mentioned above of increasing capital intensiveness in the energy, resource extraction and other industrial sectors will be off-set to a certain degree by the continual development of the postindustrial society. These sectors must be examined separately to study the question of changing capital intensiveness.

The first step in sector disaggregation is to separate the energy sector from the nonenergy sector. This separation is important when considering the changing capital intensiveness since the shifts expected in the nonenergy sector are due to the substitution effect of using relatively more nonenergy inputs in place of higher priced energy inputs, whereas in the energy sector, these shifts are due to switching to more expensive or alternative sources of energy. These two phenomena are fundamentally different and should be examined separately.

3.1 Framework for Two-Sector Economy

We begin with the two-sector model of an economy that separates the energy sector from the nonenergy sector. In this analysis, we define the energy sector in its broadest sense so that it includes energy resource exploration and mining as well as final energy distribution to the end user. Figure 12 depicts these two sectors in a simplified manner where each sector has its allocation of primary inputs, capital and labor, and imports are separated into energy and nonenergy commodities. There are flows of goods and services from the nonenergy sector into the energy sector that are distinguished as intermediate inputs X_E and payments for taxes T_E.

The output of the energy sector is divided into two components. There is a final demand* for energy which we define as household energy for heating, lighting, etc. plus

*Even though the term final demand as applied to the energy sector has some connection with the term final energy, note that the two terms arise from two completely separate disciplines and should not be confused or thought to represent the same concepts.

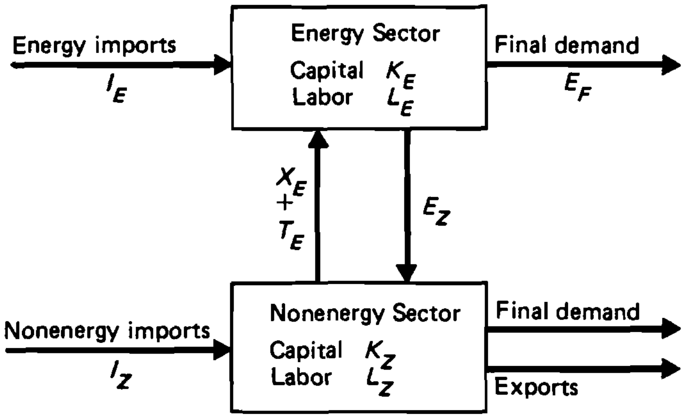

FIGURE 12 Two-sector model of an economy.

energy used for passenger transportation. The second component of energy output is used by the nonenergy sector as an intermediate input in its production process.

This same two-sector economy is depicted in Figure 13 in a flow-diagram format. With a general flow from left to right, this diagram illustrates how total GDP (which can be divided into its two primary factor components $P_K K + P_L L$) is separated into the value-added components for the energy ($\text{GDP}_E = P_K K_E + P_L L_E$) and nonenergy ($\text{GDP}_Z = P_K K_Z + P_L L_Z$) sectors*. The energy sector is shown as receiving these primary input factors plus imports I_E plus intermediate inputs X_E plus an allocation for taxes on energy T_E and producing the total value of its output $P_E E$. This energy product is divided between final consumption E_F and intermediate input to the nonenergy sector E_Z. The value of the final consumption component is shown in dashed lines rejoining the main stream of flow so that total GDP can be reconstructed and then subdivided into its consumption investment and government purchases components. The nonenergy sector is depicted as receiving primary inputs, energy inputs, and imports I_Z to produce its output Y_Z. This output can be expressed as:

$$Y_Z = \text{GDP}_Z + P_E E_Z + I_Z \tag{3}$$

3.2 Analysis of Scenario Projections

We define final demand energy as energy consumed in the household sector plus energy used for passenger transportation. In our accounting of energy uses by the MEDEE model, household requirements include space and water heating, lighting and specific uses of electricity. Passenger transportation energy includes all modes of transport. The scenario projection data given in Table A.12 of Appendix A are summarized here in Table 17.

*P, K, and L represent prices, capital services, and labor services respectively and subscripts E and Z represent the energy sector and nonenergy sector respectively.

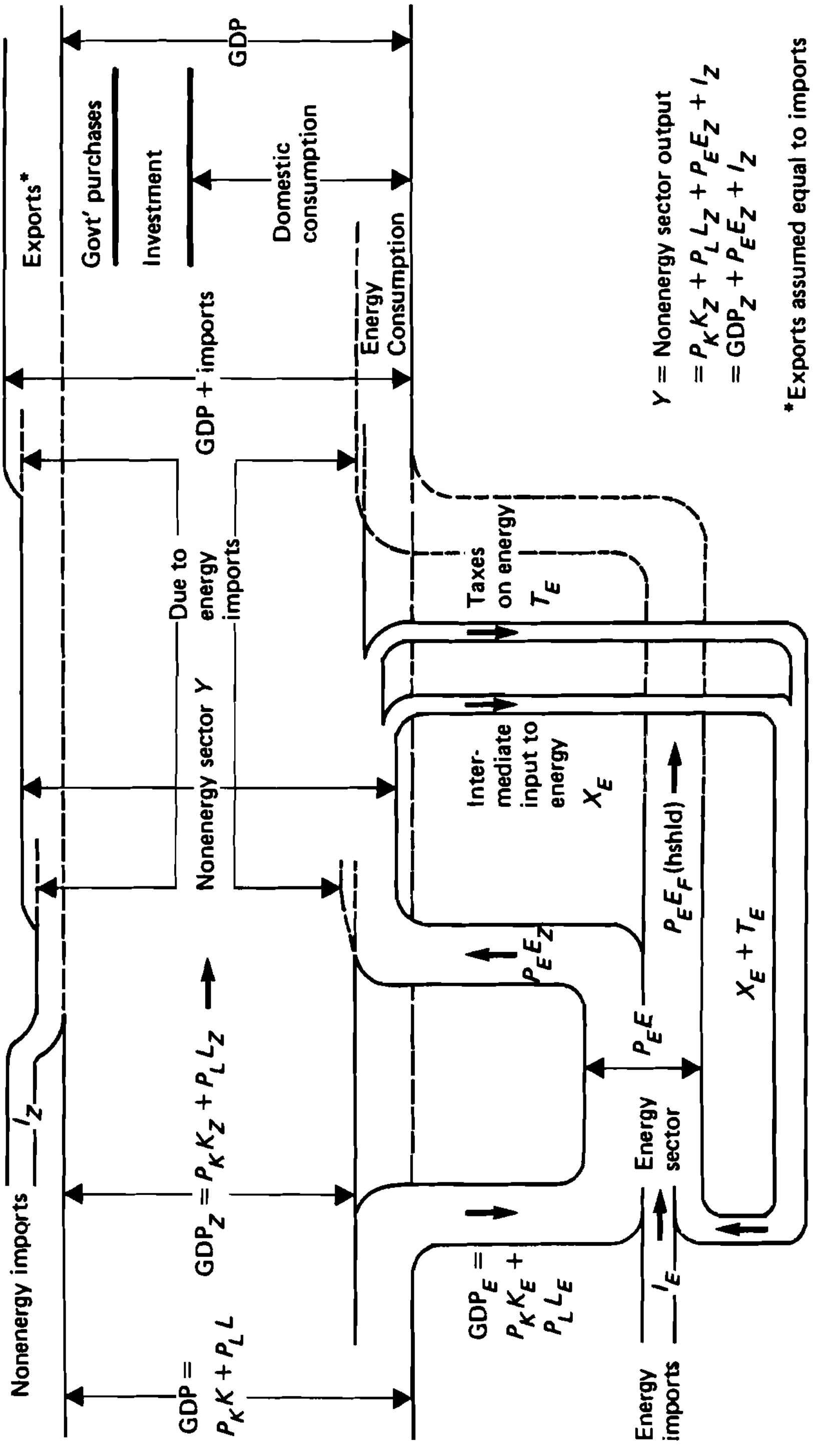

FIGURE 13 Flows in a two-sector economy.

TABLE 17 Final demand energy and intermediate input energy (GWyr/yr).

Region[c]	Final demand energy[a] 1975	High 2030	Low 2030	Intermediate input energy[b] 1975	High 2030	Low 2030
I (NA)	809	887	800	1,062	2,778	1,836
II (SU/EE)	276	662	544	1,001	3,452	2,408
III (WE/JANZ)	591	1,410	1,080	998	2,965	1,908
IV (LA)	60	619	446	145	2,021	1,210
V (Af/SEA)	57	750	577	196	2,423	1,299
VI (ME/NAf)	22	329	193	84	1,309	675

[a] Household commercial energy plus passenger transportation energy (Table A.12).
[b] Total final commercial energy including feedstocks minus final demand energy (Table A.12).
[c] Sectoral analysis is performed only for Regions I through VI for which detailed projections were made.

Energy used as an intermediate input includes feedstocks. Immediately striking is the final demand projection for Region I where energy use drops slightly from 1975 to 2030 in the Low scenario and increases only 10 percent in that period in the High scenario. This is primarily due to the mandated automobile efficiency standards in North America.

We examine the relationship between each of these two categories of energy use and the economy by means of the income and price elasticity (γ, β) model of eqn. (2). With that model, we compare energy projections with economic activity projections including the effect of price. For interpretation of final demand energy projections, it is natural to use total GDP as the measure of economic activity. For analyzing intermediate input energy with this model, several points must be raised.

Figures 12 and 13 and eqn. (3) above defined intermediate input energy and the nonenergy sector of the economy. The scenario projections were defined somewhat differently and so these variables cannot be precisely calculated. The energy sector as defined by the MEDEE model includes only the energy conversion industry. Other sector components (mining energy commodities, transmission and distribution of energy) included in the energy sector here are allocated elsewhere in MEDEE. Thus we cannot readily separate either the GDP component or the intermediate input energy requirements of these missing subsectors. For the application of the (γ, β) model here, we relate intermediate input energy increases as defined in Table 17 to total GDP increases as defined in Table A.3, Appendix A. That is, rather than make the small adjustments to these data as implied by eqn. (3) (adjustments which compensate each other anyway), we use the GDP and energy data as mentioned above.

To apply the (γ, β) model of eqn. (2), we use the same values for the relative price increase that we introduced in Section 2: a factor of 2.4 increase for Region III and 3.0 for all other regions. The values of the income elasticity γ and price elasticity β which satisfy eqn. (2), for each case, can be represented by straight lines on a graph of γ vs β as shown earlier in Figures 10 and 11 for the aggregate economy. In all cases, the results show the familiar pattern that the developing regions have values of γ greater than those for the developed regions and that the value of unity for γ generally serves to separate the developed from the developing regions.

Several observations result from this analysis as described below.

3.2.1 Comparing High Scenario with Low Scenario

In all cases, the values for γ (for a given β) are larger for the Low scenario than for the High scenario. This is consistent with the general trend that the income elasticities decrease with increasing economic development: that is, the High scenario has a higher level of economic development and therefore the long-term average values of γ should be less for the High than the Low. Another interpretation of this same result is that the High scenario has larger price elasticities (βs) than the Low scenario: that is, there were stronger conservation effects assumed in the development of the High rather than in the Low scenario.

3.2.2 Comparing Final Demand Energy with Intermediate Input Energy

A comparison of the two categories of energy use (household plus passenger transport energy and intermediate input energy) shows that the elasticities for the regions are very different for the final demand category but reasonably close together for the intermediate input category of energy use. Also, in the High scenario, the developed regions have higher βs and lower γs for the final demand category than for the intermediate input category, whereas for the developing regions the two categories are almost identical. In the Low scenario, the effect for the developed regions is less dominant, but for the developing regions the final demand category has lower βs and higher γs than the intermediate input category. These results can be represented as follows:

For final demand energy relative to intermediate input energy:

Regions	High scenario	Low scenario
Developed (I, II, and III)	Higher βs Lower γs (very pronounced)	Higher βs Lower γs (less pronounced)
Developing (IV, V, and VI)	Same elasticities	Lower βs Higher γs

For the developed regions, an interpretation of these results is that GDP growth would be accompanied by relatively lower growth (more conservation) in the final demand for energy than in the requirements for intermediate input energy. Conversely, for the developing regions, and especially in the Low scenario, GDP growth would be accompanied by relatively higher growth in the final demand for energy (which is strongly linked to population) than for intermediate input energy.

3.2.3 Comparing Passenger Transportation Energy with Household Energy

In this comparison, the High and the Low scenarios exhibit the same result. For Region I only, passenger transportation energy has higher βs and lower γs than household energy. For all other regions the opposite is true. This result indicates the very high efficiency improvements and conservation potential that were realized in these projections for Region I. Equally important is the assumed saturation effect on passenger transportation, which was assumed would apply in this region.

3.3 Framework for Five-Sector Economy

In Section 3.1, we defined a two-sector economy with an energy sector and a nonenergy sector. The nonenergy sector can, of course, be disaggregated further. In particular, we examine the industry sector apart from other sectors but for all regions.

For scenario projection purposes, many sectors were accounted for separately in the MEDEE model. These sectors are agriculture, mining, manufacturing (in four subsectors), construction, and services. Transportation (freight and passenger) and household energy uses were separated as well. For our analysis purposes here, we define the industry sector as the mining, manufacturing, and construction sectors of the MEDEE model.

Figure 14 indicates the energy and nonenergy flows in a five-sector model based on MEDEE and defines the industry sector which will be analyzed in detail in Section 5. The industry sector receives imports I_I and intermediate inputs X_I from all other sectors and combines these with its own primary inputs of capital and labor to produce its output.

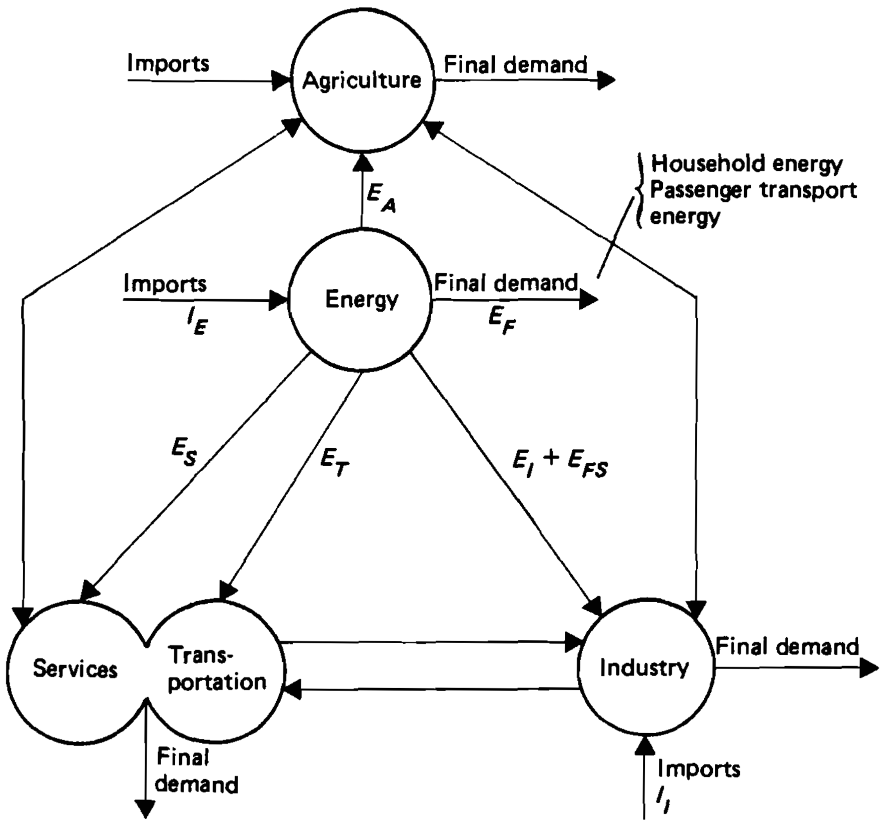

FIGURE 14 Five-sector model of an economy.

The energy inputs are separated into normal energy commodities E_I and commodities that are used as feedstocks E_{FS}. Its total output Y_I can be expressed as:

$$Y_I = \mathrm{GDP}_I + P_E E_I + P_E E_{FS} + I_I + X_I \tag{4}$$

In our analysis of this sector, we will make the simplifying assumption that imports plus intermediate inputs maintains a constant share of output so that we need only consider the primary input factors GDP_I and the energy term. Since we will be examining the substitution effect of nonenergy inputs for energy inputs we will consider only those energy inputs that are used as energy E_I and consider the feedstock component as another intermediate input included with X_I.

4 ENERGY–NONENERGY SUBSTITUTION AND TECHNOLOGICAL DEVELOPMENT: A MODEL

The objective of this analysis is to examine the substitution between energy and other factors of production and how this substitution affects both the price of energy and the structure of the economy in general. In Section 3, the accounting structure was described within which we identify and measure energy as an intermediate input and how the energy sector interacts with the other sectors of the economy. The vehicle for analyzing factors of production and substitution is the production function. In this section, we specify the family of production functions that we use, we define the elasticity of substitution of factors of production and give some examples to assist in the interpretation of these concepts in our application. This approach follows that of Manne 1977.

As described earlier, the factors of production that we consider are capital, labor, and energy. In the explication of the basic concepts immediately following, we examine the case with only two unspecified factors of production. We will later identify one factor x as energy and the other z as a combination of the primary inputs capital and labor. The z factor can eventually be split into its two basic components.

In an ideal production system, a production function defines the amount of output or product that can be produced from the specified quantities of inputs. In conceptual form, all quantities are measured in real, physical units. If we denote the output product in some units by y and the two input factors in their units by x and z, then the production function f defines the maximum feasible output for any combination of inputs, that is:

$$y = f(x,z) \tag{5}$$

We will be interested mainly in the combinations of x and z that yield a given y or simply the substitution of x for z (or vice versa) from some given mix that will maintain the same quantity of output y.

4.1 Static Economy

The first question that arises with respect to substitution is how much of one factor is required to substitute for another factor. In Figure 15, the combinations of factors x and

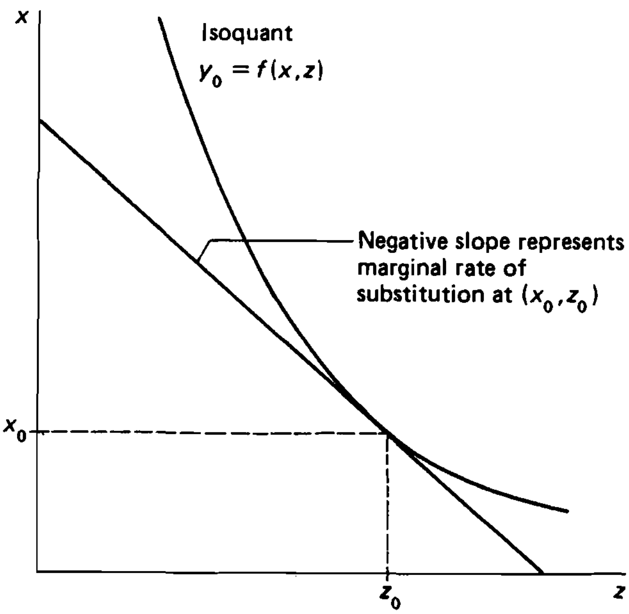

FIGURE 15 Isoquant and marginal rate of substitution.

z that could be used to produce a given output are illustrated by a curved line called an *isoquant*. At any point on this isoquant, there is a tradeoff between using more of one factor and less of the other. We formally define this tradeoff as the *marginal rate of substitution* of x and z, which is denoted $R(x,z)$ and defined as:

$$R(x,z) = -\frac{\mathrm{d}x}{\mathrm{d}z} = \frac{f_z}{f_x} \tag{6}$$

where f_x and f_z denote the partial derivatives of the production function f with respect to x and z. The marginal rate of substitution is illustrated in Figure 15 as the slope of the isoquant. It is reasonable to assume that R increases as more and more x is substituted for z as illustrated in the figure. This implies that the isoquants of constant output are convex to the origin. It is clear that, except for the case of a production function of the form $f = ax + bz$ in which the isoquants are straight lines, the marginal rate of substitution depends on the mix of inputs.

Another concept that measures the substitutability of input factors is the *elasticity of substitution*. (See for example Allen 1967.) Denoted by σ, it is defined by:

$$\sigma = \frac{\mathrm{d}\log(x/z)}{\mathrm{d}\log R(x/z)} \tag{7}$$

with output y held constant. In a different form, it can be expressed as

$$\sigma = \frac{z}{x} R \frac{\mathrm{d}(x/z)}{\mathrm{d}R} = \frac{\dfrac{\mathrm{d}(x/z)}{x/z}}{\dfrac{\mathrm{d}R}{R}} \tag{8}$$

which is explained below.

As with all elasticities, this concept is a ratio of two relative changes. What is initially confusing, perhaps, is that the numerator is a relative change ($\mathrm{d}u/u$) of a variable that is itself defined in relative terms ($u = x/z$). Expressed in words, the elasticity of substitution is the ratio of the relative change in the (relative) mix of inputs to the relative change in the marginal rate of substitution of these inputs. Thus for an elasticity of unity, a 1 percent change in the relative amounts of x and z is accompanied by a 1 percent change in the marginal rate of substitution. That is, for constant output, a small shift toward using more x is accompanied by a similar small increase in the marginal rate of substitution so that any *further* shifts toward more x will require relatively more x. For an elasticity of 0.25, for example, a 1 percent change in relative amounts of x and z will be accompanied with a 4 percent change in the marginal rate of substitution. Figure 16 shows several isoquants that exhibit constant but different elasticities of substitution.

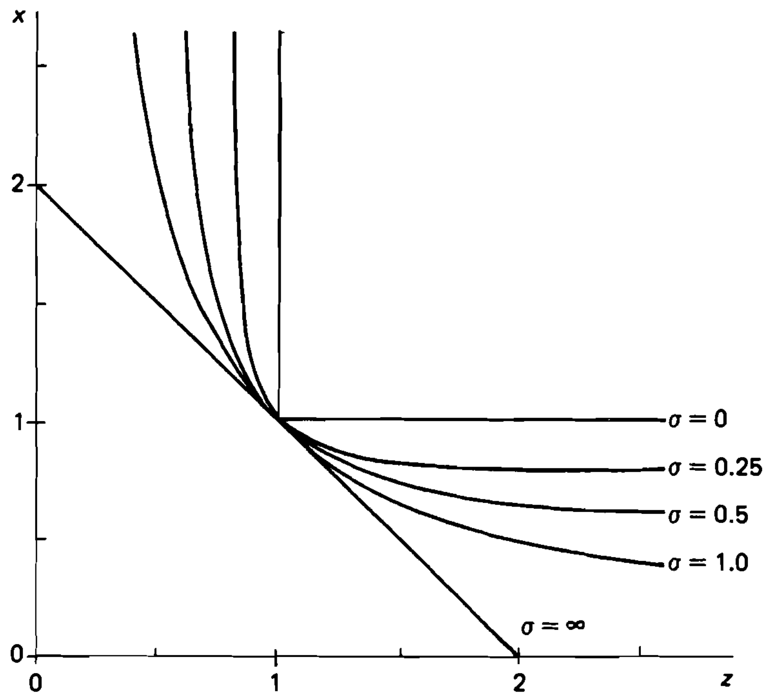

FIGURE 16 Isoquants for different values of elasticity of substitution.

We now introduce two specific forms for the production function; one is the Cobb-Douglas and the other is the constant elasticity of substitution (CES) form. The Cobb-Douglas production function has the form:

$$y = x^{\alpha} z^{\beta} \tag{9}$$

where α and β are greater than zero. For constant returns to scale, $\alpha + \beta$ must be unity and then $\beta = 1 - \alpha$. In this case, it is straightforward to show that the elasticity of substitution is unity and it can also be shown that the Cobb-Douglas production function with constant returns to scale is the *only* production function with $\sigma = 1$.

The second specific form of production function to be used in this analysis is the CES production function, which takes the form:

$$y = \left(ax^{\rho} + bz^{\rho}\right)^{\frac{1}{\rho}} \tag{10}$$

where a and b are positive constants and ρ is a parameter not equal to zero. The elasticity of substitution of this production function is:

$$\sigma = \frac{1}{1-\rho} \tag{11}$$

It can also be shown that eqn. 10 is the *only* form of production function with constant returns to scale that has a constant elasticity of substitution. The isoquants of Figure 16 are derived from this production function (except for the limiting case of $\rho = 0$ and $\sigma = 1$ for which this form is consistent with the Cobb-Douglas form).

In order to gain the full potential of production function analysis, we assume that production is based on profit maximization under perfect competition. Under these conditions, producers take prices as given and production is determined by equating the marginal productivity of each factor of production to its price. In mathematical form, this implies that the prices for x and z are given by:

$$p_x = f_x \qquad \text{and} \qquad p_z = f_z \tag{12}$$

For the CES production function of eqn. (10) these equilibrium prices are:

$$p_x = ax^{\rho-1}(ax^{\rho} + bz^{\rho})^{(1-\rho)/\rho} = a\left(\frac{y}{x}\right)^{1-\rho} \tag{13}$$

$$p_z = bz^{\rho-1}(ax^{\rho} + bz^{\rho})^{(1-\rho)/\rho} = b\left(\frac{y}{z}\right)^{1-\rho} \tag{14}$$

These prices are measured in the physical units of the product y or, equivalently, in an appropriate numéraire (say monetary) with the product price defined as unity.

The conditions already assumed for the definition of the CES production function and the prices above are sufficient to ensure that the value of the product can be exactly divided into the value contributed by the factors of production, that is:

$$y = p_x x + p_z z \tag{15}$$

which can be verified by substituting the expressions for p_x and p_z from eqns. (13) and (14).

Using the assumption regarding prices of eqn. (12), the definition of the elasticity of substitution σ can be restated in relative price terms. Since the marginal rate of substitution R is simply the ratio of the prices of x and z, eqn. (8) can be stated as follows

$$\sigma = \left[\frac{\mathrm{d}(x/z)}{x/z}\right] \Big/ \left[\frac{\mathrm{d}(p_z/p_x)}{p_z/p_x}\right] \tag{16}$$

Thus the elasticity of substitution is the ratio of the relative change of the relative mix of x and z to the relative change of the relative prices of z and x. The relative amount of x decreases if the relative price of x increases.

The relationship between the elasticity of substitution and the more common price elasticity can be investigated by means of eqns. (13) or (14). Considering the use of the factor of production x, eqn. (12) can be rewritten as:

$$x = a^{1/(1-\rho)} y\, p_x^{-1/(1-\rho)} \tag{17}$$

which is:

$$x = a^{\sigma} y\, p_x^{-\sigma} \tag{18}$$

where σ is the elasticity of substitution as given by eqn. (11).

The normal definition of a price elasticity relates the change in use of a commodity to the change in its price after all other changes have occurred in the economy. Thus, this definition compares two equilibrium states of the economy, before and after the price change. The price elasticity τ of x is defined by:

$$\tau = \frac{p_x}{x} \frac{\mathrm{d}x}{\mathrm{d}p_x} \tag{19}$$

From eqn. (18), this becomes:

$$\tau = -\sigma + \frac{p_x}{y} \frac{\mathrm{d}y}{\mathrm{d}p_x} \tag{20}$$

That is, the price elasticity is the elasticity of substitution (with opposite sign) plus the elasticity of change of output y to a change in price of x. Without a further assumption, the second term of eqn. (20) cannot be evaluated. One must be careful in making this evaluation to guarantee that the price elasticity of eqn. (19) makes sense. Only the changes of output y *due to the change in price of* x should be counted. If the states of an economy are compared at different times during which there happened to be a price change, there may have been other factors affecting output y. A growing economy is an obvious example. Between two points in time, the price of x may increase but output and the use of x may also increase due to overall growth. This is not the change in y meant in eqn. (20).

If the output is relatively independent of the price of x, then the price elasticity is numerically equal to the elasticity of substitution. That is, for *constant output* we have:

$$\tau = -\sigma \tag{21}$$

A better approximation to the full price effect can be achieved by assuming that the quantity of factor z is held constant and the output is allowed to change. In this case, we have:

$$\frac{dy}{dp_x} = \frac{dy}{dx}\ \frac{dx}{dp_x} = p_x\ \frac{x\tau}{p_x} = x\tau \tag{22}$$

with z *held constant*. Then by substituting into eqn. (20), we get:

$$\tau = -\sigma/[1-(p_x x)/y] = \frac{-\sigma}{1-s} \tag{23}$$

where s is the relative value share of x in output y. In the case of energy, its value share is relatively small so that τ and σ are approximately equal in magnitude.

4.2 Technological Development

To this point in our development, we have been dealing with a static economy. We will eventually apply these concepts in a dynamic situation. In the developed economies, historical data analysis usually indicates that capital–output ratios, labor–output ratios and energy–output ratios decline over time as output is increasing. The production functions introduced above cannot explain these changes so that further assumptions or modifications must be made.

One such modification is the introduction of the concept of technological development. In its simplest form, this concept allows for more product to be produced from the same physical inputs as time progresses. In mathematical form, it can be defined as an exponentially increasing multiplicative factor so that output y is given as follows:

$$y = e^{\delta t} f(x,z) \tag{24}$$

where t represents time (in years) and δ is (approximately) the annual percentage increase in output per unit of input.

Treating technological development in this way implies that all (or both) inputs enjoy the same rate of technological development or improvement with time. This is, of course, a simplification. It is not intended, however, that this multiplicative factor should represent ***all*** the effects which contribute to the decreasing output–input ratios. Output per physical unit of labor (labor productivity) is not entirely due to technological development nor is the factor $e^{\delta t}$ intended to represent all of labor productivity – similarly for capital and energy inputs. We separate technological development as a factor of overall improvement in product per unit input because it is an important factor which has provided more for less in the past and we assume that it will continue to some extent for the future. The factor $e^{\delta t}$, therefore, is the average technological development factor which is assumed to apply to all inputs and other "more for less" factors are represented otherwise. In particular, labor productivity increases over and above those due to technological development are assumed to be included in the definition of the measurement of the labor input. Thus, labor input is not measured in man-hours or like units but in "labor-equivalent" units relative to a base year that represents the differential productivity increases. The price of these inputs is defined accordingly to account for their "observed" value in the production function formulation. For example, if labor productivity increases apart from those due to technological development could be represented by a percentage increase, k per year, then the labor input could be defined as $e^{kt}L$ where L is measured in physical units.

Taking account of the $e^{\delta t}$ factor of eqn. (24), our expressions for the prices of x and z change slightly. Using the CES form of the production function, these prices are now:

$$p_x = e^{\delta t} f_x = e^{\delta t} a \left(\frac{f}{x}\right)^{1-\rho} = a\, e^{\rho\delta t} \left(\frac{y}{x}\right)^{1-\rho} \tag{25}$$

and

$$p_z = e^{\delta t} f_z = e^{\delta t} b \left(\frac{f}{z}\right)^{1-\rho} = b\, e^{\rho\delta t} \left(\frac{y}{z}\right)^{1-\rho} \tag{26}$$

It is easy to see that with $\delta = 0$, these reduce to eqns. (13) and (14). The comparable expression to eqn. (18) for x as a function of p_x is

$$x = a^{\sigma} e^{-(1-\sigma)\delta t} y\, p_x^{-\sigma} \tag{27}$$

where σ is the elasticity of substitution as given by eqn. (11).

4.3 Dynamic Economy

We gain some insight into the implication of the production function formulation and the equilibrium price assumptions if we examine these equations as defining a system that evolves in time. This system is determined by eqns. (24), (25), and (16) in the five variables x, y, z, p_x, and p_z. Once the production function f and technological development parameter δ are given then the evolution of the system from some initial point is determined once two of the five variables are specified. We will be interested in the dynamics of this system for various assumptions about the changes in price of x (which will represent energy in our later application) but initially we gain better understanding of this system by examining some simple cases.

If inputs x and z are both held constant over time at values x_0 and z_0, then output y is given by:

$$y = e^{\delta t} f(x_0, z_0) = e^{\delta t} f_0 \tag{28}$$

which increases at the rate δ of technological development. The equilibrium prices of x and z are given by eqns. (25) and (26) as:

$$p_x = e^{\delta t} f_x(x_0, z_0) = p_{x0} e^{\delta t} \tag{29}$$

and

$$p_z = e^{\delta t} f_z(x_0, z_0) = p_{z0} e^{\delta t} \tag{30}$$

These prices increase at the same rate as technological development which is consistent with the assumption of prices being equal to marginal productivity. Notice that the output y still divides exactly into the value share for x and z since the initial condition must satisfy:

$$p_{x0} x_0 + p_{z0} z_0 = f_0 \tag{31}$$

As a second case, assume that output y increases with growth rate g and that there is no relative price change between x and z. Then:

$$y = y_0 e^{gt} \tag{32}$$

$$x = x_0 e^{(g - \delta)t} \tag{33}$$

and

$$z = z_0 e^{(g - \delta)t} \tag{34}$$

so that the growth in output is maintained by growth in inputs x and z at a rate of $g - \delta$ to account for the technological development.

In an earlier section, we defined an elasticity ϵ as the ratio of the relative change in energy to the relative change in gross output or GDP. If input x is interpreted as an energy input, then this elasticity becomes:

$$\epsilon = \frac{dx/x}{dy/y} \tag{35}$$

In this simple growth case, dx/x is $g - \delta$ and dy/y is g so that:

$$\epsilon = \frac{g - \delta}{g} = 1 - \frac{\delta}{g} \tag{36}$$

For small economic growth with $g = \delta$ then this elasticity is zero, that is, with economic growth due to technological development only there is no increase in inputs (zero energy growth).With $g \gg \delta$ then this elasticity is close to but smaller than unity. For $g = 5\delta$, $\epsilon = 0.8$.

Notice that with this model of an economy which results in the definition of eqn. (36) for the energy–GDP elasticity, this elasticity is always less than unity (assuming that δ and g are both positive). Thus it cannot explain the development of a developing economy in the aggregate since we have already seen that this elasticity is usually greater than unity in these cases. The implication is that a single production function cannot properly explain the aggregate economy *over time* because the developing economy is changing rapidly in texture such that it *does* require more energy for the "same" aggregate output as the economy shifts from agriculture to energy-intensive industry. This model may be useful, however, for certain reasonably homogenous sectors of a developing economy and, in fact, we will apply it to the industry sector of six regions in Section 5.

To examine the effects of changing prices, it is useful to use the specific CES production functions. In this case, we can express the quantity of inputs required as a function of price as shown, for example, in eqn. (27). By rearranging eqn. (27) we have:

$$x = \frac{y}{e^{\delta t}} \left(\frac{p_x}{ae^{\delta t}} \right)^{-\sigma} \tag{37}$$

which shows very clearly that if output y and price p_x increase at the rate δ then the equilibrium quantity of x remains constant. It is useful to define all the variables of this system in terms of their initial or base year values. Thus the measurement of the quantitites of x, y, and z become relative to, or multiples of, base year values and the initial conditions of the system can be set at unity. With $t = 0$ and x, y, and z at unity, the initial prices for x and z are a and b, respectively, as can be seen from eqns. (25) and (26) provided that the price of y is defined to be unity. Then p_x/a becomes the price of x relative to its base year value and we denote this price as p_x^r. We similarly define p_z^r. Equation (37) can be simplified to:

$$x = \frac{y}{e^{\delta t}} \left(\frac{p_x^r}{e^{\delta t}} \right)^{-\sigma} \tag{38}$$

which allows us to make a very important observation: there is no effect on the use of input factor x *due to substitution* as long as its price relative to the base year value *increases at the rate of technological development*. If the price of x is held constant (in real terms), the effect is to increase substitution to use *more* x because it is undervalued vis-à-vis other inputs and marginal productivity. A constant price in real terms is therefore a decreasing price relative to other inputs but is still constant relative to the price of the output y.

To continue with our examination of the dynamics of this system, we require an expression of the time rate of change of x. By differentiating eqn. (38) with respect to t we obtain:

$$\frac{\dot{x}}{x} = \frac{\dot{y}}{y} - (1 - \sigma)\,\delta - \sigma \frac{\dot{p}_x^r}{p_x^r} \tag{39}$$

If we now let g and π (both possibly time varying) represent the growth rates $\dot{y}/y$ and $\dot{p}_x^r/p_x^r$, respectively, then:

$$\frac{\dot{x}}{x} = g - \delta - \sigma(\pi - \delta) \tag{40}$$

That is, the growth rate of x is equal to the growth rate of y minus technological development and minus the elasticity of substitution times the growth rate of the price of x in excess of the "normal" price increase due to technological development.

Whenever the price of x is different from that due to technological development ($\pi \neq \delta$) then there is substitution between x and z. This substitution causes a change in the marginal productivity of z and so its price will change. By using the basic relation:

$$y = p_x x + p_z z \tag{41}$$

and the already derived dynamics of x and p_x we can show that:

$$\frac{\dot{p}_z}{p_z} = \delta - (\pi - \delta)\frac{s}{1-s} \tag{42}$$

where s is the value share of x in y, that is:

$$s = \frac{p_x x}{y} = a^{\sigma} e^{-(1-\sigma)\delta t} p_x^{1-\sigma} \tag{43}$$

If x is interpreted as the energy input then its value share is a small part of total GDP. Even if this value share changes by a factor of two in the future due to real price increases, the fraction $s/(1 - s)$ is still small and so eqn. (42) shows that the price of z is affected only slightly even if π is substantially larger than δ. The expression for the growth rate of z itself comparable to eqn. (40) is:

$$\frac{\dot{z}}{z} = g - \delta + \sigma(\pi - \delta)\frac{s}{1-s} \tag{44}$$

which shows, as expected, that if $\pi > \delta$ then z grows faster than would normally be required $(g - \delta)$ but that the required increase is small because of the value share fraction $s/(1 - s)$.

A development similar to that above which resulted in eqns. (42) and (44) results in expressions for p_z and z as a function of p_x. These are presented here and will be useful later:

$$p_z^r = e^{\delta t}\left[\frac{1 - a(e^{-\delta t}p_x^r)^{1-\sigma}}{1-a}\right]^{1/(1-\sigma)} \tag{45}$$

$$z = \frac{y}{e^{\delta t}}\left[\frac{1-a}{1 - a(e^{-\delta t}p_x^r)^{1-\sigma}}\right]^{\sigma/(1-\sigma)} \tag{46}$$

We see immediately that if p_x^r increases only at the rate of technological development ($e^{\delta t}$) then p_z^r increases also at this rate and z increases only to the extent that output y increases above technological development. The expression in the square brackets of eqn. (46) to the power $\sigma/(1 - \sigma)$ defines the relative amount of other input (z) required over and above its normal value ($y/e^{\delta t}$), the increase which is due to substitution when p_x^r is higher than $e^{\delta t}$.

In summary, if we treat eqns. (24), (25), and (26) as defining a dynamic system, we can choose any two variables from x, y, z, p_x, p_z as independent and the remaining are determined by the system. In particular, if we choose y and p_x by specifying their growth rates over time (g and π) then x is given by eqn. (40), p_z by eqn. (42) and z by eqn. (44) where s is already defined by eqn. (43) in terms of p_x.

Finally, we can express the changing role of x in the economy by the ratio of its growth rate to that of y. This elasticity ϵ is given by

$$\epsilon = \frac{\dot{x}/x}{g} = 1 - \frac{\delta}{g} - \sigma\frac{\pi - \delta}{g} \tag{47}$$

Typical parameter values are $g = 5$ percent per year, $\delta = 0.5$ percent per year and $\sigma = 0.25$. If then the price of x increases by 2.5 percent per year over some period, we have

$$\epsilon = 1 - 0.1 - 0.1 = 0.8 \tag{48}$$

for that period. Thus we see that the substitution effect can be approximately equal in importance to the technological development effect in reducing the demand for energy. We examine the scenario projection data with these models in Section 5.

5 ENERGY–NONENERGY SUBSTITUTION AND TECHNOLOGICAL DEVELOPMENT: ANALYSIS OF SCENARIO PROJECTIONS

The model just described can be usefully applied in two ways in analyzing the scenario projections. For the industry sector itself, it can be applied to all regions, whether developed or developing, because within this sector, the possibilities for substitution from energy inputs to nonenergy inputs and for technological development are more easily understood. Another application for this model is the nonenergy sector in total as defined in Section 3 but this application must be restricted to the developed regions. As noted in the description of the model, the effects of both substitution (with increasing energy prices) and technological development contribute to using less energy per unit output. We have already seen that developing regions are projected to require more energy per unit of aggregate output (ϵs and γs are greater than unity) not because of inefficiencies but because of a shift in the sectoral composition of the developing economy. For the developed regions, on the other hand, the sectoral shifts are less pronounced and the application of the (δ, σ) model of technological development and substitution will have a meaningful interpretation. We examine the intermediate input energy consumption by the nonenergy sector of the economy for Regions I, II, and III first and then examine the industry sector (mining, manufacturing, and construction) for Regions I through VI later.

In the application of the (δ, σ) model described in Section 4, we use scenario data to define GDP or output, energy consumption, and the relative price increase of energy. Then we calculate the values of the parameters δ and σ which are consistent with these data. This calculation is based on eqn. (38) which, when interpreted with input x as energy E (relative to its base year value), is written as follows:

$$E = e^{-(1-\sigma)\delta t} y (P_E^r)^{-\sigma} \tag{49}$$

By rearrangement, this equation gives an expression for σ in terms of δ as:

$$\sigma = \frac{\delta T + \log (E/y)}{\delta T - \log (P_E^r)} \tag{50}$$

where T specifies the particular time period of 55 years (from 1975 to 2030) in our applications.

After we examine the range of values of σ and δ which satisfy eqn. (50) for each region and scenario we arbitrarily choose a specific combination for each application for illustrative purposes in order to examine further implications of the (δ, σ) model. These other implications involve the degree of substitution of nonenergy inputs for energy inputs, the price changes for the nonenergy inputs due to substitution, and the relative contribution in the scenario projections.

The effect on the price of the nonenergy inputs Z due to substitution is given by eqn. (45). This drop in price relative to what the price would have been without substitution is given by:

$$(P_Z^r)\dagger = e^{-\delta T} P_Z^r = \left[\frac{1 - a(e^{-\delta T} P_E^r)^{1-\sigma}}{1 - a}\right]^{1/(1-\sigma)} \tag{51}$$

where $(P_Z^r)\dagger$ is the price of Z with substitution relative to its price without substitution and a is the relative value of energy in the total output y at the beginning of the time period. The term $e^{-\delta T}$ adjusts the relative price P_Z^r for the "natural" price increases of the nonenergy inputs due to technological development (see Section 4). Once the relative price of the nonenergy inputs is known, the relative change in price between energy and nonenergy inputs can be calculated.

Finally, the increase in use of nonenergy inputs due to substitution is given by eqn. (46).

$$(Z^r)\dagger = \left[\frac{1 - a}{1 - a(e^{-\sigma T} P_E^r)^{1-\sigma}}\right]^{\sigma/(1-\sigma)} = (P_Z^r)\dagger^{-\sigma} \tag{52}$$

where $(Z^r)\dagger$ is the quantity of inputs Z required with substitution relative to that without substitution.

5.1 The Aggregate Nonenergy Sector

Our definition of the nonenergy sector was given in Section 3.1 and is illustrated in Figure 12. In this application of the (δ, σ) model, we analyze the same data as were analyzed in Section 3 with the (γ, β) model. The data for the relative increase in GDP are taken from Table A. 3 in Appendix A. The energy input to this sector, as depicted in Figure 12, is intermediate input energy and is given in Table 17. The relative price increase for energy is as used throughout this report (2.4 times for Region III and 3.0 times otherwise).

The values of δ and σ as defined by eqn. (50) are shown graphically in Figure 17 for Regions I, II, and III for both the High and Low scenarios. This figure shows that relatively greater improvements in terms of output per unit of energy are projected for Region II in both the High and Low scenarios than for Regions I and III since combinations of δ and σ are larger for Region II. That is, Region II has a higher rate of technological development (δ) or a higher elasticity of substitution (σ) (or both) such that by 2030 equivalent output is being produced with less energy input. Similarly, for Regions I and III, the High scenario projections represent greater technological development and/or substitution than the corresponding Low scenario. This figure also shows that if technological development is not included in the model (the case of $\delta = 0$) the elasticities of substitution implied by the projections are very large – between 0.34 and almost 0.8 for the three regions.

In order to determine the implied price decrease of the nonenergy inputs and the relative increase in use of these inputs due to substitution [eqns. (51) and (52)], we choose specific values of δ and σ from Figure 17. For this purpose, we arbitrarily choose those values as defined by the dashed line in the figure. These values, given in Table 18, range between 0.24 percent per year and 0.68 percent per year for technological development

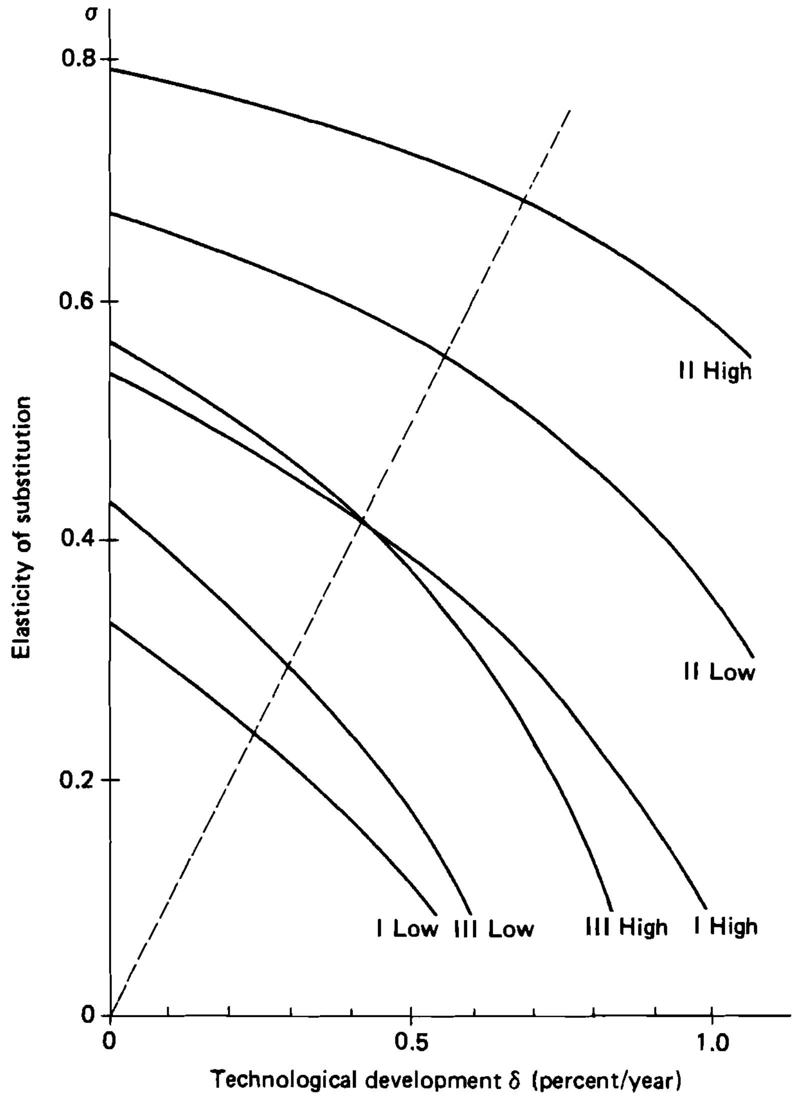

FIGURE 17 Technological development and substitution in the nonenergy sector in developed regions.

which seem reasonable given our definition of this concept.* The corresponding elasticities of substitution also range from 0.24 to 0.68 as a consequence of our selection of points. These may appear low compared to what other analyses have indicated but are lower because of the inclusion of the technological development factor.

*These should not be interpreted as labor productivity increases since in our definition, technological development is only one component of productivity increases.

TABLE 18 Application of the (δ, σ) model to the nonenergy sector.

Region	Technological development[a] δ (percent/year)	Elasticity of substitution[a] σ	Value share of energy[b] a (percent)	Energy/nonenergy relative price[c]	Increase in nonenergy inputs[d] (percent)
High scenario					
I (NA)	0.42	0.42	3.2	2.5	1.6
II (SU/EE)	0.68	0.68	7.7	2.2	4.8
III (WE/JANZ)	0.42	0.42	3.2	2.0	1.1
Low scenario					
I (NA)	0.24	0.24	3.2	2.8	1.2
II (SU/EE)	0.55	0.55	7.7	2.4	4.6
III (WE/JANZ)	0.30	0.30	3.2	2.1	0.9

[a] Representative values of technological development δ (percent/year) and elasticity of substitution σ as shown in Figure 17.
[b] Ratio of intermediate input energy payments [calculated with 1975 energy use data and base year (1972) final energy prices (Table 13)].
[c] See page 53.
[d] Shows percentage increase of nonenergy inputs required with substitution due to energy price increase relative to inputs required without substitution.

For these specific values of technological development (δ) and substitution (σ), it is possible to calculate the relative contribution of these two factors to overall energy conservation. This can be done by using eqn. (47) which expresses the energy–GDP elasticity ϵ in terms of δ, σ, and growth rates of output and prices. From that equation, the relative importance of δ and σ in reducing ϵ from unity can be easily derived. Following this procedure, we see that technological development contributes from 36 percent to 46 percent to energy conservation (and substitution, the remaining 64 percent to 54 percent) according to this model.

To examine the implications of the (δ, σ) model further, we require estimates of the value share, in the base year, of energy as an input to the nonenergy sector (parameter a in eqns. (51) and (52)). For this parameter, we estimate the total payments for the intermediate input energy and compare them with total GDP. Final (delivered) energy prices were discussed in Section 2 and summarized in Table 13. These prices include all factors, including taxes, that make up the delivered energy price. Using the given prices for Regions I and III and the Region I prices for Region II, we calculate energy payments using final energy consumption data from Table A.12 for freight transportation, for the service and industry sectors and including feedstocks. The resulting value share parameters, as shown in Table 18, range from 3 percent to almost 8 percent.

The data for δ, σ, and a in the first three columns of Table 18 can be used to calculate the extent of the substitution of nonenergy inputs for energy inputs. Equation (51) gives the relative *decrease* in nonenergy input prices. This decrease is relative to what prices would be if there were no energy price increase to cause the substitution. Based on the data given, this decrease would range from 0.92 to 0.97 depending on the region. The combination of the energy price increase and this nonenergy price decrease gives a relative price differential between these two inputs of between 2.0 and 2.8. It is important to understand the reason why this input relative price is less than the overall relative increase in energy price (either 3.0 or 2.4 depending on region). The (δ, σ) model allocates part of the energy price increase to increases in productivity due to technological development (at the rate of $e^{\delta t}$). As indicated in Section 4 where the model was described, the energy price increase which causes substitution between energy and nonenergy inputs must be increases over and above the "normal" price increases due to efficiency improvements of technological development. It is the energy price increases in excess of that due to technological development which when combined with the price decrease of nonenergy input that defines the relative price change of these two inputs.

Finally, as given in Table 18, eqn. (52) implies that the nonenergy inputs must be increased because of substitution by 1–1½ percent in Regions I and III and almost 5 percent in Region II. The much larger value for Region II is due to the estimated large value share (7.7 percent) of energy in the economy in the base year. These are increases over and above what would be required to produce the increased output to make up for the substitution away from energy inputs.

Having applied both the (δ, σ) and (γ, β) models to the nonenergy sector allows us to make a comparison of these two models. According to the (δ, σ) model, energy requirements are defined by eqn. (49) whereas for the (γ, β) model eqn. (2) applies. Rewriting this latter equation in the notation of this section gives:

$$E = y^{\gamma}(P_E^r)^{\beta} \tag{53}$$

A comparison with eqn. (49) indicates that for equivalence we must have:

$$\beta = -\sigma \tag{54}$$

and

$$y^{\gamma} = e^{-(1-\sigma)\delta t} y \tag{55}$$

The equivalence of β and σ is quite natural given the interpretation of σ as an approximation to a price elasticity as shown in Section 4, eqn. (20). The equivalence implied by eqn. (55) shows that the decreasing energy–output ratio, observed in historical data analysis and projected to continue even stronger in the future, is accounted for very differently in the two models. In the (γ, β) model, this characteristic is some sort of economy of scale (larger y implies less energy per unit y). In the (δ, σ) model this decreasing ratio is due to technological development as a function of time (with a correction due to substitution).

The two models may be compared in numerical terms by interpreting the same scenario projection data. If we use the values for δ and σ shown in Figure 17 and in Table 18 and if we assign $\beta = -\sigma$, then values for γ can be calculated from eqn. (55) for exact model equivalence. The calculation shows that γ would be between 0.92 and 0.94 for the High scenario projections (Regions I to III) and 0.89 to 0.92 for the Low scenario projections. These values are within the range given earlier (Table 15) for aggregate final energy and are somewhat higher than the historical values for aggregate final energy for these regions given in Table 12. It has been noted, however, that final demand energy has lower γs than intermediate input energy in the developed regions (Section 3.2.2). Thus one would expect that the income–GDP elasticities (γs) calculated for the nonenergy sector (based on intermediate input energy) would have higher values than the aggregate economy.

5.2 The Industry Sector

The (δ, σ) model of substitution and technological development perhaps most naturally applies to the industry sector. It is here where energy is truly an intermediate input in a production process. Because the industry sector is reasonably well defined and similar in all regions, this application can be made to all regions (except Region VII for which detailed sectoral projections were not made).

As outlined in Section 3.3 and illustrated in Figure 14, we define the industry sector, for analysis purposes here, as the mining, manufacturing, and construction sectors as defined in the MEDEE model. The energy input is taken to be the intermediate input energy excluding feedstocks (which are not substitutable by capital and labor in a way similar to intermediate input energy). The base year and scenario projection data for value added by and energy input to the industry sector are given in detail in Table A.12 and are listed in Table 19.

As defined in Section 3.3, the output y of the industry sector for this analysis is the value added plus payments for energy. The payments for energy have been estimated by using the values for final energy times the appropriate final energy price. The base year (1972 for prices) prices for the industry sector are given in Table 14 of Section 2. We use \$60/kWyr for Region III and \$30/kWyr for all other regions. Values for 2030 are taken to be 2.4 times the Region III and three times base year values for all other regions. The resulting estimates for energy payments are shown in Table 19 for all regions.

The ratio of energy payments to total output is also given in Table 19. We use only the base year values for the application of the (δ, σ) model, but these ratios are also shown for 2030 for the High and Low scenario projections. The increase in energy share between 1975 and 2030 for the industry sector is significantly different from similar increases examined earlier (Table 16) for the aggregate economies. As can be calculated from the data of Table 19, these shares increased from 33 to 68 percent (High scenario) and from 50 to 95 percent (Low scenario) for the developed Regions I, II, and III. These increases are greater than the aggregate economy increases shown earlier to be from 18 to 35 percent (High) and from 37 to 69 percent (Low). For the developing Regions IV, V, and VI, however, the reverse is true. For both the High and Low scenario projections, these energy shares increase from 2.0 to 2.3 times base year values for the industry sector while for the aggregate economy increases are shown in Table 16 to be 3.0 to 3.8 times. This comparison of the industry sector with the aggregate economy indicates that the industry sector for all regions is relatively similar while the conservation in the developed regions and the huge increase in energy shares projected for the developing regions are primarily due to other than the industry sector (i.e., to agriculture, household, and transportation).

The results of the application of the (δ, σ) model to the industry sector projections, according to eqn. (50), are illustrated in Figure 18 for the High scenario. In this figure, combinations of δ and σ are plotted that are consistent with the scenario projection data. These results are very similar to Regions I, II, and III for the nonenergy sector (Figure 17). Region II exhibits the largest values of δ and σ while Regions I and III are

TABLE 19 Data for application of (δ, σ) model to the industry sector in six regions.

Region	Industry[a] value added (10^9 \$)	Final energy[b] (GW)	Energy payments[c] (10^9 \$)	Output[d] y (10^9 \$)	Energy share[e]
1975					
I (NA)	478	619	19	497	3.7
II (SU/EE)	429	680	20	449	4.5
III (WE/JANZ)	980	651	39	1,019	3.8
IV (LA)	112	101	3	115	2.6
V (Af/SEA)	81	134	4	85	4.7
VI[f] (ME/NAf)	26	22	1	27	2.4
2030 High scenario					
I (NA)	1,997	1,466	132	2,129	6.2
II (SU/EE)	2,756	1,956	176	2,932	6.0
III (WE/JANZ)	4,046	1,767	254	4,300	5.9
IV (LA)	1,499	922	83	1,582	5.2
V (Af/SEA)	1,186	1,536	138	1,324	10.4
VI[f] (ME/NAf)	1,018	622	56	1,074	5.2
2030 Low scenario					
I (NA)	1,184	1,015	91	1,275	7.2
II (SU/EE)	1,791	1,422	128	1,919	6.7
III (WE/JANZ)	2,443	1,142	164	2,607	6.3
IV (LA)	849	531	48	897	5.3
V (Af/SEA)	619	764	69	688	10.0
VI[f] (ME/NAf)	447	292	26	473	5.6

[a] Value added (\$1975) in mining, manufacturing, and construction sectors excluding energy sector (see *f*). Data resulting from detailed scenario projections.
[b] Excluding feedstocks, data from Table A. 12.
[c] Using 1972 base year prices of \$60/kWyr for Region III and \$30/kWyr for all other regions for 1975 (see Table 14) and \$144(2.4 × \$60) for Region III and \$90 (3.0 × \$30) for all other regions for 2030.
[d] The sum of value added and energy payments.
[e] Energy payments expressed as a percentage of output.
[f] The mining sector has been excluded in Region VI.

similar but with much lower values than Region II. The developing Regions IV, V, and VI are grouped together but with still lower values of technological development and substitution.

As in the previous application of this model, we choose specific but arbitrary combinations of δ and σ as shown in Figure 18 and calculate the implied relative prices of energy inputs to nonenergy inputs and increases in requirements for nonenergy inputs due to substitution. For the three developed regions, these results for the industry sector (Table 20) are comparable to those for the entire nonenergy sector as given in Table 18. The additional results for the developing Regions IV, V, and VI indicate somewhat higher energy/nonenergy relative price increases. But the combination of these higher relative prices and lower elasticities of substitution result in estimates for increased use of the nonenergy inputs due to substitution very similar to those for Regions I and III.

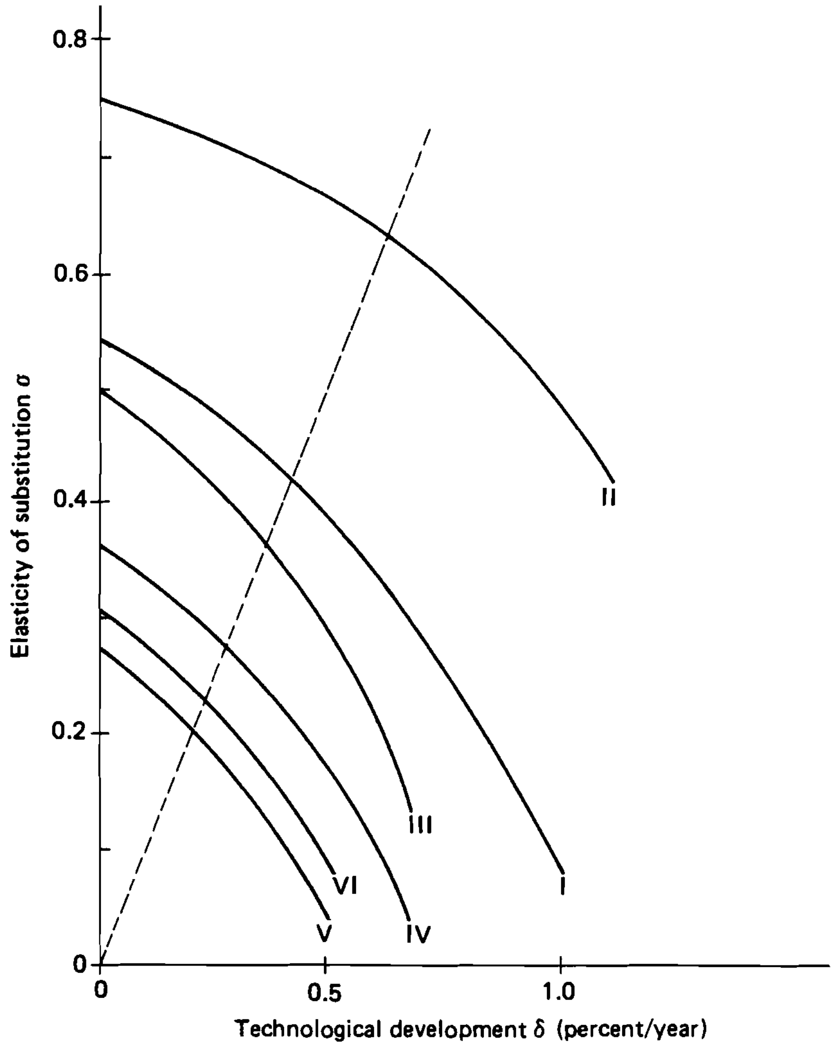

FIGURE 18 Technological development and substitution in industry in the High scenario.

5.3 Conclusions

The purpose of the examination of the scenario projections by means of an aggregate model like the (δ, σ) model was to understand better these projections with respect to energy prices, technological development, and substitution of other factors of production for energy.

As shown in detail earlier in this section, examples of model parameter values that are consistent with the scenario projections for the aggregate nonenergy sector show that technological development may be from about 0.3 to 0.7 percent per year and elasticities of substitution may also be from about 0.3 to 0.7. These values combine with our price assumptions to indicate that technological development may account for from 36 percent

TABLE 20 Application of the (δ, σ) model to the industry sector[a].

Region	Technological development δ (percent/year)	Elasticity of substitution σ	Value share of energy a (percent)	Energy/nonenergy relative price	Increase in nonenergy inputs (percent)
High scenario					
I (NA)	0.42	0.42	3.7	2.5	1.9
II (SU/EE)	0.63	0.63	4.5	2.2	2.6
III (WE/JANZ)	0.36	0.36	3.8	2.0	1.2
IV (LA)	0.27	0.27	2.6	2.7	1.0
V (Af/SEA)	0.20	0.20	4.7	2.9	1.5
IV[b] (ME/NAf)	0.22	0.22	2.4	2.8	0.8
Low scenario					
I (NA)	0.30	0.30	3.7	2.7	1.6
II (SU/EE)	0.53	0.53	4.5	2.4	2.5
III (WE/JANZ)	0.30	0.30	3.8	2.1	1.1
IV (LA)	0.26	0.26	2.6	2.7	1.0
V (Af/SEA)	0.23	0.23	4.7	2.8	1.7
VI[b] (ME/NAf)	0.18	0.18	2.4	2.8	0.7

[a]See Table 18 for explanation of column headings.
[b]The mining sector has been excluded from Region VI.

to 46 percent of projected energy conservation with the remainder coming from price-induced substitution.

The primary usefulness of the (δ, σ) model is to examine substitution of factors of production. The scenario projections generally assume a significant shift towards more capital-intensive production processes. This shift is most evident in the energy sector itself as documented in Energy Program Group 1981 and Kononov and Por 1979. Shifts to higher capital intensiveness in other resource sectors is also expected, but has not been examined in this work. The shift examined here is the substitution of capital and labor factors of production in place of energy due to projected price increases of energy. As mentioned in Section 3, this effect is a small change in a large sector (the nonenergy sector) whereas the increased capital intensiveness of the energy sector is a large change in a (relatively) small sector.

Based on the (δ, σ) model interpretation of the scenario projections, the increase in nonenergy inputs (capital and labor), due to the price increase of energy, is about 1 to 1½ percent in Regions I and III for the nonenergy sector. Much greater shifts were evident in Region II – almost 5 percent. This model, however, did not separate capital and labor as separate inputs; the shifts noted are from energy to some combination of more capital and labor. The split between these two primary inputs would depend on many factors, including relative price changes, not quantified in the scenario projections. Results for the industry sector alone are similar with increases of nonenergy inputs of 0.7 to 1.9 percent in all regions except Region II where the increase was about 2.5 percent.

In summary, with respect to increases in capital intensiveness our projections indicate large increases in the energy sector (documented elsewhere), and significant increases in the aggregate nonenergy sector, as well as the industry sector, due to energy price changes. Other effects, such as changes due to other resource price increases have not been examined.

ACKNOWLEDGMENTS

I am grateful to Wolf Häfele, Leader of the Energy Systems Program for guidance, inspiration, and the environment for performing the work reported here. I am grateful to Paul Basile for constant interaction during this work and helpful comments and suggestions on earlier drafts of this report.

Other members of the IIASA Energy Systems Program who, through their contributions, have made this work possible are: Malcolm Agnew, Christina Derstroff, Claire Doblin, John Eddington, Alois Hölzl, Arshad Khan, Alexander Papin, Jyoti Parikh, and Leo Schrattenholzer.

REFERENCES

Allen, R.G.D. (1967) Macro-Economic Theory. London: Macmillan Press.

Alterman, R. (1977) The Energy/Real Gross Domestic Product Ratio–An Analysis of Changes During the 1966–1968 Period in Relation to Long-Run Trends. Bureau of Economic Analysis Staff Paper No. 30. Washington, D.C.: U.S. Department of Commerce.

Basile, P.S. (1980) The IIASA Set of Energy Models: Its Design and Application. RR-80-31. Laxenburg, Austria: International Institute for Applied Systems Analysis.

Bureau of the Census. 1978. Statistical Abstract of the U.S., 1977. Washington, D.C.: U.S. Department of Commerce.

Chant, V.G. (1981) Scenario Projections for Region VII, China and Centrally Planned Asian Economies. Forthcoming IIASA Working Paper.

Doblin, C. (1979) Historical Data Series. WP-79-87. Laxenburg, Austria: International Institute for Applied Systems Analysis.

Energy Program Group (1981) Energy in a Finite World: A Global Systems Analysis Report by the Energy Systems Program Group of the International Institute for Applied Systems Analysis, Wolf Häfele, Program Leader. Cambridge, Massachusetts: Ballinger.

Hicks, N. L. (1976) A model of trade and growth for the developing world. European Economic Review, 7: 239–255.

Hogan, W.W. (1980) Dimensions of energy demand. Selected Studies of Energy: Background Papers for Energy: The Next Twenty Years, H.H. Landsberg ed. Cambridge, Massachussetts: Ballinger.

Keyfitz, N. (1977) Population of the World and its Regions 1975–2050. WP-77-7. Laxenburg, Austria: International Institute for Applied Systems Analysis.

Khan, A.M., and A. Hölzl (1982) Evolution of Future Energy Demands till 2030 in Different World Regions: An Assessment Made for the Two IIASA Scenarios. RR-82-14. Laxenburg, Austria: International Institute for Applied Systems Analysis.

Kononov, Yu.O., and R. Por (1979) The Economic IMPACT Model. RR-79-8. Laxenburg, Austria: International Institute for Applied Systems Analysis.

Lapillone, B. (1978) MEDEE-2: A Model for Long-term Energy Demand Evaluation. RR-78-17. Laxenburg, Austria: International Institute for Applied Systems Analysis.

Manne, A. (1977) Energy economy interactions: the fable of the elephant and the rabbit? Appendix B, Volume 2, Energy and the Economy. Energy Modeling Forum. Stanford, California: Stanford University, Institute for Energy Studies.

OECD (1978) Main Economic Indicators, April. Paris: Organization for Economic Cooperation and Development.

Schrattenholzer, L. (1981) The Energy Supply Model MESSAGE. RR-81-31. Laxenburg, Austria: International Institute for Applied Systems Analysis.

UN (1976) Yearbook of National Accounts Statistics, Volume II. New York: United Nations.

UN (1978) Monthly Bulletin of Statistics. January. New York: United Nations.

WAES (1977) Energy: Global Prospects 1976–2000. Workshop on Alternative Energy Strategies. New York: McGraw-Hill.
WEC (1978) World Energy Resources 1985–2020. The World Energy Conference. Sevenoaks, Kent: IPC Science and Technology Press.
World Bank (1977) World Bank Atlas, 12th Edition. Washington, DC: World Bank.

APPENDIX A: RECENT HISTORICAL AND SCENARIO PROJECTION DATA BY REGION 1950–2030

TABLE A. 1 Population by region 1950–1975 ($\times 10^6$).

Region	1950	1955	1960	1965	1970	1975
I (NA)	166	182	199	214	226	237
II (SU/EE)	268	289	311	331	346	363
III (WE/JANZ)	431	454	479	508	533	560
IV (LA)	164	188	216	247	283	319
V (Af/SEA)	797	875	980	1,110	1,258	1,422
VI (ME/NAf)	67	76	86	98	114	133
VII (C/CPA)	599	648	704	767	836	912
World	2,492	2,712	2,975	3,275	3,596	3,946

SOURCE: C. Doblin, Historical Data Series, September 1979, IIASA WP-79-87.

TABLE A. 2 GDP[a] by region 1950–1975 [10^9 US$ (1975)].

Region	1950	1955	1960	1965	1970	1975
I (NA)	727	893	1,008	1,270	1,487	1,670
II (SU/EE)	135	233	364	491	693	930
III (WE/JANZ)	681	869	1,111	1,471	1,971	2,385
IV (LA)	86	111	140	182	234	340
V (Af/SEA)	104	128	152	189	247	340
VI (ME/NAf)	24	35	47	74	111	190
VII (C/CPA)	61	102	132	166	222	320
World	1,818	2,371	2,954	3,843	4,965	6,175

[a]In constant 1975 US$ using 1975 prices and 1975 official exchange rates. The appropriate US GDP implicit price deflator to convert to 1980 US dollars is 1.41.

SOURCE: C. Doblin, Historical Data Series (see Table A.1) using the following sources: *Yearbook of National Accounts Statistics*, 1976, Vol. II, United Nations, *World Bank Atlas*, 12th edition, 1977, World Bank, *Main Economic Indicators*, OECD, April 1978.

TABLE A. 3 GDP by region 1975–2030 [10^9 US$ (1975)].

Region	High scenario 1975	1985	2000	2015	2030
I (NA)	1,670	2,535	4,126	5,889	7,926
II (SU/EE)	930	1,515	2,729	4,571	7,658
III (WE/JANZ)	2,385	3,633	5,999	8,688	11,693
IV (LA)	340	620	1,272	2,193	3,569
V (Af/SEA)	340	597	1,207	2,112	3,488
VI (ME/NAf)	190	381	900	1,668	2,918
VII (C/CPA)	320	521	939	1,573	2,450
World	6,175	9,800	17,170	26,700	39,700
Region	Low scenario 1975	1985	2000	2015	2030
I (NA)	1,670	2,265	3,049	3,592	4,170
II (SU/EE)	930	1,445	2,420	3,504	4,713
III (WE/JANZ)	2,385	3,260	4,452	5,566	6,656
IV (LA)	340	540	918	1,430	2,229
V (Af/SEA)	340	543	924	1,398	1,995
VI (ME/NAf)	190	328	643	959	1,310
VII (C/CPA)	320	443	690	999	1,345
World	6,175	8,820	13,100	17,450	22,400

TABLE A. 4 GDP per capita by region 1950–1975 [US$ (1975)].

Region	1950	1955	1960	1965	1970	1975
I (NA)	4,380	4,907	5,065	5,935	6,580	7,046
II (SU/EE)	504	806	1,170	1,483	2,003	2,562
III (WE/JANZ)	1,580	1,914	2,319	2,896	3,698	4,259
IV (LA)	524	590	648	737	827	1,066
V (Af/SEA)	130	146	155	170	196	239
VI (ME/NAf)	358	461	547	755	974	1,429
VII (C/CPA)	102	157	188	216	266	351
World	730	874	993	1,173	1,381	1,565

SOURCE: Tables A. 1 and A. 2.

TABLE A. 5 GDP per capita by reigon 1975–2030 [US$ (1975)].

Region	High scenario 1975	1985	2000	2015	2030
I (NA)	7,046	9,864	14,528	19,500	25,160
II (SU/EE)	2,562	3,855	6,259	9,788	15,950
III (WE/JANZ)	4,259	5,946	8,822	11,950	15,250
IV (LA)	1,066	1,462	2,212	3,165	4,480
V (Af/SEA)	239	321	477	686	980
VI (ME/NAf)	1,429	2,165	3,644	5,523	8,270
VII (C/CPA)	351	475	706	1,015	1,430
World	1,565	2,035	2,820	3,750	4,980
Region	Low scenario 1975	1985	2000	2015	2030
I (NA)	7,046	8,813	10,736	11,890	13,240
II (SU/EE)	2,562	3,677	5,550	7,503	9,820
III (WE/JANZ)	4,259	5,336	6,547	7,660	8,680
IV (LA)	1,066	1,274	1,600	2,060	2,800
V (Af/SEA)	239	292	366	454	560
VI (ME/NAf)	1,429	1,864	2,603	3,175	3,710
VII (C/CPA)	351	404	519	645	780
World	1,565	1,830	2,150	2,450	2,810

SOURCE: Table 2 and Table A. 3.

TABLE A. 6 Primary commercial energy consumption[a] by region 1950–1975 (GW).

Region	1950	1955	1960	1965	1970	1975[b]
I (NA)	1,138	1,340	1,532	1,850	2,363	2,654
II (SU/EE)	419	631	855	1,156	1,462	1,835
III (WE/JANZ)	665	855	1,026	1,353	1,825	2,256
IV (LA)	61	92	127	166	247	338
V (Af/SEA)	59	86	124	178	266	328
VI (ME/NAf)	10	15	26	35	59	126
VII (C/CPA)	33	82	224	202	285	461
World	2,385	3,101	3,914	4,940	6,507	7,998[c]

[a] Apparent inland consumption for each region (excludes international bunkers). Hydro and nuclear generated electricity counted on primary equivalent basis.

[b] Data for 1975 were compiled from a variety of sources and may not be fully compatible with data for earlier years.

[c] Excludes 210 GW for bunkers.

SOURCE: C. Doblin, Historical Data Series (see Table A. 1) for all regions except Region VII which comes from V. Chant "Scenario Projections for Region VII: China and Centrally Planned Asian Economies", IIASA Working Paper, forthcoming.

TABLE A. 7 Primary commercial energy consumption by region 1975–2030, High and Low scenarios (TW).

Region	High scenario 1975	1985	2000	2015	2030
I (NA)	2.65	3.01	3.89	4.96	6.02
II (SU/EE)	1.84	2.48	3.69	5.23	7.33
III (WE/JANZ)	2.26	2.99	4.29	5.75	7.14
IV (LA)	0.34	0.63	1.34	2.32	3.68
V (Af/SEA)	0.33	0.64	1.43	2.70	4.65
VI (ME/NAf)	0.13	0.30	0.77	1.47	2.38
VII (C/CPA)	0.46	0.78	1.44	2.54	4.45
World	8.21[a]	10.83	16.83	24.97	35.65

Region	Low scenario 1975	1985	2000	2015	2030
I (NA)	2.65	2.83	3.31	3.68	4.37
II (SU/EE)	1.84	2.30	3.31	4.15	5.00
III (WE/JANZ)	2.26	2.69	3.39	3.97	4.54
IV (LA)	0.34	0.56	0.97	1.53	2.31
V (Af/SEA)	0.33	0.57	1.07	1.75	2.66
VI (ME/NAf)	0.13	0.27	0.56	0.90	1.23
VII (C/CPA)	0.46	0.63	0.98	1.51	2.29
World	8.21[a]	9.85	13.59	17.50	22.39

[a] Including 0.21 TW for international bunkers.
SOURCE: IIASA ENP.

TABLE A. 8 Primary energy consumption per capita by region 1950–1975 (kW/cap).

Region	1950	1955	1960	1965	1970	1975[a]
I (NA)	6.9	7.4	7.7	8.6	10.5	11.2
II (SU/EE)	1.6	2.2	2.7	3.5	4.2	5.1
III (WE/JANZ)	1.5	1.9	2.1	2.7	3.5	4.0
IV (LA)	0.36	0.47	0.57	0.67	0.87	1.06
V (Af/SEA)	0.07	0.10	0.13	0.16	0.21	0.23
VI (ME/NAf)	0.15	0.20	0.30	0.36	0.52	0.95
VII (C/CPA)	0.06	0.13	0.32	0.26	0.34	0.51
World	0.97	1.14	1.31	1.51	1.81	2.08

[a] See [b] Table A. 6 and [a] Table A. 7.
SOURCE: Tables A. 1 and A. 6.

TABLE A. 9 Primary energy consumption per capita by region 1975–2030 (kW/cap).

Region	High scenario 1975	1985	2000	2015	2030
I (NA)	11.2	11.7	13.7	16.4	19.1
II (SU/EE)	5.0	6.3	8.5	11.2	15.3
III (WE/JANZ)	4.0	4.9	6.3	7.9	9.3
IV (LA)	1.1	1.5	2.3	3.3	4.6
V (Af/SEA)	.23	.34	.56	.88	1.3
VI (ME/NAf)	.95	1.69	3.11	4.87	6.74
VII (C/CPA)	.51	.71	1.08	1.64	2.60
World	2.08	2.25	2.77	3.50	4.47
Region	**Low scenario 1975**	**1985**	**2000**	**2015**	**2030**
I (NA)	11.2	11.0	11.7	12.2	13.9
II (SU/EE)	5.0	5.9	7.6	8.7	10.4
III (WE/JANZ)	4.0	4.4	5.0	5.4	5.9
IV (LA)	1.1	1.3	1.7	2.2	2.9
V (Af/SEA)	.23	.31	.42	.57	.75
VI (ME/NAf)	.95	1.52	2.28	2.99	3.48
VII (C/CPA)	.51	.58	.74	.98	1.34
World	2.08	2.05	2.24	2.46	2.81

SOURCE: Table 2 and Table A. 7.

TABLE A. 10 Final commercial energy[a] by region 1950–1975 (GW).

Region	1950	1955	1960	1965	1970	1975[b]
I (NA)	960	1,087	1,206	1,430	1,787	1,871
II (SU/EE)	359	531	704	922	1,138	1,277
III (WE/JANZ)	549	690	796	1,013	1,336	1,588
IV (LA)	49	73	100	133	191	255
V (Af/SEA)	50	71	104	147	212	253
VI (ME/NAf)	9	13	22	29	48	106
VII (C/CPA)	30	73	193	168	244	393
World	2,006	2,538	3,125	3,842	4,956	5,743

[a] Data for 1950–1970 are estimated from primary energy statistics accounting for average losses and electricity conversion.

[b] Data for 1975 were compiled from a variety of sources and may not be fully compatible with data for earlier years.

TABLE A. 11 Final commercial energy[a] by region 1975–2030, High and Low scenarios (GW).

Region	High scenario 1975	1985	2000	2015	2030
I (NA)	1,871	2,130	2,628	3,181	3,665
II (SU/EE)	1,277	1,702	2,387	3,122	4,114
III (WE/JANZ)	1,589	2,195	3,035	3,769	4,375
IV (LA)	255	486	1,005	1,700	2,641
V (Af/SEA)	253	497	1,063	1,916	3,174
VI (ME/NAf)	106	231	578	1,041	1,638
VII (C/CPA)	393	675	1,234	2,091	3,196
World	5,744	7,916	11,930	16,820	22,800

Region	Low scenario 1975	1985	2000	2015	2030
I (NA)	1,871	2,015	2,257	2,460	2,636
II (SU/EE)	1,277	1,617	2,171	2,616	2,952
III (WE/JANZ)	1,589	1,963	2,393	2,738	2,988
IV (LA)	255	425	733	1,119	1,656
V (Af/SEA)	253	442	802	1,287	1,877
VI (ME/NAf)	106	205	434	649	868
VII (C/CPA)	393	548	845	1,217	1,589
World	5,744	7,215	9,635	12,090	14,570

[a] Including feedstocks.

TABLE A. 12 Final energy consumption by sector 1975–2030, Region I (NA) (GWyr/yr).

Sector	1975	High scenario 1985	2000	2015	2030	Low scenario 1985	2000	2015	2030
Agriculture	34	47	64	78	88	42	52	56	61
Industry[a]	619	785	1,031	1,260	1,466	730	852	934	1,015
Service	162	172	201	226	248	158	166	173	179
Transportation	541	546	651	836	1,013	522	560	625	684
of which, passenger	(398)	(334)	(314)	(365)	(392)	(330)	(304)	(325)	(338)
Households	411	432	464	493	495	428	450	467	462
Total commercial final (excl. feedstocks)	1,768	1,983	2,410	2,894	3,309	1,880	2,080	2,254	2,401
Feedstocks	104	147	218	287	355	136	177	206	235
Total commercial final (incl. feedstocks)	1,871	2,130	2,628	3,181	3,665	2,015	2,257	2,460	2,636
Noncommercial[b]	0	0	0	0	0	0	0	0	0

[a]Mining, manufacturing, and construction.
[b]Firewood, animal waste, etc.

TABLE A. 12 Final energy consumption by sector 1975–2030, Region II (SU/EE) (GWyr/yr).

Sector	1975	High scenario 1985	2000	2015	2030	Low scenario 1985	2000	2015	2030
Agriculture	28	38	52	65	72	38	55	70	82
Industry[a]	680	892	1,212	1,515	1,956	847	1,117	1,308	1,422
Service	73	94	135	185	241	87	116	139	159
Transportation	224	297	418	569	786	283	376	463	549
of which, passenger	(56)	(86)	(125)	(169)	(213)	(77)	(105)	(131)	(152)
Households	220	272	348	410	449	265	326	372	392
Total commercial final (excl. feedstocks)	1,225	1,592	2,165	2,745	3,504	1,519	1,990	2,351	2,604
Feedstocks	51	110	222	377	610	98	180	265	348
Total commercial final (incl. feedstocks)	1,277	1,702	2,387	3,122	4,114	1,617	2,171	2,616	2,952
Noncommercial[b]	44	44	44	44	44	44	44	44	44

[a]Mining, manufacturing and construction.
[b]Fire wood, animal waste, etc.

TABLE A. 12 Final energy consumption by sector 1975–2030, Region III (WE/JANZ) (GWyr/yr).

Sector	1975	High scenario 1985	2000	2015	2030	Low scenario 1985	2000	2015	2030
Agriculture	27	39	53	62	58	34	39	41	39
Industry[a]	651	876	1,217	1,513	1,767	783	927	1,047	1,142
Service	68	81	114	148	188	75	100	121	144
Transportation	313	475	708	932	1,114	406	526	624	689
of which, passenger	(188)	(289)	(415)	(530)	(604)	(241)	(307)	(360)	(384)
Households	403	542	664	747	806	501	592	658	696
Total commercial final (excl. feedstocks)	1,462	2,012	2,756	3,402	3,933	1,799	2,183	2,491	2,710
Feedstocks	126	183	279	367	443	164	210	247	278
Total commercial final (incl. feedstocks)	1,589	2,195	3,035	3,769	4,375	1,963	2,393	2,738	2,988
Noncommercial[b]	0	0	0	0	0	0	0	0	0

[a]Mining, manufacturing, and construction.
[b]Fire wood, animal waste, etc.

TABLE A. 12 Final energy consumption by sector 1975–2030, Region IV (LA) (GWyr/yr).

Sector	1975	High scenario 1985	2000	2015	2030	Low scenario 1985	2000	2015	2030
Agriculture	1	4	13	27	40	4	12	24	36
Industry[a]	101	193	382	625	922	163	259	378	531
Service	3	6	14	24	38	6	12	24	42
Transportation	105	195	410	713	1,154	172	304	473	716
of which, passenger	(32)	(61)	(133)	(243)	(402)	(55)	(105)	(174)	(277)
Households	28	51	98	148	217	49	88	123	169
Total commercial final (excl. feedstocks)	238	449	915	1,537	2,372	394	674	1,023	1,503
Feedstocks	17	37	89	163	268	31	58	96	153
Total commercial final (incl. feedstocks)	254	486	1,004	1,699	2,640	425	733	1,119	1,656
Noncommercial[b]	109	109	109	109	109	109	109	109	109

[a]Mining, manufacturing and construction.
[b]Fire wood, animal waste, etc.

TABLE A. 12 Final energy consumption by sector 1975–2030, Region V (Af/SEA) (GWyr/yr).

Sector	1975	High scenario 1985	2000	2015	2030	Low scenario 1985	2000	2015	2030
Agriculture	4	18	56	123	188	17	50	104	154
Industry[a]	134	265	258	949	1,536	228	375	561	764
Service	2	5	15	30	47	5	11	19	28
Transportation	76	130	274	520	909	121	224	380	607
of which, passenger	(32)	(54)	(124)	(266)	(499)	(51)	(106)	(204)	(358)
Households	25	54	106	167	251	50	102	154	219
Total commercial final (excl. feedstocks)	242	472	999	1,788	2,931	421	762	1,219	1,772
Feedstocks	11	25	63	128	242	21	40	68	104
Total commercial final (incl. feedstocks)	253	497	1,063	1,915	3,173	442	802	1,287	1,876
Noncommercial[b]	344	344	344	344	344	344	344	344	344

[a] Mining, manufacturing, and construction.
[b] Fire wood, animal waste, etc.

TABLE A. 12 Final energy consumption by sector 1975–2030, Region VI (ME/NAf) (GWyr/yr).

Sector	1975	High scenario 1985	2000	2015	2030	Low scenario 1985	2000	2015	2030
Agriculture	1	2	8	16	26	2	7	13	20
Industry[a]	40	101	261	459	670	90	193	270	334
Service	1	3	11	27	55	3	10	18	35
Transportation	42	82	200	363	612	68	143	225	314
of which, passenger	(8)	(18)	(47)	(102)	(209)	(16)	(37)	(64)	(105)
Households	14	24	49	79	120	24	44	65	88
Total commercial final (excl. feedstocks)	97	213	530	944	1,482	187	396	591	791
Feedstocks	9	19	48	97	155	19	38	57	77
Total commercial final (incl. feedstocks)	106	231	578	1,041	1,638	205	434	649	868
Noncommercial[b]	10	10	10	10	10	10	10	10	10

[a] Mining, manufacturing and construction.
[b] Fire wood, animal waste, etc.

TABLE A. 12 Final energy consumption by sector 1975–2030, Region VII (C/CPA) (GWyr/yr).

		High scenario				Low scenario			
Sector	1975	1985	2000	2015	2030	1985	2000	2015	2030
Agriculture, Industry[a]	232								
Service									
Transportation	31								
of which, passenger									
Households	117								
Total commercial final[c] (excl. feedstocks)	380	650	1,178	1,976	2,996	528	810	1,157	1,499
Feedstocks[d]	13	25	56	115	200	20	35	60	90
Total commercial final (incl. feedstocks)	393	675	1,234	2,091	3,196	548	845	1,217	1,589
Noncommercial[b]									

[a]Mining, manufacturing, and construction.
[b]Fire wood, animal waste, etc.
[c]Excluding feedstocks.
[d]Estimated on cross-regional GDP per capita basis.

TABLE A. 13 Electricity consumption as a fraction of final energy[a] by region 1950–2030 (percent).

Region	Historical 1950	1975	High scenario 2000	2030	Low scenario 2000	2030
I (NA)	4.5	13.0	21.8	26.7	22.4	27.9
II (SU/EE)	3.6	9.2	16.1	22.9	15.2	21.6
III (WE/JANZ)	5.8	13.8	19.2	25.6	20.0	26.3
IV (LA)	5.3	7.0	11.8	16.7	11.0	16.1
V (Af/SEA)	3.2	3.8	8.6	14.2	7.2	10.8
VI (ME/NAf)	3.3	5.2	7.8	11.9	7.8	11.0
VII (C/CPA)	1.3	3.7	4.8	6.3	4.8	6.3
World	4.6	11.1	16.1	19.8	16.4	20.3

[a] Electricity consumed by the user (which is typically 85 percent of generation) computed as a fraction of final energy excluding feedstocks.

APPENDIX B: THE SEVEN WORLD REGIONS OF THE IIASA ENERGY PROGRAM

Region I: North America (NA)

Highly developed market economies with energy resources.

Canada
United States of America

Region II: The Soviet Union and Eastern Europe (SU/EE)

Highly developed centrally planned economies with energy resources.

Albania
Bulgaria
Czechoslovakia
German Democratic Republic
Hungary
Poland
Romania
Union of Soviet Socialist Republics

Region III: W. Europe, Japan, Austrialia, New Zealand, South Africa, and Israel (WE/JANZ)

Highly developed market economies with relatively low energy resources.

Member Countries of the European Community

Belgium
Denmark
France
Germany, Federal Republic of
Ireland
Italy
Luxemburg
Netherlands
United Kingdom

Other Western European Countries

Austria
Cyprus
Finland
Greece
Iceland
Norway
Portugal
Spain
Sweden
Switzerland
Turkey
Yugoslavia

Others

Australia
Israel
Japan
New Zealand
South Africa

Region IV: Latin America (LA)

Developing economies with some energy resources and significant population growth.

Argentina
Bahamas
Belize
Bolivia
Brazil
Chile
Colombia
Costa Rica
Cuba
Dominican Republic
Ecuador
El Salvador
Guadeloupe
Guatemala
Guyana
Haiti
Honduras
Jamaica
Martinique
Mexico
Netherlands Antilles
Nicaragua
Panama
Paraguay
Peru
Puerto Rico
Surinam
Trinidad and Tobago
Uruguay
Venezuela
Other Caribbean

Region V: Africa (Except Northern Africa and South Africa), South and Southeast Asia (Af/SEA)

Slowly developing economies with some energy resources and significant population growth.

Africa

Angola
Benin
Botswana
Burundi
Cameroon
Cape Verde
Central African Republic
Chad
Congo
Ethiopia
Gabon
Gambia
Ghana
Guinea
Guinea Bissau
Ivory Coast
Kenya
Lesotho
Liberia
Madagascar
Malawi
Mali
Malta
Mauritania
Mauritius
Morocco
Mozambique
Namibia
Niger
Nigeria
Reunion
Rwanda
Senegal
Sierra Leone
Somalia
Sudan
Swaziland
Tanzania, United Republic of
Togo
Tunisia
Uganda
Upper Volta
Western Sahara
Zaire
Zambia
Zimbabwe

Asia

Afghanistan
Bangladesh
Brunei
Burma
Comoros
Hong Kong
India
Indonesia
Korea, Republic of (South)
Macau
Malaysia
Nepal
Pakistan
Papua New Guinea
Philippines
Singapore
Sri Lanka
Taiwan
Thailand
East Timor
West South Asia n.e.s.

Region VI: Middle East and Northern Africa (ME/NAf)

Developing economies with large energy resources.

Member Countries of the Organization of Arab Petroleum Exporting Countries (OAPEC)

Algeria	Libyan Arab Republic
Bahrain	Qatar
Egypt	Saudi Arabia
Iraq	Syrian Arab Republic
Kuwait	United Arab Emirates

Others

Iran
Jordan
Lebanon
Oman
Yemen
Yemen, People's Democratic Republic of

Region VII: China and Centrally Planned Asian Economies (C/CPA)

Developing centrally planned economies with energy resources.

China, People's Republic of
Kampuchea, Democratic (formerly Cambodia)
Korea, Democratic Republic of
Laos, People's Democratic Republic of
Mongolia
Viet-Nam, Socialist Republic of

APPENDIX C: ENERGY UNITS AND CONVERSION FACTORS

Abbreviation

k = kilo	10^3	kWh =	kilowatt-hour
M = mega	10^6	kWyr =	kilowatt-year (8760 kWh)
G = giga	10^9	BTU =	British Thermal Unit
T = tera	10^{12}	cal =	calorie
		J =	joule

Energy Units – exact but rounded

1 kWh	=	3413 BTU	10^6 BTU	=	293 kWh
1 kWyr	=	$29.9 \cdot 10^6$ BTU	10^6 BTU	=	0.0334 kWyr
1 kWh	=	860 kcal	10^6 kcal	=	1163 kWh
1 kWyr	=	0.0982 kcal	10^6 kcal	=	0.133 kWyr
1kJ	=	0.948 BTU	1 BTU	=	1.055 kJ

Weight and Volume Units of Energy Products – approximate

Coal – metric ton (1000 kg) of coal equivalent (mtce)
- 1 mtce is defined as $7.00 \cdot 10^6$ kcal
  - which is $27.78 \cdot 10^6$ BTU or 0.929 kWyr

Oil* – barrel (bbl), metric ton of oil equivalent (mtoe)
- 1 bbl oil is defined as $5.80 \cdot 10^6$ BTU which is 0.194 kWyr
- 1.10^6 bbl/day is then 70.83 GW
- 1 mtoe is defined as 7.30 bbl which is 1.417 kWyr

Gas – cubic meter (m^3)
- 1 ft^3 natural gas is defined as 1000 BTU
- 1 m^3 natural gas is then $0.0353 \cdot 10^6$ BTU or 1.18 kWyr

$1 \cdot 10^{12}$ BTU	=	0.0334 GWyr	1 GWyr	=	$29.9 \cdot 10^{12}$ BTU
$1 \cdot 10^6$ mtce	=	0.929 GWyr	1 GWyr	=	$1.076 \cdot 10^6$ mtce
$1 \cdot 10^6$ mtoe	=	1.417 GWyr	1 GWyr	=	$0.706 \cdot 10^6$ mtoe
$1 \cdot 10^6$ bbl	=	0.194 GWyr	1 GWyr	=	$5.15 \cdot 10^6$ bbl
$1 \cdot 10^9$ m^3 n.g.	=	1.18 GWyr	1 GWyr	=	$0.847 \cdot 10^9$ m^3 n.g.
$1 \cdot 10^6$ bbl/day	=	70.8 GW	1 GW	=	$0.014 \cdot 10^6$ bbl/day

*World average crude S.G. 0.86 or API33.

WATER DEMAND FOR GENERATING ELECTRICITY: A Mathematical Programming Approach with Application in Poland

J.C. Stone, F.D. Singleton, Jr.
University of Houston, Industry Studies Program, Houston, Texas, USA

M. Gadkowski, A. Salewicz
Institute of Meteorology and Water Management, Warsaw, Poland

W. Sikorski
International Institute for Applied Systems Analysis, Laxenburg, Austria

SUMMARY

This report documents a water demand study developed as a collaborative effort between the International Institute for Applied Systems Analysis (IIASA), Laxenburg, Austria; the Institute of Meteorology and Water Management (IMGW), Warsaw, Poland; and the Industry Studies Program of the University of Houston, Houston, Texas, USA. Participants in the study developed and applied a mathematical programming model of resource use in an electric power plant. The model specifically represents a hypothetical, coal-fired plant located on the Wisła (Vistula) River in Poland. The modeling techniques, however, have very general applicability.

Section 1 of the report provides some background information and introduction. Section 2 is a nonmathematical description of the model. The principal decision variables with respect to plant design and operation are identified, and the objective according to which the decisions are made is specified to be minimization of the costs of annual operation. Applicable constraints limiting the design and operating options are identified next. These constraints relate primarily to standards of air and water quality. Logical conditions pertaining to the technical options also require the use of a limited number of integer (0,1) variables in the model. The model explicitly represents plant operations in each of a number of user-defined seasons and simultaneously optimizes plant design and plant operation in all of the defined seasons.

Section 3 describes in detail the principal options of plant design and operation, making extensive use of flow diagrams. Modeled options relate to fuel provision and the cooling system. Two grades of coal are available for use, and two alternative modes of coal transport, railroad and slurry pipeline, are modeled. The optimal choice depends on cost

and on air and water pollution standards. The options for the cooling system are extensive and include:

1. *How much the temperature of cooling water rises in condensing the exhaust steam from the turbine*
2. *Whether or not a cooling tower is used and, if so, whether water from the tower is discharged or recycled*
3. *Whether the flow of cooling water across each of six condensers is independent or the flow passes across two paired condensers*
4. *How much the temperature of cooling water falls when circulated through a cooling tower*
5. *How much the concentration of dissolved solids is allowed to build up in a cooling tower with recycle flow*
6. *Whether to discharge or treat the so-called blowdown extracted from the flow through a cooling tower with recycle*
7. *Whether or not to dilute heated cooling water (with additional river water) before discharge to the river*
8. *Whether or not to recirculate some amount of heated cooling water to maintain a minimum required temperature at the inlet to the condenser*

The optimum choice over these options depends on a complex interplay of cost, water pollution constraints, and also air pollution constraints through the effects on plant thermal efficiency of alternative cooling system configurations.

Following the discussion of design and operating options for the plant, the structure of the model is described in detail. Specifically, modeling correspondences are established between plant processes and model columns and between flows of materials or energy and model rows. Some general issues in establishing these correspondences are briefly discussed. The specification of model structure is completed by detailing the mathematical formulation of identified constraints, e.g., those relating to air and water pollution, and of an accounting structure for water use.

How the model's structure is filled in with specific numerical coefficients is described next. In practice, the coefficients are specified by using so-called matrix generators, which automate the calculations. The general logic behind the specification of coefficients is described in the report. The section concludes with a brief discussion of the availability of data for the model, generally good, and a few comments on the definition of seasons.

Section 4 focuses on the use of the model, and includes a brief discussion of procedures for operating the model, its size, and computability. A wealth of information is available from the model. In particular, it can be used to estimate the capital and operating costs, resource demands and pollution loads that result from operating the plant under a wide variety of conditions. The report presents the results of some illustrative analyses of water demand performed with the model. These include calculation of derived demand curves for water withdrawals and heat discharges, of the trade-off between water losses and water withdrawals, and of the effects on the marginal and average costs of electricity caused by reducing water withdrawals. The results are not definitive but highlight the power of the method and the importance of an integrated approach to studying water demand and other aspects of industrial resource use.

1 INTRODUCTION

Mathematical programming has for some time been an important tool for modeling industrial operations. Such models have seen widespread application to the solution of scheduling, resource allocation, and transportation problems. Models have also been developed for analyzing and forecasting industrial activities under new economic and/or regulatory conditions, and since the early 1970s, serious attempts have been made to expand them to include considerations of residuals generation and management. Many of these attempts have their conceptual origins in the work of Russell (1973). Plant-level models of petroleum refining (Russell 1973) and of iron and steel production (Russell and Vaughn 1976) have been developed at Resources for the Future in the USA. Plant- and industry-level models have been developed at the University of Houston, USA, for electricity generation, petroleum refining, and manufacture of several important chemical products, such as chlorine and caustic soda, ammonia and other nitrogenous fertilizers, ethylene and other organic chemicals, synthetic rubber, and certain plastics and polyesters (Thompson et al. 1976, Thompson et al. 1977, Thompson et al. 1978). Plant-level models of paper mills have been developed by Sawyer et al. (1976).

The water demand study in this report developed as a collaborative arrangement between the International Institute for Applied Systems Analysis (IIASA), Laxenburg, Austria; the Institute of Meteorology and Water Management (IMGW), Warsaw, Poland; and the Industry Studies Program of the University of Houston, Houston, Texas, USA. The operational objective of this collaborative effort was the development and application of a mathematical programming model of a hypothetical, coal-fired power plant located on the Wisła (Vistula) River, Poland. This choice of focus reflected the recognition that electricity generation is an enormously important component of industrial water demands. The problem, while hypothetical, deals with sufficiently realistic issues to render the results of the analysis useful to Polish decision-makers. The objective of the modeling effort was thus analytical rather than predictive – specifically, the development of a tool for quantifying the impact on water demand of alternative resource prices and standards for both pollutant discharges and environmental quality.

Figure 1 provides a geographical perspective on the modeled decision problem. The plant is assumed to be located on the middle reach of the Vistula River and has a rated capacity of 3000 megawatts (net). The potentially substantial water demands of the power plant are supplied exclusively from the river, with the minor exception of slurry water recycle. The significant quantities of coal required to fire the plant must be transported from the Silesia mining region, approximately 300 kilometers distant. Two alternative grades of coal are available – run-of-mine or "regular" coal and washed or "beneficiated" coal – and two modes of transport possible: railroad and slurry pipeline. A third option of barge transport was dismissed as currently uneconomical. The principal economic decisions for the plant are: the mix of coal types to burn, the mode of coal transport, and the design and operation of the plant cooling system.

The configuration of the cooling system is the principal determinant of water demand for the plant. Flow levels in the middle reach of the Vistula are not so low as to demand direct restrictions on the intake of water. However, problems with heat discharge render it impossible to operate an entirely "once-through" cooling system the whole year round. The problem, therefore, is to determine the optimal design and schedule of operating

FIGURE 1 The geographical setting of the modeled problem.

modes for a cooling system which can operate in an appropriate combination of open- and closed-cycle modes, depending upon the situation (see Section 3.1.3 for definitions of these terms). The optimal design and pattern of operation are a complicated function of capital and operating costs, meteorological and hydrological conditions, environmental quality standards, and any prices or charges imposed on water withdrawals, water consumption, and effluent discharges.

The provision of boiler fuel is also modeled in some detail, both because of the importance of fuel provision in power plant economics and because of a desire to make the model robust enough to enable the study of issues other than water demand. Each of the problems of coal supply, coal transport, and air emissions control is important enough in its own right, but various water-related aspects of the fuel provision issue also merit consideration in the present study (see Section 3.1.1).

The problems of water management in a power plant cannot be completely divorced from other aspects of plant design and operation. Water is only one of the basic factors of production, and accurate modeling of the derived demand relationships for water requires due consideration of the full range of relevant factor substitutions in production activities. For electricity generation it is probably sufficient to consider three factors: capital, water, and fuel. To this end, the present study has developed a model of resource use in electric energy generation which is believed to represent the variables and constraints of greatest importance in determining water demand, and also provide a modeling base for analysis of other relevant issues.

The discussion of the case study is divided into three major parts. First, a general description of the structure and components of the mathematical model is provided, in essentially nonmathematical terms. Second, the process of model construction and specification is briefly outlined. In particular, basic process options are identified and depicted in the form of flow diagrams. Components of these flow diagrams are then related to corresponding rows and columns in the programming model; the formulation of model constraints is described; and the procedures for specifying important model coefficients are discussed. The section concludes with some brief comments on the available data for specifying model coefficients and a note on seasonality. Third, we give a brief discussion of model operation, size and computability; a description of the kinds of analyses which can be performed with the model; and a summary and analysis of representative model results.

2 A NONMATHEMATICAL DESCRIPTION OF THE MODEL

In this present section we describe the structure and substance of the model in conceptual terms, without resorting to complicated algebraic notation. We address each of the principal components of the programming model in turn: decision variables, objective function, and constraints. We also include some discussion of integer requirements and of the structural representation of seasonality in the model.

Our model of resource use in electricity generation belongs to the general class of mixed-integer programming problems. It can be conceptually specified as follows:

Minimize

- Annual net costs of production

Subject to

- Seasonal production requirements
- Seasonal constraints on discharges to the water
- Seasonal constraints on discharges to the air
- Nonnegativity of decision variables (simple constraints to prevent logical and physical absurdities)
- Integer (0,1) requirements on certain variables

2.1 Decision Variables

The set of process variables (columns) in a programming model is typically composed of two classes of model activities: a set of decision variables which represent the array of controllable real-world options; and a set of "artificial" variables which perform certain logical, accounting, and integrating functions within the model. The latter set is fairly extensive and quite important in the operation of our model but merits no particular discussion. The emphasis is more on the process combination decisions which together provide the optimal solution for the plant.

Needless to say, electricity generation is a complex process involving a myriad of decision points in both plant design and day-to-day plant operation. The model developed for this study identifies a limited number of design and operating decisons which are believed to be the most significant determinants of water and fuel use patterns in the modeled plant. These key decisions are listed here; a more detailed description is provided in Section 3.1. The principal design decisions modeled are:

- Design temperature rise of cooling water across plant condensers
- Capacity of the cooling tower and water treatment facilities
- Capacity of slurry coal transport facilities (if any)
- Height of the stack for diffusing gaseous discharges

The principal (seasonal) operating decisions are:

- Basic flow pattern of plant cooling water, which itself comprises a set of decisions
- Disposition of cooling tower blowdown
- Disposition of slurry water (if any) and other briny streams
- Mix of alternative coal types burned

Two other important decisions are predetermined. First, the size of plant is given as 3000 MW net, divided into six basically identical blocks (or units) of 500 MW net each. Second, since by its nature the modeled facility is a baseload plant, the level of output is essentially determined by the number of blocks in operation at a given time and the expected rate of utilization for operational units. In a new baseload plant, this rate of utilization will tend to be high, and it is furthermore desirable to maintain it fairly constant. For present modeling purposes, therefore, it can be reasonably assumed that the average utilization rate is constant, at least over a short enough period of time. In terms of defining the problem for our study, this means that the size of plant and level of output (in net terms) cease to be economic decision variables. Gross capacity and output will vary because of the impact of various decision variables on plant efficiency (see Section 3.1.3).

Logically, the domain of relevant operating decisions is dependent upon the design decisions, and the impact on operating decisions must be considered in the design decisions. The patterns of water withdrawal, consumption, and discharge are derived results of these operating and design decisions.

2.2 Objective Function

The cost-minimizing objective function specified for the model may be resolved into the following components:

1. Annualized charge for capital investments
2. Operating costs (or penalties) for the following activities in each season:
   - electric energy generation
   - water withdrawals and water consumption
   - water handling and treatment
   - waterborne residuals discharges

   - coal supply
   - coal transportation and handling
   - coal combustion (including sulfur penalty)
3. Cost reduction applied for extra supplies of coal transported by pipeline (if any)

The annualized capital charge of 12 percent is based on a 4 percent depreciation charge and an 8 percent discount rate. The other cost coefficients, as well as the capital investment requirements to which the capital charge is applied, are based on either engineering estimates or policy specifications. While it is not appropriate here to detail the engineering cost estimates, we identify the following policy-dependent prices and penalties, which may be varied by the user for purposes of demand analysis and impact evaluation:

- Price of water withdrawals
- Price of water consumption (losses)
- Penalty for heat discharges
- Penalty for dissolved solids discharges in excess of a defined standard (except the discharges from open-cycle cooling systems)
- Penalty per percent of sulfur per ton of coal combusted
- Price of coal

We specify a cost-minimization objective for a number of reasons. First, a proper derived demand analysis requires that all factor inputs be evaluated according to a common unit of measure, and monetary cost is a commonly used criterion for analysis of industrial production activities. Second, this specification seems consistent with the planning structure of the industry and economy. Third, because of the essentially predetermined output profile of a baseload plant, a profit-maximizing objective would reduce to cost minimization anyway. Finally, using monetary cost permits a comparison between the indirect values and prices derived by our model with those of other models and applications using the same measure.

Our choice of objective function does not imply that the optimum "social" decision for design and operation of the power plant is necessarily based on production cost minimization alone; this decision may require a much broader purview and consideration of nonmonetary objectives. To some extent we have been able to incorporate some of these broader social perspectives and objectives in the form of constraints, prices, and penalties in the programming model. These specifications can in turn be used in performing economically sound analyses of cost and derived demand for use in the social decision process. In other cases, the relevant social considerations may not be so readily parameterized, and analysis proceeds by solving the model under various assumptions (or scenarios) so as to obtain some quantitative measure of the social trade-offs.

2.3 Constraints

As is the case with most complex programming models, a significant portion of the constraint set for our model is composed of equations representing logical conditions, performing accounting functions, and assuring proper materials and energy balances. These equations are essential and are discussed in Sections 3.2 and 3.3. In addition the model includes three subsets of constraints which, in the more conventional sense of the term, represent actual requirements or limitations imposed on plant activities. We briefly describe each of these.

Seasonal production requirements. The time pattern of plant output levels is translated into the model as a set of seasonal production requirements specifying the total number of megawatt-hours which must be generated (for transmission) in each season. These requirements take the form of a (greater than) row constraint for each season, and the dual values (shadow prices) associated with these rows may be interpreted as marginal costs of producing electricity in each of the seasons.

Seasonal constraints on discharges to the water. Four types of constraints are imposed on discharges of waterborne residuals. The first two are based on defined ambient standards, while the latter two are defined standards for the effluent stream itself. These standards may be summarized as follows:

1. Maximum allowable increase in river temperature
   - 4°C in June, July, August
   - 5°C in September
   - 6°C in all other months
2. Maximum allowable river temperature
   - 30°C
3. Maximum allowable temperature of plant discharge
   - 35°C
4. Maximum concentration of dissolved solids in discharge (except that from open-cycle cooling systems)
   - 500 mg/l

In constraint (4) higher concentrations are not strictly prohibited, but a penalty is applied for each kilogram of excessive solids discharge. In the model only the stricter of constraints (1) and (2) is specified for a given month. It is not readily determined whether this constraint is more or less strict than constraint (3) in a given month; hence, both constraint (3) and the stricter of constraints (1) and (2) are specified in the model.

The algebraic formulation of these constraints is somewhat complicated because of a need to express quantity-weighted averages in terms of quantities not known until the model solution is calculated. By careful formulation of intermediate accounting structures, however, each standard is ultimately expressed as a single (less than) constraint for each season. Interpretation of the dual values for these constraints requires algebraic manipulation to express them in meaningful terms.

Seasonal constraints on discharges to the air. An ambient standard for the maximum allowable ground-level concentration of sulfur dioxide is established by policy. For any given season, the difference between this standard and an expected background concentration may be interpreted as the maximum allowable concentration which may be produced by emissions from the power plant in that season. In order to incorporate the ambient standard in the model, it is necessary to translate this concentration allowance into an emission constraint for the modeled coal combustion activities. This translation has been accomplished with the aid of an atmospheric dispersion model developed by IMGW. Solutions to this model have determined – for each season and for a range of alternative stack heights over 150 meters – the maximum ratio of regular to beneficiated coal that can be combusted at full load consistent with the allowed increment in ground-level sulfur dioxide concentration. This ratio can in turn be converted into upper limits on the amounts of regular coal and of total coal – regular plus beneficiated – that can be combusted in a given season at a particular stack height.

In the model these upper limits take the form of two row constraints for each season. These constraints directly limit the quantities of coal combusted to amounts specified internally by the design choice of stack height; that is, for each additional meter of stack height constructed, an increment is added to the allowable amounts of regular and total coal combustion. The dual values for these constraints, only one of which can be binding in any season, represent the potential savings to the plant of burning one more ton of coal given a fixed stack height as determined in the solution.

2.4 Integer Requirements

A limited number of integer (0,1) variables are included in the model to impose certain logical constraints on plant design and to insure proper consideration of the economies of scale in slurry pipeline construction. Because the capacity of the power plant is predetermined, scale economies can be properly accounted for by calculating costs appropriate to an installation containing six 500 megawatt blocks. It is important, however, to insure that only one "type" of power plant is constructed with respect to the design temperature rise across the condenser; this requires integer variables. A similar integer control structure is required to insure complete and exclusive construction of only one size of slurry pipeline instead of linear bits and pieces of pipelines of various sizes.

2.5 Seasonal Structure

We incorporate the time dimension in the model by dividing the year into a number of seasons and modeling plant operations in each season in accordance with seasonally specified values for exogenous variables. These seasonal operations are tied together by certain annual resource constraints and by a fixed design of installed capital equipment. Thus, the optimal design decision is a function of the operating conditions in all seasons, and the optimal pattern of operations in a given season is dependent upon the operations in all other seasons through the common demands on annual resources and the design configuration. Again, the optimal overall decision requires a simultaneous determination of the design decision and all seasonal operating decisions, consistent with the seasonal time pattern of specified exogenous variables.

The essence of this interdependence and simultaneity must be incorporated in the mathematical structure of the model. Fortunately, this is not especially difficult. Seasonality is handled in a straightforward manner by defining separate column variables and constraints to represent plant operations in each of the defined seasons. The structure of each seasonal submatrix is virtually identical, but for each season a separate set of parameters represents charges for water use and residuals discharges, available supplies of water and other resources, and allowable discharges to the air and water. The coefficients of the electricity generation processes also vary, thus reflecting the impact of output level and of meteorological and hydrological factors on the operating conditions of the power plant and cooling system. A careful distinction is made between activities representing the provision of capital capacity for a given process (a one-time occurrence) and the operation of that process in each of the defined seasons. In each seasonal activity, capital capacity (if relevant) is treated much as any other required input, and a separate (one-time) activity is modeled to jointly provide capital capacity for all defined seasons.

3 MODEL CONSTRUCTION AND SPECIFICATION

In this section we describe the construction and specification of the model, following a typical logical sequence in the development of a progamming model. First, the basic process options are identified and depicted, where helpful, in the form of flow diagrams. Second, modeling correspondences are established between the components of the flow diagrams and the rows and columns of the model matrix. Third, model constraints are logically and algebraically formulated, and, fourth, the coefficients of model column activities are specified. We conclude the section with some comments on data availability (an issue which must always be kept in mind when developing the structure of a model) and a note on seasonality.

3.1 Basic Process Options

With the aid of several flow diagrams, the basic process options represented in the programming model are outlined. Figure 2 shows an overview of processes and materials flows with emphasis on activities outside the basic electricity generation processes. Figure 3 displays in greater detail the processes contained in the box for the electric power plant in Figure 2; it identifies the major flows of water, steam, and fuel-related materials in the power plant. Subsequent flow diagrams show the alternative configurations for the plant cooling system and are essentially a detailed expansion of the processes and flows in the dashed rectangle of Figure 3.

3.1.1 Fuel Provision Activities

Figure 2 gives an overview of the entire operation, with emphasis on the activities related to fuel provision. The coal supply for the modeled plant is assumed to be obtained from four Silesia mines with a combined annual capacity of 20 million (10^6) metric tonnes. This total is perhaps twice the expected coal requirement for the power plant. Mined coal may be transported directly to the plant site by railroad or may be beneficiated (crushed, washed, and gravimetrically separated) to produce a coal of higher heat content and lower ash and sulfur content. The quality characteristics of these two available coal types are given in Table 1.

The beneficiated coal may be transported to the plant site via railroad or slurry pipeline. Three alternative capacity options are considered for the slurry pipeline: 4.5, 9, and 16 million (10^6) metric tonnes per year. The largest capacity option represents transport

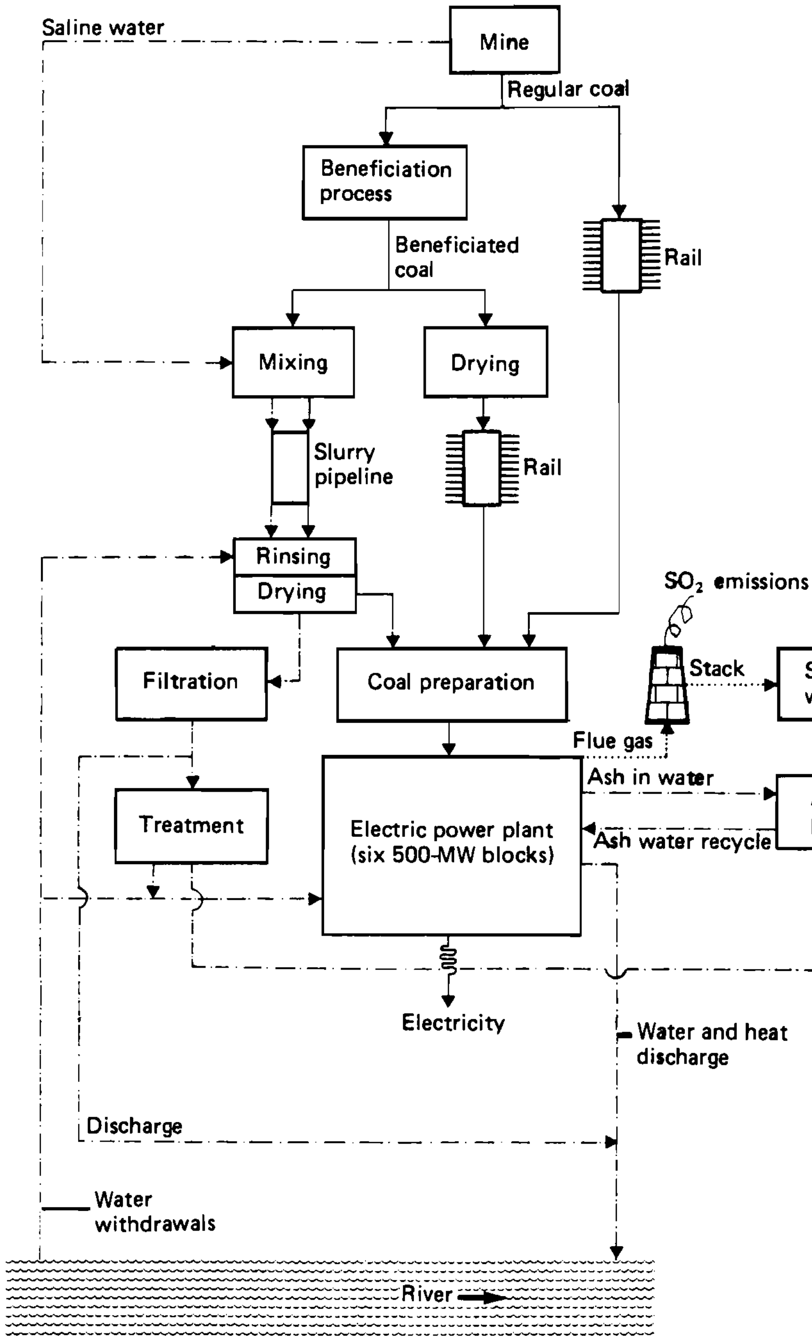

FIGURE 2 Flows of processes and materials in the generation of electricity with emphasis on coal handling and combustion, where – – – shows river water, – · – shows polluted water, ——— shows coal, and · · · · · shows flue gas or solid waste.

TABLE 1 Characteristics of run-of-mine and beneficiated coal.

	Heat content (kcal/kg)	Ash content (%)	Sulfur content (%)
Run-of-mine (regular)	4,400	26.4	2.5
Beneficiated	5,300	12.7	1.4

of the maximum yearly production of the four available mines, minus losses of 25 percent in the beneficiation process. The excess coal transported by this largest pipeline may be supplied to other users, with an appropriate benefit recorded in the objective function for the power plant.

We did not model two other coal transport options because preliminary cost calculations demonstrated them to be currently uneconomical in all circumstances. The first is slurry transport of regular grade (run-of-mine) coal, the cost effectiveness of which is always inferior to slurry transport of beneficiated coal on a delivered kilocalorie basis. This is because of the inferior heat and ash content characteristics of the regular grade coal and because the crushing and watering required for slurry transport are essentially the first two steps of the beneficiation process anyway.

The second uneconomical option is barge transport of either grade of coal which, in the case of the largely undeveloped Vistula River, is, at least for the present, inferior to railroad transport. This demonstrable inferiority arises from higher estimated unit costs and from the necessity for extra storage facilities at the power plant to insure adequate coal supplies during winter months, when navigation is inhibited by ice on the river.

None of these mining, beneficiation, or transportation processes is modeled in any great detail. Emphasis is on accurate representation of the costs of these operations and of the water balances for the slurry pipeline. We assume a one-to-one ratio for the water/coal mixture in the slurry; and IMGW estimates water losses – primarily through absorption – at 12 percent.

Another consideration concerning cost and water use involves water management in the mining region. Planners believe that the water used for slurry preparation and transport could be supplied from the large volumes of saline wastewater generated in mining operations. The major technical question to be resolved with respect to this option is the corrosive potential of the wastewater on the pipeline itself. If saline water usage proves feasible, a significant disposal problem will be alleviated as some of the wastewater is transported away from the mining area, where river flow is naturally low. From a social point of view, the economics of the slurry pipeline should incorporate these benefits, and the model includes an appropriate reduction in the operating costs of the pipeline to account for them.

The cost to be balanced against this benefit arises from the logical consequence that, at the plant site, slurry-transported coal must be dewatered, and the separated water must be discharged or treated for use in plant operations. We make the operational assumption that the slurry water is discharged through the same channel as the plant cooling water. This routing has the effect of somewhat diluting the solids concentration of the slurry water and the elevated temperature of the cooling water. While the flow of slurry water is not great – of the order of 0.5 cubic meters per second for the maximum size pipeline – the dissolved solids concentration of the stream may be as high as 10,000 mg/l. This concentration renders its disposal a nontrivial water management consideration, and the optimal decision depends upon the price of water withdrawals and on any environmental standards or effluent charges on dissolved solids discharges. The management of slurry water is thus one of the areas of interaction between the issues of water demand and of the provision of boiler fuel.

The other important consideration affecting the provision of boiler fuel is the extent of constraints and/or charges on gaseous discharges from the plant. We assume that the plant employs the most efficient available electrostatic control measures for particulate emissions and that these emissions do not require explicit analysis. We do, however, consider emissions of sulfur oxides in more detail. These emissions are subject to penalties based on the sulfur content of combusted coal and are further constrained to be in accordance with established standards for ambient concentrations of SO_2. The available alternatives for "control" of these emissions are the mix of run-of-mine and beneficiated coal combusted – the plant cannot operate entirely on regular coal because of the SO_2 standards – and the height of the stack, which affects dispersion of gaseous discharges rather than emission levels. Thus, there is an obvious interdependence between these considerations of gaseous discharges and the choice of coal supply and transport. As already indicated, the transport considerations represent an area of interaction between water use and boiler fuel.

There is, however, another area of interaction related to the impact of the cost of boiler fuel on the economic substitutability of cooling systems. The reduction in plant thermal efficiency attributable to the utilization of a cooling tower results in a higher fuel requirement per net kilowatt-hour of generation. This energy penalty must be considered, along with the additional capital requirements, in the comparative economics of open- and closed-cycle cooling systems. Proper evaluation of this energy penalty in turn requires consideration, at least to the extent of costing, of the full range of fuel provision activities from coal supply, to transport, to combustion in accordance with applicable standards for gaseous residuals discharges.

Finally we consider the disposal of solid waste from coal handling and combustion operations only to the extent of assignment of costs. We incorporate estimates of the average water requirements for removal of ash from the boiler, but the small magnitude of ash water flow does not justify detailed consideration – both data collection and modeling – of the weather-dependent management problem of managing the water in the ash pond. We use the ash pond frequently in our modeling as a convenient sink for small but dirty wastewater streams. This seems an acceptable approximation in light of the far greater significance of cooling water flows, which are at least 10 times as great even in the case of a closed-cycle system. The routing also makes operational sense because of the dilution and settling of materials in the ash pond.

3.1.2 Electricity Generation Processes

Figure 3 illustrates the major interrelationships among the most basic processes for power generation. Flows to and from the boundaries of this figure directly correspond to the flows entering and leaving the power plant shown in Figure 2. Figure 3 shows the basic water use patterns for process cooling, boiler make-up, and ash removal. Certain other minor water uses, such as cleaning water for the boiler, are omitted from the figure but

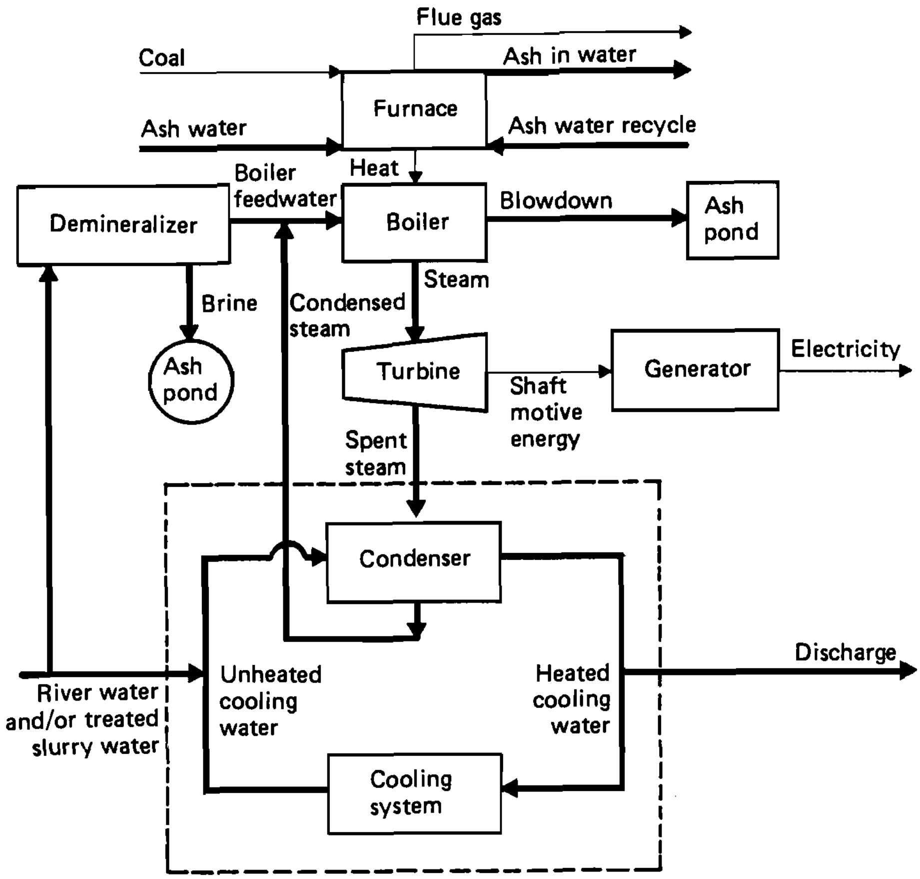

FIGURE 3 Basic unit processes for the electric power plant.

are included in the modeling analysis. Also illustrated are two typical uses of the ash-pond sink for "disposal" of small waste streams.

Of the three types of water use depicted, the boiler make-up and ash water flows are fairly small. The more substantial flows used in process cooling and the alternative configurations of the cooling system merit further consideration.

3.1.3 Cooling System Options

Figure 4 is a basic reference diagram of the eight major cooling system options (A–H) considered in our study; Figures 5–9 highlight one or more of the flow patterns shown in Figure 4. The basic options are characterized as follows:

(A) Temperature rise across condensers
(B) Type of cooling system
(C) Single or series condensers
(D) Wet bulb approach factor for cooling tower

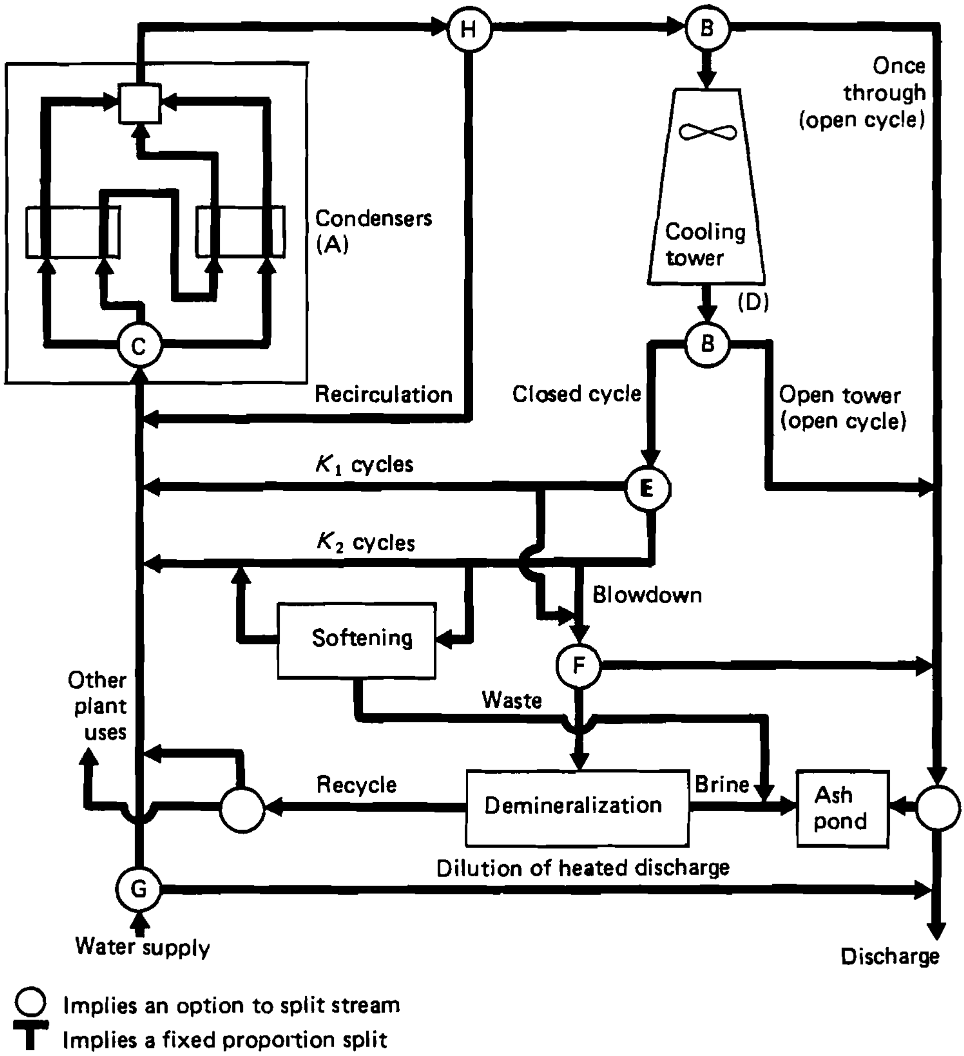

FIGURE 4 Cooling system options.

(E) Cycles of concentration in cooling tower
(F) Treatment of cooling tower blowdown
(G) Dilution of heated discharge
(H) Recirculation for temperature maintenance

Temperature rise across condensers (A). The process of heat exchange in a condenser condenses the turbine exhaust steam at the expense of an increase in the temperature of cross-current cooling water. The magnitude of this increase in cooling water temperature ΔT is a design decision variable which, for a given rate of waste heat removal H, determines the necessary rate of flow of cooling water across the condenser Q. In brief

$$H/c = Q\Delta T \tag{1}$$

where c is the appropriately scaled heat capacity of water. As can be seen, water flow Q is a decreasing function of ΔT, and the choice of ΔT is an important determinant of water demand in the plant.

As an additional important consideration, the value of ΔT determines – for given inlet water temperature and equipment design – the condensing temperature of the turbine exhaust steam. Because the pressure on the exhaust end of the turbine is an increasing function of this temperature, it follows that an increase in ΔT decreases the pressure drop across the turbine, with a resultant loss of generating power. This decrease in thermal efficiency results in an increase in both water and fuel requirements for a given level of net output.

Because both of these effects influence operating conditions throughout the plant, and because a condenser and its accessories must be designed for operation over a fairly narrow range of flow rates and ΔT, the choice of ΔT is a fundamental decision variable in plant design. In this study we consider three discrete options for ΔT; only one of these options may be chosen by the model.

Type of cooling system (B). The two decision nodes labeled B in Figure 4 represent the second fundamental choice in the cooling system configuration. Depending upon the flow routings at each of these points, the resulting configuration may be classified as one of the following basic types, or a combination of the three:

1. Open-cycle sytem
   a. "once-through"
   b. "open-tower"
2. Closed-cycle system

In Figure 5 the basic flow pattern for a once-through system is indicated by the broken lines; in Figure 6 that for an open-tower system is similarly indicated. In both cases, water from the river is pumped directly across the condensers and then discharged back into the river. This basic flow pattern characterizes these systems as open-cycle. In the once-through system, the discharge to the river is direct, and the temperature of the discharge stream is essentially the same as that at the outlets from the condensers. In the open-tower system, the condenser outlet water is pumped through a cooling tower before being discharged; this lowers the temperature of the discharge stream to that in the cooling tower basin (see option D for the determinants of basin temperature). The open-tower system has two important effects on water demand. First, water consumption is increased, relative to a once-through system, because of evaporative and drift losses in the tower. Second, overall water withdrawals must increase, again relative to a once-through system, because the energy requirements of the pumps and fans for the tower (assumed to be mechanical draft) increase the gross energy generation necessary to produce the same level of net output.

In our analysis we have crudely estimated the evaporative losses from a once-through cooling system that are caused by the spreading of heated cooling water over the river surface. As this is a very complicated problem involving a number of variables not otherwise considered in this analysis, we have used for the present an approximation based on more

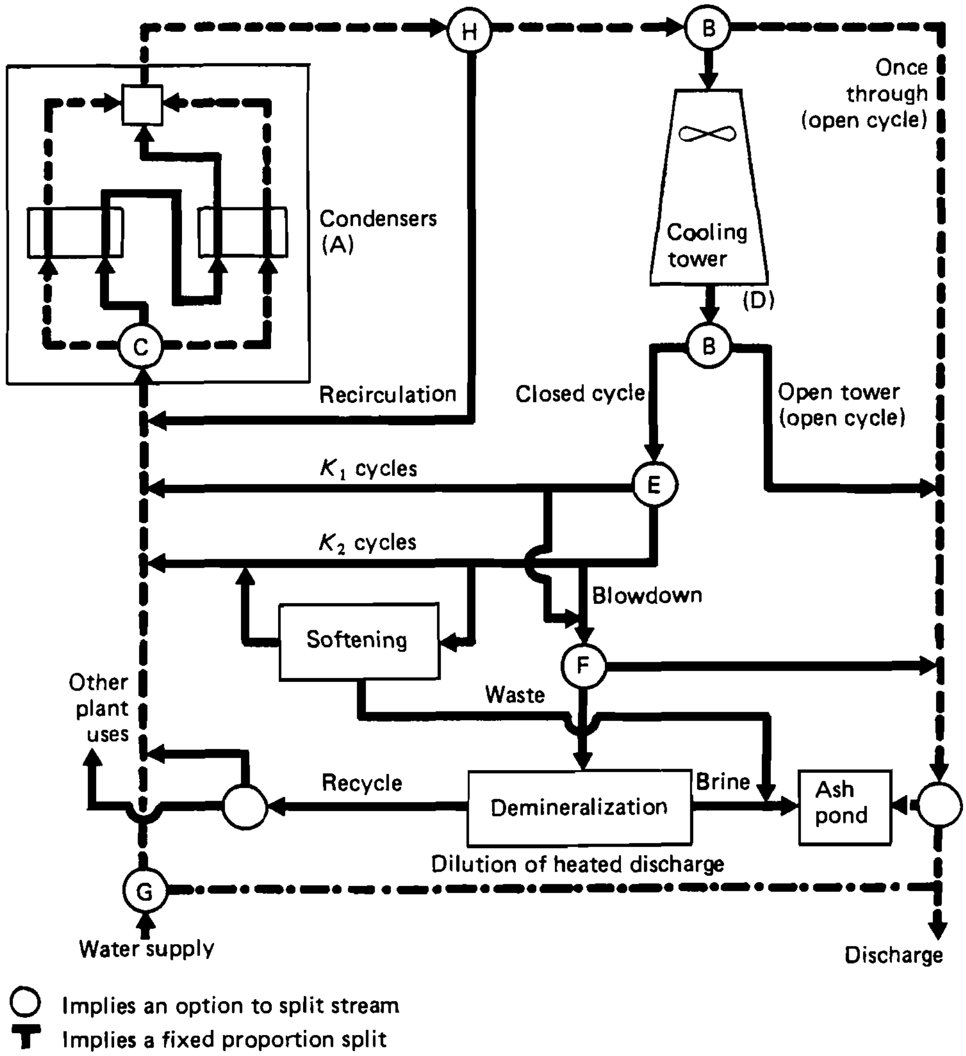

FIGURE 5 Flow pattern for a once-through cooling system (indicated by broken line), where A–H are cooling system options.

straightforward formulas for losses in the cooling tower. In general, the losses from a once-through system are less, perhaps 25 to 50 percent less, than those from a cooling tower system.

In either open-cycle system, it is possible – as shown at the bottom right of Figures 5 and 6 – to divert a small proportion of the cooling water discharge to the ash-removal system. In general, there is no reason not to employ this routing since it decreases slightly both heated water discharges and river water withdrawals for ash removal.

Figure 7 illustrates the basic flow pattern of a closed-cycle system. Now the emphasis is on the recycle routing at node B under the cooling tower. This flow pattern reduces the potential discharges from the system to the amount of blowdown collected at node F.

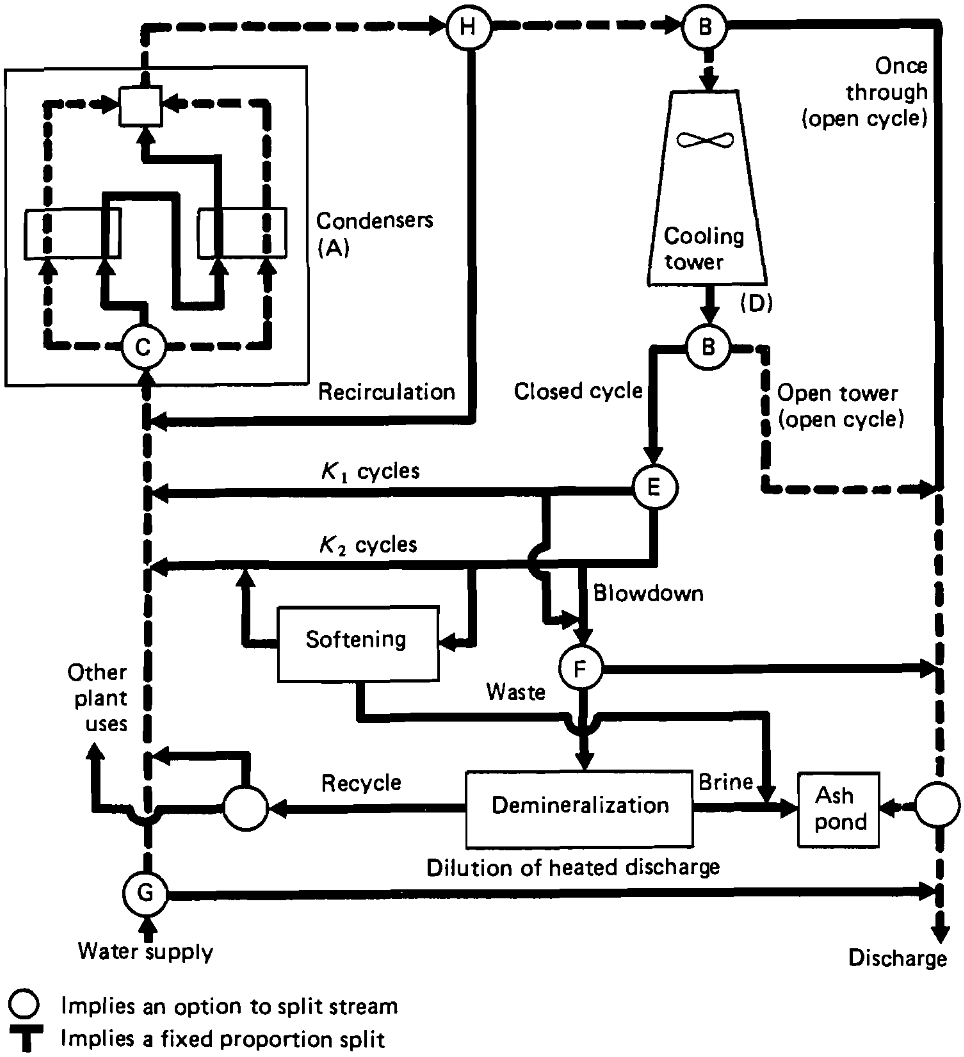

FIGURE 6 Flow pattern for an open-tower cooling system (indicated by broken line), where A–H are cooling system options.

This blowdown stream is extracted from the recirculating cooling water in order to maintain an acceptable concentration of dissolved solids in the system; this concentration would otherwise be continuously increasing because of the evaporative water losses in the cooling tower. The magnitude of blowdown is quite small, generally about 1 percent of the total flow of recirculating cooling water. The only withdrawal requirements of the closed-cycle system are a make-up stream to account for evaporative and drift losses, and blowdown extraction.

While drastically reducing water withdrawals for cooling purposes, the closed-cycle system increases water consumption (relative to that of a once-through system) because

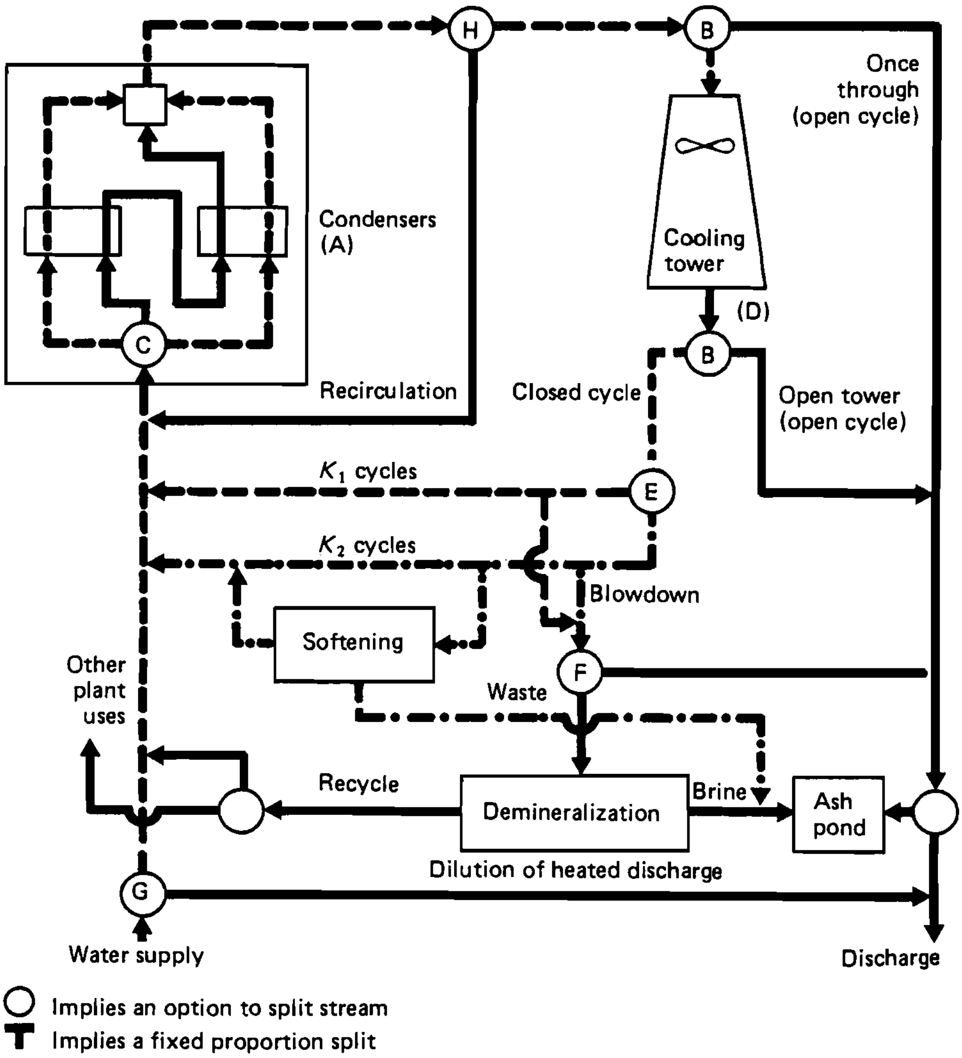

FIGURE 7 Flow pattern for a closed-cycle cooling system (indicated by broken line), where A–H are cooling system options.

of water losses in the tower. Similarly, heat discharges are rendered virtually insignificant by closing the system, but discharges of dissolved solids may become a problem because of the higher solids concentration of the blowdown (see option F). There are also two effects on plant thermal efficiency. The first involves the additional energy requirements for the pumps and fans as described for the open-tower system. The second relates to the temperature of the recycle water from the cooling tower. To the extent that this temperature is higher than that of the river water, the plant suffers a loss in thermal efficiency relative to that of an open-cycle system. This is because (for a given ΔT) the higher temperature cooling water increases the condensing temperature of turbine exhaust steam.

While this higher temperature is typical, under certain conditions the recycle water may actually be cooler than the river water (see option D). In this case the steam cycle thermal efficiency is improved, but this effect is outweighed by the additional energy requirements for the pumps and fans.

The essence of the water management problem at the power plant is determining an optimal combination of the three "pure" types of cooling systems (once-through, open-tower, and closed-cycle). This decision is an operating decision as well as a design decision, because the flow patterns through existing equipment can be altered to fit a given situation. (There is also an important interdependence between these decisions and the design choice of ΔT.) As a very simplified generalization, we can say that it is presumably necessary to construct a large enough cooling tower to assure compliance with heat discharge standards during low river flow and high temperature conditions. Beyond that, the tower capacity may be expanded and/or the time pattern of flows in the cooling system may be altered in optimal response to the time pattern of other environmental quality constraints, of meteorological and hydrological conditions, and of prices and charges for water withdrawals, water consumption, and effluent discharges.

Single or series condensers (C). In the normal mode of operation for the cooling system, the flows through the condensers of the various blocks (or units) are independent, although they may share the same channels for water intake and discharge. This "single condensers" mode of operation is illustrated by the broken lines in the box representing condensers in Figure 7. Under certain conditions, however, it may prove advantageous to route the heated cooling water from the outlet of one condenser to the inlet of a paired condenser. This alternative "series condensers" mode of operation is illustrated by the solid flow lines in the box in Figure 7. The series configuration has two economic and water use advantages. First, the cooling water requirements for the paired condensers are only a little over half those for singly operated condensers. Second, in the case of open-tower and closed-cycle systems, the increased outlet temperature from the second paired condenser means a higher temperature at the top of the cooling tower. For a given basin water temperature, this results in a greater temperature drop across the tower and accordingly more effective heat rejection. This improvement may allow for construction of a smaller cooling tower. The optimal configuration decision must weigh these advantages against the decline in thermal efficiency implied by the higher cooling water temperature in the second paired condenser.

Wet bulb approach factor for cooling tower (D). The water temperature in the cooling tower basin T_B is related to the wet bulb temperature T_W and a so-called wet bulb approach factor P, which depends upon cooling tower design, fan speed, and other considerations. We make the fairly typical assumption that

$$T_B = T_W + P \tag{2}$$

where all magnitudes are in degrees Centigrade.

This wet bulb approach factor affects the efficiency of heat rejection in the cooling tower – and therefore its necessary size – as well as the temperatures of the discharge stream in an open-tower system and of the recycle stream in a closed-cycle system. These temperatures in turn have definite implications for environmental quality and thermal efficiency. For low enough values of T_W and P, T_B may actually be lower than the river water temperature. This situation reduces somewhat the energy penalty for a closed-cycle cooling tower and enhances the capacity of an open-tower discharge to dilute the excess heat in a once-through discharge. In this study we use the value of the wet bulb approach factor as a kind of proxy design and operating option for the cooling tower. Four discrete values of P are incorporated as options, and linear combinations are allowed to increase the flexibility of the model in representing the design and operation of the cooling tower.

Cycles of concentration in cooling tower (E). The make-up water requirements for a closed-cycle system are a function of the evaporative losses in the cooling tower, the naturally occurring solids content of the make-up water (i.e., the river), and a so-called cycle factor K. This cycle factor further determines the amount and dissolved solids concentration of cooling tower blowdown. The following relationships hold:

1. Make-up requirements decrease with K
2. Blowdown decreases with K
3. Blowdown solids concentration increases with K

A maximum value of K is essentially determined by the concentration and composition of dissolved solids in the make-up water and the allowable build-up of solids of that composition in the cooling system. This base maximum value of K can be increased by removal of solids from the system or by softening a fraction of the cooling water to render a given solids concentration less harmful to the mechanical equipment. This latter option is considered here and is represented by decision node E in Figure 7. If no treatment is employed, the relevant flow pattern is that indicated by the upper broken flow line. In this case, the base cycle factor K_1 is 3. If a fraction of the recycle stream is treated, the flow pattern is that of the lower, dashed-dotted line, and the cycle factor increases. Our study models treatment of an amount of water equivalent to the make-up requirement, and this process increases the cycle factor K_2 to 6. We assume that the small waste stream from the treatment process is routed to the ash pond.

Treatment of cooling tower blowdown (F). The cooling tower blowdown collected at node F must be disposed of in an optimal manner consistent with liquid effluent discharge standards and effluent charges. Direct discharge of this blowdown is illustrated in Figure 8 by the upper, dashed-dotted flow line at node F. Some fraction of this discharge may be routed to the ash pond as indicated. Alternatively, all or some of the blowdown can be demineralized, producing a clean recycle stream for plant use. This option is illustrated in Figure 8 by the lower broken flow path from node F. The briny waste stream from this process is assumed to be routed to the ash pond. Demineralization of all cooling tower blowdown essentially eliminates discharges from a closed-cycle cooling system.

Dilution of heated discharge (G). Under certain conditions the temperature of the cooling water discharge may exceed the standard imposed on discharge temperature. In this case it may be advantageous to use a certain amount of river or other available water to "dilute" the heated discharge to an acceptable temperature. This incidental option is illustrated by the dashed-dotted flow line across the bottom of Figure 5. This procedure does not, of course, change the value of the total heat load added to the river; it just reduces the temperature differential at the discharge outlet.

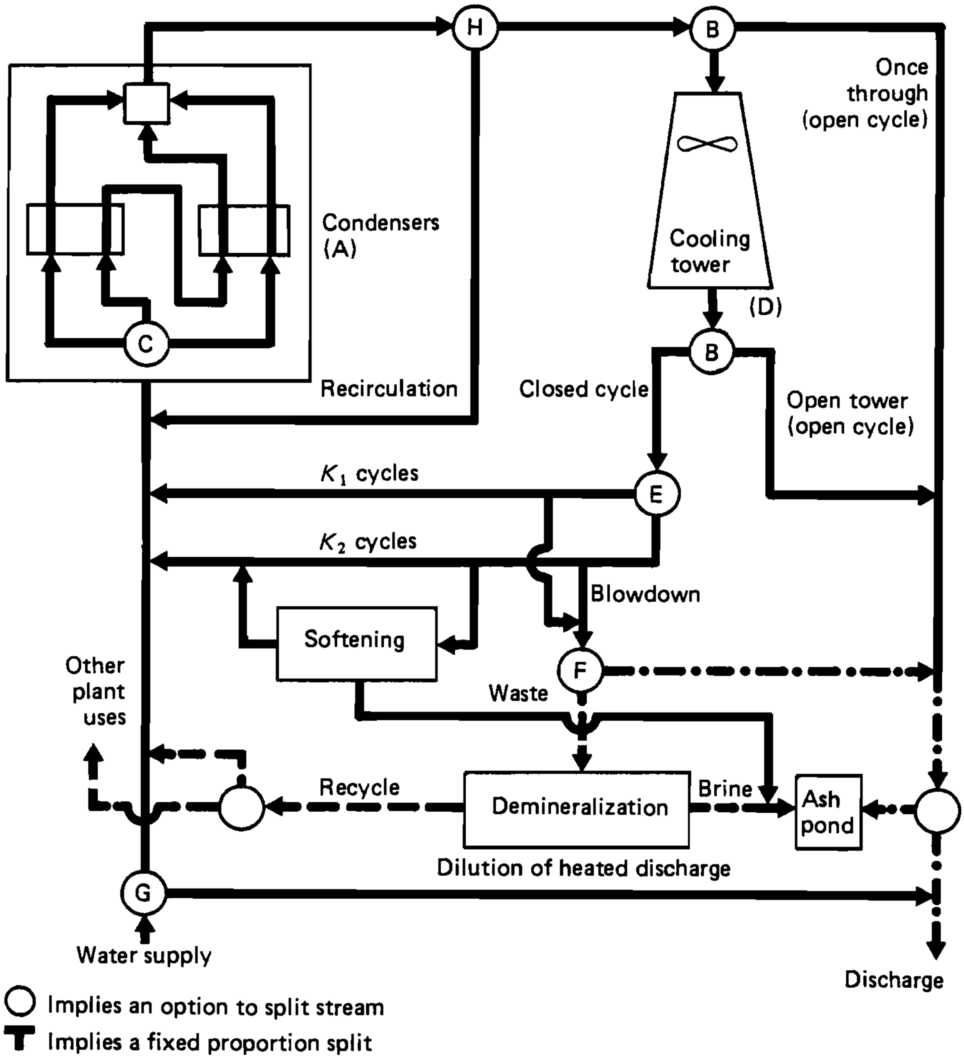

FIGURE 8 Disposition of cooling tower blowdown (indicated by dashed and dashed–dotted lines), where A–H are cooling system options.

Recirculation of condenser outlet water for temperature maintenance (H). The design of the condensers is such that a minimum inlet temperature of 10°C must be maintained. During some parts of the year, however, the temperature of the river – and even that of the recycle stream from a closed-cycle system – may fall below 10°C. In such a situation, the minimum inlet temperature can be maintained by recirculating just enough of the heated outlet water from the condensers to bring the inlet water temperature up to 10°C. This flow pattern is depicted by the dashed-dotted line at node H in Figure 9. Logically, the remaining flow of water proceeding to discharge or cooling tower circulation is reduced by the amount of this recirculation. Water withdrawals are similarly reduced, although the effect is somewhat complicated in the case of a closed-cycle system. If the river water

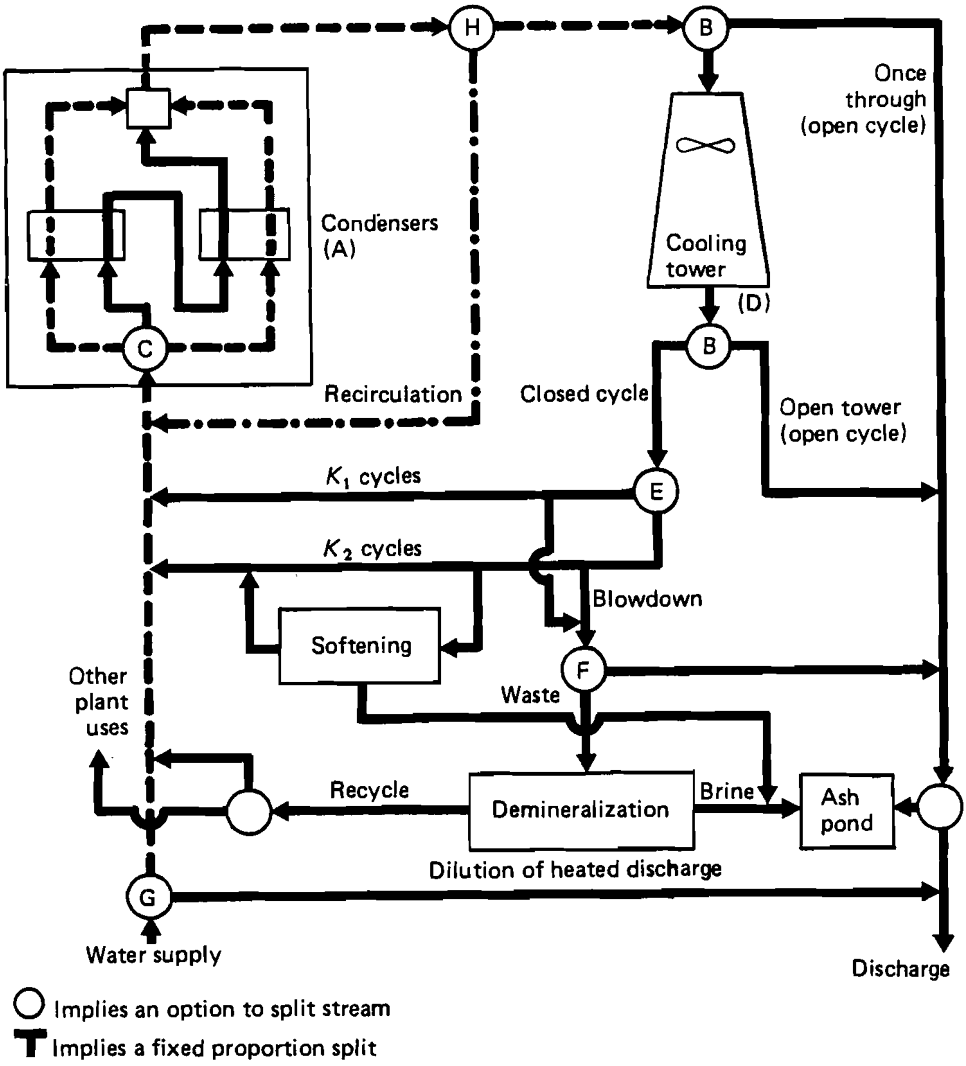

FIGURE 9 Recirculation of condenser outlet water (indicated by dashed–dotted line), where A–H are cooling system options.

temperature is less than 10°C but the temperature of cooling tower recycle is greater than 10°C, minimum condenser inlet temperature can be maintained by a proper combination of open- and closed-cycle flows.

3.2 Correspondence of Flows and Processes to Model Rows and Columns

Once the relevant material flows and unit processes have been identified (see Figures 2–9), the next modeling task is to develop a correspondence between these flows and processes and the rows and columns of the mathematical programming model. There are any number of ways in which this can be done. At one extreme, a one-to-one correspondence may be developed between each material flow and a model row and between each unit process and a model column. At the other extreme, an entire complex operation can be represented by a single column, with rows defined only for those materials with a net flow across the boundary of the operation. In practice, the correspondence employed is usually a compromise between the two extremes, and the modeler's choice depends upon a number of modeling and budgetary considerations. Four of these – model size, extent of true options, identification of important flows and process options, and linear and integer relationships – are identified here because of their general applicability and because of their particular importance in the formulation of our model.

The first consideration is *model size.* Budgetary or data processing limitations almost inevitably constrain the size of model which can be manageably manipulated and successfully solved. Generally a trade-off must be made between manageability/computability and the degree of material flow and process detail explicitly represented in the model. This directly conditions the kinds of correspondences which can be made between material flows and rows and between unit processes and columns. This is particularly so in models which attempt to capture the time dimension by representing flows and processes in each of a number of specified time periods. This trade-off regarding model size is an important factor in the resolution of the next two considerations.

The second consideration is the *extent of true options* in the flow and process configurations modeled. Given the model size consideration, it makes little sense to explicitly represent unit processes (and related flows) whose activity levels relative to other processes are logically fixed rather than being actual decision variables. In some cases the distinction is dictated by the basic technical relationships of the modeled technology; in other cases it is a consequence of a modeling decision not to model certain design or operation options. This leads to the third, related, consideration which is an identification of the *important flows and process options.* Here, too, it makes little sense to expand the size of the model with detail on flows and processes which do not significantly interact with the principal decisions, constraints, and flow patterns that are the target of the modeling analysis. In many cases, the flow diagrams themselves are an early stage in this simplification; the figures presented thus far already reflect considerable simplification of the water, energy, and residuals flows in the power plant.

The fourth consideration arises from the representation of power plant activities in terms of *linear and integer relationships.* Such a representation is motivated by the powerful algorithms and software available for solving linear programs and so-called mixed-integer programs with a manageable number of integer variables. This is not to say that the underlying relationships of electricity generation are linear (indeed, they are not), but rather that for a given application these relationships may be adequately approximated by well-formulated linear relationships, possibly supplemented by integer variables. The implication for model formulation is that the correspondence between unit processes and model columns should be defined so that the cost and input–output coefficients of linear model columns are independent of the activity levels of all model columns. As illustrated later, these correspondences may subsume in one column highly nonlinear relationships, or a group of linear columns may be used to piecewise-approximate a nonlinear relationship. Supplemental integer variables may be used to incorporate such considerations as mutual exclusiveness or "all-or-none" decisions, and they may further be used to ensure that the linear segments of a piecewise-approximated relationship are selected in the proper order.

To show how these four correspondence considerations relate to the construction of our model, we can illustrate the derivation of rows and columns from the various flow diagrams through a partial matrix tableau. A matrix tableau displays the rows and columns of the programming model and identifies the nonzero matrix coefficients which define model relationships. A partial tableau focuses on a particular subset of model rows and columns and as such may not display all nonzero entries in a given row or column. For present purposes, numerical values for many coefficients are not tabulated both because the values are subject to user discretion and because such generality allows for shorthand representation of several rows or columns as a generic class. The existence of positive coefficients is indicated in the tableaus by "+", and negative coefficients are indicated by "–". Rows and columns identified as seasonal in the tableaus are structurally replicated in the model as many times as there are seasons defined.

We use several partial matrix tableaus in the discussion of modeling correspondences and constraint formulations. As an aid in relating these tableaus to each other and to the overall model structure, Table 2 shows the different classes of rows and columns in the complete model. Classes of activities relating to coal (supply, transport, and combustion), air emissions, power plant construction and operation, and water use are given vertically; classes of rows pertaining to cost, coal, air emissions, heat, electricity, and water use are given horizontally. As can be seen, many parts of the matrix have little or no interaction with other parts, and the partial tableaus reflect these logical separations.

We can best identify one specific point of the model's structure in the context of Table 2. A logical accounting row is used in the model to accumulate the total capital investment in the power plant. A specified fraction of the investment (12 percent here) is prorated as an annual capital charge and "transferred" to the objective function by a special column. The objective function coefficient of this column is thus a convenient focus for altering or parameterizing the capital discount rate. As a further note, certain activities are seen to have entries in both the objective function and capital investment rows. The objective function coefficients for these activities represent the unit maintenance costs of the activities and are in addition to the annual capital charge.

3.2.1 Modeling Correspondences: Coal Transport and Combustion

Table 3 presents the partial matrix tableau corresponding to the coal transportation activities depicted in Figure 2. The correspondence applied is straightforward and almost one-to-one. This approach does not yield the minimum number of rows and columns but expands the size of the model somewhat for the sake of ease and flexibility in altering or parameterizing certain cost or technical coefficients. The number of rows and columns is kept small by modeling coal supply, beneficiation, and transport activities on an annual basis. This simplification is based on the assumption that monthly variations in these activities do not significantly affect costs or the pattern of water use in the power plant.

Separate column variables are defined for each of the activities of mining (supplying) coal, beneficiating coal, and transporting each type of coal from the mine to the power plant. Slurry transportation is modeled by three integer column variables, each representing the construction and (by assumption) uniform annual operation of a given capacity pipeline. As a simple example of the true option correspondence criterion, the logically

TABLE 2 Overview of model structure.

		Annual capital charge	Coal supply and transport	Coal combustion	Air emissions accounting	Air emissions accounting
		Logical	Annual	Seasonal	Seasonal	Annual
Cost (objective function)	Annual minimum	.12	+	+		+
Capital investment	Logical = 0	–1				
Coal	Annual ⩾ 0		+	–		
Air emissions constraints	Seasonal ⩽ 0			+		
Air emissions accounting	Seasonal = 0			+	–	
Air emissions accounting	Annual = 0				+	–
Heat to boiler	Seasonal ⩾ 0			+		
Intake water	Seasonal = 0			–		
Water handling capacity	Seasonal ⩾ 0					
Electricity generation	Seasonal ⩾ 0					
Wastewater	Seasonal = 0		+			
Water discharge constraints	Seasonal ⩽ b					
Water use accounting	Seasonal ⩽ 0					
Water use accounting	Annual = 0					
Integer control rows	Logical ⩽ or = 1		+ 1 Slurry			

necessary processes for drying beneficiated coal prior to rail transport and for mixing and drying coal on either end of the slurry pipeline are subsumed in the column variables for the transportation activities. Similarly, the coal preparation activities at the power plant are subsumed in column variables for plant construction and operation. Each slurry column variable provides a given quantity of slurry water at the power plant in each modeled season; two column variables are defined for each season to represent the options of discharging slurry water or treating it for plant use. A single column variable records the benefit of any excess coal transported to the Middle Vistula region by the slurry pipeline.

Plant construction	Electricity generation and cooling	Water discharge	Water treatment	Water use accounting	Water use accounting
Build	Seasonal	Seasonal	Seasonal	Seasonal	Annual
+	+		+		+
+					
Stack —					
	—				
	—		+	+	
+	—				
ΔT options —	+				
	+	—	—		
		+/–		+/–	
		+/–		+/–	
				+	—
ΔT options + 1					

In terms of the rows defined for this sector of the model, only material flows directly affecting fuel and water use at the plant are represented; water flows at the mine are not explicitly modeled. Hence, there are annually specified rows for regular and beneficiated coal at both the mine and the power plant and seasonally specified rows for slurry water, intake water, and ash water at the power plant. The cost row (objective function) may be considered a material flow or a purely logical or accounting row. A logical row must also be defined to insure that only one slurry column variable is chosen, and another is defined to insure that excess coal benefits are applied only to slurry-transported coal.

TABLE 3 Partial matrix tableau: coal transportation.

		Coal supply	Coal beneficiation	Rail transport – regular coal	Rail transport – beneficiated coal
		Annual	Annual	Annual	Annual
Cost (objective function)	Annual minimum	+	+	+	+
Regular coal at mine	Annual $\geqslant 0$	1	–1.25	–1	
Beneficiated coal at mine	Annual $\geqslant 0$		1		–1
Regular coal at plant	Annual $\geqslant 0$			1	
Beneficiated coal at plant	Annual $\geqslant 0$				1
Slurry wastewater	Seasonal $= 0$				
Plant intake water	Seasonal $= 0$				
Ash water (pond)	Seasonal $= 0$				
Constraints on discharge to water	Seasonal $\leqslant b$				
Integer control row – slurry	Logical $\leqslant 1$				
Control row – excess coal benefits	Logical $\geqslant 0$				

Table 4 presents the partial matrix tableau corresponding to the coal combustion activities depicted at the lower right of Figure 2 and at the top of Figure 3. (To a certain extent, the separation of furnace and boiler in Figure 3 is a modeling abstraction.) Coal combustion is represented by two column variables in each season, one for regular and one for beneficiated coal. These variables convert a ton of coal into a calculated amount of kilocalories of usable heat in the boiler (a seasonally defined row). Water required for ash removal is recorded explicitly in the (seasonal) ash water row. Solid waste is represented only by its disposal cost incorporated in the cost coefficients for the combustion column variables. A sulfur accounting is made through logical rows defined for each season and annually. Seasonally specified column variables transfer the seasonal sulfur accounting to the annual row, and the coefficient in this row (identified in the tableau as "ratio") can be used to apply proportionately different penalties in the various seasons. An annually specified column variable records the total sulfur penalty in the cost row.

Slurry pipeline option 1 Annual Integer	Slurry pipeline option 2 Annual Integer	Slurry pipeline option 3 Annual Integer	Excess coal benefits Annual	Slurry water discharge Seasonal	Slurry water recycle Seasonal	Other matrix entries
+	+	+	–		+	+
–4.5	–9	–16				
						–
4.5	9	16	–1			–
+	+	+		–1	–1	
					.95	+/–
					.05	+/–
				+/–		+/–
1	1	1				
4.5	9	16	–1			

The key relationship in Table 4 is that between the combustion column variables and the column variables defining the height of the dispersion stack. As indicated in Section 2, this relationship indirectly models the constraint imposed on plant operation by the ambient air quality standard for sulfur dioxide. (There is no explicit row representation for flue gas or sulfur dioxide.) External to the programming model, an atmospheric dispersion model is used to calculate the maximum amount of regular and of total coal which can be combusted in a given season consistent with the air quality standard. These amounts are dependent on the height of the dispersion stack, and this dependence is incorporated in the model by means of seven explicit column variables, which together construct a stack of optimal height. The first such variable is constrained to provide a stack of minimum height (150 meters); the remaining six provide increments of up to 25 meters each. These columns piecewise-approximate a nonlinear relationship of increasing incremental capital costs per increment to the allowable quantities of coal combustion. Opposite signs of the

TABLE 4 Partial matrix tableau: coal combustion.

		Build minimum stack	Build higher stack	Burn regular coal	Burn beneficiated coal	Sulfur accounting	Sulfur penalty	Annual capital charge	Other matrix entries
		Fixed = 1	6 options (each ≤ 1)	Seasonal	Seasonal	Seasonal	Annual	Logical	
Cost (objective function)	Annual minimum			+	+		+	.12	+/–
Capital investment	Logical = 0	+	+					–1	+
Regular coal at plant	Annual ≥ 0			–1					+
Beneficiated coal at plant	Annual ≥ 0				–1				+
Constraint on total coal combustion	Seasonal ≤ 0	–	–	1	1				
Constraint on regular coal combustion	Seasonal ≤ 0	–	–	1					
Heat to boiler	Seasonal ≥ 0			+	+				–
Ash water	Seasonal = 0			–	–				+/–
Sulfur accounting	Seasonal = 0			+	+	–1			
Sulfur accounting	Annual = 0					Ratio[a]	–1		

[a]Used to apply proportionally different charges in each season.

coefficients for the stack-building and combustion column variables in the two rows constraining coal combustion imply that adequate stack height must be provided for coal combustion in all seasons. The model optimally balances stack costs against differential coal combustion costs.

3.2.2 Modeling Correspondences: Electricity Generation and Cooling System

The water withdrawal and discharge activities shown in both Figures 2 and 3 are represented by separate columns defined for each season. The interaction between these columns and a system of accounting rows and columns for water use charges and discharge constraints is rather complex, and is discussed in Section 3.3. We consider now the rest of the unit processes and flows shown in Figures 3 and 4. In short, the correspondence applied here is much at the opposite extreme of that applied to the coal transportation and combustion activities. Almost all of the processes depicted are subsumed into a single column variable representing electricity generation and a particular configuration of the cooling system. (The exceptions to this scheme are nodes F and G in Figure 4 and the unlabeled node in the lower right of the same figure. The column variables representing these decision points are shown in Tables 7 and 8.)

The combination of generation and cooling processes in a single column variable is motivated by all of the previous correspondence criteria, although reduction in model size may not be readily apparent. The true option criterion is applied to the combination of the boiler, turbine, generator, and condenser as no additional uses for the steam or turbine shaft energy are modeled. Similarly, demineralization of boiler feedwater is essential, and since no other uses are modeled for the demineralized water or the demineralization unit, it makes sense to combine the unit with the other four. (We assume that optional demineralization of cooling tower blowdown would involve a separate and cheaper unit since the treated water need not be of boiler purity.)

This combination of processes not only eliminates the need to define separate column variables for each process, it also eliminates the need to explicitly define rows to represent steam, shaft energy, or boiler feedwater. The important flow criterion is used to avoid row definitions for demineralizer brine or boiler blowdown; these small flows are assumed to be routed to the ash pond. This criterion is also used to aggregate all minor water flows for such purposes as boiler cleaning and resin regeneration in the demineralizer. These water inputs are furthermore indistinguishable (in source) from cooling water intake and demineralizer input for boiler feedwater; hence, all water inputs are aggregated into a single row for water intake.

This combination of unit processes and flows yields a fairly simple input–output structure for the electricity generation activity: water and boiler heat in and electricity and ash water out. The key modeling correspondence, however, involves the relationship between the generation activity and the cooling system. While conceptually (and to a large extent physically) separable, the generation and cooling processes are subsumed in a single column variable to maintain linearity in model relationships (the fourth correspondence criterion). As discussed earlier, the net heat rate for electricity generation depends upon the configuration of the cooling system, and the water input for cooling purposes in turn depends upon the net heat rate. Because of this interdependence, it is not possible to accurately define linearly separable column variables for generation and cooling processes; the heat and water input coefficients of the generation activity would be dependent upon the activity levels of the column variables representing cooling system options. Thus, the modeling correspondence applied defines (for each season) a number of column variables representing prespecified combinations of the generation activity (at a given condenser ΔT), a single or series flow pattern across the condenser, and a particular choice of options for the cooling system configuration. The resulting column enumeration scheme is summarized in Table 5; the options identified can be readily related to the options and decision nodes discussed in the context of Figures 4 through 9.

TABLE 5 Enumeration of plant design and operating mode combinations.

Design/mode	Combinations (in each season)		
Cooling system type	Once-through	Open-tower	Closed-cycle
Condenser ΔT	3	3	3
Single vs. series condensers	(Series not used)	2	2
Wet bulb approach factor	Not applicable	4	4
Cycles of concentration for closed-cycle cooling tower	Not applicable	Not applicable	2
Recirculation for maintenance of condenser inlet temperature[a]	1 or 2[b]	1 or 2[b]	1 or 2[c]
Total column variables defined	3 or 6	24 or 28	48–96

[a]When necessary. Two options are available:
1. Recirculation of sufficient amount of condenser outlet water
2. Combination of open-cycle and closed-cycle flow, if temperature of closed-cycle recycle exceeds 10°C

[b]Two options are defined if (and only if) river temperature is below 10°C and temperature of closed-cycle recycle exceeds 10°C for at least one of the defined wet bulb approach factors.

[c]If river temperature is below 10°C, two options are defined only for those combinations with a wet bulb approach factor which produces a recycle temperature greater than 10°C.

The column variables enumerated for each season represent "pure" system configurations; each represents a particular combination of fully implemented process options. While only one choice of condenser ΔT is allowed, mixed system configurations with respect to the other options are modeled via linear combinations (in the programming model solution) of the column variables for pure system types. This mixing by linear combination applies not only to combinations of once-through, open-tower, and closed-cycle cooling systems but also to combinations of single and series condenser flow patterns and to combinations of wet bulb approach factors or cooling tower cycle factors. Thus, the model indirectly has many more configurations available than the particular "pure" options enumerated at the identified decision points. Of course, these linear combinations are linear approximations to complicated nonlinear relationships, but it is believed that this approximation is significantly better than that accomplished by defining separate column variables to represent each of the modeled processes or decision points. From a computational viewpoint, this improved approximation is paid for by a marked increase in the number of column variables, but at the same time a significant number of rows is saved. In our model, this saving in the number of rows keeps the incremental computational burden of added columns within acceptable limits.

TABLE 6 Partial matrix tableau: interaction between generation/cooling and capacity provision activities.

		Plant construction	Plant construction	Provide water intake capacity	Provide cooling tower capacity	Provide softening unit capacity	Generation and cooling	Generation and cooling	Annual capital charge	Other matrix entries
		ΔT option 1	ΔT option 2				ΔT option 1	ΔT option 2		
		Integer	Integer	Build	Build	Build	Seasonal	Seasonal	Logical	
Cost (objective function)	Annual minimum	+	+	+	+	+	+	+	.12	+/–
Capital investment	Logical = 0	+	+	+	+	+			–1	+
Integer control row – ΔT options	Logical = 1	1	1							1
Electricity generation – ΔT option 1	Seasonal $\geqslant 0$	–					1			
Electricity generation – ΔT option 2	Seasonal $\geqslant 0$		–					1		
Water intake capacity	Seasonal $\geqslant 0$			1			–	–		–
Cooling tower capacity	Seasonal $\geqslant 0$				1		(–)[a]	(–)[a]		–
Softening unit capacity	Seasonal $\geqslant 0$					1	(–)[a]	(–)[a]		–

[a] If relevant.

A partial matrix tableau of the considerable number of column variables defined for a given season would be more cumbersome than useful. Instead Tables 6 and 7 are used to illustrate two important kinds of interaction between the generation/cooling column variables and other sectors of the model matrix.

Table 6 shows the relationship between seasonally defined generation/cooling activities and column variables defined to represent construction of various power plant units. Only two options for condenser ΔT are illustrated. As in all tableaus, rows and columns identified as seasonal are structurally replicated in the model as many times as there are seasons defined. The tableau illustrates two important aspects of model structure. First, the capital construction ("build") activities provide capacity in all defined seasons. The level of capacity provision depends upon the maximum seasonal requirement, as determined by the activity levels of the generation/cooling column variables; there may be excess capacity in seasons with less than the maximum capacity requirement. Second, the quantity of electricity to be generated in each season is specified by means of the (negative) coefficients of the integer plant construction activities in the seasonal electricity generation

TABLE 7 Partial matrix tableau: disposition of cooling water effluent.

		Generation with once-through cooling	Generation with open-tower cooling	Generation with closed-cycle cooling	Discharge once-through effluent
		Seasonal (given ΔT)	Seasonal (given ΔT)	Seasonal (given ΔT)	Seasonal (matched)
Cost (objective function)	Annual minimum	+	+	+	
Heat to boiler	Seasonal $\geqslant 0$	–	–	–	
Intake water	Seasonal $= 0$	–	–	–	
Electricity generation (given ΔT)	Seasonal $\geqslant 0$	1	1	1	
Ash water	Seasonal $= 0$	+	+	+	
Once-through effluent[a]	Seasonal $= 0$	+			–1
Open-tower effluent[a]	Seasonal $= 0$		+		
Closed-cycle blowdown[a]	Seasonal $= 0$			+	
Discharge accounting	Seasonal $\leqslant 0$				+/–
Control row[b]	Seasonal $= 0$	(–)	(–)	(+)	

[a]At known temperature and dissolved solids content.
[b]Used only when condenser inlet temperature maintenance is necessary and can be achieved by combination

rows. Since only one of the (0,1) integer variables can be chosen, these rows define not only how much electricity must be generated but also which class of generation/cooling activities (with respect to condenser ΔT) must be used to provide it.

Table 7 shows the interaction between generation/cooling activities and column variables for the disposition of cooling water effluent. These latter variables in turn interact with the structure for discharge constraints and water use accounting described in Section 3.3. The important observation here is that separate sets of rows are defined in each season for once-through, open-tower, and closed-cycle effluent. The once-through effluent rows are differentiated by temperature of the effluent stream, which is essentially determined by river temperature and condenser ΔT; thus, there are as many once-through effluent rows in a given season as there are options for condenser ΔT (three in this study). The open tower effluent rows are also differentiated by temperature, which in this case is determined by wet bulb temperature and the approach factor for the cooling tower. Thus, there are as many open tower effluent rows in a given season as there are options for the cooling tower wet bulb approach factor (four in this study). The dissolved solids concentration of

Ash pond once-through effluent	Discharge open-tower effluent	Ash pond open-tower effluent	Discharge closed-cycle blowdown	Ash pond closed-cycle blowdown	Recycle closed-cycle blowdown	Other matrix entries
Seasonal (matched)	Seasonal (matched)	Seasonal (matched)	Seasonal (matched)	Seasonal (matched)	Seasonal (matched)	
					+	+/–
						+/–
					.95	+/–
						–
1		1		1	.05	+/–
−1						
	−1	−1				
			−1	−1	−1	
	+/–		+/–			+/–

of open- and closed-cycle flow.

open-cycle effluent is not represented in the model, as no constraints or charges are imposed on the solids content of such discharges. The situation is quite the reverse, however, for closed-cycle effluent. There, the rows for cooling tower blowdown are differentiated by dissolved solids concentration, which is determined by the concentration in the intake water and the number of cycles for the tower. Since the flow of blowdown is quite small relative to river flow and open-cycle discharges, the differences in temperature of blowdown at different wet bulb approach factors are ignored, and only two blowdown rows are defined for each season (one for each cycle option). The temperature of the stream is approximated by using the average of the four wet bulb approach factors.

As indicated in the tableau, all open-cycle effluent streams may be discharged to the river (subject to constraints and charges) or routed to the ash pond. The same two options apply to closed-cycle cooling tower blowdown, and a third option is defined for demineralization and recycle of this stream. Briny waste from the demineralizer is routed to the ash pond. Since the ash water row is defined as an equality, no more cooling water effluent may be disposed of in this manner than is required for ash removal. It is important to recognize that specific column variables for discharge, ash pond routing, and demineralization/recycle are matched to each cooling water effluent row. In this manner, the proper concentration-dependent costs can be assigned to the demineralization options, and stream temperatures and dissolved solids concentrations are well-defined for the discharge activities. This characteristic of the formulation is essential for proper interaction with the model structure for discharge constraints and water use accounting.

TABLE 8 Partial matrix tableau: seasonal water use accounting and discharge constraints.

		Total water withdrawals QW	Dilution of heated discharge QF	Once-through discharge QO	Open-tower discharge
		Seasonal	Seasonal	Seasonal	Seasonal
Intake water	Seasonal $= 0$	1	-1		
Water discharge	Seasonal $= 0$			1	1
Water losses	Seasonal $\leqslant 0$	1	-1	$+e$	
Constraint on temperature rise in river	Seasonal $\leqslant QR(DT)$	DT	$-DT$	$TO - TR$	$TC - TR$
Constraint on maximum discharge temperature	Seasonal $\leqslant 0$		$TR - TM$	TO	TC
Heat discharge	Seasonal $\leqslant 0$			$(TO - TR)/C$	$(TC - TR)/C$
Excess dissolved solids discharge	Seasonal $\leqslant 0$				

3.3 Formulation of Model Constraints and Water Use Accounting

In Section 2 we identified three important classes of constraints in the model: seasonal production requirements, seasonal constraints on discharges to the water, and seasonal constraints on discharges to the air. Here we describe the formulation of the constraints on discharges to the water along with the general model structure for water use accounting. The formulation of the other two classes of constraints has already been discussed in the context of Table 4 (air emission constraints) and Table 6 (electricity generation requirements).

The structure devised for discharge constraints and water use accounting is depicted in two partial matrix tableaus. Table 8 displays the constraint and accounting structure for a given season, while Table 10 shows the interaction between four seasonal column variables and a set of annually defined rows and column variables which apply specified charges or penalties for water withdrawals, water losses, heat discharges, and dissolved solids discharges (in excess of the prescribed standard). Table 9 defines the abbreviations used for parameters of the important coefficients in Table 8.

Table 8 reflects the complexity of the model structure, which arises from the nature of the constraints themselves. Some of the constraints require calculation of weighted averages for which the weights are activity levels of column variables that are unknown before the model is solved. For simplicity of notation, the once-through, open-tower, and closed-cycle discharge variables are treated as though a single variable represented each class; in the model, however, there are a number of column variables in each class. Each such variable is treated in the same manner.

Closed-cycle discharge	Slurry water discharge	Total water discharge *QD*	Total water losses *QL*	Total heat discharge	Excess dissolved solids discharge	Other matrix entries
Seasonal	Seasonal	Seasonal	Seasonal	Seasonal	Seasonal	
						+/–
1	1	–1				
		–1	–1			
$TB - TR$	$TS - TR$	$-DT$				
TB	TS	$-TM$				
$(TB - TR)/C$	$(TS - TR)/C$			–1		
$DB/1{,}000$	$DS/1{,}000$	$-SD/1{,}000$			–1	

TABLE 9 Definition of parameters used in Table 8.

QR	Total river flow in the season
DT	Maximum allowable temperature increase in river; calculated as the minimum of (1) the specified temperature increase allowance for the season, either 4°, 5°, or 6°C, and (2) the difference between maximum allowable river temperature, 30°C, and upstream river temperature
TR	Upstream river temperature
TO	Temperature of once-through discharge (condenser outlet temperature)
TC	Temperature of open-tower discharge (cooling tower basin temperature)
TB	Temperature of closed-cycle discharge (cooling tower basin temperature modified somewhat by presence of wastewater from a pretreatment unit)
TS	Temperature of slurry water discharge
TM	Maximum allowable discharge temperature (35°C)
C	Heat capacity of water
DB	Dissolved solids concentration of closed-cycle discharge
DS	Dissolved solids concentration of slurry water discharge
SD	Concentration standard for dissolved solids in discharge (500 mg/l multiplied by a seasonal proportionality constant, if desired)
e	Coefficient expressing evaporative losses in the river per unit of once-through discharge

We have adopted the convention that total withdrawals from the river QW include withdrawals for dilution purposes only QF; this gives rise to the negative unity coefficient for the dilution variables in the intake water row. This structure implies that any charges for water intake are also paid for dilution withdrawals. Should this not be the desired charging scheme, it is necessary only to remove the dilution variable coefficients in the rows for intake water and for the temperature rise constraint. Water withdrawn for use in the plant QI is simply $QW - QF$.

The row for water discharge simply accumulates the total discharge of cooling water and slurry water. This total, as reflected in the activity level of the total water discharge variable QD, is essential to the formulation of the discharge constraints.

The water loss accounting row accumulates losses QL as the difference between plant intake and discharge plus an estimate of the in-river losses caused by once-through discharge QO. Algebraically, the row states

$$QW - QF + e(QO) - QD - QL \leqslant 0$$

This can be rearranged as

$$QL \geqslant QW - QF + e(QO) - QD = (QI - QD) + e(QO)$$

which is the desired accounting when equality holds. (The inequality is merely a modeling convenience which improves computability and allows for the possibility of negative losses without defining another column. Negative losses might occur because of slurry water discharge.)

By appropriately defining DT as indicated in Table 9, the modeled constraint on temperature rise in the river reflects the stronger of the two policy conditions on maximum temperature rise and maximum downstream temperature (see the definition of water discharge constraints in Section 2). In notation, this constraint requires that

$$TR' \leqslant TR + DT$$

where TR' is the temperature of the river downstream of the plant (after complete mixing).

The key to formulating the constraint is expressing TR' in terms of variables contained in the model. Logically, this temperature is the flow-weighted average of the upstream river temperature and the plant discharge temperature TD; the weights are river flow remaining after plant intake and plant discharge. Hence

$$\frac{(QR - QI)TR + QD(TD)}{(QR - QI) + QD} \leqslant TR + DT$$

$$(QR - QI)TR + QD(TD) \leqslant (QR - QI)(TR + DT) + QD(TR + DT)$$

$$QD(TD - TR - DT) \leqslant (QR - QI)DT$$

$$QI(DT) + QD(TD - TR) + QD(-DT) \leqslant QR(DT)$$

$$(QW - QF)DT + QD(TD - TR) + QD(-DT) \leqslant QR(DT)$$

$$QW(DT) + QF(-DT) + QD(TD - TR) + QD(-DT) \leqslant QR(DT)$$

The constraint form used in the model is obtained directly from this last inequality by appropriately resolving $QD(TD - TR)$ into the various components of total discharge (i.e., once-through, open-tower, closed-cycle, and slurry water).

The constraint on maximum discharge temperature is obtained by a reformulation similar to that applied above. The flow-weighted average temperature of the mixed discharge and dilution streams must not exceed the specified maximum. In notation,

$$\frac{QF(TR) + QD(TD)}{QF + QD} \leqslant TM$$

$$QF(TR) + QD(TD) \leqslant (QF + QD)TM$$

$$QF(TR - TM) + QD(TD) + QD(-TM) \leqslant 0$$

The constraint form used in the model is obtained by resolving $QD(TD)$ into the four discharge components.

The row for accounting total heat discharges straightforwardly accumulates the incremental heat content of each discharge stream. By definition, this heat loading (per period of time) is the discharge volume multiplied by the temperature differential (between discharge and river) and then divided by the heat capacity of water. The column variable for heat discharge records the total amount of this heat load added to the river (over the course of a season).

The accounting for excess dissolved solids discharges is applied, by specification, to closed-cycle and slurry water discharges only. Since taxation of the excess is applied on the basis of a quantity of solids, the coefficients in the accounting row must be scaled in order to convert concentration multiplied by discharge volume (per season) into the appropriately measured quantity of solids. The row thus accumulates solids discharged in blowdown and slurry water and subtracts a nonpenalized allowance determined by the product of the specified concentration standard and the discharge volume. The difference, if positive, is recorded by the activity level of the column variable for excess dissolved solids discharges. We include the volume of open-cycle discharges in determining the nonpenalized allowance, but do not count the solids content of open-cycle discharge. This convention can be easily changed, either to exclude open-cycle volume or to include open-cycle solids.

Shifting focus to the annual application of charges and penalties for water use, Table 10 details the four points of intersection between the seasonal and annual accounting structures. The structure is quite straightforward, although not the most efficient in terms of the number of rows and columns defined. The motivation for this structure is the same as that alluded to earlier for sulfur accounting. The formulation allows for the specification of proportionately different charges and penalties in different seasons while at the same time defining a limited number of base values for these charges and penalties, which can be easily accessed for alteration or parameterization. These base values are recorded as positive objective function coefficients in the four annual accounting columns. Seasonal values are specified through the "ratio" entries in the seasonal accounting columns. Each ratio coefficient is the ratio between the seasonal value and the base value in the annual column. This feature is employed in our study to "zero-out" withdrawal and loss charges in March, April, and May (high river flow months) and to zero-out heat discharge taxes in December through February (when inhibition of freezing may be a benefit). Parametric analysis on the base charges and taxes is reported in Section 4.

3.4 Specification of Model Coefficients

Once the row and column structure for the programming model has been established, matrix coefficients must be specified. This task may vary greatly in complexity from one sector of the model to another. In many cases coefficient specification amounts to little more than arranging basic data in a manner that is consistent with respect to units and the period of time over which flows are averaged and measured. Such is the case, for example, with most of the coefficients for coal transportation and combustion (Tables 3 and 4) and with the coefficients for water use accounting and discharge constraints (Tables 8 and 10, noting some overlap with Table 7). In other cases, however, coefficient specification is computationally complex because the coefficient represents the net effect of many technical relationships. Such is the case with the coefficients for allowable coal combustion in the stack-building column variables and with most of the coefficients for activities related to electricity generation and cooling. The procedures developed for specifying these coefficients are central to the modeling analysis.

3.4.1 Use of Matrix Generators

Operationally, the coefficient matrix for our programming model is specified through the use of so-called matrix generators. Essentially, a matrix generator is a specialized computer program designed to accept raw data and instructions from the user and to calculate (according to specified mathematical and logical relationships) the input–output

TABLE 10 Partial matrix tableau: water use charges and penalties.

		Water withdrawal charge	Water loss charge	Heat discharge penalty	Excess solids discharge penalty	Total water withdrawals	Total water losses	Total heat discharge	Excess dissolved solids discharge	Other matrix entries
		Annual	Annual	Annual	Annual	Seasonal	Seasonal	Seasonal	Seasonal	
Cost (objective function)	Annual minimum	+	+	+	+					+/–
Accounting row – water withdrawal charge	Annual = 0	–1				Ratio[a]				
Accounting row – water loss charge	Annual = 0		–1				Ratio[a]			
Accounting row – heat discharge penalty	Annual = 0			–1				Ratio[a]		
Accounting row – excess solids discharge penalty	Annual = 0				–1				Ratio[a]	
Intake water	Seasonal = 0					1				+/–
Water losses	Seasonal ⩽ 0					1	–1			+/–
Heat discharge	Seasonal ⩽ 0							–1		+/–
Excess dissolved solids discharge	Seasonal ⩽ 0								–1	+/–

[a]Used to apply proportionally different charges in each season.

coefficients for each of a specified set of column variables in the programming model. Utilization of such a program is particularly useful (often necessary) when calculations are numerous and/or complex and especially when such calculations must be performed repeatedly according to different specifications of the arguments. In our model, the seasonal and other multiple-option structures give rise to a high degree of repetition for calculations ranging from trivial to extremely complex (even iterative). In short, the model developed for this study could not be specified without the aid of matrix generators.

Five independent (FORTRAN-coded) matrix generators have been developed to produce the entire programming model matrix. One of these programs specifies the column variables related to coal transportation and combustion. Three key programs specify the large number of column variables representing electricity generation and cooling, as well as the columns representing disposal of cooling water effluent. A final program generates everything else, primarily additional water-handling activities, certain construction activities, and accounting procedures for the constraints and charges on waterborne discharges.

3.4.2 Coefficient Specification

For the coal transportation and combustion sector (Tables 3 and 4), much of the process of coefficient specification involves accumulating the various cost components for the operation of a modeled activity. These accumulated costs must then be expressed in terms of a unit level of operation of the defined column variable, which in the case of the integer variables for the slurry pipeline amounts to an entire year of operation. Slurry wastewater in a given season is simply a loss-adjusted fraction of annual flow, which is in turn the product of coal-carrying capacity and the assumed water-to-coal ratio (one in this case). Heat delivered to boiler per ton of coal combustion is defined as the heat content of the coal divided by an assumed parameter for boiler efficiency. Ash water input is proportional to the ash content of the coal, and the coefficient in the seasonal sulfur accounting row is nothing more than the fractional sulfur content of the particular grade of coal.

As indicated previously, the coefficients for the two (seasonal) coal combustion constraints involve more complicated calculations. Most of this analysis was performed "off-line," and the matrix generator serves only to convert the results of this analysis to a form and units consistent with the structure of the programming model. The basic logic and intent of the analysis were briefly outlined in the nonmathematical description of the model in Section 2.

Coefficient specification is relatively simple for the tableaus relating to water use accounting and discharge constraints (Tables 8 and 10). Here most of the work has already been done in the formulation of the structure itself. The logical function of the coefficient within this structure straightforwardly dictates its numerical assignment. As can be seen in the two tableaus and the definitions provided in Table 9, the coefficients are either basic data inputs or simple mathematical operations on those inputs.

The most complex specification task is the derivation of the column vector representations for the electricity generation/cooling system combinations. This is a multistep procedure involving three separate matrix generators (one for each type of cooling system). Ignoring the operational separation of these programs, the basic procedure may be summarized as follows.

First, an enumeration is made of the different combinations of plant design and operating modes to be considered; Table 5 is an example of such an enumeration. Second, the number of seasons to be considered is defined and a tabulation is made of the plant design and operating combinations considered sensible operating schemes in each season. (Essentially, this is a determination of the seasons during which the recirculation and series condenser options are to be considered.) For each defined season a tabulation is also made of various plant and environmental factors influencing the operation of the steam cycle or heat removal components of the power plant. The steam cycle operation is influenced by the plant utilization rate and the temperature of the water in the cooling system. Cooling system performance and resulting water temperature are influenced by river water temperature, dry and wet bulb atmospheric temperatures, and humidity.

Third, a set of design operating conditions is calculated for each plant type configuration on the basis of data on nominal operating conditions for a typical 500-MW generating unit in Poland. Estimates of power requirements for pumps, fans, electrofilters, and other incidentals are employed to convert from a gross to a net basis of operation. The key operating conditions calculated (all unitized on one net megawatt-hour of production) are net steam cycle heat rate, net overall heat rate, and net cooling rate.

Fourth, for each combination of plant design and operating mode, a progression is made through each defined season of operation in order to calculate variations from the design operating conditions brought about by seasonal variations in the plant and environmental factors. Two functional relationships are central to this determination. The first calculates the steam cycle heat rate as a function of steam condensing temperature and the plant throttle factor.* This factor has a fundamental effect on steam cycle efficiency and is a function of the plant utilization rate, plant up-time, and the net-to-gross operating ratio. The steam condensing temperature can be related to the outlet temperature of condenser cooling water, which is in turn a function of cooling water flow rate, condenser cooling water inlet temperature, and the required rate of waste heat removal. Since this last factor is in turn a function of the steam cycle heat rate, a certain circularity results in the functional relationship. This problem is resolved by means of an iterative convergence calculation on the throttle factor, the condenser flow rate, and the condenser inlet and outlet temperatures. We derived the functional form for the relationship (and particularly the dependence on throttle factor) from data published by the United States Environmental Protection Agency. Constants of the equation appropriate to Polish plant conditions were obtained by fitting the equation to data on nominal turbine performance for a 500-MW generating unit. (It was necessary to assume that the Polish data correspond to a throttle factor of one.) Figure 10 shows sample curves and the fitted data points.

The second important functional relationship involved in calculating seasonal operating conditions is a determination of cooling tower performance (when relevant) based upon the cooling water flow rate and the environmental factors listed previously. The important outputs of this determination are the temperature of the cooling tower basin water and the required dimensions of the cooling tower itself. In the case of a closed-cycle system, the temperature of the recycle water feeds back into the steam cycle equation because of its influence on condenser inlet temperature. Tower size also feeds back into the steam cycle equation because the pump and fan energy requirements for a given size tower affect the net-to-gross ratio and hence the throttle factor. These determinations must accordingly be part of the convergence loop for the steam cycle equation.

*The throttle factor may be defined as the ratio of the actual rate of heat delivery to steam (under a given operating condition) to the nominal rate of heat delivery to steam for a given plant design.

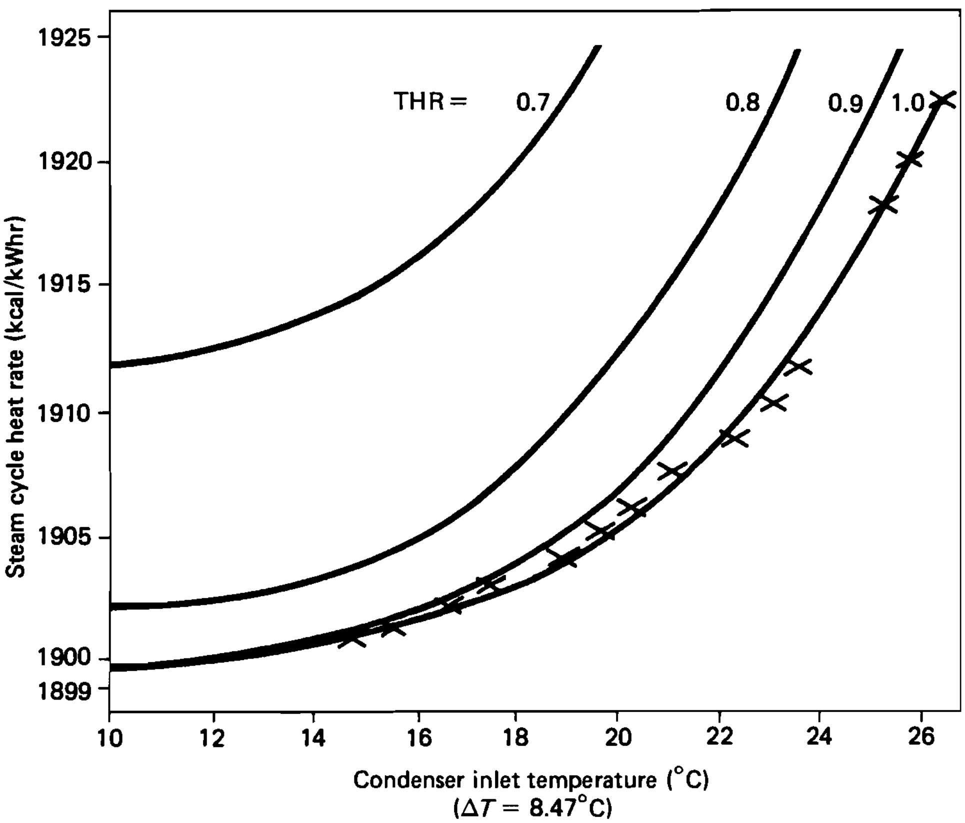

FIGURE 10 Steam cycle relationship. THR indicates throttle factor.

The final step in this procedure (for a given plant type, operating mode, and season) is specification of the actual input–output coefficients for a column variable, based on the important operating conditions determined in the convergence loop. As depicted in Tables 6 and 7, the specified inputs are boiler heat, water, and installed capacity (generation, water intake, cooling tower, softening unit). The specified outputs are electricity (one megawatt-hour net), ash water, and cooling water effluent of a known temperature and dissolved solids concentration. Since the characteristics of the effluent are known at this stage in the procedure, the coefficients of the column variables for disposition of the effluent are also specified.

All of these calculations and coefficient specifications are performed automatically by the matrix generators for each plant design, season, and operating mode selected by the user.

3.5 Data Availability

Aside from its educational value, a mathematical programming model is only as good as the economic and technical data available for defining its coefficients. We were able to construct a fairly complex programming model for this study because the data were deemed good enough to justify it. For the most part, the data base was collected by the IMGW research team and is specific to Polish conditions. Where gaps appeared during the course of model development, technical information based on similar technologies in the USA was employed, but use of cost data from the USA was successfully avoided.

Some of the more important components of the collected data base include the following:

1. A set of highly detailed specifications for the design characteristics of the power plant
2. Engineering cost estimates for the construction and design of power generation and water treatment processes
3. A tabulation of average monthly values for a wide range of meteorological and hydrological variables needed in the analysis, including a monthly specification of low flows in the river (flows exceeded 90 and 95 percent of the time)
4. A set of relationships and parameters for calculating the size of cooling tower required to dissipate a given amount of waste heat under specified meteorological conditions (plus the costs of tower construction)
5. A specification of the physical, chemical, and combustion properties of the two available grades of coal
6. Engineering cost estimates for the various coal handling and combustion processes
7. An assessment of the water management benefits accrued from the use of saline wastewater in the slurry pipeline
8. A full specification of relevant environmental standards and constraints
9. A set of relevant prices and penalties for various aspects of water and coal use, along with ranges of variation in these values for use in water demand and other analyses

On the whole, the data base is more than sufficiently reliable to produce sound modeling results. Those aspects of the data base in greatest need of further refinement are: (1) the cost structures for coal beneficiation, slurry transport, and certain incidental water treatment processes; and (2) the benefit assessment for use of saline wastewater in the slurry pipeline.

3.6 Seasonality

Throughout our discussion, the concept of seasons has been frequently employed, but generally with an intentional vagueness as to number and duration. The key determinations which must be made in defining model seasons are: (1) how short a time period is necessary to accurately capture the important time-dependent variations in operating conditions; and (2) how short a time period can be manageably considered in the modeling analysis (which involves not only model size but also data collection and interpretation of results). In general, there must be some trade-off between accuracy of representation and manageability. In this study we define 12 "seasons" corresponding to the months of the year.

Treating the time-dependent conditions in order of increasing complexity, we note that policy specifications tend to show the least time-dependent variation. In our model, a month-by-month specification of charges and standards is perfectly adequate and manageable. Output levels for a baseload plant may also be reasonably assumed to be constant over a short period of time; the most significant variation is caused by the schedule of planned plant maintenance which calls for shutdown of each block at least once a year. In our study, the knowledge that these shutdowns are concentrated in the summer months and require an average of six weeks for completion allows us to make a straightforward specification of the fraction of plant capacity in operation in a given month. Applying a constant baseload utilization rate to this operating fraction provides a monthly time pattern of plant output levels.

As is to be expected, the time pattern of meteorological and hydrological conditions demonstrates the shortest period of variation. Ultimately the availability of data and the manageability of the problem formulation dictates the choice of time period. For this study, monthly data are available for the most important meteorological/hydrological conditions, and careful design renders the problem manageable at this level of detail.

The model specifications for the defined time periods need not be based on average values, nor is it necessary to define approximately uniform time periods. These choices depend on the analyst's conception of the proper context for optimizing plant design. For example, it may be considered appropriate to optimize plant design according to expected values for the time pattern of operating conditions. On the other hand, it may be desirable to design the plant to meet a time pattern of "worst possible" conditions or conditions exceeded in adversity only 5 or 10 percent of the time. Perhaps the most sophisticated treatment would involve an optimization of design and operation in accordance with a time pattern of both average and critical conditions, with time periods for each defined in relation to expected frequencies of occurrence of the various sets of operating conditions. In the present case, manageability and data considerations dictated a composite approach employing monthly time periods, average meteorological factors, and low flow in the river defined as that with a 90 percent probability of being exceeded monthly. The model structure is sufficiently flexible, however, to allow for easy redefinition of time periods and operating conditions.

4 USE OF THE MODEL

The previous sections have dealt primarily with a description of the model and its development; this section deals with three aspects of model use. First, a few comments are made on the operation of the model, its size and computability. Second, a brief discussion is provided of the kind of information available from the model and its potential uses. Third, some representative results are presented based on preliminary analyses performed with the model in the latter stages of its development at IIASA.*

4.1 Model Operation, Size, and Computability

A serious attempt has been made in the development of the model to render it accessible to users without a great deal of mathematical programming experience. To use

*Ultimately the model was transferred to IMGW computer installations in Warsaw.

the model it is necessary to execute five FORTRAN matrix generators, collect the various sectors of the matrix produced by these programs, and then solve the model using an available solution algorithm. Accordingly, a user must have some knowledge of the host computer system, FORTRAN, and the available mathematical programming software.

From the standpoint of model specification, a user with only a general understanding of model intent and structure can produce a matrix by defining three modest data tables. These tables contain key cost specifications, meteorological and hydrological data for each season, and policy-dependent discharge constraints, prices, and penalties for each season. Through these tables the user also selects the number and length of seasons, and the number and nature of important options such as temperature rise across the condenser and cooling tower wet bulb approach factor. The matrix generators automatically expand on the other kinds of options described in this report. By this procedure, the model expands or contracts in a structurally consistent manner to accommodate the level of detail desired by the user. This frees the user to concentrate on parameter refinement and definition of desired analyses, rather than on the details of model structure. The more experienced user, naturally, may desire to alter the inner workings of the matrix generators in order to modify the structure of the model or the nature of available options.

In its present form the model encompasses 12 month-long seasons, 3 options for condenser ΔT, 4 options for the cooling tower approach factor, 2 coal types, and 3 slurry pipeline options. In addition to these specifications, the model includes the full range of fuel provision and water management options selected for this study. At this level of detail, the model contains approximately 350 rows and 1,400 columns.

These dimensions do not constitute an especially large problem, and continuous linear programming solutions posed no particular difficulties on an IBM 370/168 computer employing the SESAME linear programming system. An integer algorithm, however, was not readily available within the time constraints for the study. Fortunately, because of the limited number of integer variables, it was possible to heuristically determine optimal solutions – often by inspection and occasionally, in case of doubt, by limited enumeration. On the whole, our computing experience with the model has been highly favorable.

4.2 Information Available and Potential Uses

One of the major advantages of programming models is the wealth of information which can be derived from well-conceived patterns of model solutions. Our model can be straightforwardly applied to estimate the capital and operating costs as well as the resource demands and pollution loads that result from operation of the power plant under a wide variety of conditions. Standard parametric and ranging techniques can be employed to test the sensitivity of these estimates to model assumptions and specifications. Using such techniques to identify the important constraints and cost values conditioning the model's solution not only contributes to an understanding of the real-world system but also indicates which aspects of model development should be most closely double-checked for accuracy and reasonableness.

The potential also exists for expanding the boundaries of the problem to include a direct interface between the programming model and models of water and air quality. Our present method employs such environmental models in the background as a means of calculating rigid discharge constraints, but makes no attempt to determine the environmental impacts of relaxing or tightening those constraints and to compare such an impact to the economic effect on power plant operations. Such an approach can be a useful means of evaluating public policy and the costs of environmental protection. It is, perhaps, most profitably implemented by means of a direct interface between the emission level component of the programming model and the residual load component of the corresponding environmental model. Residual loads are then traced through the environmental model to determine the impact of plant operations on environmental quality. This technique has been successfully employed in a number of documented cases (e.g., Spofford 1976). Such an interface can, but need not, involve a simultaneous solution of disparate models according to some unitary objective criterion. It can also be used more informally to assess the trade-offs between air and water pollution or between economic and environmental objectives of social policy.

The primary purposes of this case study and model were to investigate the patterns of water use in a power plant on the Vistula River and to estimate the demands for water, both as a process input and as a medium for disposal of process wastes. IMGW therefore developed a slate of variants for the seasonal charges for water withdrawals, water losses, heat discharges, and dissolved solids discharges. Some fraction of the many possible combinations of these variants can be investigated to determine the induced changes in optimal plant design and operation. These changes map out derived demand functions for water in its various capacities; such functions may be determined jointly or independently. Shifts in these functions brought about by changes in model constraints or parameters can also be studied, both for their own sake and as a means to identify important interdependencies among various water uses or among water use, fuel use, and air pollution considerations. This is only a cursory listing of the kinds of analyses that can be performed with the Vistula model; it would not be unrealistic to assert that the primary limits to the information that can be obtained are the imagination and stamina of the analyst, and perhaps the computing budget.

4.3 Representative Model Results

Model analyses performed at IIASA were directed almost exclusively to the impact of variations in the charges (prices) for water withdrawals and losses, although some less extensive variations in the penalty for heat discharges and the price of coal were also investigated. We did not analyze the impact of changing the constraints on discharges to the water and air or the penalty on excess dissolved solids discharge. While we summarize key results of these limited analyses in this section, it is important to remember that model solutions contain a great deal more information than that presented here.

The (base) price for water withdrawals was varied in fixed steps over a range from 0.0 to 5.0 złoty (Zł) per cubic meter (1.0 Zł = 100 groszy ≅ 0.03 US dollars, at the time of the study, 1977–78). The charge for water losses was fixed at 25 times the price for water withdrawals. Initial penalties for heat and excess dissolved solids discharges were set at 0.5 Zł/10^6 kcal and 0.5 Zł/kg, respectively. Alternate heat discharge penalties of 1.0 and 2.0 Zł/10^6 kcal were investigated at three different water prices. The minemouth price of regular grade coal was specified as 320 Zł/ton for most of the modeling analyses, but this price was increased to 1000 Zł/ton (at three different water prices) to investigate the interaction between thermal efficiency and water use. All model constraints were held constant throughout the analyses.

We can make three generalizations about the model results. First, the maximum-size slurry pipeline proves to be the preferred mode of coal transportation in all cases. This consistently preferred option underscores a need to carefully verify the cost and feasibility assessments reflected in model specifications. Ideally, an investigation should be made of the range of costs over which the slurry (at any size) remains the preferred option.

Second, the maximum of the three specified options for condenser ΔT proves to be the preferred option for plant type in almost all model solutions. This preference arises both from reduced water flows and from lower capital costs relative to the other two options. The sharp rise in coal prices, however, shifts the preference to the middle option, indicating a dominance of the improvement in thermal efficiency over both increased water flows and capital costs. More sophisticated sensitivity analysis would be required to determine the precise switchpoint and/or to determine the relative importance of water flow vs. capital cost in the choice of condenser ΔT. It also seems that future analysis would be improved by providing a yet higher option for ΔT and removing the lowest option.

Third, the model solutions show great variation in the patterns of water use and in the marginal costs of electricity from season to season (i.e., from month to month). This is, of course, the expected result given the considerable seasonal variation in operating conditions, constraints, and prices and penalties. As a weak generalization, the open-tower cooling configuration seems to be a preferred option for complying with discharge constraints. The costs specified for make-up water treatment (even at three cycles) render a closed-cycle system the option of last resort. This sensitivity points to a need to carefully verify the treatment costs applied in the model.

Rather than presenting more specific results by season in this report, we can communicate the "flavor" of the model results by using certain annual totals or weighted averages. Since withdrawal and loss charges and heat discharge penalties are not applied in certain seasons, the annualized results presented must inevitably dilute somewhat the impact in price-sensitive seasons; impacts are nonetheless quite visible.

Figure 11 illustrates the derived demand relationship for water withdrawals, given the standard specifications for coal price and heat discharge tax. The axes are defined according to the convention in economics, even though price is specified and quantity observed. Withdrawal quantity is the annual total expressed in m^3/sec; this expression allows for a comparison with river flow over the middle reach of the Vistula. Mean annual flow is 297 m^3/sec, and low flows with a 10 percent probability of being exceeded range from as low as 89 m^3/sec in fall and winter to 249 m^3/sec in the spring.

Line segments connecting observation points in the graph are provided as an aid to visualizing the general shape of the relationship. They do *not* represent the response surface of the programming model. This response surface is actually a step function following the basic pattern indicated in the graph. Each step in this function identifies a range of prices over which the optimal process configuration in the model does not change. Since we specified alternative prices *a priori* rather than determining them by a parametric algorithm (which finds switchpoints in the model solution) our analysis did not identify all of the steps in the response surface. As a result, a given observation may represent either an endpoint or an interior point of the relevant step.

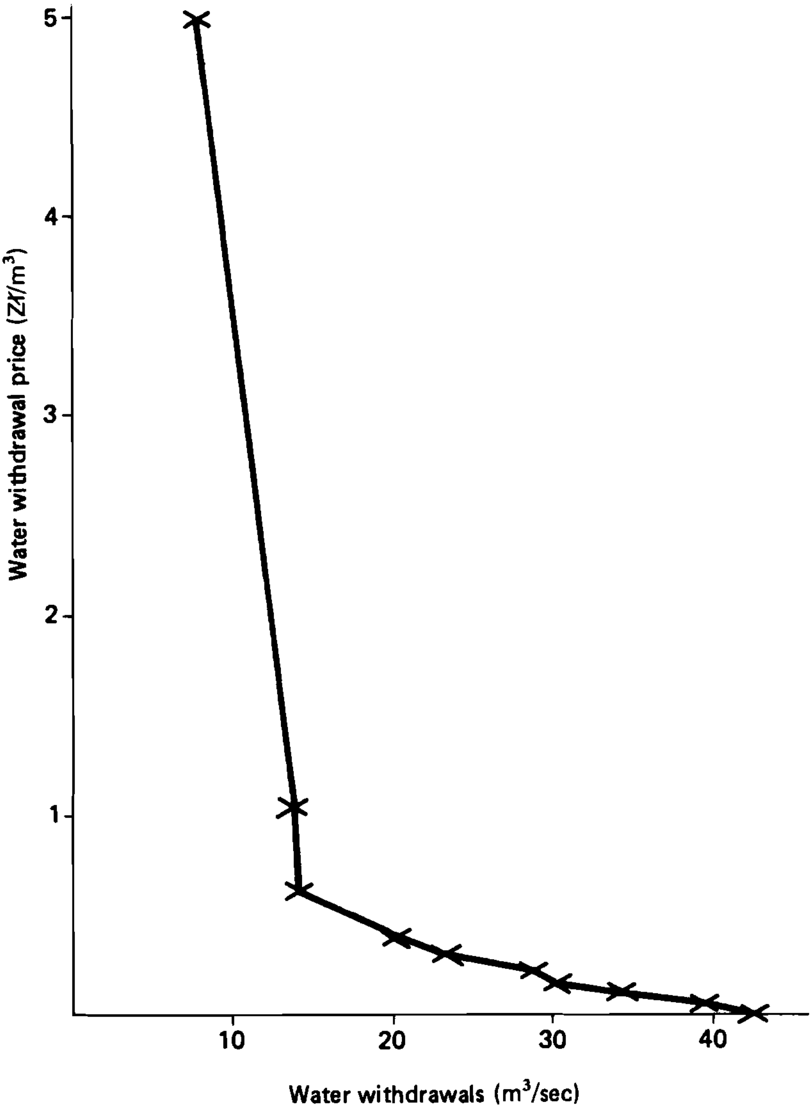

FIGURE 11 Derived demand for water withdrawal.

This limitation notwithstanding, the basic price sensitivity of withdrawal demand is readily apparent in Figure 11. Withdrawals decrease significantly as price is raised from 0.0 to 0.6 Zł/m^3, but higher prices produce only modest reductions on an absolute scale. On a proportional scale, the pattern is roughly similar, but the change at 0.6 Zł/m^3 is not as abrupt. This can be seen in Figure 12 which plots the same results on a logarithmic scale.

The significance of a logarithmic plot is that the slope of a demand curve (or, more precisely, the reciprocal of the slope) can be interpreted as a price elasticity of demand. The price elasticity of demand is a standard economic measure of sensitivity defined as

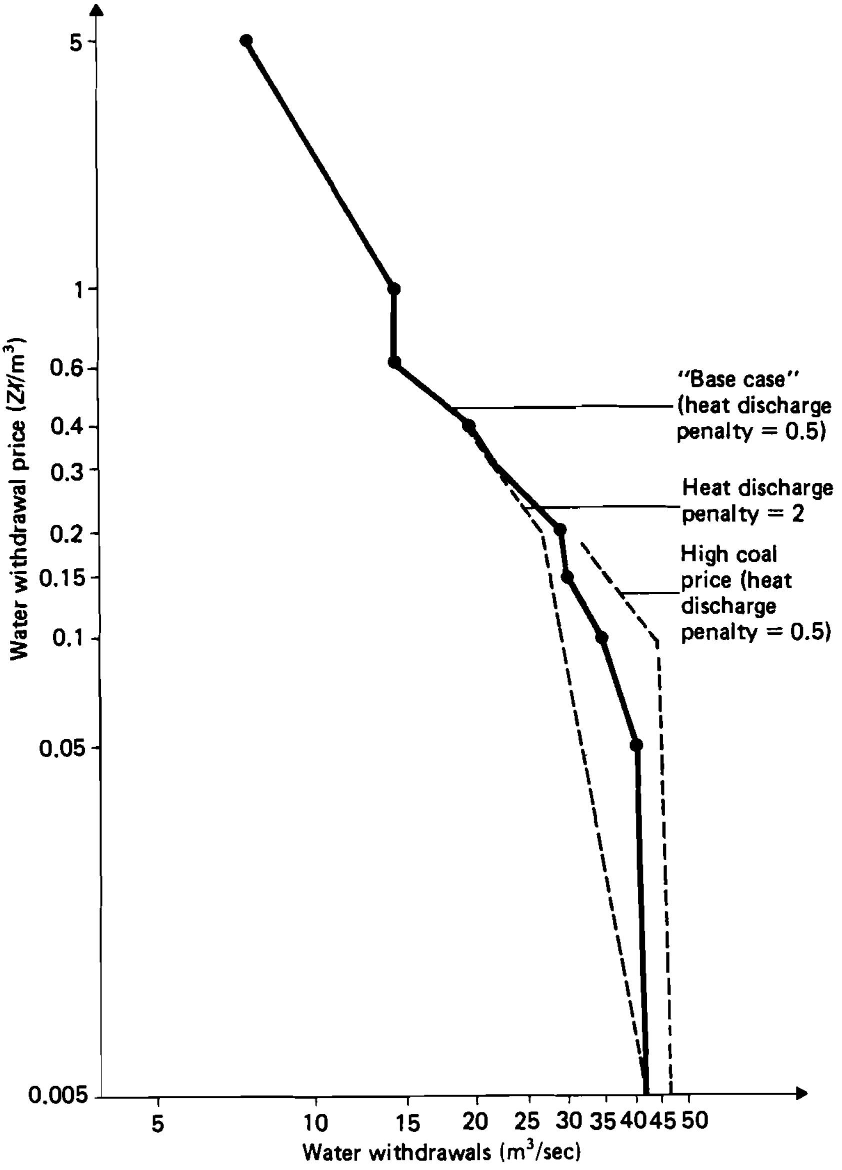

FIGURE 12 Derived demand for water withdrawal (logarithmic plot).

the percentage change in quantity divided by the percentage change in price. For very small changes in price, a point elasticity is defined as

$$(\mathrm{d}Q/\mathrm{d}P)(P/Q) = \mathrm{d}\ln Q/\mathrm{d}\ln P$$

From this arises the significance of a logarithmic plot. For larger variations in price, the so-called arc elasticity of demand defines an average elasticity between two price-quantity points as

$$(Q_2 - Q_1)(P_1 + P_2)/(P_2 - P_1)(Q_1 + Q_2)$$

This is the most appropriate quantitative measure for our results, while the logarithmic plot aids in their visual interpretation. (Note that because the underlying model response surface is a discontinuous step function, the elasticity interpretations must be rather loose.)

Over the price range from 0.0 to 0.05 Zł/m^3, the arc elasticity is merely −0.02, confirming the visual impression of an inelastic range. Demand becomes more elastic over the price range from 0.05 to 0.6 Zł/m^3, for which the arc elasticity is −0.56. The apparent changes in elasticity over this range are typical of linear programming model response surfaces, but no rigorous interpretations can be made here because the observation points do not necessarily represent switchpoints in the model solution. Demand again becomes quite inelastic over the price range from 0.6 to 1.0 Zł/m^3 (and possibly beyond), but a less inelastic range is indicated somewhere between 1.0 and 5.0 Zł/m^3.

Figure 12 also shows shifts in the derived demand relationship for water withdrawals brought about by separate increases in the heat discharge penalty and the coal price. A higher coal price brings about increased water withdrawals at each price investigated. This substitution of water for energy reflects the lower value of condenser ΔT chosen at the high coal price. Although higher water prices were not investigated at the high coal price, the near convergence of the graphs at a water price of 0.2 Zł/m^3 supports the logical prior hypothesis that the graphs will approach each other as higher water prices dictate greater and greater use of closed-cycle cooling. Higher water prices may also raise the value of condenser ΔT chosen under a high coal price.

The impact on water withdrawals of a fourfold increase in the heat discharge penalty is almost unnoticeable at the 0.0 and 0.4 Zł/m^3 withdrawal prices. Some divergence is apparent at the 0.2 Zł/m^3 withdrawal price, but the large apparent divergence at 0.05 Zł/m^3 is probably caused only by the absence of an observation in that range for the higher heat discharge penalty. These results indicate a dominance of withdrawal price over heat discharge penalty, given the constraints defined for discharges. Further evidence of this dominance is provided in Figure 13 which shows derived demand relationships for water as a medium for heat dissipation. Three curves illustrate the "penalty-responsiveness" of heat discharges at three different prices for water withdrawal. As is readily apparent from the spread of the three curves, heat discharges are much more sensitive to the price of water withdrawal than to the penalty for heat discharge. Again, present information allows this conclusion only for the set of discharge constraints defined on temperature and heat.

These results reflect the logical complementarity between water withdrawals and heat discharges. With a few minor exceptions, the process substitutions to decrease (increase) withdrawals simultaneously decrease (increase) heat discharges – and vice versa. The opposite relationship is for the most part demonstrated between water withdrawals and water losses (principally because of the losses in cooling towers). Figure 14 shows the general increase in water losses as the process configuration responds to higher and higher prices for water withdrawal. (The initial decrease in water losses results from a shift to a higher wet bulb approach factor in open-tower cooling flows. This shift lowers the temperature differential across the tower and decreases evaporative loss.) The largest part of the increase in water losses occurs over the range in which once-through and then open-tower

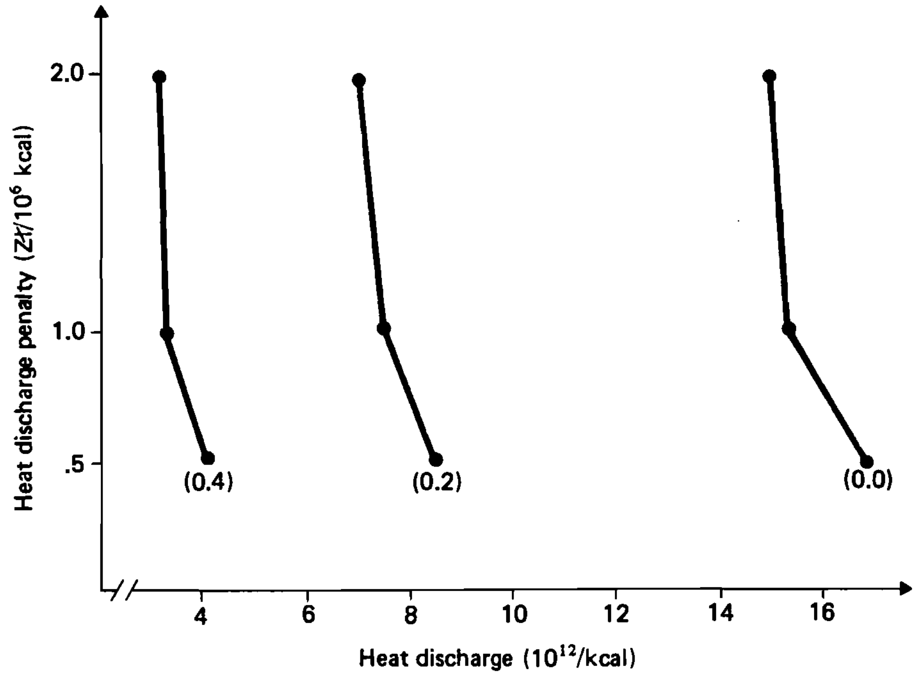

FIGURE 13 Derived demand for heat discharge. Water withdrawal prices are shown in parentheses.

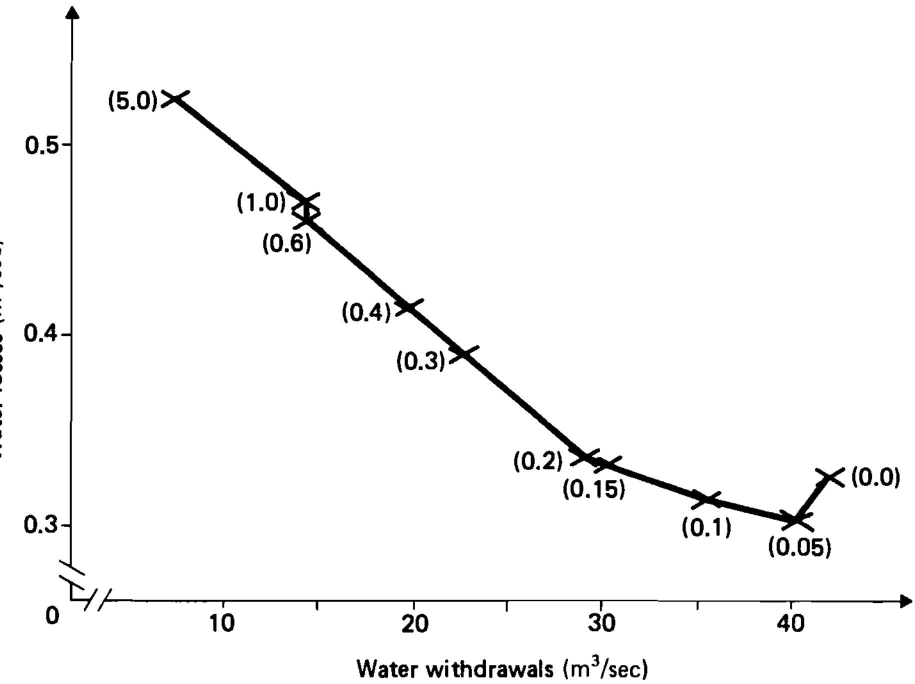

FIGURE 14 Water losses vs. water withdrawals. Water withdrawal prices are shown in parentheses.

flows are progressively replaced by closed-cycle configurations. Interestingly, the relationship is linear over much of the response range investigated, with incremental increases in water losses amounting to around 1 percent of incremental savings in water withdrawals.

We have focused exclusively on water use relationships without any indication of the cost consequences of the changes in process configuration. Since it is a cost minimization, after all, which determines the patterns of water use (subject to the defined constraints), these cost consequences are also of interest. In the end they must be borne by someone, whether or not model prices permit an interpretation of the costs as proper social costs. As an indication of these cost consequences, Figure 15 shows the average and marginal costs of plant operation as water withdrawals are varied in response to the programmed variation in withdrawal prices. Both cost figures include the outlays for withdrawal and

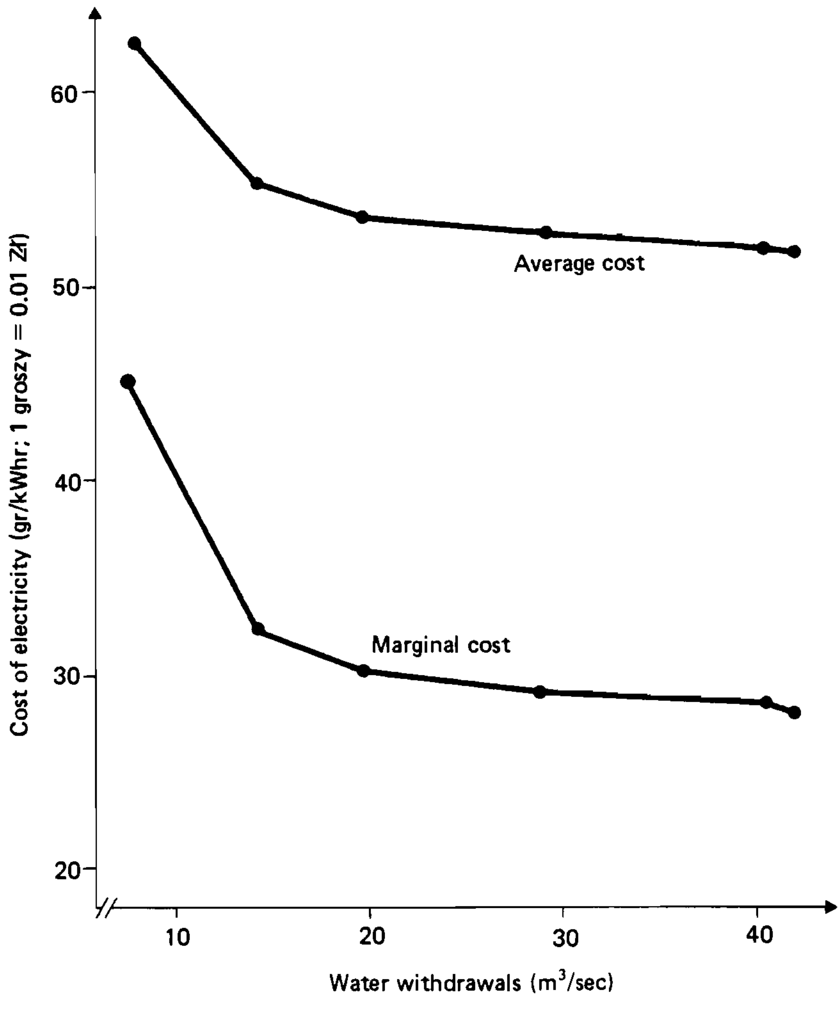

FIGURE 15 Cost of electricity vs. water withdrawals.

loss charges and for penalties on heat and excess dissolved solids discharges. Average costs are significantly higher than marginal costs because the model structure and solution essentially treat the costs of plant installation and slurry operation as fixed cost components. As the construction of the cooling tower, water intake station, blowdown demineralizer, and combustion stack are modeled linearly, the capital costs of each of these units are reflected in the marginal cost for at least one season; this cost in turn shows up in the (weighted average) marginal cost of Figure 15 as well as in the average cost.

Figure 15 shows that an initial 66 percent decrease can be attained in water withdrawals at a fairly minor increase in electricity cost; average costs increase only 7 percent while marginal costs increase 15 percent. In absolute terms, electricity costs per kWhr increase by less than 0.16 groszy for each m^3/sec of reductions in water withdrawals. The final steep increment is considerably more costly in both absolute and relative terms. The incremental cost per m^3/sec of withdrawal savings is over 1.1 gr/kWhr in this range, and the proportional cost increases are approximately threefold higher than those observed over the flatter range. This result is properly reflective of the economic law of diminishing returns, and identification of this high cost region is essential to any cost-based determination of the socially optimal rate of water withdrawal.

While a myriad of other economic and resource use relationships are contained in even the limited set of analyses performed at IIASA, it is hoped that the results selected for presentation here sufficiently illustrate the analytical potential of the programming model. In particular, these results should demonstrate the usefulness of programming models for extracting information about water demand relationships which might not be available in the statistical record.

5 CONCLUSION

In this report we have addressed the objectives, structure, and development of a mathematical programming model of resource use in electricity generation. We applied the methodology elaborated to the modeling of a hypothetical coal-fired power plant on the middle reach of the Vistula River in Poland. While this application is quite specific, the basic methodology is inherently general and may be applied in other geographical and economic contexts. The modeling results presented in Section 4 are illustrative and should not be interpreted as definitive quantitative assessments of the identified water demand issues. The results do highlight, however, the significant interrelationships between the various dimensions of water demand and the importance of taking an integrated approach to the study of industrial water demand relationships.

ACKNOWLEDGMENTS

The authors wish to acknowledge and thank a host of colleagues and friends for their assistance and cooperation in the conception and development of the Vistula Case Study and its model of electricity generation:

IIASA

Janusz Kindler, Leader of the Water Demand Research Task for project conception, initiation, and management

William Orchard-Hays for assistance in solving the model
Denise Promper for clerical assistance and logistics
Vicky Hsiung for typing assistance

Institute of Meteorology and Water Management (IMGW) and other Polish Organizations

Zdzislaw Kaczmarek, Director of IMGW, for project conception, initiation, and management
Jerzy Pruchnicki, Deputy Director of IMGW, for air pollution modeling and management
Karol Budzinski (IMGW) for air pollution modeling
Hanna Spoz-Dragan (IMGW) for meteorological and hydrological data
Ewa Czarnecka (IMGW) for clerical assistance, interpretation, and logistics
Aleksander Laski (Hydroproject) for model review and advice, water policy specifications
Czestaw Mejro (Warsaw Technical University) for model review and advice

University of Houston, Industry Studies Program

Russell G. Thompson, Director, for project conception, initiation, and supervision

Reviewers

George B. Dantzig, Stanford University
Trevor C. Hughes, Utah State University

This study was supported in part with funds provided by Stiftung Volkswagenwerk, Hannover, Federal Republic of Germany.

REFERENCES

Russell, C.S. (1973) Residuals Management in Industry: A Case Study of Petroleum Refining. Baltimore and London: Johns Hopkins University Press.

Russell, C.S., and J. Vaughn (1976) Steel Production, Processes, Products, and Residuals. Baltimore and London: Johns Hopkins University Press.

Sawyer, J.H., Jr., B.I. Bower, and G.O.G. Löf (1976) Modeling process-substitutions by LP and MIP. In R.M. Thrall et al., eds., Economic Modeling for Water Policy Evaluation. Amsterdam: North Holland Publishing Company.

Spofford, W.O., Jr., C.S. Russell, and R.A. Kelley (1976) Environmental Quality Mangement – An Application to the Lower Delaware Valley. Research Paper R-1. Washington, D.C.: Resources for the Future, Inc.

Thompson, R.G., J.A. Calloway, and L.A. Nawalanic, eds. (1976) The Cost of Clean Water in Ammonia, Chlor-Alkali and Ethylene Production. Houston, Texas: Gulf Publishing Company.

Thompson, R.G., J.A. Calloway, and L.A. Nawalanic, eds. (1977) The Cost of Electricity: Cheap Power Vs. a Clean Environment. Houston, Texas: Gulf Publishing Company.

Thompson, R.G., J.A. Calloway, and L.A. Nawalanic, eds. (1978) The Cost of Energy and a Clean Environment. Houston, Texas: Gulf Publishing Company.

STOCHASTIC WATER REQUIREMENTS FOR SUPPLEMENTARY IRRIGATION IN WATER RESOURCE SYSTEMS

Zdeněk Kos
International Institute for Applied Systems Analysis, Laxenburg, Austria

SUMMARY

In semi-humid and humid climates of the temperate zone, supplementary irrigation water requirements depend on meteorological conditions. A mathematical model is developed to assess monthly time series of irrigation water requirements, based on Penman's equation and calibrated on the basis of data obtained from irrigation systems in Czechoslovakia. In the model, monthly time series of temperature, relative humidity, sunshine, wind velocity, and precipitation are used as input data. Because of the persistence phenomena often noted in irrigation practices, the correlation between the current irrigation water requirements and those of the previous month is taken into account. The statistical properties of irrigation water requirements are analyzed as the basis for the generation of a synthetic water requirement time series. The model can be used for long-term planning of water resource systems incorporating supplementary irrigation water use, as is shown in the case of the Labe River catchment area in Czechoslovakia.

1 PROBLEM DEFINITION

In dry regions, irrigation water requirements exhibit a more or less regular cyclic form with only slight deviations from year to year, so that conventional attitudes to irrigation planning and modeling are adequate. However, in semi-humid and humid areas, supplementary irrigation is closely related to the variability of factors such as precipitation and potential evapotranspiration. This should be proved not only qualitatively but also quantitatively on the basis of data from some irrigation systems.

Meteorological data are the records of stochastic events, so the supplementary irrigation water requirements that depend on them are also stochastic. In long-term planning of water resource systems, including large-scale irrigation, the stochastic character of irrigation water requirements should be reflected on the same basis, and with the same accuracy, as other input variables. A monthly time series of flows is commonly adopted for this purpose as an appropriate input into water resource system (WRS) models. Therefore, a monthly time series of irrigation water requirements could also be adopted as an adequate form of input to these models, bearing in mind the purpose of long-term planning of large-scale irrigation.

In keeping with this main aim of the model, a prescriptive rather than descriptive model is adequate in order to create a tool with approximately the same accuracy as the other inputs and to quantify the effects of alternative irrigation and WRS designs. Otherwise, the WRS model would be too cumbersome for engineering and planning purposes.

As the results of this study will be used for long-term WRS planning, the aggregation of some data is necessary. Therefore, the influences of the type of soil, vegetation, and agricultural production on irrigated fields are aggregated into calibration coefficients, and are not taken into account as variables. Meteorological data are the only variables used for determining monthly time series.

The monthly time series is an adequate form of input for all principal kinds of WRS models, i.e.,

- deterministic simulation models, when observed time series are used directly as inputs;
- an implicit stochastic model, where the basis of synthetic time series generation is the observed (or on the observed data calculated) time series;
- an explicit stochastic model, where the parameters of the compound probability distribution are determined on the basis of the set of input time series (observed or generated).

From this analysis, it can be concluded that the most appropriate form of irrigation requirement inputs into WRS models is the time series based on climatic data, as related to large-scale irrigation policies and methods.

2 ANALYSIS OF IRRIGATION WATER REQUIREMENTS

One of the objectives of water resource systems planning, including irrigation, may be to supply water for irrigation in such a way as to maximize the net economic return of a farm, or a whole system, or to maximize the yields of marketable products. The latter objective will be attained (e.g. Skogerboe 1977), if soil water is not the limiting factor in plant growth.

The total quantities of water affecting the soil in a month during the vegetative period can be expressed in the following water budget equation (Fleming 1975):

$$\Delta S_t = P_t - E_t - R_t - G_t - U_t \tag{1}$$

where

ΔS_t = the change in water storage (mainly as soil water in an unsaturated zone);
P_t = precipitation (mainly rainfall);
E_t = evapotranspiration;
R_t = surface run-off;
G_t = subsurface flow;
U_t = underflow (deep percolation);
t = month.

The term $(R_t + G_t + U_t)$ can be used to express the unused (ineffective) part of precipitation equal to $(1 - \alpha)P_t$. Equation (1) can then be simplified to

$$\Delta S_t = \alpha_t P_t - E_t \tag{2}$$

The coefficient α is not constant and depends on many hydrological and soil conditions. However, keeping in mind the aim of the study and the aggregated character of the data, an approximation by a constant value (or determined only by precipitation) can be admitted.

The maximum value of E_t under given meteorological conditions is the potential evapotranspiration PE_t that occurs when the soil water content is not a limiting factor in evaporation and transpiration. This state can be reached by adding an amount of irrigation water, I_t. The water budget can then be expressed by

$$I_t = PE_t - \alpha_t P_t + \Delta S_t \tag{3}$$

Considering the losses in delivering irrigation water to the field (expressed by a coefficient k), the equation will be

$$I'_t = k(PE_t - \alpha_t P_t + \Delta S_t) \tag{4}$$

This equation was derived in a slightly different form by Holy (1979) for the whole vegetative period.

At the beginning of the vegetative period, the term ΔS_t can be considered as the available store of water due to winter precipitation. For planning purposes, Holy (1979) recommended the following values according to the permeability of soils:

Low: 23–55 mm
Mean: 26–45 mm
High: 12–21 mm

The depth of the active soil layer is assumed to be 0.3–0.6 m.

The individual terms in eqns. (3) and (4) will now be analyzed further, with the emphasis on the potential evapotranspiration term, as this is crucial in determining irrigation water requirements.

3 POTENTIAL EVAPOTRANSPIRATION

The best method of determining potential evapotranspiration would be its measurement under field conditions, but because this is not technically or economically feasible, sample measurements are used. Sampling may involve the measurement of soil moisture and the indirect calculation of evapotranspiration; or the lysimeter method may be used, whereby some crop (usually grass) is planted in tanks and the losses of water used to maintain satisfactory growth are measured. In general, the conditions in the tank may not closely simulate actual field conditions, and the results thus obtained may not be reliably extrapolated to a much larger area (Veihmeyer 1964). Nevertheless, the reliability of various methods of evapotranspiration estimation on the basis of measured meteorological data is often determined by comparison with lysimetric measurements. This is one of the contradictions that this study attempts to analyze.

3.1 Evapotranspiration Estimation

The basis for the determination of evapotranspiration is the physical process of evaporation, regardless of the evaporating medium (water surface, soil, vegetation, etc.). In hydrology, the term evaporation refers to the evaporation from a water surface, and evapotranspiration refers to the evaporation from soil and vegetation (but evaporation can also include evapotranspiration from bare soil). It is commonly accepted that evaporation and evapotranspiration under conditions of abundant water supply (i.e., potential evapotranspiration) are governed by the same physical laws and can be expressed by the same, or similar, formulae. Attitudes to this process differ among authors, and the following methods have been used: energy budget approach, aerodynamic approach, eddy flux measurement, heat flow measurement of sap flux and the empirical or semi-empirical method (Rodda *et al.* 1976), water budget method, energy budget method, aerodynamic profile method, eddy correlation method, combination method, and empirical formulae (WMO 1966). This classification is not unique; other authors distinguish humidity methods (e.g., Ivanov 1954, Pýcha 1965), methods using primarily temperature (Linacre 1977), and multiple correlation methods (Christiansen 1968, Christiansen and Hargreaves 1969, Kos 1969). As the classification of methods is not the primary aspect of this study, that used here is rather arbitrary.

3.1.1 Water Budget Method

The basic water budget method requires an inflow of water to the soil profile, an outflow, and a change in storage. Determination of these relations is the basic aim of hydrological models describing the dynamics of water in soil. However, only short time intervals are required; the longest acceptable interval for these deterministic hydrological simulation models is one day.

The choice of the appropriate model for this study is very difficult, as each one has its advantages and disadvantages (e.g., US Army Corps of Engineers SSARR model; Stanford Watershed model; British Road Research model; Dawdy and O'Donell model; Boughton model; Huggins and Monke model; Hydrocomp simulation model; Kutchment model; Hyreun model; Lichty, Dawdy, and Bergmann model; Kozak model; Mero model; USDAHL model; Institute of Hydrology model; Vemuri and Dracup model; Water Resources Board "Disprin" model; UBC watershed and flow model; Shih, Hawkins, and Chambers model; Leaf and Brink model; and Balek Dambo model). The application of deterministic hydrological simulation models is also not straightforward, and will be considered in the second phase of this study. For the estimates in this study, only a simple procedure is necessary.

3.1.2 Energy Budget Method

The energy budget method assumes that the energy received by a surface through radiation equals the energy used for evaporation and for heating the air and the soil, plus any advective energy. For monthly balances, the energy used in heating the soil and the advective energy may be neglected (Veihmeyer 1964), and the energy balance can then be written as follows:

$$Q_s - Q_r - Q_b - Q_h - Q_e = 0 \tag{5}$$

where

Q_s = solar radiation incident on the soil (or vegetation) surface;
Q_r = reflected solar radiation;
Q_b = net energy lost by a body of soil and vegetation through the exchange of long-wavelength radiation;
Q_h = energy conducted from a body of soil and vegetation to the atmosphere as heat;
Q_e = energy utilized for evapotranspiration.

Other authors use different terminology in the energy budget (e.g. WMO 1966), i.e.,

$$E = R_n - S - A \tag{6}$$

where

E = energy due to evaporation;
R_n = net radiation flux;
S = soil heat flux;
A = sensible heat flux,

or

$$R_n = E(1 + B) + S \tag{7}$$

where B is the Bowen ratio.

From the engineering point of view, the energy budget method cannot be used without an additional empirical approach, as there are not enough data for its application (Balek 1980).

3.1.3 Aerodynamic Profile and Eddy Correlation Methods

The classical Thornthwaite and Holzman relation (1939, 1942) gives evaporation as a function of wind speed u and the specific humidity of air q at different heights above the ground (z_1, z_2)

$$E = \frac{-k^2 \sigma (q_2 - q_1)(u_2 - u_1)}{(\log z_2/z_1)^2} \tag{8}$$

where

E = evaporation;
σ = density of air;
q_1 and q_2 = specific humidities at heights z_1 and z_2, respectively;
u_1 and u_2 = wind speeds at heights z_1 and z_2, respectively;
k = Kármán's constant.

This equation is valid under strictly neutral conditions; otherwise, it gives very high results due to the breaking of the logarithmic profile law. This aerodynamic profile method, which requires precise determination of wind and water vapor profiles near the evaporating surface, is therefore suitable for short-term studies, but cannot be used as a routine method (WMO 1966). The same holds true for the eddy correlation method, which uses measurements of vertical turbulent fluxes in the atmosphere. It involves the measurement of short-period fluctuations in vertical wind velocity and water vapor at some arbitrary level.

3.1.4 Combination Methods and Empirical Formulae

From an analysis of all evapotranspiration estimation methods at monthly intervals from the standpoint of irrigation requirements determination in this study, it seems that the only adequate ones are combinations of methods and empirical formulae. As there are many of these (e.g. Seuna 1977 lists ten methods and formulae), the most commonly used will be listed in abbreviated form here, and in detail in Appendix A, and some will be discussed as to their possible application for the purpose of this study. In this listing, PE_t is the potential evapotranspiration in period t.

Penman

$PE_t = f$(sunshine, temperature, relative humidity, wind velocity)

Linacre

$PE_t = f$(temperature, relative humidity)

Thornthwaite

$PE_t = f$(temperature)

Blaney and Criddle

$PE_t = f$(temperature, crop coefficient)

Turc

$PE_t = f$(temperature, solar radiation, precipitation, yield, crop coefficient)
$PE_t = f$(temperature, solar radiation, humidity)

Johansson

$PE_t = f$(solar radiation, wind velocity)

Ivanov

$PE_t = f$(temperature, relative humidity)

Ostromecki and Alpatjev

$PE_t = f$(saturation deficit, crop coefficient)

Pýcha

$PE_t = f$(saturation deficit, crop coefficient, temperature)

Makking, Stephens, Jensen, Jensen and Haise

$PE_t = f$(solar radiation, temperature)

McIlroy

$PE_t = f$(atmospheric pressure, net radiation, soil heat flux, wind velocity, humidity)

Christiansen and Hargreaves (multicorrelation)
PE_t = f(solar radiation, temperature, wind velocity)

Baier and Russelo (multicorrelation)
PE_t = f(temperature, solar radiation, wind velocity, saturation deficit)

Morton
PE_t = f(temperature, relative humidity, sunshine, areal evapotranspiration).
A brief discussion of Morton's method is included in Appendix C.

3.2 Comparison of Evapotranspiration Formulae

Many authors have compared evapotranspiration values estimated by a combination of methods and empirical formulae (e.g., WMO 1966, Penman 1963, Rodda *et al.* 1976, Blaney and Criddle 1966, Christiansen 1968, Schulz 1973, Seuna 1977). Some of these comparisons were for semi-humid climatic conditions (e.g., Penman 1954, 1963), but most of them referred to arid and semi-arid zones.

Measurement of data from which the potential evapotranspiration is computed depends on local site conditions, since there is no way to measure the evapotranspiration that depends purely on meteorological conditions.

Some authors claim that the best methods are those based on net radiation, but since this is difficult to measure, it is therefore calculated from the total incoming radiation and other values, such as the amount of sunshine. In some formulae, the temperature and amount of sunshine are considered to be good indicators of radiation, and can be used for monthly intervals. According to Tanner (1967), these methods give lower values in spring and higher values in autumn since there is a time lag between radiation and temperature readings due to the storage of heat in the ground.

For the purpose of this study, the comparisons made by Johansson (1970) are important, as they were done for monthly values and in a semi-humid climate of the temperate zone (Sweden). He compared the calculations from the formulae of Penman, Thornthwaite, Blaney and Criddle, and Turc, with his own, and the results were as follows. Johansson's formula gave highest radiation values in spring and the beginning of summer. Almost as high as Johansson's values were those of Penman for May and June. Thornthwaite's formula gave highest values in August and September, while Johansson and Penman gave the lowest values. This seems to confirm the suggestion of the time lag between radiation and temperature readings.

The values calculated from the formula of Blaney and Criddle were profoundly different. Their formula was derived for arid regions and was therefore not applicable to humid and semi-humid areas.

The adequacy of evapotranspiration formulae can also be judged from the standpoint of the time and space intervals to which they are applied. The Swedish International Hydrological Decade (IHD) Commission (see Forsman 1969) recommended Penman's, McIlroy's, and Konstantinov's formulae for monthly values on the micro- and meso-scales (1 m–1 km), and Budyko's formula for annual values on the meso- and macro-scales (1–100 km).

McGuinness and Parmele (1972) investigated evapotranspiration rates in Ohio (using the US Weather Bureau method based on Penman's formula) for different periods of time (1 day to 1 month), and obtained very close correlations (coefficient of multiple correlation $R = 0.96$), taking into account only the number of months t and days d:

$$PE_{t,d} = (0.179d + 1.235t - 0.0858t^2 - 0.0082td - 3.834)/10 \tag{9}$$

For $d = 30$, this equation reduces to

$$PE_t = (1.54 + 0.989t - 0.0858t^2)/10 \text{ (ft)} \tag{10}$$

For instance, for June ($t = 6$), this formula gives 0.439 ft (134 mm), which supports the statement above that evapotranspiration and consequently irrigation requirements in arid and semi-arid areas are more or less constant and are not dependent on meteorological deviations, as are those in semi-humid zones.

In Finland, Seuna (1977) calculated evapotranspiration rates in 20 regions using the US Weather Bureau formula (based on Penman's equation). The accumulation of heat in the ground was not taken into account, but the same differences as stated above occurred.

Mustonen and McGuinness (1968) criticized the lysimeter method as a basis of measuring field evapotranspiration because it gives higher values due to advection, especially over shorter periods. This effect is more pronounced in arid regions, but it may also be noticeable during dry periods in semi-humid zones. For instance, in Arizona, evapotranspiration according to net radiation was 6.4 mm/day, but the lysimeter method gave a value 159% greater. In the UK, Penman found that lysimetric measurements over a three-day interval were 112% higher than net radiation.

Riou (1977) based his theory on Penman's equation. Using a more general thermodynamic approach, he concluded that in evapotranspiration the two main terms in Penman's equation (radiation and vapor flow) are influenced by vegetation in different ways, and he therefore used the term "apparent" saturation deficit. The same effect can be achieved using different empirical coefficients for these terms, as shown in the model described in Section 5.

Brochet and Gerbier (1977) also used Penman's equation as a basis. They suggested a correction of radiation and vapor flow terms, which then led to a correction of the regression constants in Penman's equation.

Perrier (1977) stated that some differences in methods and results were the consequences of unequal notation by different authors, so that incomparable values are then discussed. He therefore suggested a classification of evaporation phenomena, explaining different definitions of evaporation and evapotranspiration.

3.3 Penman's Equation

As a result of the comparisons made in Section 3.2, it can be stated that the choice of the "best" equation to calculate evapotranspiration is not an easy one. However, some of the equations can be excluded for semi-humid climatic conditions, some are not used as they do not use all the available information, and the results of others do not differ significantly.

According to the comprehensive evaluation of Penman's equation made by Rodda *et al.* (1976), which gives many references, and to the facts that it was derived for a semi-humid climate and, according to Jensen's statement (1973), gives best results with proper calibration, Penman's equation was taken as the basis of the irrigation water requirements model. This decision was supported by the recommendations of the WMO and the practice of the FAO/WMO agroclimatology surveys. The equation will now be described in detail; the general form is

$$PE_t = f_t E_0 \tag{11}$$

where PE_t is the potential evapotranspiration in period t (mm/month), and f_t is a factor converting potential evaporation E_0 to PE_t. For the northern hemisphere, Penman suggested the following.

t	f_t
March	0.7
April	0.7
May	0.8
June	0.8
July	0.8
August	0.8
September	0.7
October	0.7

$$E_0 = \frac{\Delta R_n + \gamma E}{\Delta + \gamma} = \text{potential evaporation (mm/month)} \tag{12}$$

where

γ = psychrometric constant (= 0.49 mm °C^{-1} = 0.65 mbar °C^{-1});

Δ = slope of the saturation vapor pressure curve of air (mm °C^{-1}). In the model, this is approximated by $\Delta = 0.3559e^{T/18}$ mm °C^{-1}, where T is the mean monthly air temperature;

R_n = energy budget or net radiation (mm/month);
= H/L, where H = net radiation (J cm^{-2}/month or cal cm^{-2}/month);

L = latent heat of evaporation (1 mm ≈ 59 cal cm^{-2} ≈ 247 J cm^{-2}). The value of L at 12 °C was considered; for 20 °C it would be 245 J cm^{-2}. In the model, it was taken to be constant.

Because net radiation is not usually measured, it was calculated from measured data as follows:

$$\begin{aligned} &H = R_c - R_b, \qquad R_n = R_c/L - R_b/L \\ &R_c = R_a(1 - r)(a + bn/N) \end{aligned} \tag{13}$$

TABLE 1 Mean monthly intensity of solar radiation on a horizontal surface, R_a^d/L (mm/day) (after Criddle).

Latitude (°N)	M	A	M	J	J	A	S	O
70	4.3	9.1	13.6	17.0	15.8	11.4	6.8	2.4
60	6.8	11.1	14.6	16.5	15.7	12.7	8.5	4.7
50	9.1	12.7	15.4	16.7	16.1	13.9	10.5	7.1
40	11.0	13.9	15.9	16.7	16.3	14.8	12.2	9.3
30	12.7	14.8	16.0	16.5	16.2	15.3	13.5	11.3
20	13.9	15.2	15.7	15.8	15.7	15.3	14.4	12.9

R_a = maximum solar radiation (J cm^{-2}/month or cal cm^{-2}/month). See Table 1 for R_a^d/L (mm/day); $R_a/L = R_a^d/LD$, where D is the number of days in a month;
r = surface albedo (0.05 for water);
n = duration of sunshine (h/month);
N = maximum possible duration of sunshine (h/month). See Table 2 for N^d, then $N = N^d D$, where D is the number of days in a month;
a,b = constants: $a = 0.18$; $b = 0.55$ (other values of a and b given by WMO (1974) for tropical and humid zones differ slightly; original values used in our model have been recommended by the WMO for the semi-humid temperate zone);
R_b = back-reflected radiation (J cm^{-2}/month or cal cm^{-2}/month).

$$R_b = \sigma T_a^4(0.56 - 0.09\sqrt{e_d}\,)(0.1 + 0.9\, n/N) \tag{14}$$

where
σT_a^4 = black-body radiation (J cm^{-2}/month or cal cm^{-2}/month) at mean air temperature T_a (K);
σ_d = Stefan–Boltzmann's constant $\approx 1.17 \times 10^{-7}$ cal cm^{-2} K^{-4}/day;
σ = $\sigma_d D$ (cal cm^{-2} K^{-4}/month);
e_d = saturation vapor pressure at the dewpoint (mm);
E = vapor flow parameter (mm/month).

The constants in eq. (14) may vary with latitude (Rodda *et al.* 1976), but only slightly.

TABLE 2 Maximum possible duration of bright sunshine in hours per day (N^d calculated after Veihmeyer).

Latitude (°N)	M	A	M	J	J	A	S	O
60	11.6	13.9	16.9	17.8	17.7	15.4	12.3	10.0
50	11.9	13.3	15.4	15.7	15.8	14.4	12.2	10.7
40	12.0	12.9	14.4	14.5	14.7	13.7	12.1	11.1
30	12.1	12.6	13.7	13.7	13.9	13.3	12.0	11.5
20	12.1	12.3	13.2	13.0	13.3	12.9	11.9	11.8

According to Penman's later studies

$$E = 0.35(e_a - e_d)(0.5 + 0.54\,w)D \tag{15}$$

where

e_a	=	saturation vapor pressure at mean air temperature (mm);
e_d	=	saturation vapor pressure at the dewpoint (mm);
w	=	mean wind velocity 2 m above the ground (m s^{-1});
D	=	number of days in a month.

Note: In SI units, e_a and e_d should be expressed in millibars (mbar), but the measured values available are in millimeters of mercury, so that the expression in mbar would require a double recalculation. For WMO recommendations concerning the use of Penman's formula, see Appendix B.

Some attempts have been made to simplify Penman's equation; for instance, Linacre (1977) suggested the formula

$$E_0 = \frac{700T_m/(100 - A) + 15(T - T_d)}{80 - T} \tag{16}$$

where

E_0	=	evaporation (mm/day);
T	=	mean temperature (°C);
	=	$T_d + 0.006h$, h = elevation (m);
A	=	latitude (degrees);
T_d	=	mean dewpoint temperature (°C).

Linacre noted that typical monthly values may differ by as much as 0.5 mm/day in the calculation of evaporation from a lake surface. In fact, Linacre's method requires only air temperature and relative humidity as input data (the dewpoint temperature T_d can be calculated from the relative humidity and vice versa; the same applies to saturation vapor pressure e_d at the dewpoint). This method is therefore only suitable for locations where these data are available for evaporation estimation.

Linacre's formula was tested on the input data used in this study and it was found that in comparison with Penman's equation, it overestimated evaporation in the late months of the vegetative period. However, when an empirically determined correction coefficient Z was introduced, the deviations of both methods in the vegetative period were less than 5% in 60% of compared pairs, and the maximal deviation was 20% in April.

The formula for potential evapotranspiration PE_t was $PE_t = E_0/Z$, where E_0 is evaporation calculated from eq. (16).

t	Z
April	1.7
May	1.8
June	1.9
July	2.0
August	2.5
September	3.2

Summarizing Penman's equation, it could be expressed as F_p or F_m, i.e.,

$$PE_t = F_p(r, n/N, e_a, e_d, w, T_a) = F_m(r, n, T_a, T_b, w) \tag{17}$$

where T_b is the wet bulb temperature (°C), F_p is a combination of eqs. (9)–(13), and F_m is the function of measured values n, T_a, T_b, w, and estimated albedo (r). Other values have been defined.

The sensitivity of this equation to errors or deviations in the measured values has been analyzed by Howard and Lloyd (1979), who concluded that the errors in the input parameters were found to affect the evapotranspiration estimates significantly, particularly those that were very sensitive to marginal variations in the albedo regression constants (a and b) and temperature measurements. In turn, evapotranspiration was found to be the most significant variable in the water balance. On the other hand, errors in wind speed and sunshine measurements were far less critical (this fact also supports Linacre's simplification).

4 PRECIPITATION

The second important part of the calculation of irrigation requirements is the evaluation of effective rainfall. This can be done on the basis of continuous precipitation records, or hourly, daily or monthly rainfall values. Accurate hydrological evaluation requires time intervals not longer than one hour (Balek 1980), but for preliminary planning purposes, longer intervals can be used. The effective rainfall is evaluated on the basis of average or prevailing conditions. The most common methods use a coefficient of effectiveness α (see eq. (2)), the determination of which is discussed below.

It can be taken for granted (Holy 1980) that α is closely related to the coefficient of run-off c from irrigated fields, i.e.,

$$\alpha = 1 - c - r \tag{18}$$

where r is the coefficient of evapotranspiration during the precipitation interval. This value is often neglected, mainly because of uncertainty in the determination of c. In this case $\alpha = 1 - c$ is used, and further analysis concerns the run-off coefficient c.

Härtel (1925) was one of the first scientists to deal with this problem using

$$c = n_1\, n_2\, n_3\, n_4 \tag{19}$$

where n_1 represents the length of the field. In calculating the amount of irrigation required, the length of the field (in m) is greater than the critical value, and a constant value n_1 = 0.55 is used. The second term, n_2, represents the amount of forest cover; where there is little or none, 0.95–0.9 is used for the coefficient. The slope of the field is expressed by n_3: for hilly country, 0.8 is suggested, and for plains 0.6 (according to other authors, such as Cermak and Brenda 1971). The last term, n_4, represents the permeability of the soil. The following table gives a summary of these terms according to various authors.

Coefficient of run-off (c).

Author	Slope (%)	Soil permeability: Almost impermeable	Minimum	Mean	Maximum
Härtel (1925)	Hilly	0.38	0.33	0.31	0.29
Ven Te Chow (1964)	7	0.25–0.35		0.15–0.20	
	2	0.13–0.17		0.10–0.15	
Kostjakov (1951)	5	0.3–0.6	0.25–0.45	0.20–0.30	0.15–0.25
	< 1	0.25–0.40	0.20–0.40	0.15–0.25	0.10–0.20
Cermak and Brenda (1971)	10	0.54	0.45	0.37	0.24
	< 5	0.38	0.32	0.26	0.18

Other authors have also investigated the run-off coefficient c, such as Hudson (1973), Němec (1972), Ogrosky and Mockus (in Ven Te Chow 1964), Rodda *et al.* (1976), and Fleming (1975). The last author evaluated the role of c in hydrological models. The coefficient can be used in simple models based on the "black-box" approach, but on the other side of the complexity scale, deterministic hydrological simulation models such as the Stanford model can be used (this approach attempts to introduce physical relevance to the equations and formulae in the model, but more detailed data on time and area are required). In the present study a compromise between the two methods was achieved by means of physically based calculations of evapotranspiration and a simple evaluation of the effective precipitation.

If the systems and sensitivity analyses of the WRS show that a more detailed investigation is necessary, a conceptual model can be used. Then, instead of a run-off coefficient, other process parameters are necessary. These can obtained by a combination of measured data and indirect assessment in the process of model calibration. In the choice of the model, one that is readily available and relatively simple (in terms of the number of inputs and calibrated parameters) is preferred.

5 MODEL OF IRRIGATION WATER REQUIREMENTS

Having discussed all the main terms in eq. (4), the irrigation water requirements model can be formulated as follows:

$$WI_t = k_1 f_t \frac{\Delta}{\Delta+\gamma} R_{n,t} + k_2 f_t \frac{\gamma}{\Delta+\gamma} E_t + k_3 P_t + k_4 WI_{t-1} + C \tag{20}$$

where WI_t are irrigation water requirements, the first two terms express the potential evapotranspiration (corresponding to PE_t in eq. (4)), and the third term represents the precipitation P_t. The fourth term was not directly used in eq. (4), but it may have some relation to changes in the soil moisture content expressed by the last term in eq. (4). The last term is the intercept C, which can be taken to be a constant part of the effective precipitation.

In eq. (20), four coefficients k_1, k_2, k_3, k_4, and the intercept C have been used. The factor f_t converts the potential evaporation to potential evapotranspiration (see eq. (11));

$R_{n,t}$ is Penman's net radiation in period t (see eq. (12)); E_t is the vapor flow parameter in period t (see eq. (15)); P_t is the precipitation in period t; WI_{t-1} are irrigation water requirements in the previous time period $t-1$; γ is the psychrometric constant; and Δ is the slope of saturation vapor pressure.

The coefficients k_1, k_2, and k_3 have been suggested *a priori* from physical and operational considerations, and these can be explained as follows:

$$k_1 = kk_e g \qquad k_2 = kk_e h \qquad k_3 = kk_e \alpha \tag{21}$$

where k is a coefficient (see eq. (4)) giving the losses due to transportation and distribution of water in irrigated fields (the typical value for sprinkling irrigation is $k = 1.1-1.2$), and k_e is the coefficient of exploitation, giving the degree to which the irrigation capacity has been exploited (in the WRS discussed later, this was approximately 0.2–0.4 for the present state and 0.9 for the future).

The main difference between eqs. (4) and (20) is that the evapotranspiration term has been split into two parts by using weighting coefficients g and h. If $g = h = 1$, then it is apparent that the first two terms will produce evapotranspiration PE_t calculated by Penman's equation and multiplied by the coefficient kk_e (see eq. (21)). According to the results of the model application in this study, and comments by Barton (1979), Brutsaert and Stricker (1979), and Brochet and Gerbier (1977), different values (i.e., $h \neq g$) can be used. This is due to the fact that in irrigation system management, water is supplied at a lower rate than that indicated by the requirements of potential evapotranspiration. Some crops are only partly irrigated and, at some times, potential evapotranspiration occurs. When good irrigation practices are followed, the moisture content of the soil in the most productive areas never drops significantly below the field water capacity. However, such soil surfaces cannot usually be called saturated, and some modification to the evapotranspiration formula is necessary. Barton (1979) suggested the equation

$$PE_t = \frac{\alpha\Delta}{\alpha\Delta + \gamma} R_n + \frac{\gamma}{\alpha\Delta + \gamma} E \tag{22}$$

where α is a constant. Brutsaert and Stricker (1979) used a similar equation:

$$PE_t = (2\beta - 1)\frac{\Delta}{\Delta + \gamma} R_n + \frac{\gamma}{\Delta + \gamma} E \tag{23}$$

where β is a constant. Both of these equations indicate that modified weights for the terms R_n and E might be used; in model (20) Penman's original values were modified by the weighting coefficients g and h.

The coefficient α refers to the rainfall effectiveness (see eq. (18) discussed in Section 4). The term WI_{t-1} with coefficient k_4 was used to introduce autocorrelation due to soil water storage and the persistence of weather conditions and irrigation practices. This reflects the fact that every kind of man-controlled operation is affected by human as well as physical factors. The positive and relatively high values of k_4 (see eqs. (27) and (30)) indicate the influence of long-term irrigation policies ("If the irrigation of some crop has started it will continue till the end of the vegetative period."). The initial values of WI_{t-1} can be considered to be negligible ($WI_0 = 0$).

As a second method of taking into account soil moisture storage and the persistence of irrigation practices and weather conditions, the previous irrigation index can be used, derived experimentally to be:

$$i_t = 0.75 \log(WI_{t-1} + 7.0) \tag{24}$$

Then eq. (20) can be modified to

$$WI_t = i_t\left(k_1 f_t \frac{\Delta}{\Delta+\gamma} R_{n,t} + k_2 f_t \frac{\gamma}{\Delta+\gamma} E_t\right) + k_3 P_t + C \tag{25}$$

For cases where only temperature and relative humidity had been measured (or temperature with a dry and wet bulb), Linacre's simplification with the described correction was used. The following modification to the irrigation water requirements model was then used:

$$WI_t = k_1 PE_t + k_3 P_t + k_4 WI_{t-1} + C \tag{26}$$

where $PE_t = E_0/Z$, E_0 is calculated from eq. (16), and Z was evaluated as described above.

6 APPLICATIONS OF THE MODEL

The model was applied to two irrigation subsystems in the Labe River catchment area in Czechoslovakia, namely, the Vltava III and Vltava V irrigation systems (from now on called the V-III-V system), and the Celakovice–Vsetaty irrigation system (denoted as the C-V system; see Figure 1). The technique used was sprinkling irrigation, and both systems were observed during 1970–76. In this period, no water supply deficiency was observed in either system, for the following reasons.

The V-III-V system draws water mainly from the confluence of the Labe and the Vltava Rivers. On the Vltava River there is a cascade of reservoirs, which is used for electricity generation, and serves to regulate the river flow through Prague. This low-flow augmentation is not fully utilized downstream of Prague and the withdrawal of water for irrigation is a complementary use.

The C-V system takes water from the Labe River, the flow of which is regulated by the Roskos dam. The capacity of this dam has not yet been fully utilized, and the withdrawals of water in the observed period were not limited by low flows. Therefore, both irrigation systems used in the calibration of the model were supplied with as much water as required during the calibration period, i.e., with no reduction due to deficits.

It is intended to use the model of irrigation water requirements for the Czechoslovakian general water plan for irrigation and water resource systems for the year 2000, using measurements of water withdrawals by pumping stations in the Labe River basin. The prevailing soil type is a chernozem with a silty loam texture, and typical crops grown include cereals (40%), sugar beet (8%), potatoes (10%), vegetables (10%), alfalfa (27%), and others (5%). The intensity of agriculture on irrigated fields can be demonstrated by the crop yields: wheat 0.4 kg m^{-2}, sugar beet 4.5 kg m^{-2}, potatoes 1.5 kg m^{-2} (spring), 2.3 kg m^{-2} (autumn), and alfalfa 0.8–1.0 kg m^{-2} (hay). The area of cultivated land under irrigation is approximately 100 km^2.

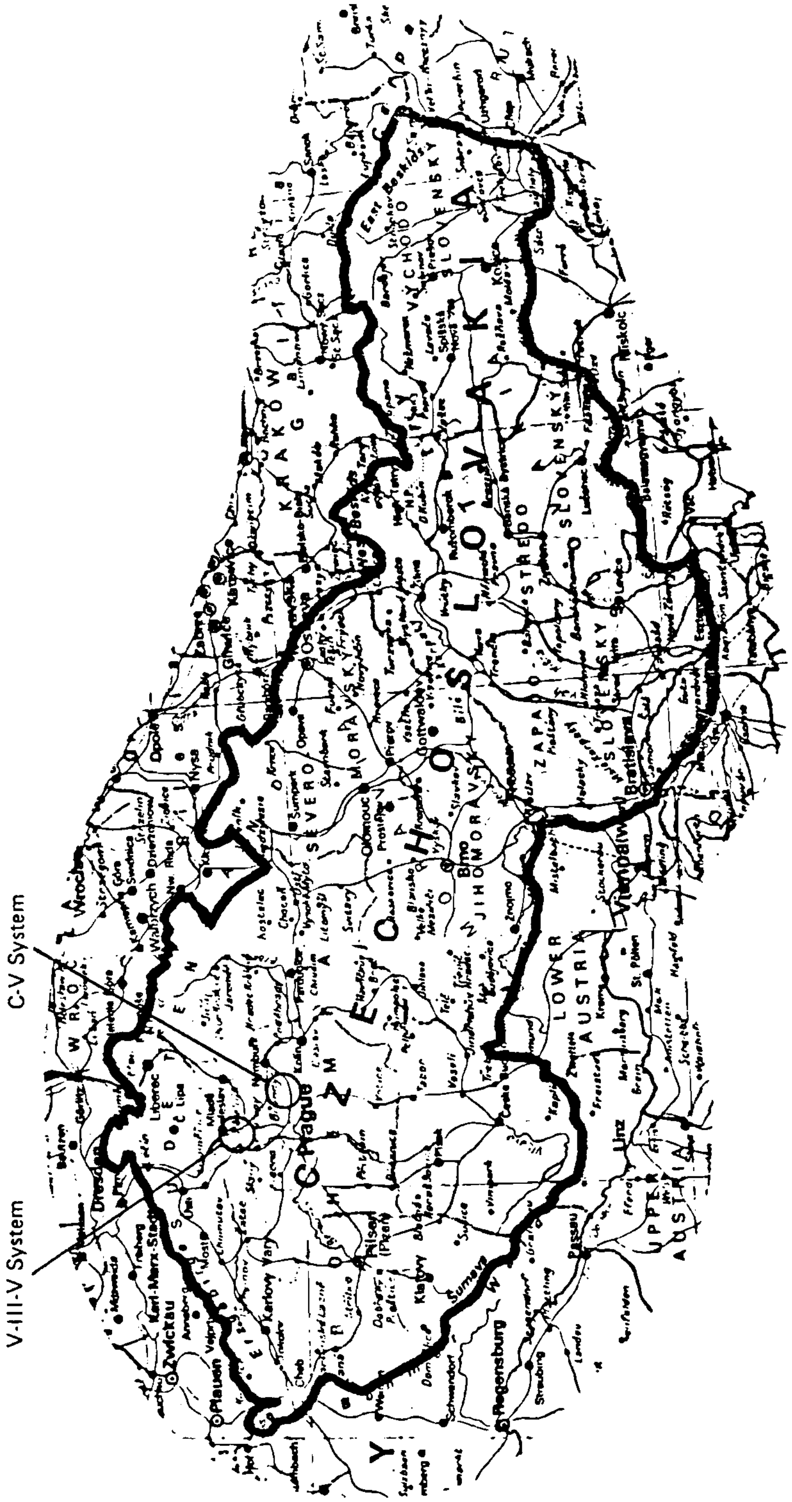

FIGURE 1 Location of irrigation systems.

TABLE 3 Input variables in regression analysis: V-III-V system (mm). $A = i_t[\Delta/(\Delta + \gamma)]R_{n,t}$; $B = i_t[\gamma/(\Delta + \gamma)]E_t$. Other variables are explained in eqs. (20) and (25).

	M	WI_{t-1}	P_t	$\frac{\Delta}{\Delta+\gamma}R_{n,t}$	$\frac{\gamma}{\Delta+\gamma}E_t$	WI_t	Previous irrigation index WI_{t-1}	P_t	A	B	WI_t
1970	6	0.24	75.50	81.90	17.40	2.67	0.24	75.50	52.81	11.22	2.67
	7	2.67	48.90	74.70	23.10	13.61	2.67	48.90	55.20	17.07	13.61
	8	13.61	106.30	57.00	9.60	2.24	13.61	106.30	56.18	9.46	2.24
	9	2.24	23.60	28.80	11.10	0.68	2.24	23.60	20.86	8.04	0.68
1971	4	0.00	16.50	33.30	14.40	0.33	0.00	16.50	33.30	14.40	0.33
	5	0.33	124.30	57.60	13.20	1.48	0.33	124.30	37.38	8.57	1.48
	6	1.48	109.70	59.10	14.70	0.10	1.48	109.70	41.14	10.23	0.10
	7	0.10	9.30	84.30	19.80	12.47	0.10	9.30	53.83	12.64	12.47
	8	12.47	57.20	68.10	22.20	26.52	12.47	57.20	65.85	21.47	26.52
	9	26.52	37.70	26.40	9.30	7.89	26.52	37.70	30.20	10.64	7.89
1972	4	0.00	24.20	27.60	15.90	0.71	0.00	24.20	27.60	15.90	0.71
	5	0.71	76.10	53.70	17.40	1.98	0.71	76.10	35.73	11.58	1.98
	6	1.98	78.90	73.20	16.80	6.72	1.98	78.90	52.34	12.01	6.72
	7	6.72	40.70	75.30	14.10	13.78	6.72	40.70	64.24	12.03	13.78
	8	13.78	51.50	57.00	14.70	9.03	13.78	51.50	56.33	14.53	9.03
	9	9.03	37.30	24.30	6.90	0.85	9.03	37.30	21.96	6.24	0.85
1973	4	0.00	47.30	27.00	18.30	1.47	0.00	47.30	27.00	18.30	1.47
	5	1.47	54.70	62.40	18.60	3.41	1.47	54.70	43.42	12.94	3.41
	6	3.41	44.10	80.70	19.50	10.62	3.41	44.10	61.59	14.88	10.62
	7	10.62	69.00	72.90	20.70	24.72	10.62	69.00	68.13	19.35	24.72
	8	24.72	14.10	68.10	18.90	26.72	24.72	14.10	76.68	21.28	26.72
	9	26.72	9.90	29.70	17.40	14.60	26.72	9.90	34.03	19.94	14.60
1974	4	0.00	10.00	33.30	22.20	15.70	0.00	10.00	33.30	22.20	15.70
	5	15.70	70.10	54.90	18.90	3.91	15.70	70.10	55.83	19.22	3.91
	6	3.91	65.80	65.10	18.90	6.26	3.91	65.80	50.67	14.71	6.26
	7	6.26	54.30	61.20	28.20	11.88	6.26	54.30	51.53	23.74	11.88
	8	11.88	44.70	65.10	21.30	13.61	11.88	44.70	62.30	20.38	13.61
	9	13.61	38.90	30.30	13.20	6.41	13.61	38.90	29.86	13.01	6.41
1975	4	0.00	19.90	30.90	18.30	0.30	0.00	19.90	30.90	18.30	0.30
	5	0.30	65.50	55.80	15.30	2.91	0.30	65.50	36.14	9.91	2.91
	6	2.91	62.00	66.30	14.40	5.55	2.91	62.00	49.52	10.76	5.55
	7	5.55	48.50	78.30	17.40	15.58	5.55	48.50	64.52	14.34	15.58
	8	15.58	20.90	65.40	17.10	20.32	15.58	20.90	66.40	17.36	20.32
	9	20.32	20.90	33.00	8.40	9.31	20.32	20.90	35.55	9.05	9.31
1976	4	0.00	17.50	33.00	16.80	2.98	0.00	17.50	33.00	16.80	2.98
	5	2.98	55.50	63.30	26.10	16.24	2.98	55.50	47.43	19.56	16.24
	6	16.24	32.00	83.10	26.10	16.11	16.24	32.00	85.15	26.74	16.11
	7	16.11	29.50	78.00	30.30	38.39	16.11	29.50	79.78	30.99	38.39
	8	38.39	37.50	59.10	25.20	26.37	38.39	37.50	73.45	31.32	26.37
	9	26.37	29.50	24.60	9.60	11.16	26.37	29.50	28.11	10.97	11.16

The coefficients in eq. (20) were determined for the V-III-V system by linear regression analysis, using the input data shown in Table 3:

$$k_1 = 0.176 \quad k_2 = 0.669$$
$$k_3 = -0.082 \quad k_4 = 0.486 \quad C = -11.61$$

Then eq. (20) for the observed period becomes

$$WI_t = 0.176 f_t \frac{\Delta}{\Delta+\gamma} R_{n,t} + 0.669 f_t \frac{\gamma}{\Delta+\gamma} E_t - 0.082 P_t + 0.486\, WI_{t-1} - 11.61 \tag{27}$$

A comparison between observed and calculated data is shown in Figure 2.

To calculate the coefficient of exploitation k_e and the weighting coefficients g and h, some assumptions have to be made since there are only two equations for the three unknowns, i.e.,

$$k_1 = kk_e g = 0.176$$
$$k_2 = kk_e h = 0.669$$

The coefficient k was evaluated as $k = 1.11$ (i.e., efficiency 90% and $k = 1/\text{efficiency}$). The relation between g and h was based on the following.

As stated earlier, the maximum yield seems to be connected with potential evapotranspiration. If Penman's equation is used to calculate the potential evapotranspiration in the original form (eq. (12)), then the weighting coefficients in eq. (21) will be $g = h = 1$, and their sum will therefore be $g + h = 2$. In eq. (20), the condition $g = h = 1$ is not required, but a weaker condition, $g + h = 2$. With this equation, the following system can be obtained:

$$k_e g = 0.176/1.11 = 0.158$$
$$k_e h = 0.669/1.11 = 0.603$$
$$g + h = 2$$

and the resulting values are

$$k_e = 0.381 \quad g = 0.41 \quad h = 1.59$$

If a maximum feasible coefficient of exploitation estimated by $k_e = 0.9$ has to be reached, then the regression coefficients k_1, k_2, k_3, and the intercept C have to be multiplied by the ratio of actual and maximum coefficients, i.e., $d = 0.9/0.381 = 2.36$. Equation (20) then becomes:

$$WI_t = 0.415 f_t \frac{\Delta}{\Delta+\gamma} R_{n,t} + 1.579 f_t \frac{\gamma}{\Delta+\gamma} E_t - 0.194 P_t + 0.486\, WI_{t-1} - 27.4 \tag{28}$$

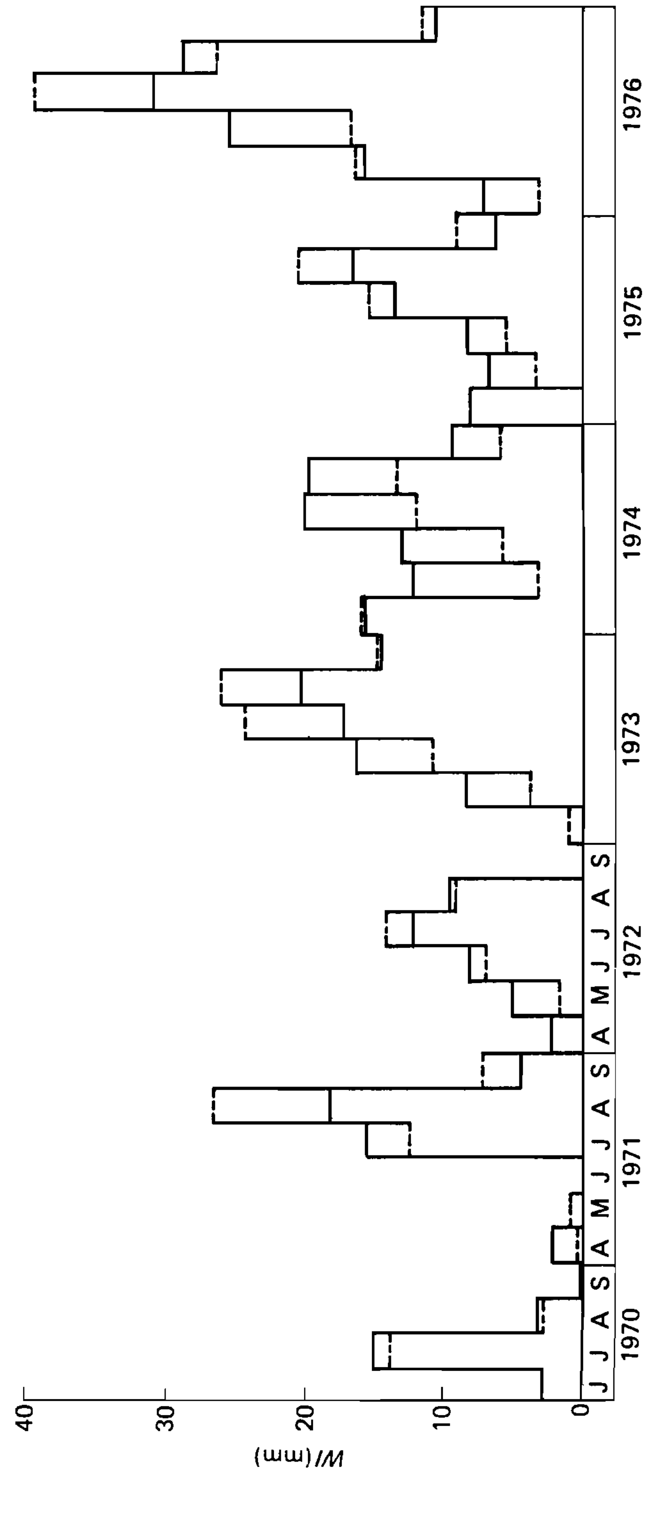

FIGURE 2 Calculated and observed *WI* values for the V-III-V system (mm): ——, calculated from eq. (27); - - -, observed.

The multiregression coefficient of correlation is 0.873, indicating a close correlation (further details are given below). For the same V-III-V system, eq. (25) was calibrated by regression analysis and the resulting coefficients were

$$k_1 = 0.307 \qquad k_2 = 0.478$$
$$k_3 = -0.080 \qquad C = -8.48$$

Equation (25) then becomes:

$$WI_t = i_t\left(0.307 f_t \frac{\Delta}{\Delta+\gamma} R_{\mathrm{n},t} + 0.478 f_t \frac{\gamma}{\Delta+\gamma} E_t\right) - 0.080 P_t - 8.48 \tag{29}$$

The resulting multiregression coefficient of correlation is 0.846.

For the C-V system, the following results were obtained:

$$k_1 = 0.149 \qquad k_2 = 0.356$$
$$k_3 = -0.119 \qquad k_4 = 0.438 \qquad C = -1.49$$

and eq. (20), based on the input data in Table 4, becomes:

$$WI_t = 0.149 f_t \frac{\Delta}{\Delta+\gamma} R_{\mathrm{n},t} + 0.356 f_t \frac{\gamma}{\Delta+\gamma} E_t - 0.119 P_t + 0.438\, WI_{t-1} - 1.49 \tag{30}$$

The goodness-of-fit of the model is apparent from Figure 3. If the same procedure is used to calculate the coefficients k_e, g, and h, then $k_\mathrm{e} = 0.228$, $g = 0.59$, and $h = 1.41$ will be obtained. For maximum possible utilization ($k_\mathrm{e} = 0.9$), k_1, k_2, k_3, and C can be multiplied by the ratio $d = 0.9/0.228 = 3.95$, and eq. (20) then becomes:

$$WI_t = 0.590 f_t \frac{\Delta}{\Delta+\gamma} R_{\mathrm{n},t} + 1.409 f_t \frac{\gamma}{\Delta+\gamma} E_t - 0.470 P_t + 0.438\, WI_{t-1} - 5.90 \tag{31}$$

The relation of the individual terms in eq. (31) to irrigation water requirements can be expressed by the individual correlation coefficients $r_{i,d}$ relating the independent variable i, and the dependent variable (irrigation water requirements) d. The degree of the explained part of the relation is characterized by the multiple correlation coefficient R_i, where i denotes the number of independent variables (e.g., R_3 takes into account the first three components: the radiation term, and vapor flux term of evapotranspiration and precipitation). The reliability of the derived equation can also be tested by the F-test. The critical values of the F-test (F_crit) of the α value of significance ($\alpha = 0.05$) were:

$i =$	2	3	4
F_crit	3.2	2.8	2.6

Because the sampling values of the F-test were much greater, the relation is highly significant. The values of $r_{i,d}$, R_i, and F_i were as follows.

TABLE 4 Input variables in regression analysis: C-V system (mm). $WI_t^1 = WI_t/2.22$, $WI_{t-1}^1 = WI_{t-1}/2.22$; $A = i_t[\Delta/(\Delta + \gamma)]R_{n,t}$; $B = i_t[\gamma/(\Delta + \gamma)]E_t$. Other variables are explained in eqs. (20) and (25).

							Previous irrigation index				
	M	WI_{t-1}^1	P_t	$\frac{\Delta}{\Delta+\gamma}R_{n,t}$	$\frac{\gamma}{\Delta+\gamma}E_t$	WI_t^1	WI_{t-1}^1	P_t	A	B	WI_t^1
1970	6	1.66	13.00	81.90	17.40	6.58	1.66	13.00	57.59	12.23	6.58
	7	6.58	26.00	74.70	23.10	6.11	6.58	26.00	63.48	19.63	6.11
	8	6.11	95.00	57.00	9.60	2.44	6.11	95.00	47.78	8.05	2.44
	9	2.44	21.00	28.80	11.10	3.87	2.44	21.00	21.06	8.12	3.87
1971	4	0.00	12.00	33.30	14.40	1.80	0.00	12.00	33.30	14.40	1.80
	5	1.80	98.00	57.60	13.20	2.63	1.80	98.00	40.80	9.35	2.63
	6	2.63	110.00	59.10	14.70	0.39	2.63	110.00	43.60	10.84	0.39
	7	0.39	5.00	84.30	19.80	9.86	0.39	5.00	54.91	12.90	9.86
	8	9.86	60.00	68.10	22.20	9.36	9.86	60.00	62.66	20.43	9.36
	9	9.36	35.00	26.40	9.30	4.66	9.36	35.00	24.03	8.47	4.66
1972	4	0.00	26.00	27.60	15.90	1.21	0.00	26.00	27.60	15.90	1.21
	5	1.21	94.00	53.70	17.40	1.86	1.21	94.00	36.82	11.93	1.86
	6	1.86	66.00	73.20	16.80	6.13	1.86	66.00	52.02	11.94	6.13
	7	6.13	39.00	75.30	14.10	6.23	6.13	39.00	63.16	11.83	6.23
	8	6.23	48.00	57.00	14.70	3.28	6.23	48.00	47.94	12.36	3.28
	9	3.28	60.00	24.30	6.90	1.61	3.28	60.00	18.45	5.24	1.61
1973	4	0.00	34.50	27.00	18.30	1.43	0.00	34.50	27.00	18.30	1.43
	5	1.43	48.40	62.40	18.60	4.71	1.43	48.40	43.34	12.92	4.71
	6	4.71	47.00	80.70	19.50	7.45	4.71	47.00	64.67	15.63	7.45
	7	7.45	79.10	72.90	20.70	8.26	7.45	79.10	63.42	18.01	8.26
	8	8.26	8.00	68.10	18.90	11.26	8.26	8.00	60.45	16.78	11.26
	9	11.26	7.70	29.70	17.40	9.34	11.26	7.70	28.10	16.46	9.34
1974	4	0.00	8.40	33.30	22.20	8.45	0.00	8.40	33.30	22.20	8.45
	5	8.45	80.00	54.90	18.90	3.17	8.45	80.00	48.95	16.85	3.17
	6	3.17	73.70	65.10	18.90	4.53	3.17	73.70	49.18	14.28	4.53
	7	4.53	64.60	61.20	28.20	2.69	4.53	64.60	48.73	22.45	2.69
	8	2.69	66.10	65.10	21.30	4.83	2.69	66.10	48.15	15.75	4.83
	9	4.83	30.60	30.30	13.20	3.23	4.83	30.60	24.38	10.62	3.23
1975	4	0.00	19.90	30.90	18.30	1.43	0.00	19.90	30.90	18.30	1.43
	5	1.43	74.70	55.80	15.30	1.98	1.43	74.70	38.75	10.63	1.98
	6	1.98	41.10	66.30	14.40	5.66	1.98	41.10	47.39	10.29	5.66
	7	5.66	28.80	78.30	17.40	6.43	5.66	28.80	64.75	14.39	6.43
	8	6.43	17.50	65.40	17.10	8.52	6.43	17.50	55.34	14.47	8.52
	9	8.52	18.00	33.00	8.40	7.16	8.52	18.00	29.48	7.50	7.16
1976	4	0.00	14.00	33.00	16.80	2.51	0.00	14.00	33.00	16.80	2.51
	5	2.51	48.00	63.30	26.10	7.90	2.51	48.00	46.44	19.15	7.90
	6	7.90	25.00	83.10	26.10	8.70	7.90	25.00	73.13	22.97	8.70
	7	8.70	30.00	78.00	30.30	16.77	8.70	30.00	69.96	27.18	16.77
	8	16.77	36.00	59.10	25.20	12.71	16.77	36.00	60.99	26.01	12.71
	9	12.71	2.00	24.60	9.60	8.25	12.71	2.00	23.89	9.32	8.25

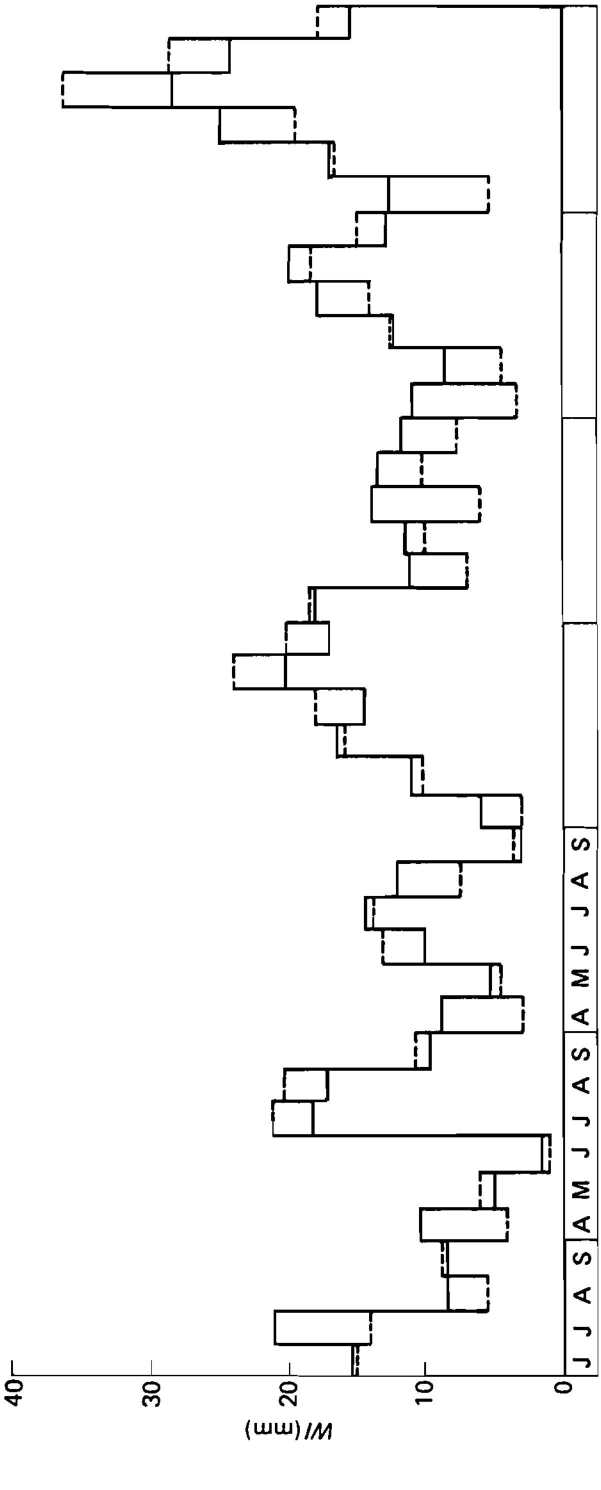

FIGURE 3 Calculated and observed *WI* values for the C-V system (mm): ——, calculated from eq. (30); - - - -, observed.

For eq. (27) and the V-III-V system:

$i =$	1	2	3	4
$r_{i,d}$	0.454	0.613	−0.296	0.534
R_i		0.631	0.716	0.873
F_i		12.2	12.5	28.0

For eq. (30) and the C-V system:

$i =$	1	2	3	4
$r_{i,d}$	0.445	0.505	−0.417	0.595
R_i		0.545	0.724	0.870
F_i		7.8	13.2	27.2

For eq. (29) using the previous irrigation index and considering $i_0 = 7.0$ as an additional parameter, the values for the V-III-V system will be:

$i =$	2	3	4
$r_{i,d}$	0.734	0.725	−0.296
R_i		0.819	0.846
F_i		25.07	22.59

Very useful indicators of the significance of the regression coefficients are their standard errors and t-values; these have been computed for eqs. (27, V-III-V system) and (30, C-V system). For eq. (27) and the V-III-V system:

$i =$	1	2	3	4
k_i	0.176	0.669	−0.082	0.486
s_{k_i}	0.051	0.117	0.032	0.080
t_i	3.45	5.72	2.56	6.07

The t-values were defined as $|k_i - 0|/s_{k_i}$. When $t_i > t_{\text{crit}}$, the hypothesis that $k_i = 0$ is rejected. The value t_{crit} (level of significance $\alpha = 0.05$; $n = 40$) = 2.02. Since the relation $t_i > t_{\text{crit}}$ is fulfilled for all i, the coefficients k_i are statistically significant.

For eq. (30) and the C-V system:

$i =$	1	2	3	4
k_i	0.149	0.356	−0.119	0.438
s_{k_i}	0.042	0.149	0.024	0.076
t_i	3.55	2.39	4.96	5.76

Since $t_i > t_{\text{crit}} = 2.02$ for all i, all the regression coefficients are statistically significant.

The results of the calibration show that irrigation water requirements are more sensitive to evapotranspiration than to precipitation. As evapotranspiration has been expressed in two terms, the irrigation water requirements are more dependent on vapor flow than on radiation, in good agreement with the observations of some authors of evaporation formulae, based on the vapor flux term only.

An interesting result is the relatively low correlation between irrigation water requirements and precipitation, which can be explained in several ways. First, the evaporation term is an index of the overall synoptic situation. High evaporation means little precipitation, and vice versa. Secondly, irrigation practices are governed more by evaporation than by precipitation. Thirdly, the intercept C can be considered to be a constant part of effective precipitation. More precisely, the effective rainfall can be considered as a linear function of precipitation:

$$P_e = \alpha P + \beta \tag{32}$$

as compared to the original equation ($P_e = \alpha' P$).

It is worth noting that there is a relatively close positive correlation between irrigation in the current month and that in the previous one, i.e., autocorrelation indicates the persistence of weather conditions and irrigation practices.

The relatively low value of α in eqs. (27)–(31) needs further discussion. According to Section 4, the expected value of α would be 0.5–0.7. At first, a fully exploited and developed irrigation system should be considered for this comparison; eqs. (28) and (31) are therefore used. Further, the intercept C is considered to be a constant part of effective precipitation. Then, for average precipitation $\bar{P}$, the following values are derived comparing $P_e = \alpha' \bar{P}$ with eq. (32) and considering the loss coefficient $k = 1.1$.

For the V-III-V system,

$$\alpha' = \frac{1}{k}\,\frac{\alpha\bar{P}+\beta}{\bar{P}} = \frac{1}{1.1}\,\frac{0.194 \times 47 + 27.4}{47} = 0.70 \tag{33}$$

and for the C-V system,

$$\alpha' = \frac{1}{k}\,\frac{\alpha\bar{P}+\beta}{\bar{P}} = \frac{1}{1.1}\,\frac{0.470 \times 42.78 + 5.90}{42.78} = 0.55 \tag{34}$$

The resulting values correspond closely to the expected ones, and are in accordance with the values of the run-off coefficient, c.

The regression analysis and calibration procedure was also carried out for eq. (26) using Linacre's formula. The resulting equations were:

(*a*) Observed V-III-V system:

$$WI_t = 0.330\,PE_t - 0.103\,P_t + 0.578\,WI_{t-1} - 12.76 \tag{35}$$

(*b*) Fully developed V-III-V system (using the transformation coefficient $d = 2.37$):

$$WI_t = 0.782\,PE_t - 0.244\,P_t + 0.578\,WI_{t-1} - 30.24 \tag{36}$$

(*c*) Observed C-V system:

$$WI_t = 0.223\,PE_t - 0.119\,P_t + 0.502\,WI_{t-1} - 2.97 \tag{37}$$

(*d*) Fully developed C-V system (using the transformation coefficient $d = 3.96$):

$$WI_t = 0.883\,PE_t - 0.471\,P_t + 0.502\,WI_{t-1} - 11.76 \tag{38}$$

The statistical parameters were as shown below.

$i =$	1	2	3
V-III-V system			
$r_{i,d}$	0.473	−0.296	0.534
R_i		0.636	0.864
F_i		12.5	35.4
C-V system			
$r_{i,d}$	0.455	−0.417	0.595
R_i		0.670	0.871
F_i		15.0	37.6

6.1 Time Series Modeling

The time series of irrigation requirements were modeled using eqs. (27), (28), (30), and (31) for the period 1931–70 (for eqs. (27) and (30) in 1931–36, see Figure 4). Equation (29) was not used because it does not give significantly better results. Since data were available from meteorological station S for Penman's equation (Table 5), these were used for time series modeling. Linacre's simplification was used for comparison only; it is only useful when temperature measurements (dry and wet bulb) are available.

The soil moisture conditions at the beginning of the vegetative period were determined to be 40 mm, and this average was used for planning purposes (Holy 1979). If this stored water is not exhausted by March, the rest will be used in April. The October values were reduced by a coefficient 0.3 because only about 30% of the area is generally utilized in this month.

For time series modeling, eqs. (27), (28), (30), and (31) should contain an error term because the compiled values give averages of WI_t and the computed series will thus have lower variances than the observed series. However, it is first necessary to determine the type of probability distribution of WI_t, which was the main aim of the analysis.

The resulting time series model of irrigation water requirements was analyzed statistically. The main input time series (based on observations at station S) was also analyzed to discover the statistical properties of the results. The averages, standard deviations, and coefficients of variation of $e1_t$, $e2_t$, and P_t are shown in Table 6, where

$$e1_t = f_t \frac{\Delta}{\Delta + \gamma} R_{\mathrm{n},t}$$

$$e2_t = f_t \frac{\gamma}{\Delta + \gamma} E_t$$

f_t, Δ, γ, R_n, and E were defined in eqs. (11)–(15), and P_t is precipitation.

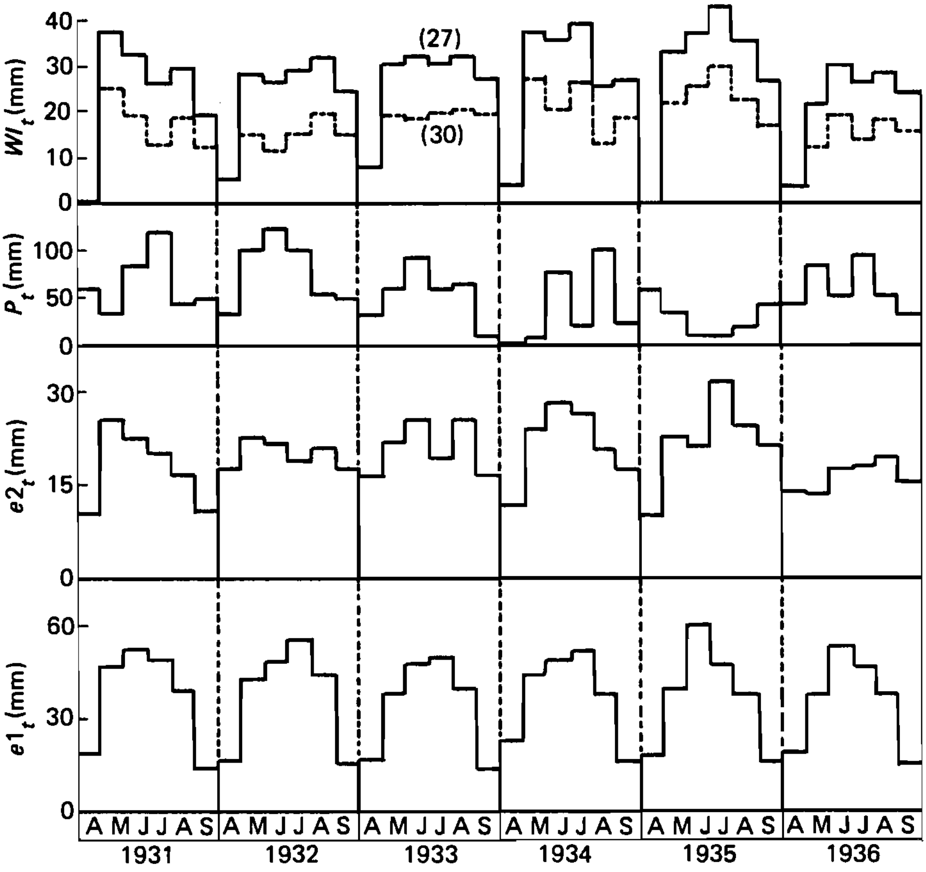

FIGURE 4 Time series of input data and irrigation water requirements of the V-III-V system (using eq. (27)), and the C-V system (using eq. (30)).

The coefficient of variation values, C_v, suggest that $e1$ is a relatively stable element ($C_v = 0.084$ on average, or 8.4%). The second evapotranspiration term expressed by vapor flux $e2$ has a higher variation ($C_v = 0.23$ on average, or 23%). Since the corresponding regression coefficients in eqs. (27)–(31) have the highest values, this term adds considerably to the final variation. Precipitation has the greatest value ($C_v = 0.52$ on average, or 52%). Therefore, in combination with a higher regression coefficient (e.g., eq. (31)), it can be an important source of variability in the resulting irrigation water requirements.

The question as to whether the differences in averages for 1931–70 and 1970–76 are statistically significant can be answered by comparing the computed t_i and t_{crit} values. Both averages and standard deviations differ, so t_{crit} values were computed by means of the formula given by Janko (1958):

$$t_{crit} = \frac{\nu_1 t_{f_1} + \nu_2 t_{f_2}}{\nu_1 + \nu_2}$$

TABLE 5 Data for Penman's equation. (M = 2: April; M = 3: May, etc.)

	M	TE	RH	W	N	R_c	R_b	E_0	PE
1970	2	7.40	0.72	3.00	3.40	3.87	1.42	2.04	1.43
	3	12.40	0.90	2.30	5.18	5.34	1.49	2.54	2.04
	4	18.10	0.72	1.70	7.72	7.15	2.02	4.13	3.31
	5	18.60	0.69	2.20	7.15	6.56	1.91	4.08	3.27
	6	17.60	0.80	1.10	5.57	5.18	1.58	2.77	2.21
	7	12.90	0.76	1.70	5.78	4.40	2.10	1.91	1.34
1971	2	9.70	0.69	2.00	5.40	4.86	1.99	2.28	1.60
	3	15.10	0.74	1.40	5.37	5.44	1.61	2.95	2.36
	4	15.20	0.77	2.00	4.31	5.25	1.32	3.08	2.46
	5	19.30	0.65	1.40	8.93	7.50	2.33	4.34	3.47
	6	19.90	0.66	1.70	7.88	6.35	2.22	3.75	3.00
	7	12.10	0.78	1.50	4.73	3.93	1.79	1.70	1.19
1972	2	8.60	0.69	2.40	3.33	3.83	1.41	2.06	1.44
	3	13.50	0.74	2.30	5.02	5.26	1.57	2.96	2.37
	4	17.10	0.72	1.70	6.51	6.47	1.80	3.76	3.00
	5	19.50	0.75	1.40	6.61	6.26	1.66	3.73	2.98
	6	17.40	0.75	1.60	5.90	5.35	1.73	2.99	2.39
	7	11.70	0.82	1.30	3.69	3.46	1.46	1.49	1.04
1973	2	6.70	0.66	2.90	3.94	4.14	1.62	2.17	1.52
	3	14.20	0.68	1.80	7.09	6.34	2.11	3.37	2.70
	4	17.30	0.70	1.90	7.94	7.26	2.13	4.18	3.34
	5	18.40	0.73	2.30	6.64	6.28	1.75	3.90	3.12
	6	18.60	0.66	1.40	8.48	6.65	2.43	3.62	2.90
	7	15.20	0.68	1.90	5.71	4.37	2.11	2.24	1.57
1974	2	9.20	0.61	2.70	5.90	5.11	2.23	2.63	1.84
	3	13.00	0.72	2.40	5.60	5.56	1.74	3.08	2.47
	4	15.40	0.74	2.40	5.48	5.90	1.60	3.50	2.80
	5	17.10	0.73	3.60	4.82	5.31	1.41	3.72	2.98
	6	19.20	0.73	2.30	7.08	5.95	1.95	3.60	2.88
	7	14.00	0.77	2.20	5.87	4.44	2.07	2.08	1.46
1975	2	8.40	0.67	2.70	4.98	4.66	1.91	2.34	1.64
	3	13.70	0.73	1.80	5.48	5.50	1.68	2.96	2.37
	4	16.50	0.74	1.50	5.34	5.82	1.54	3.36	2.69
	5	19.30	0.73	1.70	7.36	6.66	1.86	3.99	3.19
	6	19.50	0.71	1.50	7.13	5.97	1.98	3.44	2.75
	7	16.90	0.80	1.20	5.33	4.20	1.77	1.98	1.39
1976	2	8.60	0.66	2.30	5.82	5.07	2.16	2.37	1.66
	3	14.20	0.63	2.40	7.52	6.57	2.29	3.72	2.98
	4	18.20	0.61	1.90	8.52	7.59	2.38	4.55	3.64
	5	20.50	0.60	2.10	7.53	6.76	2.07	4.52	3.61
	6	17.20	0.66	2.30	6.93	5.87	2.11	3.51	2.81
	7	13.30	0.79	1.60	3.26	3.26	1.32	1.62	1.14

where

$$\nu_1 = \sigma_1^2/m\,(m = 40) \qquad \nu_2 = \sigma_2^2/n\,(n = 7)$$

For the 5% level of significance, $t_{f_1} = t_{39} = 1.68$, $t_{f_2} = t_6 = 1.94$, and σ_1 and σ_2 are the standard deviations obtained from Table 6. The values t_i were

$$t_i = \frac{|\phi_1 - \phi_2|}{\sigma_d}$$

where $\sigma_d = (\nu_1 + \nu_2)^2$, and ϕ_1 and ϕ_2 are averages from Table 6. Since $t_i < t_{\mathrm{crit}}$ in almost all cases, the hypothesis that both averages are from the same population was not rejected. The only exception was the precipitation in July, where $t_i \doteq 2.4$ and $t_{\mathrm{crit}} \doteq 2.3$. However, the difference is very small, and for a slightly lower level of significance (e.g., $\alpha = 4\%$) the relation $t_i < t_{\mathrm{crit}}$ will be fulfilled.

In order to investigate the serial dependence, the correlation coefficients r_i between successive months were computed. For $e1_t$ and P, the r_i values were smaller than r_{crit} $(f = n - 1 = 6, \alpha = 5\%) = 0.7067$ and r_{crit} $(f = n - 1 = 39, \alpha = 5\%) = 0.3084$, and so

TABLE 6 Statistical parameters of input variables from station S. ϕ = average (approx.); σ = standard deviation; C_v = coefficient of variation.

Value		A	M	J	J	A	S	ϕ
$e1_t$	ϕ_1	0.650	1.320	1.710	1.677	1.297	0.514	
1931–70	σ_1	0.059	0.132	0.139	0.138	0.102	0.035	
	$C_v(\%)$	9.1	10.0	8.2	8.2	7.9	6.8	8.4
$e2_t$	ϕ_1	0.467	0.630	0.624	0.628	0.590	0.434	
1931–70	σ_1	0.111	0.152	0.118	0.137	0.139	0.128	
	$C_v(\%)$	23.8	24.1	18.9	21.8	23.6	29.5	23.3
P_t	ϕ_1	38.8	64.9	64.9	76.8	67.8	41.6	
1931–70	σ_1	18.6	33.4	28.9	42.5	34.4	25.2	
	$C_v(\%)$	47.9	51.5	44.5	55.3	50.7	60.6	51.6
$e1_t$	ϕ_2	0.609	1.240	1.608	1.651	1.304	0.507	
1970–76	σ_2	0.042	0.074	0.179	0.143	0.077	0.045	
	$C_v(\%)$	6.9	6.0	11.1	8.7	5.9	8.9	
$e2_t$	ϕ_2	0.516	0.564	0.553	0.621	0.586	0.352	
1970–76	σ_2	0.110	0.104	0.111	0.094	0.134	0.113	
	$C_v(\%)$	21.3	18.4	20.1	15.1	22.9	32.2	
P_t	ϕ_2	34.1	72.9	69.9	49.0	51.4	31.3	
1970–76	σ_2	20.9	23.2	27.3	24.4	32.4	16.5	
	$C_v(\%)$	61.3	31.8	39.1	49.8	63.0	52.7	
$e1_t$	t_{crit}	2.338	2.295	2.407	2.388	2.347	2.406	
	t_i	2.227	2.292	1.434	0.446	0.210	0.391	
$e2_t$	t_{crit}	2.383	2.332	2.377	2.332	2.380	2.369	
	t_i	1.086	1.433	1.546	0.168	0.072	1.756	
P_t	t_{crit}	2.395	2.334	2.377	2.300	2.377	2.324	
	t_i	0.558	0.782	0.443	2.436	1.224	1.392	

these were not statistically significant. For $e2_t$ the following values for r_i were obtained:

	A–M	M–J	J–J	J–A	A–S
1931–70	−0.191	0.310	0.408	0.452	0.577
1970–76	0.041	0.675	0.257	0.035	0.222

The values for 1931–70 were statistically significant starting from May (May–June, June–July, etc.), showing a positive serial correlation.

Further analysis concerned the monthly probability distributions of $e1_{t,y}$, $e2_{t,y}$, and $P_{t,y}$, where t is the month (e.g. $t = 2$ for April, y = year = 1, 2, . . . , 40), and then the sums of these values for the whole vegetative period, namely:

$$E1_y = \sum_{t=1}^{8} e1_{t,y}$$

$$E2_y = \sum_{t=1}^{8} e2_{t,y}$$

$$PS_y = \sum_{t=1}^{8} P_{t,y}$$

The cumulative frequency curves are shown in Figures 5–24. The probabilities p_i were determined by the formula $p_i = i/(m + 1)$ where i is the rank number ($i = 1, 2, \ldots, m$) and m is the total number of observations ($m = 40$ in this case). In the middle part, approximately $0.2 < p_i < 0.8$, some points were not plotted because they were not important in an approximate fitting of theoretical distributions. In some figures the theoretical normal cumulative distribution function was fitted on probability paper, with p_i on the vertical axis. On this paper a normal cumulative distribution function is projected as a straight line.

The results of some of these tests of $e1$, $e2$, and P for May and July are given in Figures 5–10, and those of $E1_y$, $E2_y$, and PS_y are given in Figures 11–17. These results seem to show that the distributions of $e1$, $e2$, and P (Figures 9 and 10) can be regarded as normal with some outliers (one or two in the 40-year sequence). These outliers are probably not error measurements, but reflect the fact that in a semi-humid climate, conditions typical of a semi-dry or humid climate sometimes occur and may last for several months (the prevailing synoptic situation with persistent high or low pressure governing the air mass circulation).

The $E1$ values showed a normal distribution (Figure 11), but the probability distribution of $E2$ values was obviously not normal, and produced an S-shaped curve (Figure 12). The minimum value that caused this rather strange behavior was tested at the neighboring meteorological station B, and it was found that it occurred at both stations in 1955, so that the minimum at station B could not have been an outlier. Therefore, asymmetrical distributions were tested. At first, a log normal distribution with the transformation $w_y = \log E2_y$ was tested, but the result was unsatisfactory, so that $w_y = \log (E2_y - A)$ was used (with $A = 2$), and this was sufficient to transform the distribution to normal (Figures 13, 15).

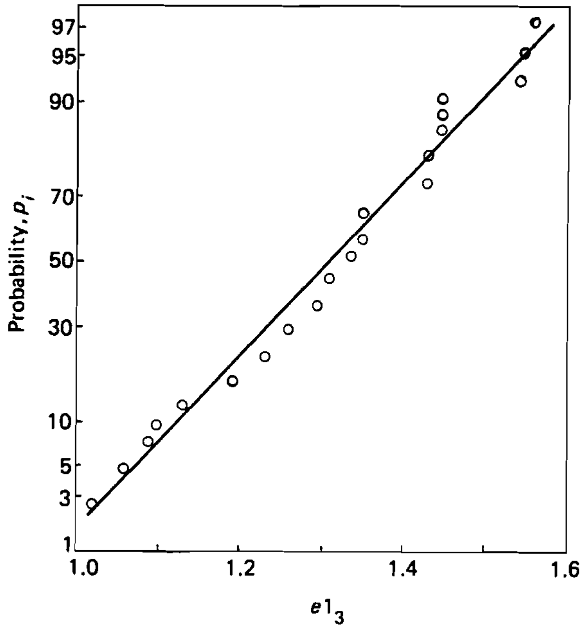

FIGURE 5 Distribution of $e1_3$ in May (daily values).

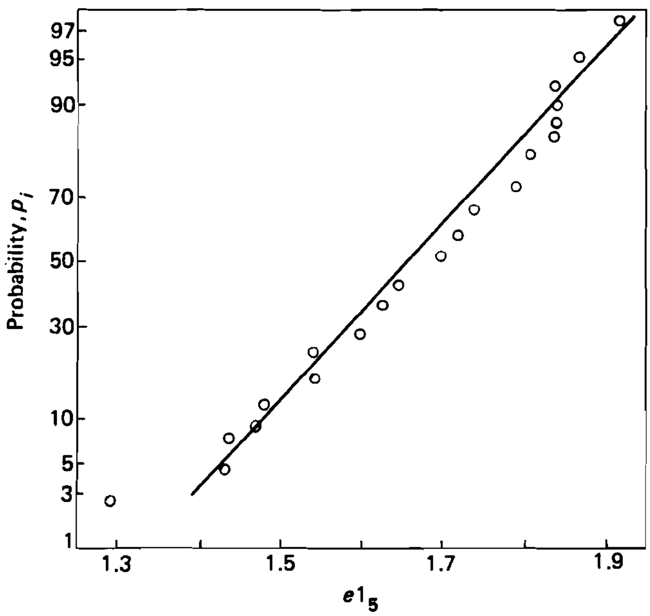

FIGURE 6 Distribution of $e1_5$ in July (daily values).

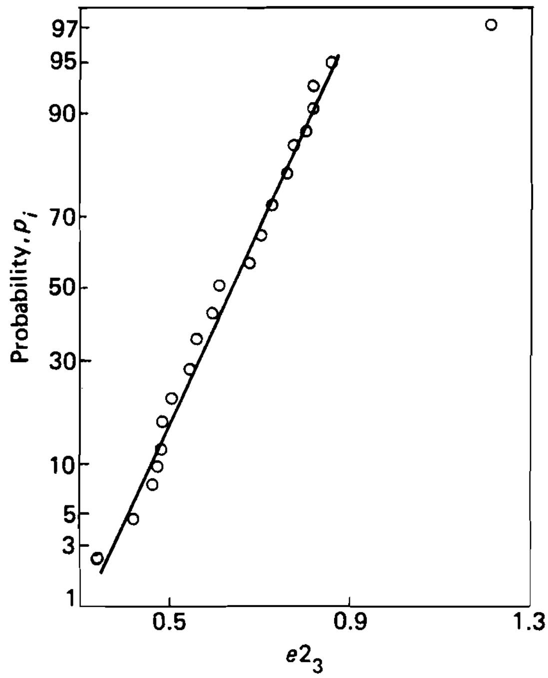

FIGURE 7 Distribution of $e2_3$ in May (daily values).

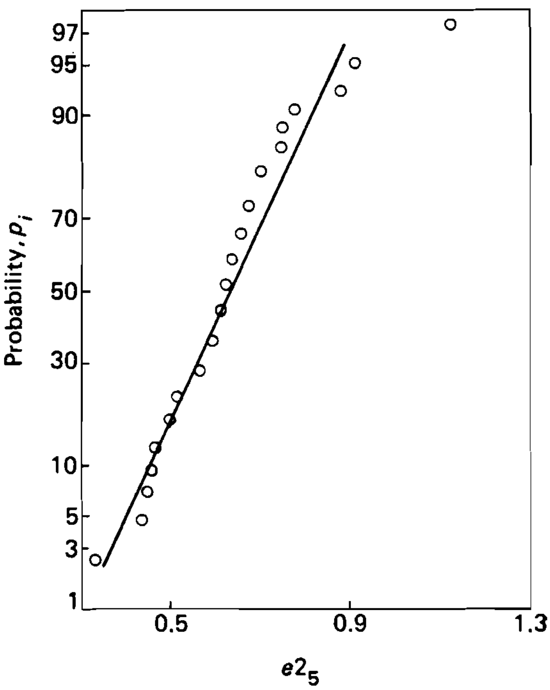

FIGURE 8 Distribution of $e2_5$ in July (daily values).

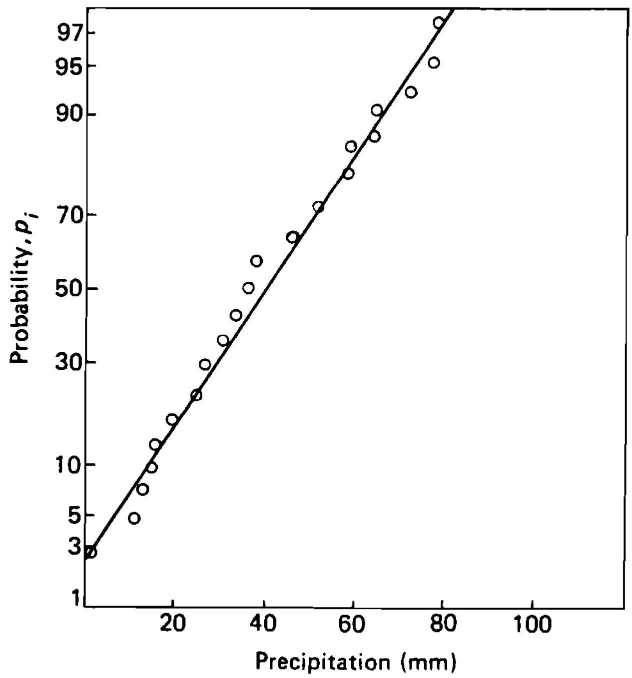

FIGURE 9 Distribution of precipitation, P_3 (May).

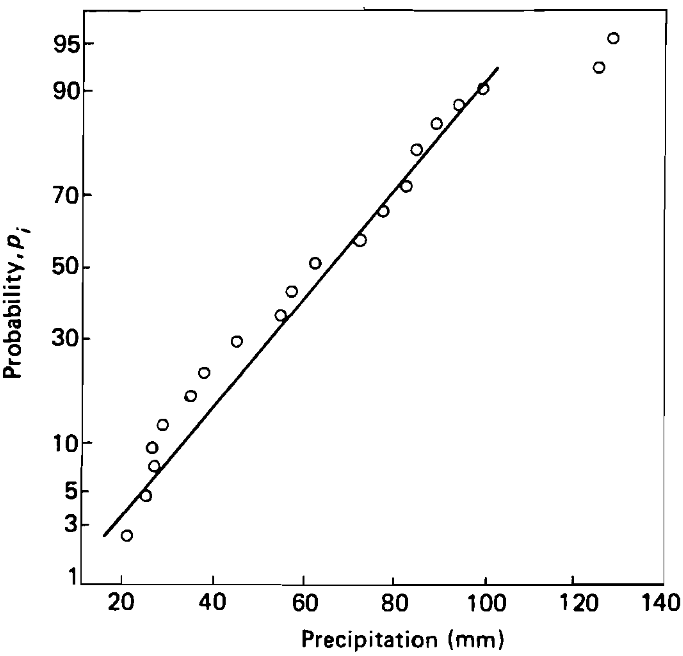

FIGURE 10 Distribution of precipitation, P_5 (July).

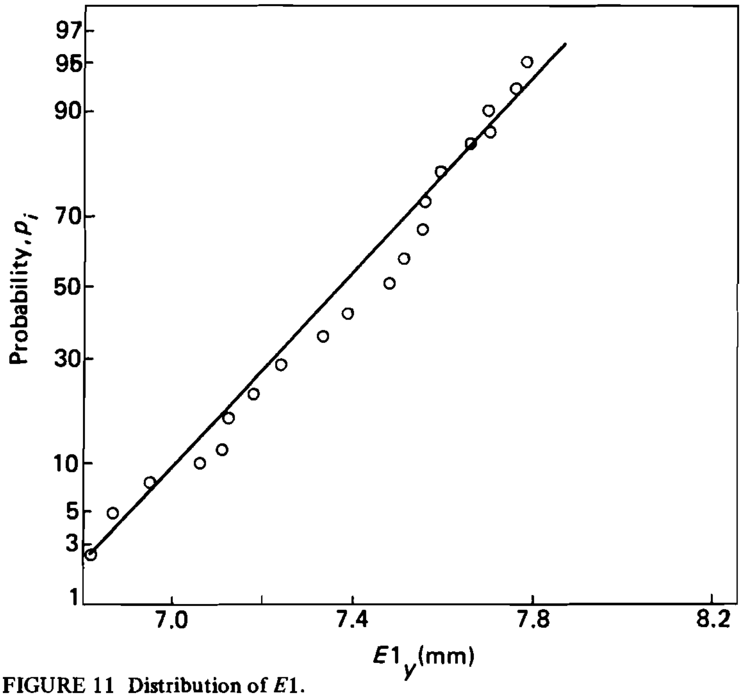

FIGURE 11 Distribution of $E1$.

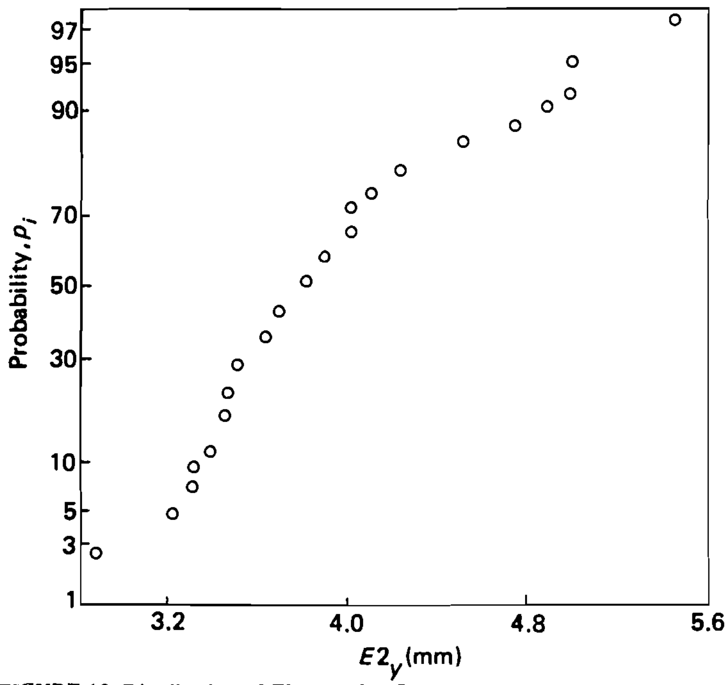

FIGURE 12 Distribution of $E2$ at station S.

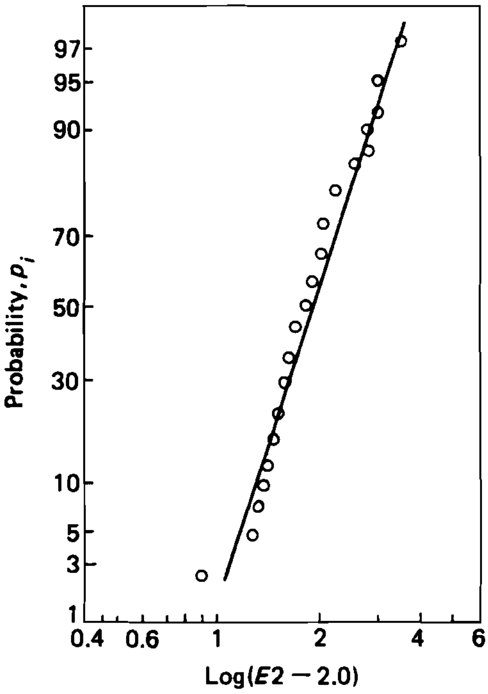

FIGURE 13 Distribution of log ($E2-2.0$) at station S.

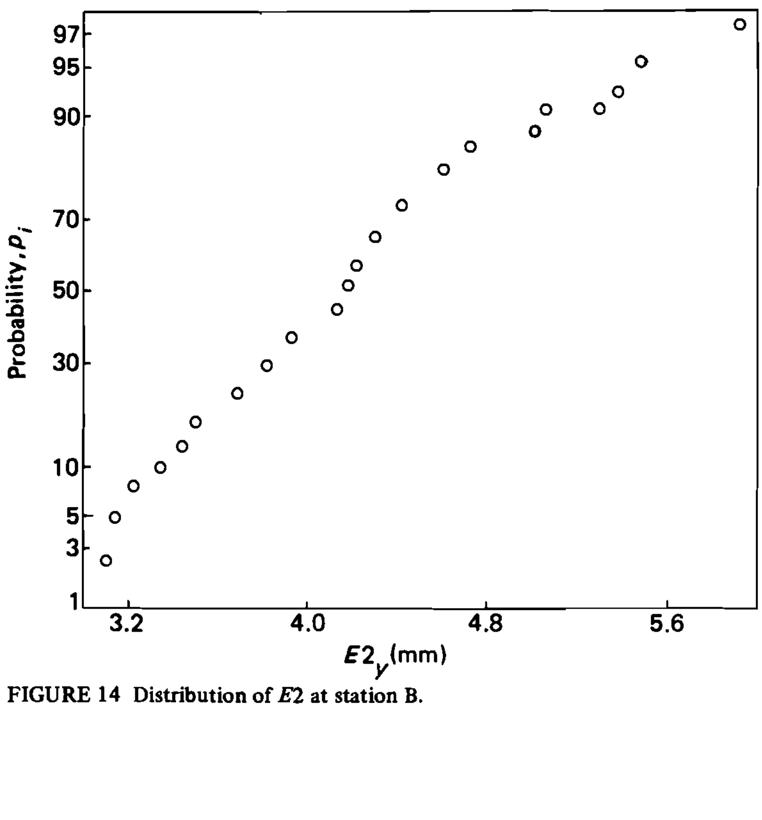

FIGURE 14 Distribution of $E2$ at station B.

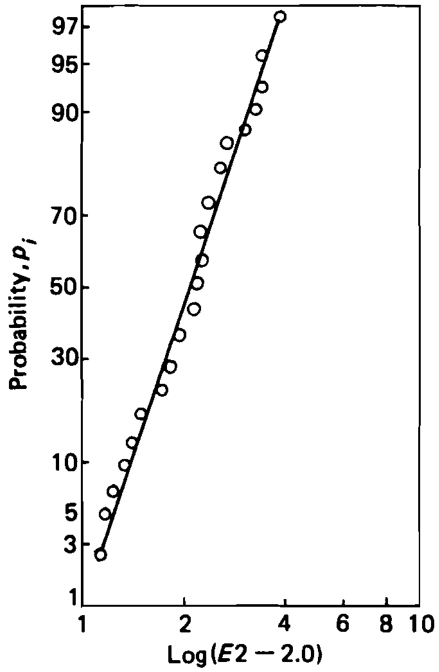

FIGURE 15 Distribution of log ($E2$ — 2.0) at station B.

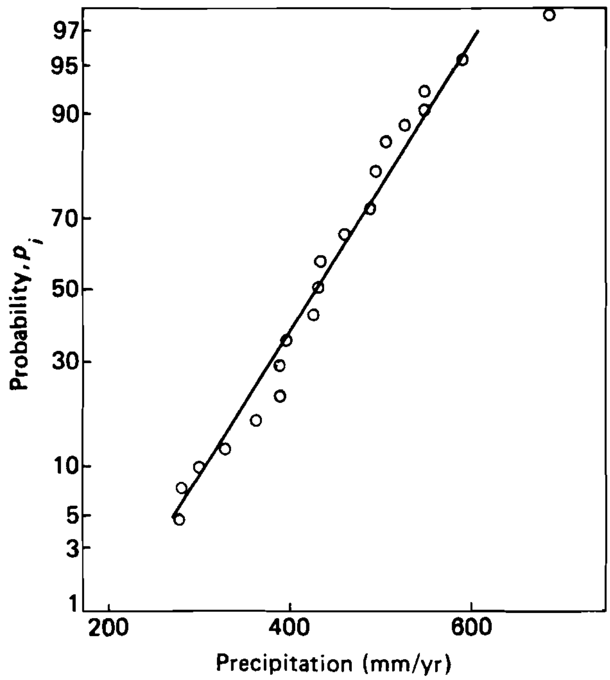

FIGURE 16 Distribution of precipitation PS at station S.

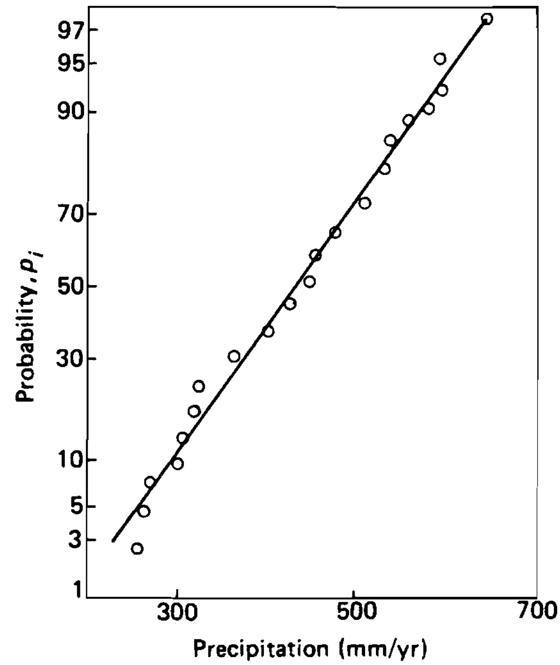

FIGURE 17 Distribution of precipitation *PS* at station B.

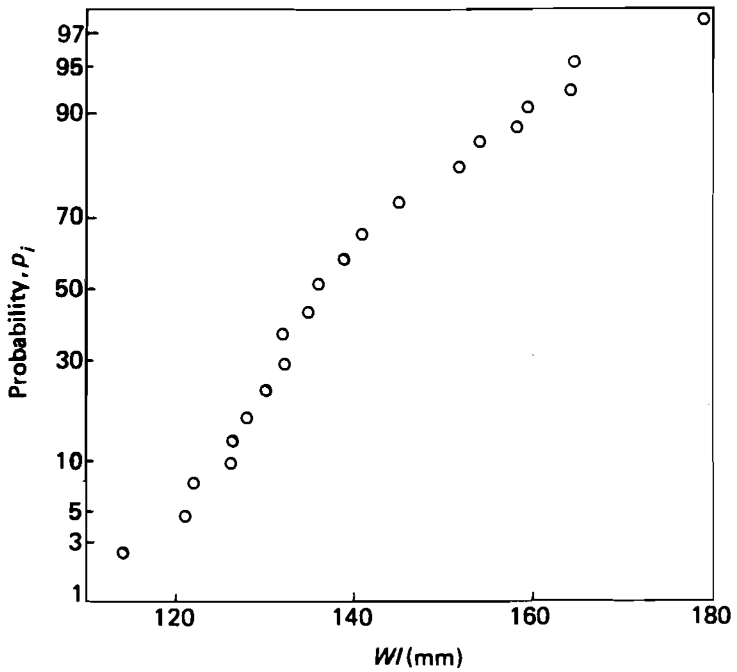

FIGURE 18 Distribution of irrigation water requirements *WI*, based on eq. (27).

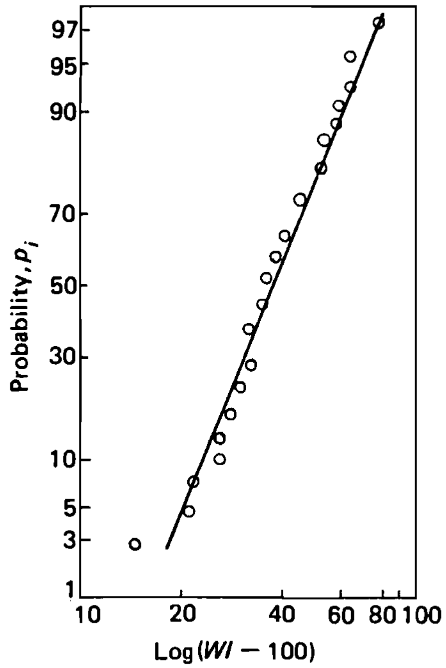

FIGURE 19 Distribution of irrigation water requirements log(*WI* — 100), based on eq. (27).

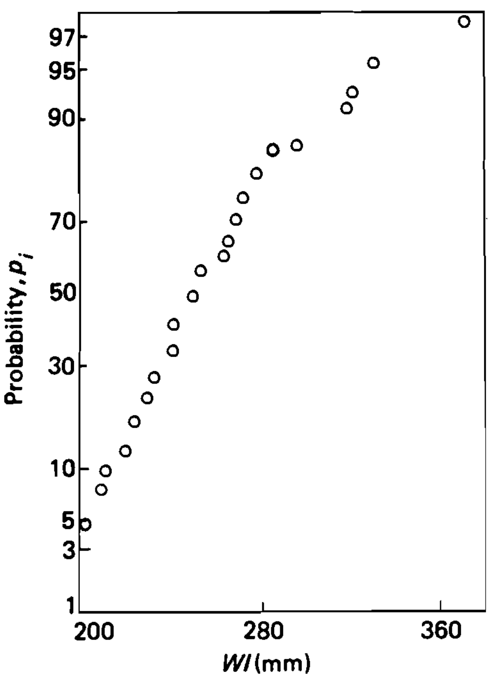

FIGURE 20 Distribution of irrigation water requirements *WI*, based on eq. (28).

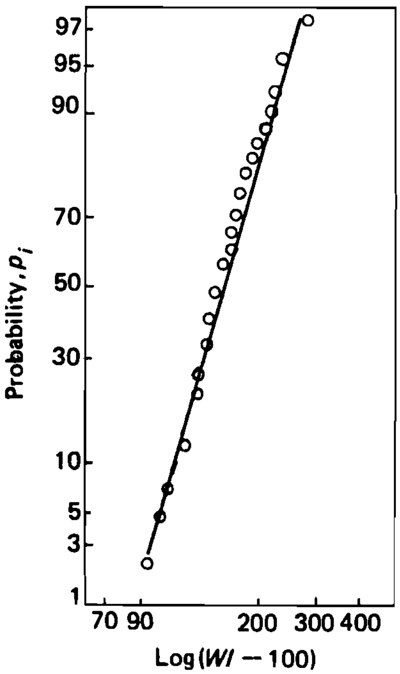

FIGURE 21 Distribution of irrigation water requirements log(WI — 100), based on eq. (28).

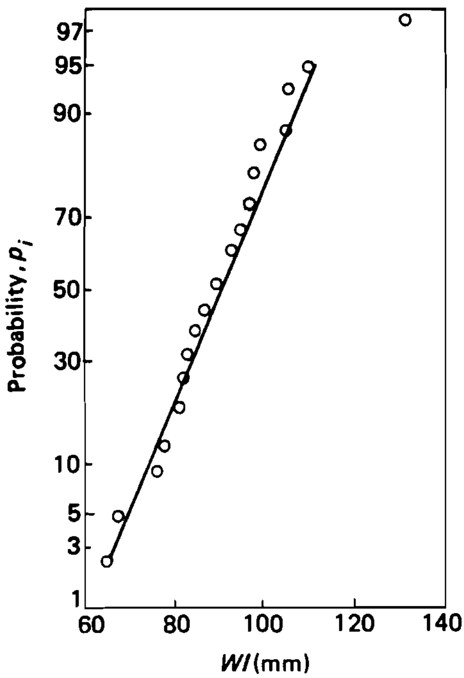

FIGURE 22 Distribution of irrigation water requirements WI, based on eq. (30).

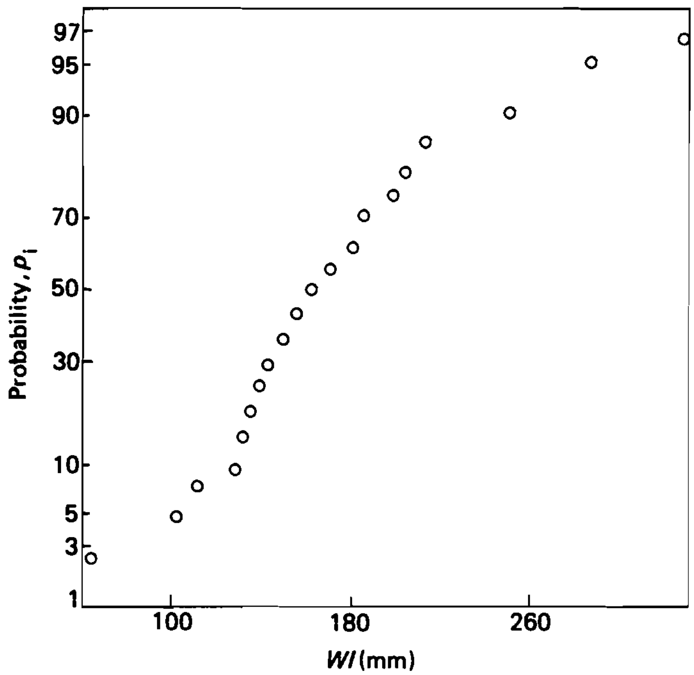

FIGURE 23 Distribution of irrigation water requirements WI, based on eq. (31).

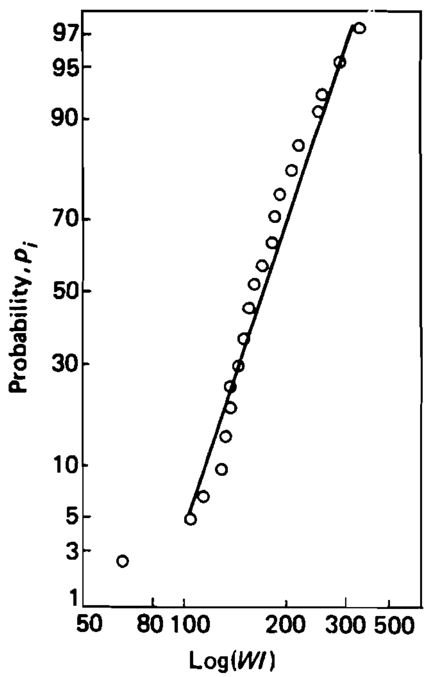

FIGURE 24 Distribution of irrigation water requirements log(WI), based on eq. (31).

The total precipitation for the vegetative period PS_y had an approximately normal distribution with an outlier on each side of the curve (minimum and maximum). This phenomenon was tested using station B values where a normal distribution fitted better (Figures 16 and 17). Because the irrigation water requirements model, WI_t, is based on a linear combination of the terms $e1_t$, $e2_t$, P_t, and WI_{t-1}, it can be expected that the distribution of WI_t will be either normal or log normal according to the prevailing component (see Figures 18–24).

First of all, the normal distribution was tested for WI_t values, but it did not fit well, and the log normal distribution with the transformation $z_t = \log(WI_t)$ was not sucessful in all cases. With the additional parameter the transformation $z_t = \log(WI_t - A)$ fitted well with the constant $A \approx 100$ for eqs. (27) and (28). In eq. (30), a normal distribution was thought to be satisfactory if the maximum value was assumed to be an outlier; otherwise, a log normal distribution with $A = 0$ gave better results.

In eq. (31), the minimum value was assumed to be an outlier and a log normal distribution was used ($A = 0$). This decision was supported by the fact that in this study, we were interested in maximum and average, rather than in minimum values, because these influence the WRS. It was stated above that a prescription model was tested, so that it is unimportant that it did not describe the occurrence of the minimum value.

Some other probability distributions were tested (e.g., Weibull and Pearson) with no significantly better fits. If all the known distributions (e.g., Johansson 1970) were tested, a better goodness-of-fit could be found. A log normal distribution, however, has some advantage in the generation of a synthetic time series. This distribution has been carefully studied by hydrologists and is therefore recommended.

Results based on time series using Penman's equation (Table 7) were compared with those based on Linacre's simplification. For this purpose, the time series based on eqs. (35)–(38) were modeled and the results are summarized in Table 8; differences can be seen in both averages and standard deviations. The main source of these differences lies in the fact that, in irrigation water requirement models, the second term of Penman's equation is decisive, whereas in Linacre's equation both terms have the same weight. This is

TABLE 7 Statistical parameters of irrigation water requirements, *WI*, at station S using Penman's equation. ϕ = average (approx.); σ = standard deviation; C_v = coefficient of variation.

		A	M	J	J	A	S	Z	ϕ
WI	ϕ	3.57	28.87	30.80	29.73	27.71	22.61	143.3	
Eq. (27)	σ	3.83	5.21	3.80	5.65	4.85	4.02		
	C_v(%)	107.3	18.0	12.3	19.0	17.5	17.8		19.1
WI	ϕ	20.85	48.26	52.80	50.27	45.50	33.50	251.2	
Eq. (28)	σ	11.44	12.30	8.97	13.35	11.46	9.49		
	C_v(%)	54.9	25.5	17.0	26.5	25.2	28.3		26.5
WI	ϕ	–	18.04	19.72	18.19	17.17	15.13	88.2	
Eq. (30)	σ	–	5.14	4.03	6.10	4.99	3.86		
	C_v(%)	–	28.5	20.4	33.5	29.1	25.5		27.3
WI	ϕ	6.81	34.07	39.90	35.47	30.50	22.16	168.9	
Eq. (31)	σ	10.05	18.17	15.65	20.66	18.06	13.57		
	C_v(%)	147.6	53.3	39.2	58.2	59.2	61.2		56.9

TABLE 8 Statistical parameters of irrigation water requirements, *WI*, at stations S and B using Linacre's equation. ϕ_B and ϕ_S = averages at stations S and B, respectively; σ_S = standard deviation at station S; C_v = coefficient of variation at station S.

		A	M	J	J	A	S	*E*	ϕ
WI	ϕ_B	2.58	26.68	28.74	28.29	24.38	19.23	129.90	
Eq. (35)	ϕ_S	1.97	25.91	28.15	27.48	24.24	19.56	127.31	
	σ_S	3.00	4.62	3.76	5.31	4.33	3.11		
	C_v(%)	152.2	17.8	13.4	19.3	17.9	15.9		18.9
WI	ϕ_B	11.58	39.49	44.35	43.30	34.03	21.82	194.58	
Eq. (36)	ϕ_S	9.50	37.66	42.96	41.38	33.70	22.59	187.79	
	σ_S	9.16	10.95	8.90	12.58	10.25	7.37		
	C_v(%)	96.4	29.0	20.7	30.4	30.4	32.6		31.5
WI	ϕ_B	–	18.36	19.34	18.65	16.42	14.17	86.94	
Eq. (37)	ϕ_S	–	17.64	19.16	18.12	16.38	14.50	85.80	
	σ_S	–	4.65	3.88	5.62	4.56	3.31		
	C_v(%)	–	26.4	20.2	31.0	27.8	22.8		25.7
WI	ϕ_B	4.03	29.40	32.43	31.43	21.79	13.51	132.59	
Eq. (38)	ϕ_S	3.29	26.47	31.53	29.16	21.77	14.18	126.40	
	σ_S	7.59	15.81	14.84	18.47	15.37	10.64		
	C_v(%)	290.6	59.7	47.1	63.3	70.6	75.2		65.5

supported by a comparison of time series values for monthly evapotranspiration. With one exception in May, the values calculated by Linacre's equation for May–September were within 10% limits, as compared with those calculated by Penman's equation. In April, the values were systematically higher, so obviously a reduction by approximately 10% (e.g., a reduction by the coefficient of 0.9) was necessary. WRS are not very sensitive to April demands and, further, these are lower because of soil water storage. This difference in April was therefore not analyzed further.

As a result of these differences, Penman's equation is recommended even when the available data for, say, station X qualify for Linacre's simplification only with some station Y with "similar conditions" that has all the necessary data. These vague terms of similarity should be specified, but generally there are not enough data to do so. Then, the decision as to whether the conditions can be regarded as similar is one for meteorological and hydrological expert judgment. If conditions can be regarded as "similar", it is recommended that the missing data from station Y be used.

This problem is connected with the common question of transferability of the results from one place (such as a meteorological station) to another. In the present study, two stations (B and S) were tested, and it was found that the main difference was in precipitation, in the $e2$ term (differences of up to 5%), and differences in the $e1$ term were the least pronounced. The stations were in similar geographical, meteorological, and hydrological conditions, about 40 km apart. Apart from precipitation, the data were transferable from one station to the other within the error of measurement.

The irrigation water requirement values are not only dependent on meteorological conditions, but also on agricultural and irrigation practices. Equations (27) and (28) derived from the V-III-V system in Czechoslovakia reflect a relatively rigid irrigation scheme in which the water requirements are insensitive to precipitation. This policy can be adopted where there is a relatively low degree of exploitation (low k_e). Therefore, it can be concluded that the transformation of eq. (27) to (28) does not reflect the changes that can occur where there is more effective use of irrigation water. Equations (30) and (31) derived from the C-V system reflect a better and more flexible irrigation system with more efficient use of water. Therefore, these equations are recommended for irrigation water requirement calculations as a time series for WRS modeling.

7 CONCLUSION AND DISCUSSION

Data concerning irrigation water requirements are essential in the planning of water resource systems (WRS). Used in the form of time series, they can be applied as a direct input into deterministic simulation models and as an indirect input into stochastic models for the derivation of the necessary statistical parameters. In the present study the elements that affect irrigation water requirements were analyzed, and it was found that evapotranspiration, precipitation, and irrigation in the previous time periods were the decisive factors. A model relating irrigation water requirements to these elements was derived and tested on two irrigation systems in Czechoslovakia.

The model is comprehensive enough to be used in other areas and under different conditions for irrigation systems in semi-humid climates in moderate climatic zones. However, it has to be based on observed data (monthly irrigation water requirements), since not only can the influence of individual terms change, but also the degree of exploitation and irrigation practices may differ from place to place, and this can have a profound effect on the resulting model parameters. It is not justifiable to calibrate the model in one area and then to use it in another that has different economic, agricultural, soil, vegetation, and irrigation conditions, because all of these factors must be taken into account in the calibration coefficients. Further research in this direction depends on the data available, and it is recommended that this work is carried out as soon as these are obtained.

The application of calibration coefficients makes use of prevailing irrigation practices, although their improvement is considered through the use of the coefficient of exploitation k_e. Long-term experience in Czechoslovakia has shown that changes in irrigation policy have little effect on the pattern of water requirements (distribution in the irrigation season), and therefore the difference between present and future irrigation policies can be evaluated using k_e.

The second step in the perfection of the model is connected with the effects of irrigation water requirements on the WRS, or vice versa. These can be analyzed by two basic methods. First, the model can be used (e.g., eq. (31)), and the area irrigated (with or without k_e) can be taken as the variable. This approach is called experimenting with the model. Secondly, experiments on the model can be done, i.e., the irrigated area is held constant, and the parameters and terms of the model can be analyzed as far as their influence on the WRS is concerned.

ACKNOWLEDGMENT

The author would like to express his gratitude to Dr. Janusz Kindler, Chairman of the Resources and Environment Area (on leave from the Institute of Environmental Engineering, Warsaw Polytechnic University, Warsaw, Poland), for his help in the preparation of the manuscript, and suggestions and comments concerning the model and its application.

REFERENCES

Balek, J. (1980) State of art of modeling of the water balance processes in the agricultural field and watershed. IIASA, REN Task Force Mtg, June.

Barton, I.J. (1979) A parametrization of the evaporation from nonsaturated surfaces. J. Appl. Meteorol. 18: 43–7.

Blaney, H.F. and W.D. Criddle (1966) Determining consumptive use for water developments. Irrigation and Drainage Specialty Conf., Las Vegas, Nevada.

Brochet, P. and N. Gerbier (1977) Une méthode opérationnelle pratique de calcul de l' évapotranspiration potentielle. La Météorologie, VI^e Série No. 11, pp25–31.

Brutsaert, W. and H. Stricker (1979) An advection–aridity approach to estimate actual regional evapotranspiration. Water Resources Res. 15: 443–50.

Cermak, M. and I. Brenda (1971) Drainage nets and land management. 2nd Conf. CVTS (N. Smokovoc).

Christiansen, J.E. (1968) Pan evaporation and evapotranspiration from climatic data. J. Irrigation and Drainage Division ASCE 94: 243–65.

Christiansen, J.E. and G.H. Hargreaves (1969) Irrigation requirements from evaporation. Trans. Int. Commun. on Irrigation and Drainage III: 23.569–23.596.

Fleming, G. (1975) Computer simulation techniques in hydrology. New York: Elsevier. p333.

Forsman, A. (1969) Mät- och beräkningsmetoder för bestämning av avdunstning. Svenska kommitten för internationella hydrologiska dekaden. Statens naturvetenskapliga forskningsråd. Report 4 (30 pp).

Härtel, O. (1925) Die Wildbach and Lawinenverbauung, Tübingen.

Holy, M. (1979) Irrigation structures. Central Board of Irrigation and Power No. 135, New Delhi (323 pp).

Holy, M. (1980) Erosion and Environment. London: Pergamon (390 pp).

Howard, K. and J.W. Lloyd (1979) The sensitivity of parameters in the Penman evaporation equations and direct recharge balance. J. Hydrol. 41: 329–44.

Hudson, N. (1973) Soil Conservation. London: Batsford.

Ivanov, N.N. (1954) The determination of potential evapotranspiration. Izvest. Vsesoyuznogo. Geograf. Obs. p22.

Janko, J. (1958) Statistical Tables. Prague: CSAV p251 (in Czech).

Jensen, M.E. (Ed.) (1966) Evapotranspiration and its role in water resources management. Proc. Conf. on Evapotranspiration, Am. Soc. Agric. Engrs, Chicago, p65.

Johansson, W. (1970) Bevattning i fältmässig odling. Rapport fran Seminarium vid Alnarp, Sverige.

Kos, Z. (1969) Linear regression model and its application in hydrology. Works and Studies No. 6 Water Courses, Prague (in Czech).

Kostjakov, A.N. (1951) Osnovy Meliovacij, Moscow: Selchozgiz.

Linacre, E.T. (1977) A simple formula for estimating evaporation rates in various climates, using temperature data alone. Agric. Meteorol. 18: 490–24.

McGuinness, J.L. and L.H. Parmele (1972) Maximum potential evapotranspiration frequency. East Central US. J. Irrigation and Drainage Division ASCE 98(IR 2), Proc. Paper 8943, pp207–14.

Morton, F.I. (1980) On the complementary relationship between potential and areal evapotranspiration. Nat. Hydrol. Res. Inst. Ottawa, Canada, p80.

Morton, F.I., R. Goard, and J. Piwowar (1980) Programs REVAP and WEVAP for estimating areal evapotranspiration and lake evaporation from climatological observations. Nat. Hydrol. Res. Inst., NHRI Paper No. 12, Ottawa, Canada, p56.

Mustonen, S.E. and J.L. McGuinness (1968) Estimating evapotranspiration in a humid region. US Dept of Agric. Tech. Bull. No. 1389.
Penman, H.L. (1954) Evaporation over parts of Europe. Proc. IASH Gen. Assembly, Rome, Publ. No. 38, pp168–76.
Penman, H.L. (1963) Vegetation and hydrology, Tech. Commun. No. 53, Commonwealth Bureau of Soils, Harpenden, UK (125 pp).
Perrier, A. (1977) Projet de définitions concernant l'évapotranspiration en fonction de considérations théoretiques et pratiques. La Météorologie VI^e Série No. 11, pp7–16.
Pruitt, W.O. (1960) Relation of consumptive use of water to climate. Trans. Am. Soc. Agric. Engrs 3(1): 9–13, 17.
Pýcha, M. (1965) Research of consumptive use of water by plants. Bratislava: VÚZA (in Czech).
Quackenbush, T.H. and J.T. Phelan (1965) Irrigation requirements of lawns. J. Irrigation and Drainage Division ASCE 91: pp11–19.
Riou, C. (1977) Rémarques sur l'évaporation des surfaces naturelles et son évaluation. La Météorologie, VI^e Série No. 11, pp17–23.
Rodda, J.C., R.A. Downing, and F.M. Law (1976) Systematic Hydrology. London: Newnes-Butterworth (399 pp).
Schulz, E.F. (1973) Problems in Applied Hydrology. Fort Collins: Water Resources Publications.
Seuna, P. (1977) On the Hydrometeorological Factors Affecting Irrigation. Helsinki: Vesihallitus (96 pp) (in Finnish).
Skogerboe, G.C. (1977) Water measurement and water management relationships. Proc. ASCE Conf. on Water Management for Irrigation and Drainage, Reno, Nevada, pp295–304.
Tanner, C.B. (1967) Measurements of evapotranspiration, in Irrigation of Agricultural Lands. Monogr. No. 11, Am. Soc. Agron., Madison, pp534–74.
Thornthwaite, C.W. and B. Holzman (1939) The determination of evaporation from land and water surfaces. Monthly Weather Rev. 67: 4–11.
Thornthwaite, C.W. and B. Holzman (1942) Measurement of evaporation from land and water surfaces. US Dept of Agric. Tech. Bull. No. 817.
Thornthwaite, C.W. and J.R. Mather (1955) The water balance, in Climatology 8(1), Lab. of Climatic Studies, Centerton, NJ.
Turc, L. (1954) Le bilan d'eaux des sols – relations entre les précipitations, l'évaporation et l'écoulement. Ann. Agron. 5: 491–596.
Veihmeyer, F.J. (1964) Evapotranspiration, in Handbook of Applied Hydrology (ed. Ven Te Chow). New York: McGraw-Hill.
Ven Te Chow (ed.) (1964) Handbook of Applied Hydrology. New York: McGraw-Hill.
WMO (1966) Measurement and Estimation of Evaporation and Evapotranspiration. WMO-No. 201, TP 105, Tech. Note No. 83 (121 pp).

BIBLIOGRAPHY

Allen, W.H. and J.R. Lambert (1971) Application of the principle of calculated risk to scheduling of supplemental irrigation, I: concepts. Agric. Meteorol. 8.
Aslyng, H.C. (1965) Evaporation, evapotranspiration and water balance investigations at Copenhagen 1955–64. Acta Agric. Scandinavia, XV(3–4): 284–300.
Aslyng, H.C. and S.E. Jensen (1965) Radiation and energy balance of Copenhagen 1955–64, R. Vet. and Agric. Coll. Yearbook 1966, Copenhagen, pp22–40.
Baier, W. (1965) The interrelationship of meteorological factors, soil moisture and plant growth. Int. J. Biometeorol. 9: 5–20.
Baier, W. and D.A. Russelo (1968) A computer program for estimating risks of irrigation requirements from climate data. Canadian Dept of Agriculture, Ottawa, Canada, TB 58, p48.
Balek, J. (1979) Water balance model DAMBO. IIASA, June, p23.
Banach, K., P. Kowalik, I. Toczylowska, and W. Wedzinski (1978) Simulation model of water management for agricultural lands. J. Hydrol. Sci. 5: 191–9.

Beven, K. (1979) A sensitivity analysis of the Penman–Monteith actual evapotranspiration estimates. J. Hydrol. 44: 169–90.
Blaney, H.F. and W.D. Criddle (1945) A method of estimating water requirements in irrigated areas from climatological data. US Dept of Agric. Soil Conservation Service.
Blaney, H.F. and W.D. Criddle (1950) Determining water requirements in irrigated areas from climatological and irrigation data. US Dept of Agric. SCS TP 96 (48 pp).
Blaney, H.F. and W.D. Criddle (1962) Determining consumptive use and irrigation water requirements. US Dept of Agric. Tech. Bull. 1275 (59 pp).
Blaney, H.F. and K.V. Morin (1942) Evaporation and consumptive use of water empirical formulae. Trans. Am. Geophys. Union 23: 76–83.
Bosen, J.F. (1960) A formula for approximation of saturation vapor pressure over water. Monthly Weather Rev. 88: 275–6.
Brunk, H.D. (1960) An Introduction to Mathematical Statistics. New York: Ginn and Co. (403 pp).
Brutsaert, W. (1965) Evaluation of some practical methods of estimating evapotranspiration in arid climates at low latitudes. Water Resources Res. 1: 187–91.
Budyko, M.I. (1948) Evaporation under natural conditions. US Dept of Commerce Israel Program Sci. 751 (130 pp; translated from Russian).
Budyko, M.I. (1956) The heat balance of the Earth's surface. US Dept of Commerce Weather Bureau PB 131692 (259 pp; translated by N.A. Stepanova, 1958).
Budyko, M.I. (1974) Climate and Life. New York: Academic Press (209 pp).
Buras, N., D. Nir, and F. Alpetovits (1973) Planning and updating farm irrigation schedules. J. Irrigation and Drainage Division ASCE 99 (IR 1), Proc. Paper 9586, pp43–51.
Businger, J.A. (1956) Some remarks on Penman's equations for evapotranspiration. Netherlands J. Agric. Sci. 4: 77–80.
Cowan, I.R. (1965) Transport of water in the soil–plant–atmosphere system. J. Appl. Ecol. 2: 221–39.
Crawford, N.H. and R.K. Linsley (1966) Digital simulation in hydrology, Stanford Watershed Model IV, Tech. Rep. 39, Dept Civil Engng, Stanford University, Stanford, California.
Curran, J.C. (1979) Regional mean Bowen ratios deduced from diurnal changes of temperature and humidity. J. Hydrol. 40: 113–21.
David, W.P. and E.A. Hiler (1970) Predicting irrigation requirements of crops. J. Irrigation and Drainage Division ASCE 96 (IR 3) Proc. Paper 7507, pp241–55.
Davies, J.A. (1967) A note on the relationship between net radiation and solar radiation. Q.J.R. Meteorol. Soc. 93: 109–15.
Doorenbos, J. and W.O. Pruitt (1974) Guidelines for prediction of crop water requirements. FAO Irrigation and Drainage Paper No. 25. Rome: FAO.
Dub, O. and J. Nemec (1969) Hydrologie. TP 34. Prague: SNTL (379 pp).
Eagleson, P.S. (1970) Dynamic Hydrology. New York: McGraw-Hill.
England, C.B. (1963) Water use by several crops in a weighing lysimeter. Agron. J. 55: 239–41.
Fritschen, L.J. (1965) Accuracy of evapotranspiration determinations by the Bowen ratio method. Bull. Int. Ass. Sci. Hydrol. 10: 38–48.
Fritschen, L.J. (1967) Net and solar radiation relations over irrigated fields. Agric. Meteorol. 5: 55–62.
Gardner, W.R. (1960) Dynamic aspects of water availability to plants. Soil Sci. 89: 63–73.
Garstka, W.U. (1978) Water resources and the national welfare, Fort Collins, WRP, CO 80552, USA (638 pp).
Gates, D.M. and R.J. Hanks (1967) Plant factors affecting evapotranspiration, in Irrigation of Agricultural Lands (Eds. R.M. Hagan *et al.*). Am. Soc. Agron.
Gay, L.W. (1969) The Regression of Net Upon Solar Radiation, Presented at 9th Conf. on Agric. Meteorol. Seattle. Am. Meteorol. Soc. (20 pp).
Hagan, R.M. and I.J. Stewart (1972) Water deficits irrigation design and programming. J. Irrigation and Drainage Division ASCE 98 (IR 2), Proc. Paper 8955, pp215–37.
Haise, J.R. (1958) Irrigation, in Agronomic Trends and Problems in the Great Plains. Adv. Agron. Vol. X. New York: Academic Press pp47–56.
Hall, W.A. and W.S. Butcher (1968) Optimal timing of irrigation. J. Irrigation and Drainage Division ASCE 94 (IR 2), Proc. Paper 5988, pp267–75.

Hallgren, G. (1977) Studies on the influences of precipitation on crop yields in Sweden with special reference to field irrigation. Ann. R. Agric. Coll. Sweden 14: 175–289.

Hanks, R.J., J.I. Stewart and J.P. Riley (1977) Four-state comparison of models used for irrigation management. Proc. ASCE Conf. on Water Management for Irrigation and Drainage, Reno, Nevada, pp283–94.

Hargreaves, G.H. (1968) Consumptive use derived from evaporation pan data. J. Irrigation and Drainage Division ASCE 94 (IR 1), Proc. Paper 5863, pp97–105.

Herschfield, D. (1964) Effective rainfall and irrigation water requirements. J. Irrigation and Drainage Division ASCE 90 (IR 2), Proc. Paper 3920, pp33–47.

Howe, G.M. (1956) The moisture balance in England and Wales based on the concept of potential evapotranspiration. Weather 11: 74–82.

Israelsen, O.W. and V.E. Hansen (1962) Irrigation Principles and Practices. New York: Wiley. (447 pp).

Jaworski, J. (1978) A mathematical model of actual evapotranspiration. J. Hydrol. Sci. 5(3–4): 179–89.

Jensen, M.E. (1966) Discussion of irrigation water requirements of lawns. J. Irrigation and Drainage Division ASCE 92: 95–100.

Jensen, M.E. (1966) Empirical methods of estimating or predicting evapotranspiration using radiation Proc. Conf. on Evapotranspiration, Am. Soc. Agric. Engrs, Chicago, pp57–61, 64.

Jensen, M.E. (1969) Scheduling irrigation with computers. J. Soil and Water Conservation 24(5): 193–5.

Jensen, M.E. and L.J. Erie (1971) Irrigation and water management, in Advances in Sugarbeet Production (Ed. R.T. Johnson *et al.*) Ames: Iowa State University Press, pp189–222.

Jensen, M.E. and H.R. Haise (1963) Estimating evapotranspiration from solar radiation. J. Irrigation and Drainage Division ASCE (IR 4), Proc. Paper 3737, pp15–41.

Jensen, M.E., J.L. Wright, and B.J. Pratt (1971) Estimating soil moisture depletion from climate, crop and soil data. Trans. Am. Soc. Agric. Engrs 14(6): 954–9.

Jensen, M.E., J.L. Wright, and B.J. Pratt (1974) Consumptive use of water and irrigation water requirements. Committee on Irrigation Water Requirements, Irrigation and Drainage Division ASCE.

Kaczmarek, Z. (1970) Statistical methods in hydrology and meteorology. Wydawn. Kom. i Laern. Warsaw 312 pp (in Polish).

Keller, W. and C.W. Carlson (1967) Irrigation of principal crops: Forage crops. Irrigation of Agricultural Lands (Eds R.M. Hagan *et al.*). Am. Soc. Agron. pp607–21.

Kharchenko, S.I. and D.M. Katz (1974) Methods for the study of water balance of irrigated lands and irrigation systems. Proc. Symp. on World Water Balance, IASH–UNESCO–WMO, Vol. II, Publ. No. 93, IASH, pp452–8.

Kindler, J. (Ed.) (1978) Proc. Workshop on Modeling of Water Demands. IIASA CP-78-06 (156 pp).

Kindler, J. (1980) The systems analysis in regional water management planning. Proc. Workshop on Water Regional Planning in the Nordic Sea, NORDFORSK Cooperative Orgn. for Research. Sweden: Kungälv.

Kindler, J., K.A. Salewicz, H. Słota, and T. Terlikowski (1979) Operation of Multiple Reservoir Systems: A Case Study of the Upper Vistula System (An Introduction). IIASA CP-79-17 (35 pp).

Kindler, J., P. Zielinski, and L. de Mare (1980) An Interactive Procedure for Multiobjective Analysis of Water Resources Allocation. IIASA WP-80-85.

Kohler, M.A. and L.H. Parmele (1967) Generalized estimates of free-water evaporation. Water Resources Res. 3(4): 997–1005.

Konstantinov, A.R. (1968) Evaporation in nature. Gidrometidet. Leningrad (Translation US Dept of Commerce Nat. Tech. Inf. Service, Springfield, VA 22151).

Kos, Z. (1964) Relation of irrigation rates to water resources: Projecting and Construction, in Water Management pp13–16 (in Czech).

Kos, Z. (1964) Irrigation construction planning and water resources reliability, in Water Management No. 3 (in Czech).

Kos, Z. (1965) Problems of development rates of irrigation: Projecting and Construction, in Water Management pp14–17 (in Czech).

Kos, Z. (1968) Economic level of irrigation withdrawals in water resource system design. PhD Thesis, Prague (in Czech).

Kos, Z. (1969) Irrigation withdrawals in water resource systems. Water Management 7: 198–200 (in Czech, English summary).

Kos, Z. (1970) Simulation models of water supply for irrigation in water resource system. ICID Bull., pp47–52.

Kos, Z. (1973) Water resource system development with catchment system optimization. Proc. Conf. on the Biosphere. Prague: CVUT pp232–9 (in Czech).

Kos, Z. (1975) Chance-constrained model of water resource systems. Proc. Int. Symp. and Workshops on Application of Mathematical Models in Hydrology and Water Resources Systems, Bratislava (in English).

Kos, Z. (1976) Stochastic hydrology and its application for water resources systems solution. Water Management J. 23: 4–5 (in Czech, English summary).

Kos, Z. (1978, 1979) (two parts). Stochastic Models of Water Resources Systems. Works and Studies No. 146 Prague: Water Research Institute, SZN (in Czech, English summary) p468.

Kos, Z. (1979) Operation of water resources systems in Czechoslovakia. IIASA Workshop on Operation of Multiple Reservoir Systems. Poland: Jodłowy Dwor, May–June (17 pp).

Kos, Z. (1979) Multimodeling of water resources systems. 12th European Regional Conf., ICID, Dubrovnik, Yugoslavia.

Kos, Z. (1979) Chance-constrained model of the water resources system in the Odra River basin. Water Management J. 27(1): 14–26 (in Czech, English summary).

Kos, Z., V. Bečvář, L. Votruba, and V. Zeman (1974) Study of the important water resource system in the River Odra basin. CWP Preliminary Study. Prague: WRDC (in Czech).

Kos, Z. and J. Dupačova (1979) Chance-constrained and simulation models of water resources systems. Econ. Math. Rev. 15(2): 178–91.

Kos, Z., A. Medla, S. Novotný, and V. Zeman (1973) Study of the important water resource system in the River Morava basin. CWP Preliminary Study. Prague: WRDC (in Czech).

Kos, Z. and D. Novák (1976) Optimization of water resources utilization in water resource systems in CSSR. Symp. ECE to Problems of Water Resources Planning. Proc. WATER/SEM. 4/R4/CCM. 4, Varna.

Kos, Z., J. Pometlo, M. Sýkora, and V. Zeman (1972) Study of the important water resource system in the upper and middle part of the Labe River basin. GWP Preliminary Study. Prague: WRDC (in Czech).

Kos, Z. and V. Zeman (1976) Water Resource Systems Design in the General Water Management Plan. Prague: SZN (in Czech, English summary) p271.

Kruse, E.G., D.C. Kincaid, and H.R. Duke (1977) Evapotranspiration estimates with the modified Penman equation. Proc. ASCE Conf. on Water Management for Irrigation and Drainage, Reno, Nevada, pp245–55.

Linacre, E.T. (1967) Climate and the evaporation from crops. J. Irrigation and Drainage Division ASCE 93 (IR 4), Proc. Paper 5651, pp61–79.

Linacre, E.T. (1969) Closing discussion: climate and evaporation from crops. J. Irrigation and Drainage Division ASCE 95: 348–52.

Linacre, E.T. and M.R. Till (1969) Irrigation timing and amounts. J. Australian Inst. Agric. Sci. 35 (3): 175–96.

Linsley, R.K., M.A. Kohler, and Y.L.H. Paulhus (1975) Hydrology for Engineers (2nd edn) New York: McGraw-Hill, p482.

Lowry, R.L. and A.F. Johnson (1942) Consumptive use of water for agriculture. Am. Soc. Civil Engrs Trans. 107: 1243–302.

McCulloch, J.S.G. (1965) Tables for the rapid computation of the Penman estimate of evaporation. East Africa Forestry J. 30: 286–295.

McCulloch, J.S.G. (1977) Examples of areal actual evapotranspiration by indirect methods. Gen. Rep. on the Tech. Conf. on Assessment of Areal Evaporation, Budapest.

McGuinness, J.L. and E.F. Bordne (1972) A comparison of lysimeter-derived evapotranspiration with computed values, US Dept of Agric. Tech. Bull. 1452 (71 pp).

McIlroy, I.C. and D.E. Angus (1964) Grass, water and soil evaporation at Aspendale. Agric. Meteorol. 1(3): 201–24.

Makking, G.F. (1957) Testing the Penman formula by means of lysimeters. J. Inst. Water Engrs 11(3): 277–88.

Molz, F.J. (1972) Simulation of post-irrigation moisture movement. J. Irrigation and Drainage Division ASCE 98(IR 4), Proc. Paper 9419, pp523–32.

Monteith, J.L. (1965) Evaporation and the environment, in The State and Movement of Water in Living Organisms. Proc. 19th Soc. for Expt. Biol. Swansea. London: Cambridge University Press pp205–34.

Olivier, H. (1961) Irrigation and Climate. London: Arnold (250 pp).

Ostromecki, J. (1965) Remarks on methods of computation of water requirements of fields and grasslands. US Dept Interior TT 67-56052. (Transl. from Polish) (23 pp).

Patil, A.C. and J.E. Christiansen (1963) Comparison of four methods of computing evaporation. University Research Project U-193, College of Engineering, Utah State University.

Pegg, R.K. (1970) Evapotranspiration and the water balance, in The Role of Water in Agriculture (Ed. J.A. Taylor). University College of Wales at Aberystwyth Memo No. 12.

Penman, H.L. (1948) Natural evaporation from open water, bare soil and grass. Proc. R. Soc. London A193: 120–46.

Penman, H.L. (1949) The dependence of transpiration on weather and soil conditions. J. Soil Sci. 1: 74–89.

Penman, H.L. (1950) Evaporation over the British Isles. Q.J.R. Meteorol. Soc. 76: 372–83.

Penman, H.L. (1955) Components in the water balance of a catchment area. Q.J.R. Meteorol. Soc. 81: 280–3.

Penman, H.L. (1956) Estimating evaporation. Trans. Am. Geophys. Union 37: 43–50.

Penman, H.L. (1956) Evaporation: an introductory survey. Netherlands J. Agric. Sci. 1: 9–29, Discussion: 87–97, 151–3.

Persaud, Ch. (1977) Potential evapotranspiration in different climatic regions of Guyana. McGill University CRS No. 11 (101 pp).

Pruitt, W.O. (1966) Empirical method of estimating evapotranspiration using primarily evaporation pans. Proc. Conf. on Evapotranspiration, Am. Soc. Agric. Engrs, Chicago, pp57–61.

Pruitt, W.O. and M.C. Jensen (1955) Determining when to irrigate. Agric. Engr 36: 389–93.

Pruitt, W.O. and F.J. Lourence (1968) Correlations of climatological data with water requirements of crops. Water Sci and Engng Paper No. 9001, Univ. of California, Davis (59 pp).

Pruitt, W.O., F.J. Lourence, and S. von Oettingen (1972) Water use by crops as affected by climate and plant factors, California Agric., pp10–14.

Pruitt, W.O., S. von Oettingen, and D.L. Morgan (1972) Central California evapotranspiration frequencies. J. Irrigation and Drainage Division ASCE 98 (IR 2), Proc. Paper 8941, pp177–84.

Prus-Chacinski, T.M. (1963) Discussion of some aspects of the hydrology of the Thames bar. Proc. Inst. Civil Engrs 24: 247–87.

Rider, N.E. (1954) Evaporation from an oat field. Q.J.R. Meteorol. Soc. 80: 198–211.

Rider, N.E. (1957) Water losses from various land surfaces. Q.J.R. Meteorol. Soc. 83: 181–93.

Ritchie, J.T., E. Burnett, and R.C. Henderson (1972) Dryland evaporative flux in a subhumid climate, III. Soil water influences. Agron. J. 64: 168–73.

Robins, J.S. (1967) Reducing irrigation requirements, in Irrigation of Agricultural Lands (Eds. R.M. Hagan *et al.*). Am. Soc. Agron. pp1144–58.

Rosenberg, N.J. (1972) Frequency of potential evapotranspiration rates in Great Central Plains. J. Irrigation and Drainage Division ASCE 98 (IR 2), Proc. Paper 8946, pp203–6.

Saxton, K.E. and A.T. Lenz (1967) Antecedent retention indexes predict soil moisture. J. Hydraulics Division ASCE 93 (HY 4), Proc. Paper 5351, pp223–41.

Seuna, P. (1973) A simple linear soil moisture model for irrigation purposes. Proc. 9th European Reg. Conf. ICID, Budapest.

Shimshi, D., D. Yaron, E. Bresler, M. Weisbrod, and G. Strateener (1975) Simulation model for evapotranspiration of wheat: an empirical approach. J. Irrigation and Drainage Division ASCE 101 (IR 1): 1–12.

Slatyer, R.O. and I.C. McIlroy (1961) Practical Climatology. Melbourne: CSIRO, and Paris: UNESCO (340 pp).

Srivastava, M.S. and C.G. Khatri (1979) An Introduction to Multivariate Statistics. New York: North-Holland (350 pp).

Stanhill, G. (1958) The accuracy of meteorological estimates of evapotranspiration. J. Inst. Water Engrs 12: 377–83.
Stephens, J.C. (1965) Discussion of estimation evaporation from insulation. J. Hydrol. Division ASCE 91 (HY 5): 171–82.
Stewart, J.I. and R.M. Hagan (1969) Predicting effects of water shortage on crop yield. J. Irrigation and Drainage Division ASCE 95 (IR 1), Proc. Paper 6443, pp91–104.
Stewart, J.I., R.M. Hagan, and W.O. Pruitt (1974) Functions to predict optimal irrigation programs. J. Irrigation and Drainage Division ASCE 100 (IR 2), Proc. Paper 10626, pp179–99.
Szeicz, G. and I.F. Long (1969) Surface resistance of crop canopies. Water Resources Res. 5: 622–33.
Tanner, C.B. (1960) Energy balance approach to evapotranspiration from crops. Proc. Soil Sci. Soc. Am. 24: 1–9.
Tanner, C.B. (1968) Evaporation of water from plants and soils, in Water Deficits and Plant Growth vol. 1 (Ed. T.T. Kozloski) New York: Academic Press, pp73–106.
Tanner, C.B. and M. Fuchs (1968) Evaporation from unsaturated surfaces: a generalized combination method. J. Geophys. Res. 73: 1299–304.
Tanner, C.B. and W.L. Pelton (1960) Potential evapotranspiration estimates by the approximate energy balance method of Penman. J. Geophys. Res. 65: 3391–413.
Thornthwaite, C.W. (1944) Report of the committee on transpiration and evaporation 1943–44. Trans. Am. Geophys. Union 25: 5.
Thornthwaite, C.W. (1948) An approach toward a rational classification of climate. Geog. Rev. 38: 55–94.
Tomlain, J. (1979) Methods of determination of actual and potential evaporation from soil surface. Meteorologicke zpravy 32: 72–7 (in Czech).
Turc, L. (1961) Evaluation des besoins en eau d'irrigation, évapotranspiration potentielle: formule climatique simplifice et mise à jour (Estimation of irrigation water requirements, potential evapotranspiration: a simple climatic formula evolved up-to-date). Ann. Agron. 12: 13–49.
USDA (1967) Irrigation water requirements. US Dept of Agric., Engng Division Soil Conservation Service, Tech. Release No. 21 (88 pp).
van Bavel, C.H.M. (1968) Discussion of climate and evaporation of crops. J. Irrigation and Drainage Division ASCE 68: 533–5.
Wilks, S.S. (1962) Mathematical Statistics. New York: Wiley (644 pp).
Windsor, J.S. and Ven Te Chow (1971) Model for farm irrigation in humid areas. J. Irrigation and Drainage Division ASCE 97: (IR 3), Proc. Paper 8355, pp369–85.
Wiser, E.H. (1965) Irrigation planning using climatological data. J. Irrigation and Drainage Division ASCE 91 (IR 4), Proc. Paper 4551, pp1–11.
WMO (1968) Practical Soil Moisture Problems in Agriculture. WMO-No. 235, TP 128, Tech. Note No. 97 (69 pp).
WMO (1974) Guide to Hydrological Practices. WMO-No. 168.
WMO (1979) Problems of Evaporation Assessment in the Water Balance (Hounam, C.E.) Rep. No. 73, WMO-No. 285.
Wu, I. and T. Liang (1972) Optimal irrigation quantity and frequency. J. Irrigation and Drainage Division ASCE 98 (IR 1), Proc. Paper 8776, pp117–33.

APPENDIX A Formulae for Evapotranspiration

Thornthwaite

$$PE_t = 16\,(10T_t/I)a$$

where

PE_t = monthly potential evapotranspiration (mm);
T_t = mean monthly air temperature (°C);
I = annual heat index

$$I = \sum_{t=1}^{12} \left(\frac{T_t}{5}\right)^{1.514}$$

$$a = 6.75 \times 10^{-7} I^3 - 7.71 \times 10^{-5} I^2 + 1.792 \times 10^{-2} I + 0.49239.$$

This formula is relatively simple and requires few input data, so that it has been one of the most commonly used (and misused) empirical equations in generating inaccurate estimates of potential evapotranspiration. This equation is valid only for the conditions of the east-central USA. Thornthwaite and Mather (1955) required that (1) the albedo of the evaporating surface must be a standard; (2) the rate of evapotranspiration must not be influenced by advection of moist or dry air; and (3) the ratio of energy utilized in evapotranspiration to that used in heating the air must remain essentially constant. Since it is questionable whether these conditions exist in the investigated area, this equation cannot be used.

Blaney and Criddle

$$PE_t = \sum_{t=1}^{8} k_t \frac{T_t P_t}{100}$$

where

PE_t = potential evapotranspiration (in/season);
k_t = monthly crop coefficient;
T_t = mean monthly air temperature (°F);
P_t = mean monthly percentage of annual daytime hours.

(This equation could be converted to SI units (i.e., mm, °C), but with some loss of simplicity.)

This formula has been analyzed by Pruitt (1960), Quackenbush and Phelan (1965), Jensen (1966), Tanner (1967), and others, who showed that it is oversimplified and that the coefficients are influenced by radiation and humidity. Furthermore, the evapotranspiration PE (or its monthly components) is strongly dependent on the crop being irrigated, which is not convenient for long-term planning.

Turc

Turc's formula (1954) was derived from lysimetric measurements giving evapotranspiration from a cultivated field as a function of available moisture and the "evaporating power of the air":

$$PE_t = \frac{P + m + V}{\{1 + [(P + m)/L + (V/2L)]^2\}^{1/2}}$$

where

PE_t = evapotranspiration (mm/10 days);
P = precipitation (mm/10 days);
m = soil moisture available for evapotranspiration (mm) (e.g., m = 10 after irrigation, m = 1 for dry soil);
V = additional moisture available for evapotranspiration (mm).

V is determined by

$$V = 25(Mc/Z)^{1/2}$$

where

- M = final yield of dry matter (dg m^{-2}; originally metric cents per hectare) (e.g., for wheat $M = 30$);
- c = crop constant (e.g., for cereals, carrots, $c = 1.00$; maize, beet, $c = 0.67$; potatoes, $c = 0.83$; peas, clover, $c = 1.17$; lucerne, alfalfa, meadow grass, $c = 1.33$);
- Z = length of growing season (days).

A radiation and temperature term giving the evaporating power of the air is given by

$$L = (1/16)(T + 2)\sqrt{Q}$$

where T is the mean air temperature over a ten-day period (°C), and Q is the mean short-wavelength radiation over a ten-day period (cal cm^{-2}).

A simplified version (Turc 1954, Johansson 1970) for the vegetative period can be written as

$$PE_t = \frac{P + 80}{\{1 + [(P + 45)/L]^2\}^{1/2}}$$

by choosing average values of m and V. Turc (1954) published a new formula:

$$PE_t = 0.013\frac{T}{T + 13}(Q + 50)\left(1 + \frac{50 - RH}{70}\right)$$

where T and Q have the same meanings as above, and RH is the relative humidity (%). This formula can be referred to in three forms: in one form PE_t is dependent on yield and crop coefficients, but this makes it cumbersome, so that it has been simplified using average estimates of the empirical coefficients. In this form only the stated inputs are necessary. The main advantage is that precipitation can be used as the input factor of evapotranspiration. However, the procedure is dependent on the conditions under which the input data were derived, and lacks physical sense, although under some conditions it affects the result very little (a change of 100% from 20 to 40 mm of precipitation changes the monthly evapotranspiration value by only 3%).

Johansson

$$PE_t = 0.14 + 3.7 \times 10^{-3}Q + 0.13w(e_m - e_d)$$

where

- PE_t = evapotranspiration (mm/day);
- Q = solar radiation (cal cm^{-2}/day);
- w = mean daily wind velocity (m s^{-1});
- $e_m - e_d$ = saturation deficit (mm Hg).

Ivanov

$$PE_t = 0.0018(25+T)^2(100-RH)$$

where

PE_t = evapotranspiration (mm/month);
T = temperature (°C);
RH = relative humidity (%).

Ostromecki, Alpatjev, and Pýcha

$$PE_t = k_c d_t$$

where
PE_t = evapotranspiration (mm/month);
k_c = crop coefficient (0.2–1.1);
d_t = sum of mean daily saturation deficits (mm Hg).
Pýcha found that k_c is dependent on the accumulated temperature:

$$\sum_{d=1}^{d+h} T_d$$

i.e., the sum of mean daily temperatures (°C) from the beginning of the growing period of a crop.

Makking

$$PE_t = 0.61 \frac{\Delta}{\Delta+\gamma} \frac{R_s}{59} - 0.12$$

where
PE_t = evapotranspiration (mm/day);
Δ, γ = (see Penman's equation);
R_s = solar radiation (cal cm^{-2}).

Stephens

$$PE_t = (0.014T - 0.37)R_s/1500$$

where
PE_t = evapotranspiration (in/day);
T = temperature (°F);
R_s = solar radiation (cal cm^{-2}).

Jensen, Jensen and Haise

$$PE_t = C(T - T_o)R_s = 0.025(T+3)R_s$$

where
PE_t = evapotranspiration (mm/day);
T = mean air temperature (°C);
R_s = solar radiation (cal cm^{-2}).

Jensen later defined C as follows:

$$C = \frac{1}{C_1 + C_2 C_H}$$

where

C_1 = $38 - 2M/305$;
M = elevation above sea level (m);
C_2 = 7.6;
C_H = $50/(e_n - e_d)$;
e_n and e_d = saturation vapor pressure at mean maximum and mean minimum temperatures (mbar), respectively.

McIlroy

$$PE_t = \frac{s}{L(s+\gamma)}(Q_n - S) + h(D - D_0)$$

where

PE_t = evapotranspiration (mm/day);
γ = (see Penman's equation);
L = latent heat of vaporization (cal g^{-1});
s = $0.63\,\Delta W/p$;
p = atmospheric pressure (mbar);
ΔW = slope of saturation vapor pressure curve at mean wet bulb temperature (mbar $°C^{-1}$);
Q_n = net radiation flux (cal cm^{-2});
S = soil heat flux (cal cm^{-2}) (for monthly data, this can be neglected);
h = wind velocity coefficient (experimentally determined)
= $0.5(1 + w)$, where w is the wind velocity (m s^{-1});
D = wet bulb temperature depression (°C) at height Z(m) above the ground;
D_0 = wet bulb temperature depression (°C) at ground level, which can be taken as $D_0 = 0$ (experimentally determined).

Christiansen and Hargreaves

$$PE_t = 0.492 R_s C_T C_w C_H$$

where

PE_t = evapotranspiration (mm/day);
R_s = solar radiation (cal cm^{-2});
C_T = $0.463 + 0.425T/20 + 0.112(T/20)^2$;
T = mean temperature (°C);
C_w = $0.672 + 0.406W/6.7 - 0.073(W/6.7)^2$;
W = mean wind velocity 2 m above ground level (km h^{-1});
C_H = $1.035 + 0.24RH/60 - 0.275(RH/60)^2$, where RH is relative humidity (%).

Baier and Russelo, Baier and Robertson

$$PE_t = 0.085[-53.39 + 0.337M + 0.531R + 0.0107Q_0 + 0.0512Q_s + 0.0977W + 1.77(e_w - e_s)]$$

where

PE_t = evapotranspiration (mm/day);
M = daily maximum temperature (°F);
R = difference between daily maximum and minimum temperatures (°F);
Q_0 = solar radiation (cal cm^{-2}/day);
Q_s = Q_0 $(0.261 + 0.616n/N)$, total daily solar energy on a horizontal surface (cal cm^{-2}/day), where n/N is the sunshine (see Penman's equation);
W = wind velocity (miles/day);
$e_w - e_s$ = vapor pressure deficit (mbar) from saturation vapor pressure at mean air temperature and at mean daily dewpoint temperature.

APPENDIX B FAO Modifications to Penman's Equation

According to the annex of the FAO Plant Production and Protection Paper No. 17 *Agrometeorological Crop Monitoring and Forecasting* (Rome, 1979), the following modifications to Penman's equation were recommended:

(*a*) Evapotranspiration should be calculated directly using an albedo of $r = 0.25$.

(*b*) A correction for elevation should be included (it is insignificant up to 150 m above sea level).

(*c*) In eq. (14), a coefficient of 0.079 should be used instead of 0.9.

(*d*) Equation (15) should be changed to $E = 0.26(e_a - e_d)(1 + 0.54w)D$

Other changes were not valid for the case analyzed.

With these changes and $f_t = 1$ for the V-III-V system (based on the input data shown in Table B.1), eq. (27) becomes

$$WI_t = 0.198 \frac{\Delta}{\Delta + \gamma} R_{n,t} + 0.853 \frac{\gamma}{\Delta + \gamma} E_t - 0.076 P_t + 0.487\, WI_{t-1} - 12.08 \qquad (27a)$$

and eq. (28) for $d = 1.90$ becomes

$$WI_t = 0.377 \frac{\Delta}{\Delta + \gamma} R_{n,t} + 1.621 \frac{\gamma}{\Delta + \gamma} E_t - 0.144 P_t + 0.487\, WI_{t-1} - 22.95 \qquad (28a)$$

The parameters $r_{i,d}$, R_i, and F_i become

$i =$	1	2	3	4
$r_{i,d}$	0.396	0.662	−0.296	0.534
R_i		0.662	0.718	0.875
F_i		14.46	12.78	28.59

Corresponding to eq. (23), α' becomes

$$\alpha' = \frac{1}{1.1} \frac{0.144 \times 47 + 22.95}{47} = 0.57$$

The resulting multiple correlation coefficient was nearly the same (0.873 and 0.875), the F-test values were higher by 2%, and the regression coefficients did not differ significantly. Thus the results using both methods are practically identical.

This modification was tested in the C-V system with approximately the same results concerning the significance of the resulting equation. For the C-V system, eq. (30) becomes (using the input data shown in Table B.1)

$$WI_t = 0.170 \frac{\Delta}{\Delta+\gamma} R_{n,t} + 0.499 \frac{\gamma}{\Delta+\gamma} E_t - 0.115 P_t + 0.442\, WI_{t-1} - 1.72$$

and eq. (31) for $d = 2.99$ becomes

$$WI_t = 0.508 \frac{\Delta}{\Delta+\gamma} R_{n,t} + 1.492 \frac{\gamma}{\Delta+\gamma} E_t - 0.345 P_t + 0.442\, WI_{t-1} - 5.14$$

The parameters $r_{i,d}$, R_i, and F_i become

$i =$	1	2	3	4
$r_{i,d}$	0.383	0.575	−0.417	0.595
R_i		0.577	0.727	0.872
F_i		9.25	13.22	27.74

$$\alpha' = \frac{\alpha \bar{P} + \beta}{\bar{P}} = \frac{0.345 \times 42.78 + 5.14}{42.78} = 0.47$$

The method of Appendix B was also used for computation in Section 6.1, but values of f_t were omitted.

This method of direct evapotranspiration determination (i.e., without the reduction coefficients f_t) was combined with the previous irrigation index. For the V-III-V system, the following modification to eq. (29) was obtained (based on the input data shown in Table B.2):

$$WI_t = i_t \left(0.365 \frac{\Delta}{\Delta+\gamma} R_{n,t} + 0.695 \frac{\gamma}{\Delta+\gamma} E_t \right) - 0.076 P_t - 8.14 \tag{29a}$$

The multiregressive coefficient was slightly lower, at 0.838, as compared with 0.846.

APPENDIX C Application of Program REVAP by Morton *et al.*

Areal evapotranspiration is an important element in the modeling of a hydrological cycle. Morton *et al.* (1980) defined it as the evapotranspiration from an area so large that the effects of evapotranspiration on the temperature and humidity of the overpassing air are fully developed.

The basic aim of Morton's investigation was to determine the complementary relationship between areal and potential evapotranspiration:

TABLE B.1 Input variables in regression analysis (method of Appendix B). $WI^{1}_{t} = WI_t/2.22$; $WI^{1}_{t-1} = WI_{t-1}/2.22$. Other variables are explained in eqs. (20) and (25).

		V-III-V system					C-V system				
	M	WI_{t-1}	P_t	$\frac{\Delta}{\Delta+\gamma}R_{n,t}$	$\frac{\gamma}{\Delta+\gamma}E_t$	WI_t	WI^{1}_{t-1}	P_t	$\frac{\Delta}{\Delta+\gamma}R_{n,t}$	$\frac{\gamma}{\Delta+\gamma}E_t$	WI^{1}_{t}
1970	6	0.24	75.50	53.70	17.40	2.67	1.66	13.00	53.70	17.40	6.58
	7	2.67	48.90	48.60	22.20	13.61	6.58	26.00	48.60	22.20	6.11
	8	13.61	106.30	36.30	10.20	2.24	6.11	95.00	36.30	10.20	2.44
	9	2.24	23.60	14.70	11.40	0.68	2.44	21.00	14.70	11.40	3.87
1971	4	0.00	16.50	19.80	14.10	0.33	0.00	12.00	19.80	14.10	1.80
	5	0.33	124.30	37.80	13.80	1.48	1.80	98.00	37.80	13.80	2.63
	6	1.48	109.70	40.20	14.40	0.10	2.63	110.00	40.20	14.40	0.39
	7	0.10	9.30	53.70	20.70	12.47	0.39	5.00	53.70	20.70	9.86
	8	12.47	57.20	41.10	22.20	26.52	9.86	60.00	41.10	22.20	9.36
	9	26.52	37.70	14.10	9.60	7.89	9.36	35.00	14.10	9.60	4.66
1972	4	0.00	24.20	17.10	15.00	0.71	0.00	26.00	17.10	15.00	1.21
	5	0.71	76.10	35.40	16.50	1.98	1.21	94.00	35.40	16.50	1.86
	6	1.98	78.90	48.60	17.10	6.72	1.86	66.00	48.60	17.10	6.13
	7	6.72	40.70	49.80	14.70	13.78	6.13	39.00	49.80	14.70	6.23
	8	13.78	51.50	35.70	15.00	9.03	6.23	48.00	35.70	15.00	3.28
	9	9.03	37.30	13.80	7.20	0.85	3.28	60.00	13.80	7.20	1.61
1973	4	0.00	47.30	16.50	17.10	1.47	0.00	34.50	16.50	17.10	1.43
	5	1.47	54.70	39.90	18.30	3.41	1.43	48.40	39.90	18.30	4.71
	6	3.41	44.10	52.80	19.50	10.62	4.71	47.00	52.80	19.50	7.45
	7	10.62	69.00	47.70	19.80	24.72	7.45	79.10	47.70	19.80	8.26
	8	24.72	14.10	40.50	19.80	26.72	8.26	8.00	40.50	19.80	11.26
	9	26.72	9.90	14.70	17.10	14.60	11.26	7.70	14.70	17.10	9.34

1974	4	0.00	10.00	19.20	20.70	15.70	0.00	8.40	19.20	20.70	8.45
	5	15.70	70.10	35.70	18.00	3.91	8.45	80.00	35.70	18.00	3.17
	6	3.91	65.80	43.50	18.00	6.26	3.17	73.70	43.50	18.00	4.53
	7	6.26	54.30	40.80	25.20	11.88	4.53	64.60	40.80	25.20	2.69
	8	11.88	44.70	40.20	20.10	13.61	2.69	66.10	40.20	20.10	4.83
	9	13.61	38.90	15.60	12.90	6.41	4.83	30.60	15.60	12.90	3.23
1975	4	0.00	19.90	18.60	16.80	0.30	0.00	19.90	18.60	16.80	1.43
	5	0.30	65.50	36.30	15.30	2.91	1.43	74.70	36.30	15.30	1.98
	6	2.91	62.00	44.40	14.70	5.55	1.98	41.10	44.40	14.70	5.66
	7	5.55	48.50	51.30	17.40	15.58	5.66	28.80	51.30	17.40	6.43
	8	15.58	20.90	40.20	17.70	20.32	6.43	17.50	40.20	17.70	8.52
	9	20.32	20.90	17.70	9.00	9.31	8.52	18.00	17.70	9.00	7.16
1976	4	0.00	17.50	19.20	15.90	2.98	0.00	14.00	19.20	15.90	2.51
	5	2.98	55.50	39.90	24.90	16.24	2.51	48.00	39.90	24.90	7.90
	6	16.24	32.00	53.40	25.80	16.11	7.90	25.00	53.40	25.80	8.70
	7	16.11	29.50	50.10	29.40	38.39	8.70	30.00	50.10	29.40	16.77
	8	38.39	37.50	36.00	24.30	26.37	16.77	36.00	36.00	24.30	12.71
	9	26.37	29.50	14.10	9.60	11.16	12.71	2.00	14.10	9.60	8.25

TABLE B.2 Input variables in regression analysis (method of Appendix B, combined with previous irrigation index). $WI_t^{1/2} = WI_t/2.22$; $WI_{t-1}^{1/2} = WI_{t-1}/2.22$. Other variables are explained in eqs. (20) and (25).

		V-III-V system					C-V system				
	M	WI_{t-1}	P_t	$\frac{\Delta}{\Delta+\gamma}R_{n,t}$	$\frac{\gamma}{\Delta+\gamma}E_t$	WI_t	$WI_{t-1}^{1/2}$	P_t	$\frac{\Delta}{\Delta+\gamma}R_{n,t}$	$\frac{\gamma}{\Delta+\gamma}E_t$	$WI_t^{1/2}$
1970	6	0.24	75.50	34.63	11.22	2.67	1.66	13.00	37.76	12.23	6.58
	7	2.67	48.90	35.91	16.40	13.61	6.58	26.00	41.30	18.87	6.11
	8	13.61	106.30	35.78	10.05	2.24	6.11	95.00	30.43	8.55	2.44
	9	2.24	23.60	10.65	8.26	0.68	2.44	21.00	10.75	8.34	3.87
1971	4	0.00	16.50	19.80	14.10	0.33	0.00	12.00	19.80	14.10	1.80
	5	0.33	124.30	24.53	8.96	1.48	1.80	98.00	26.77	9.77	2.63
	6	1.48	109.70	27.98	10.02	0.10	2.63	110.00	29.65	10.62	0.39
	7	0.10	9.30	34.29	13.22	12.47	0.39	5.00	34.98	13.48	9.86
	8	12.47	57.20	39.74	21.47	26.52	9.86	60.00	37.82	20.43	9.36
	9	26.52	37.70	16.13	10.98	7.89	9.36	35.00	12.84	8.74	4.66
1972	4	0.00	24.20	17.10	15.00	0.71	0.00	26.00	17.10	15.00	1.21
	5	0.71	76.10	23.55	10.98	1.98	1.21	94.00	24.27	11.31	1.86
	6	1.98	78.90	34.75	12.23	6.72	1.86	66.00	34.54	12.15	6.13
	7	6.72	40.70	42.48	12.54	13.78	6.13	39.00	41.77	12.33	6.23
	8	13.78	51.50	35.28	14.82	9.03	6.23	48.00	30.03	12.62	3.28
	9	9.03	37.30	12.47	6.51	0.85	3.28	60.00	10.48	5.47	1.61
1973	4	0.00	47.30	16.50	17.10	1.47	0.00	34.50	16.50	17.10	1.43
	5	1.47	54.70	27.76	12.73	3.41	1.43	48.40	27.71	12.71	4.71
	6	3.41	44.10	40.29	14.88	10.62	4.71	47.00	42.31	15.63	7.45
	7	10.62	69.00	44.58	18.50	24.72	7.45	79.10	41.50	17.23	8.26
	8	24.72	14.10	45.60	22.29	26.72	8.26	8.00	35.95	17.57	11.26
	9	26.72	9.90	16.84	19.59	14.60	11.26	7.70	13.91	16.18	9.34

1974	4	0.00	10.00	19.20	20.70	15.70	0.00	8.40	19.20	20.70	8.45
	5	15.70	70.10	36.31	18.31	3.91	8.45	80.00	31.83	16.05	3.17
	6	3.91	65.80	33.86	14.01	6.26	3.17	73.70	32.86	13.60	4.53
	7	6.26	54.30	34.35	21.22	11.88	4.53	64.60	32.49	20.07	2.69
	8	11.88	44.70	38.47	19.24	13.61	2.69	66.10	29.73	14.87	4.83
	9	13.61	38.90	15.38	12.71	6.41	4.83	30.60	12.55	10.38	3.23
1975	4	0.00	19.90	18.60	16.80	0.30	0.00	19.90	18.60	16.80	1.43
	5	0.30	65.50	23.51	9.91	2.91	1.43	74.70	25.21	10.63	1.98
	6	2.91	62.00	33.16	10.98	5.55	1.98	41.10	31.74	10.51	5.66
	7	5.55	48.50	42.27	14.34	15.58	5.66	28.80	42.42	14.39	6.43
	8	15.58	20.90	40.81	17.97	20.32	6.43	17.50	34.02	14.98	8.52
	9	20.32	20.90	19.70	9.70	9.31	8.52	18.00	15.81	8.04	7.16
1976	4	0.00	17.50	19.20	15.90	2.98	0.00	14.00	19.20	15.90	2.51
	5	2.98	55.50	29.90	18.66	16.24	2.51	48.00	29.27	18.27	7.90
	6	16.24	32.00	54.72	26.44	16.11	7.90	25.00	46.99	22.70	8.70
	7	16.11	29.50	51.25	30.07	38.39	8.70	30.00	44.94	26.37	16.77
	8	38.39	37.50	44.74	30.20	26.37	16.77	36.00	37.15	25.08	12.71
	9	26.37	29.50	16.11	10.97	11.16	12.71	2.00	13.69	9.32	8.25

$$ET + ETP = 2ETW$$

where ET is the areal evapotranspiration, ETP is the potential evapotranspiration, and ETW is the wet environment evapotranspiration (evapotranspiration that occurs from a large saturated area, with water available for evapotranspiration).

Morton (1980) demonstrated that a reduction in the water available for areal evapotranspiration makes the overpassing air hotter and drier, and that this in turn increases potential evapotranspiration as computed from meteorological variables such as temperature, dewpoint temperature, and duration of sunshine.

The relationship indicates that potential evapotranspiration is more an effect than a cause of areal evapotranspiration. Morton's theoretical investigation and empirical verification showed that the average of areal and potential evapotranspiration, i.e., $(ET + ETP)/2$, is relatively stable, and he called it the wet environment evapotranspiration (ETW).

For this value, the following regression equation was proposed by Morton *et al.* (1980):

$$ETW = 14 + 1.2 \frac{\Delta}{\Delta + \gamma} R_n \text{ (mm)},$$

where Δ (the slope of the saturation vapor pressure curve) and R_n (net radiation) are at the potential evapotranspiration equilibrium temperature, and γ is the psychrometric constant. If ETP and ETW are known, ET can be computed.

Morton *et al.* (1980) published a program, REVAP, in Fortran for computation of these values, and a simplified version of this was used in this study for the data from station B. The results indicated that the potential evapotranspiration values computed by REVAP were systematically higher than those of potential evapotranspiration (PE) computed by eqs. (11)–(15) (Penman). For the period April–September, the ETP (evapotranspiration – Morton) was 1.66 times higher than the PE in 1970–76, and 1.63 times higher in 1931–70. For the period March–October, it was 1.67 times higher in 1931–70.

Similar relations were computed for areal evapotranspiration (ET) and wet environment evapotranspiration (ETW), as shown in the table below.

		April–September	March–October
ETP/PE	1931–70	1.63	1.67
	1970–76	1.66	
ET/PE	1931–70	0.83	0.83
	1970–76	0.81	
ETW/PE	1931–70	1.23	1.25
	1970–76	1.23	

According to the complementary character of Morton's relationship, it was taken for granted that it would give lower potential evapotranspiration values than Penman's formula. This disagreement between expectations and results needs further research, especially as far as the regression equation for the determination of the ETW is concerned.

BIOGRAPHIES

Verne G. Chant, Canada

Verne G. Chant received his BASc in Electrical Engineering in 1965 and his MASc in Control Systems in 1967, both from the University of Toronto, and his PhD in Engineering-Economic Systems from Stanford University in 1972. Dr. Chant came to IIASA in January 1978 to work on energy demand and economic analysis. He is currently with Hickling-Partners Incorporated, Ottawa, Ontario. His main scientific interests include problem definition and formulation, economic analysis, application of operational research and mathematical analysis, optimization and decision analysis, as applied to problems involving economics and public policy. He is a member of the International Association of Energy Economists, the Canadian Operational Research Society and the Ottawa Association of Applied Economics.

M. Gadkowski, Poland

M. Gadkowski works at the Institute of Meterology and Water Management in Warsaw, Poland, where he is engaged in water management problems, particularly with respect to heat power plants. He received his M.Sc. in water engineering in 1956 and his Ph.D. in 1970, both from the Technical University of Warsaw. Dr. Gadkowski's professional and research interests are concerned with water dam design, water supply for large power plants, industrial water utilization, heat energy development, and environmental problems in large power plants. He has published numerous articles in these areas. As a result of his activities and fellowships in France, USA, and the FRG, he has become an experienced specialist in the field of water economics.

Zdenek Kos, Czechoslovakia

Zdenek Kos joined IIASA's Resources and Environment Area in April 1980. His research focuses on the application of mathematical models and computational procedures in regional water management. Dr. Kos is with the Technical University of Prague; he received his Ph.D. from there in 1969. In recent years he has been working on the design, modeling, and control of water resource systems, on new methods of water supply, on drainage design, and on stochastic hydrological problems. He is a member of the Czechoslovak Scientific Technical Society, the task group for reservoirs and dams of the Presidium of the Czechoslovak Academy of Sciences, and the Opponent Board of the Technical University of Prague. Dr. Kos has attended numerous international symposia and workshops and is the author of a number of books and papers.

Andrzej Salewicz, Poland

Andrzej Salewicz is the leader of the Water System Control Group of the Institute of Meteorology and Water Management, Warsaw. He received an M.Sc. in Automatic Control from Warsaw Technical University. He is currently working on the operation of multiple reservoir systems, concentrating on the case study of the Upper Vistula System.

Witold Sikorski, Poland

Witold Sikorski was at IIASA from June 1977 to September 1978. Mr. Sikorski studied Electrical Engineering at Warsaw Technical University, where he received his M.Sc. in 1973. In 1974 he completed his postgraduate studies in didactics and methodology of teaching. He is currently at the Institute of Environmental Engineering of Warsaw Technical University.

F. Dail Singleton, Jr., USA

F. Dail Singleton, Jr., received a bachelors degree in Chemical Engineering (1965) from the University of Delaware, and a doctoral degree (1971) from the University of Rochester. After working in the chemical industry, he was among the first professionals to join the Industry Studies Program at the University of Houston. His experience in industrial modeling led to an invitation to work at IIASA in 1977. Upon leaving IIASA he resumed work with the Industry Studies Program and then moved with the group to a private-sector corporation, RGT, Inc. (now Operational Economics, Inc.), where he is the Director of Systems and Engineering Analysis.

John C. Stone, USA

John C. Stone received a bachelors degree in Economics (1974) and a masters degree in Environmental Health Science (1977/78) from Harvard University. Between degrees he joined the research staff of the Industry Studies Program at the University of Houston, and through that group obtained an invitation to do work at IIASA following his masters degree. Upon leaving IIASA he continued to work with the Industry Studies Program and then moved with the group to a Houston-based private-sector corporation, RGT, Inc. (now Operational Economics, Inc.), where he has been the Director of Mathematical Modeling and Economic Analysis. He is currently pursuing a doctoral degree in Operations Research at Stanford University, USA.

IIASA
REPORTS

Volume 6 Number 2 October-December 1982
Completing Volume 6

Published quarterly

CONTENTS

Printed by NOVOGRAPHIC, Vienna, Austria.